



Impacts of (Cooperative) Adaptive Cruise Control Systems on Traffic Flow

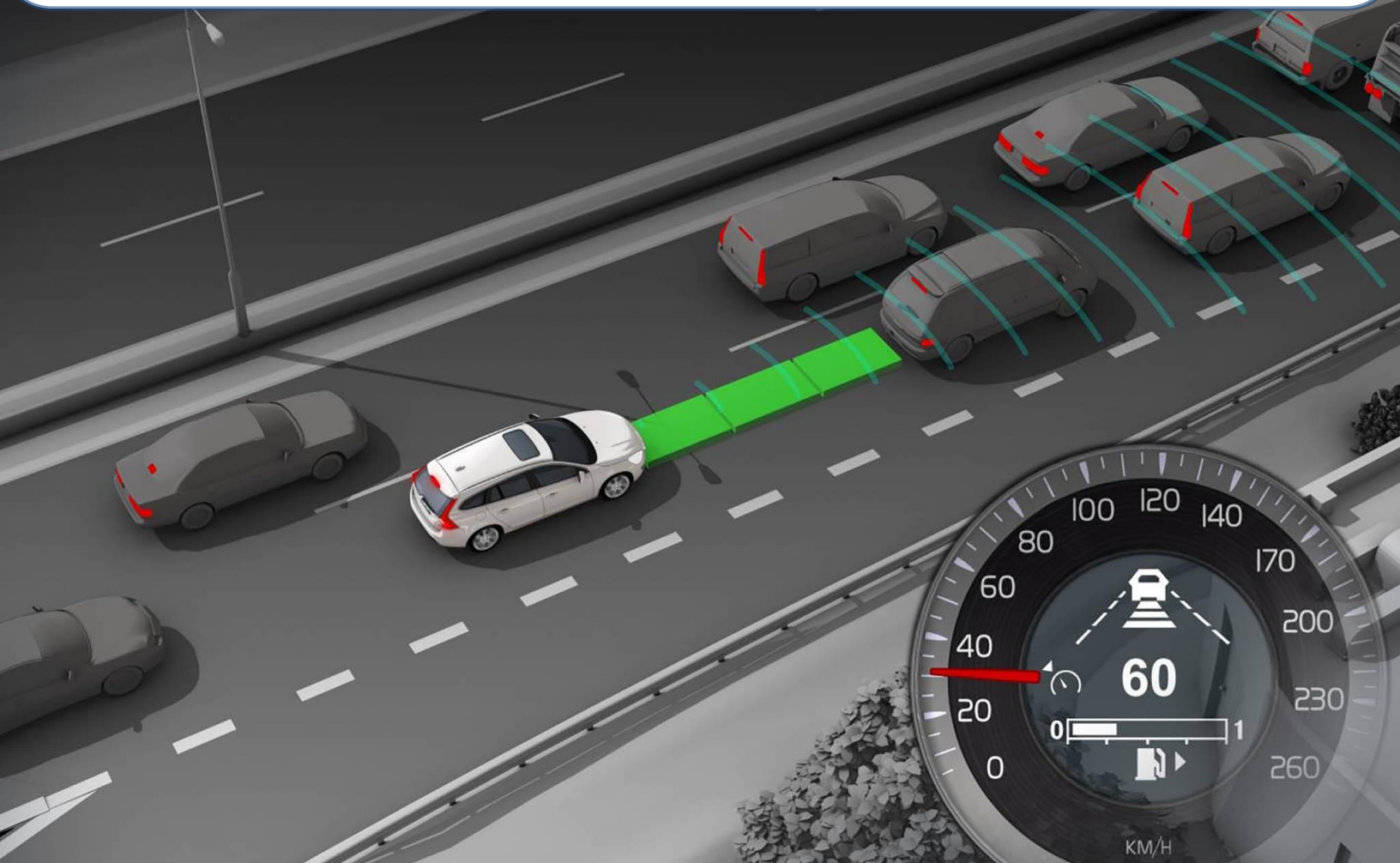
A simulation case study on the effects of (cooperative) adaptive cruise control on the A15 highway

M. Huisman
4147537



TU Delft Delft University of Technology

 **Royal HaskoningDHV**
Enhancing Society Together



Impacts of (Cooperative) Adaptive Cruise Control on Traffic Flow

A simulation case study on the effects of (cooperative) adaptive cruise control on the A15 highway

By

M. Huisman

in partial fulfilment of the requirements for the degree of

Master of Science

in Transport, Infrastructure & Logistics

at the Delft University of Technology,

Mathijs Huisman

4147537

mathijs.huisman1992@gmail.com

mathijs.huisman@rhdhv.com

Graduation committee:

Prof. Dr. Ir. B. van Arem

Chair

Delft University of Technology - Faculty of Civil Engineering and Geosciences - Department
Transport & Planning

Dr. Ir. R. Happee

Daily supervisor TU Delft

Delft University of Technology - Faculty of Mechanical, Maritime and Materials Engineering -
Department BioMechanical Engineering

Dr. Ir. M. Wang

Daily supervisor TU Delft

Delft University of Technology - Faculty of Civil Engineering and Geosciences - Department
Transport & Planning

Ing. E. Klem

Royal HaskoningDHV

Daily supervisor Royal HaskoningDHV

Ir. M. C. Verkaik-Poelman

Royal HaskoningDHV

Daily supervisor Royal HaskoningDHV

Preface

Currently, you are reading the result of approximately 8 months of researching, modelling, simulation, analysis and writing. This research is my graduation project as a component of the MSc program Transport, Infrastructure and Logistics at the Delft University of Technology. This research was executed in close cooperation with Royal HaskoningDHV.

When I first read about the topic of this research, I immediately became enthusiastic. In my opinion, the topic of (Cooperative) Adaptive Cruise Control is very interesting. Also, the field of study on traffic flow interests me and therefore, this topic was an ideal combination of these components. At the start of this project I did not have much experience in traffic modelling using simulation programs, but it was something that I was prepared to learn. After all, I am very happy with this decision, because traffic modelling is fun and interesting. This research really pushed my boundaries, because I was very determined to find effects of ACC and CACC on traffic flow and I had the chance to develop research, writing and modelling skills. Therefore, I am very glad and grateful that I got the chance to perform this research.

This research is executed under the supervision of my graduation committee consisting of Bart van Arem, Meng Wang, Riender Happee from the TU Delft and Muriel Verkaik-Poelman and Evert Klem from Royal HaskoningDHV. I would like to thank all members of my thesis committee for the enthusiasm, criticism and help to perform this research as good as possible. Also, I would like all of you for the time you took to help, coach and supervise me, although being so busy. Your passion and enthusiasm motivated me to push my limits even further.

I am very grateful for all help I received with respect to traffic modelling in Aimsun. Muriel and some other colleagues really helped me in this field. Additionally, Evert Klem and Meng Wang really helped me getting some insights during the conversations we had. Next to this, I would like to thank all other colleagues at Royal HaskoningDHV for providing me a unique insight into their work and their interest into this research. The opportunity to talk with professionals helped me in getting more insight into modelling and traffic (flow) in general.

Also, I would like to thank the other students that did their internship at the same department, because we had a lot of fun and motivated each other to improve the quality of our work and research.

Finally, I would like to thank my family, friends and my girlfriend Mirjam for supporting me throughout my study and life in general. These persons not only motivated me, but also helped me in getting the relaxation needed to keep performing at a high level.

Amersfoort, October 2016

Mathijs Huisman

Executive summary

Background

Adaptive Cruise Control (ACC) is an advanced version of cruise control which is able to automatically maintain a certain set speed and detect the speed of a directly leading vehicle and adapting speed, based on the location and speed of this predecessor. Cooperative Adaptive Cruise Control (CACC) is a further development of ACC, which adds communications with multiple vehicles. This enables CACC vehicles to send and receive speed information, enabling smoother and faster responses than ACC.

These systems take over a part of the driving tasks, which means that it influences the driving behavior of drivers and vehicles on the road. Clearly, this could have a significant effect on traffic flow performance. This research is executed to determine the effects of ACC and CACC on realistic traffic situations with multiple bottlenecks.

A wide variety of literature that study the effects of (C)ACC on traffic flow or performance is available. However, the topic is not yet well understood, since results differ from substantial increases to substantial decreases (Milanés & Shladover, 2014). Additionally, detailed studies on the effects of ACC and CACC on relatively large scale network are still lacking, since most microscopic studies are aimed on a single bottleneck or characteristic traffic situation. Therefore, this research could be of added value to this field of research and might provide extra insight into this topic.

Research method

The main objective of this thesis is to *gain an insight in the effects of (different market penetration rates of) ACC and CACC on traffic flow performance in realistic traffic situations on the highway, such as traffic situations with multiple bottlenecks and at weaving sections*. In order to reach this objective, the following research question is composed: *'What are the effects of (Cooperative) Adaptive Cruise Control on traffic flow in realistic traffic situations with multiple bottlenecks?'*

The research question is answered using a relatively simple research framework. First, a literature review was performed to gain insight in the topic and to find similarities and differences between different sources of literature. Additionally, some other microscopic simulation studies are used as a reference for the parameters input to describe (C)ACC driving behavior. Subsequently, microscopic traffic simulations with (C)ACC scenarios were performed to gain insight in the effects of these systems on traffic flow. Then, it was checked whether it is possible to represent the microscopic simulation results with mesoscopic simulation, which is significantly faster, but simplified. Subsequently, the results were analyzed, compared and assessed, after which conclusions were drawn and recommendations were given.

Simulation program and research network

The traffic simulation program Aimsun was used for simulating the effects of (C)ACC on realistic traffic situations on the highway. Both the micro- and mesoscopic simulator of Aimsun were used in this study. The microscopic behavioral models use certain simulation steps at which all data of a vehicle within the network is calculated. The longitudinal car-following behavior is described by a development of the Gipps car-following model (Gipps, 1981, 1986b). The mesoscopic simulator only calculates the points in time at which a vehicle enters or leaves a road section and could be considered as a simplification of the microscopic simulation model.

In order to assess the effects of (C)ACC on traffic flow in realistic traffic situations, a realistic traffic network was used as simulation network. The simulation network consists of the A15, at the Southern part of the ring Rotterdam, containing the junctions Ridderkerk, Vaanplein and Benelux, where congestion is found at a daily basis. Typical congestion patterns from Google (2016) and detector data from 2014 and

2016 (National Data Warehouse for traffic information, 2014, 2016) were used to calibrate the network and make the reference scenario represent a traffic situation similar to the actual traffic situations found. For microscopic calibration, the reaction time of the car and truck user class was set to 0.8 seconds. For mesoscopic calibration, the mesoscopic reaction times of the car class was set to 1.2 seconds, which is in line with the rule of thumb ($R_{meso} = 1.5 * R_{micro}$) to convert microscopic reaction time into mesoscopic reaction time. For the truck user class, mesoscopic reaction time was set to 1.6 seconds, to compensate for differences in acceleration and deceleration rates. The microscopic simulation step was set to 0.2 seconds. These user classes have no defined headway settings, because the headways applied by a manual driver differs with respect to differences in (expected) acceleration and deceleration parameters and actual travel speeds. The calibrated congestion patterns of microscopic and mesoscopic simulation showed sufficiently realistic congestion patterns. However, one of the congestion fronts could not be shown in mesoscopic simulation as a result of the defined parameter boundaries and simplifications to allow for mesoscopic modelling.

Modelling (C)ACC driving behavior and simulation scenarios

In this research, the driving behavior of all user classes was described by the empirical car-following model of Gipps (Gipps, 1981, 1986b), which was constructed to model human driving behavior. This car-following model is a safe distance model that ensures that the car-following behavior in simulation is always collision-free. In order to model (C)ACC driving behavior, the available parameters in the Gipps car-following model were manipulated in such a way that it represents (C)ACC driving behavior.

Since vehicles driving with (C)ACC systems activated show a different driving behavior to those of human drivers, it is important to model the driving behavior as a result of these systems realistically. First, these (C)ACC systems will apply the set speed if there is no constraint with respect to the speed of a leading vehicle. If the gap becomes too small according to the fixed gap settings, the systems will apply lower speeds than the desired speed and follow the leading vehicle at approximately the same speed. Additionally, Gorter (2015) indicated that ACC users apply lane changes less frequently and tend to stay in the same lane, either right or left. The same research also indicated that ACC users are more aware of the speed limits and apply slightly lower speeds than human drivers. In order to model these features, minimum desired time headways were set to model a minimum following distance of (C)ACC systems. The speed acceptance parameter that describes the maximum desired speed with respect to the speed limit was set lower than those of manual drivers to compensate for the effect of the awareness of the speed limits. Additionally, most literature studies reported that the accelerations and decelerations applied by (C)ACC vehicles are often smaller than the acceleration and decelerations human car drivers apply. Therefore, the mean maximum acceleration, maximum deceleration and normal deceleration were slightly decreased for all (C)ACC types. The (C)ACC systems modelled must work at full speed range, because in this research, it is assumed that these systems were always activated during driving. A further description of the microscopic parameter settings to describe (C)ACC driving behavior is provided in *Table 1* below, after discussing the simulation scenarios used in this research.

The simulation scenarios consist of two main components. Both the (C)ACC types and the market penetration rates were differentiated. The market penetration rates were differed from 0% to 50% of all cars (note: not trucks) with steps of 10%. With respect to the (C)ACC vehicles types, some parameters were differed to represent the driving behavior. The (C)ACC types considered in this study are subdivided in ACC, newer ACC, improved ACC and CACC. The term ACC is used to describe vehicles with ACC systems that are currently found on the road. Many of these ACC systems have a relatively small reaction time for longitudinal car-following behavior, although there still is some sensor delay. However, most of the current ACC systems are not able to detect (merging) vehicles on adjacent lanes and therefore respond very slowly to merging vehicles. To compensate for this effect, the reaction time was set at the same value as for human car drivers, while the mean headway was set to 1.6 seconds. The newer ACC vehicles are

able to detect vehicles on adjacent lanes and have decreased reaction times of 0.4 seconds. The improved ACC vehicle type is considered to be a further advancement of the ACC technology, which also uses smaller following distances. For the CACC vehicles, the reaction times and following distances are reduced even further, under the assumption that all vehicles are able to communicate with the CACC vehicles. *Table 1* provides an overview of the vehicle types included in simulation. For human car drivers, no fixed mean time headways were set, but test simulations showed that the headway applied by two equal human car drivers is approximately 1.0 second in unrestricted driving situations on the highway. The simulation step in all scenarios was set to 0.2 seconds, which allows for comparisons between all the simulated scenarios.

Table 1 - Overview of (C)ACC vehicle types and main microscopic parameter settings

	Reaction time [s]	Mean time headway [s]	Mean maximum acceleration [m/s ²]	Mean normal deceleration [m/s ²]	Mean maximum deceleration [m/s ²]
Car	0.8	- (\approx 1.0)	2.8	-3.5	-7
ACC	0.8	1.6	2.5	-2.5	-6
Newer ACC	0.4	1.6	2.5	-2.5	-6
Improved ACC	0.4	1.2	2.5	-2.5	-6
CACC	0.2	0.8	2.5	-2.5	-6

Microscopic simulation results

Average speeds over the network decrease for increasing market penetration rates of ACC. Average densities and delay time over the network increase for increases in ACC equipage, which indicates that these vehicle types have a negative effect on traffic flow. For the 40% and 50% ACC scenarios, a significant deterioration in traffic flow performance was found, which seems that the capacity limits at several local bottlenecks has been reached at these market penetration rates. In general, the introduction of ACC results in deteriorations in traffic flow. Additionally, the total number of lane changes decreases for increasing market penetration rates of ACC.

With respect to newer ACC, a very small deterioration is found at early moments of simulation as a result of increasing percentages of newer ACC, which can be explained by the lower speed acceptance parameters for the simulated (C)ACC systems in general. However, at some point in time, a small improvement in average speed can be gained with respect to the reference scenario without any ACC vehicles. This increase can already be gained at 10% market penetration rates of newer ACC, where congestion is significantly reduced on some local bottleneck locations. Further increases in market penetration lead to small changes in average speed. Additionally, densities increase for increasing percentages of newer ACC at the early evening peak, because the speed acceptance of these vehicles is lower, resulting in slightly larger travel times. However, after 17:30 hours approximately, when the congestion is starting to resolve again, the average densities decrease for increasing percentages of newer ACC. The average delay time decreases as a result of the introduction of newer ACC. A 10% market penetration rate significantly reduces delay time in comparison with the reference scenario, while relatively small further gains can be found until 30%. Between 30% and 50% newer ACC penetration, substantial improvements are found again, as a result of significant improvements in traffic situations at local bottlenecks in the network.

For the improved version of ACC, the results are very similar to the results for newer ACC. The small differences are that some effects are found at earlier moments in time or for lower market penetration rates, indicating small further improvements in comparison with newer ACC systems.

When looking at simulation results of the CACC scenarios, it was found that the improvements were most significant for these vehicle types. Average speeds increase and densities decrease for increasing market penetration rates of CACC from the start of congestion until the end of simulation. The delay time is

seriously reduced for all increasing percentages of CACC, although the improvements are smaller from 30% CACC and higher, in comparison with 10% and 20% equipment rates of CACC, indicating that most congestion on local bottlenecks is already solved for penetration rates of 30%, under the assumption that all vehicles are able to communicate with the CACC vehicles. The improvements between the 40% and 50% CACC scenarios are very small, which indicates that it is probable that no further gains can be achieved at high penetration rates. However, it is very important to understand that the results will be less optimistic when communication capabilities of individual vehicles are taken into account.

With respect to bottlenecks where extreme braking rates are applied, all (C)ACC vehicle types were found to have a positive effect. This effect could be explained by the lower deceleration parameters and reduced reaction times, which means that the ACC and CACC vehicles have a dampening effect on the severe braking rates applied. This leads to a stabilization of traffic and decrease of congestion.

When a capacity bottleneck, such as a lane drop, is considered, it was found that ACC and newer ACC systems show decreases in traffic flow performance. This could be explained by the fact that the potential achievable road capacity reduces as a result of the larger following distances applied by ACC systems. Therefore, the theoretical capacity reduces, resulting in an increase in congestion at capacity bottlenecks. This effect was not found for the improved ACC and CACC vehicles, which indicates that these vehicles are able to apply headways that are equal or even smaller than the headways manual car drivers generally apply, resulting in equal or positive effects.

When considering on-ramps as potential bottlenecks, ACC and newer ACC showed negative effects as a result of relatively large desired headways. For improved ACC, no differences with the reference situation was found, which indicates that the mean time headway should at least be as small as 1.2 seconds to prevent increases in congestion near on-ramps, as a result of increasing market penetration rates of ACC. With respect to CACC vehicles, positive effects were found, which are caused by the decrease in severity and consequences of braking actions as a result of merging vehicles, indicating a dampening and stabilizing effect of CACC systems.

With respect to weaving sections, the effects of ACC are generally negative as a result of larger following distances of ACC vehicles, which results in decreases in potential capacity. For all other (C)ACC types, both positive and negative effects are found on weaving sections. It seems that this effect is mainly due to the lay-out and characteristics of the respective weaving sections considered. At weaving sections of limited length or weaving sections with connections with limited capacity, the effects of introducing (C)ACC are generally negative. However, for normal weaving sections that do not suffer from connections with limited capacity or very limited weaving section length, the effects of increasing the market penetration rates of (C)ACC are generally positive.

Additionally, a homogenizing effect in terms of speed, density and flow differences between lanes was found for increasing market penetration rates (C)ACC on road sections at capacity. This indicates that (C)ACC systems are able to homogenize traffic on sections at capacity or in congestion, which is a positive effect. However, it is important to note that this effect was only found on road sections at capacity.

Furthermore, the average amount of lane changes per vehicle type was tested on six characteristics road sections, where it was found that ACC vehicles indeed apply less lane changes than human car drivers. However, for newer ACC, improved ACC and CACC, the average amount of lane changes was generally higher than human car drivers, which should not be the case according to Gorter (2015). However, this effect could be explained by the reductions in reaction time, which ensures that the minimum acceptable gaps in the gap acceptance model reduce. Therefore, a reduction in reaction time directly leads to an increase in the average amount of lane changes found in simulation.

Although microscopic simulations provided credible and reasonable results to assess the effects of ACC and CACC on traffic flow, the microscopic simulator is not fully able to simulate all specifications and features of (C)ACC. Firstly, the simulator does not always apply the defined minimum desired time headway, because it is sometimes overruled by the V_b component of the car-following model, which results in unrealistic driving behavior. This is one of the consequences of applying a safe distance car-following model. Additionally, it is currently impossible to model activation and deactivation of these (C)ACC systems. Also, it should be able to influence lane-changing behavior in an additional way, to model the (C)ACC users that tend to change lanes less frequently. Currently, the reaction time applies for both longitudinal and lateral driving behavior, while current ACC systems react fast to vehicles in longitudinal direction, but slower or not at all to vehicles in lateral direction. Another effect that cannot be captured in microscopic simulations in Aimsun yet is that CACC vehicles can use two types of driving behavior, because these systems would function as an ACC if the leading vehicle has no communication abilities and as CACC if the leading vehicle is able to communicate. Since the assumption that all vehicles have the capability to communicate with CACC vehicles was made in this research, microscopic simulation results of CACC scenarios are more positive than in studies where communication abilities between vehicles are taken into account as a (variable) vehicle characteristic.

Mesoscopic simulation results

In the exploration on whether it is possible to obtain similar results as found in microscopic simulation by using mesoscopic simulation, it was found that the general rule of thumb to translate microscopic reaction times into mesoscopic reaction times ($R_{meso} = 1.5 * R_{micro}$) did not provide satisfactory results when fixed headway settings were used in microscopic simulation. Actually, the multiplication factors that provided the best fit between microscopic and mesoscopic simulation results were different for every (C)ACC user class defined in this research. The microscopic reaction time and mean time headway parameter seem to have the most significant influence on the multiplication factor needed to translate microscopic reaction times into mesoscopic reaction times. Generally, it seems that the more restricting the (microscopic) time headway parameters are with respect to the microscopic reaction time settings, the higher the multiplication factor should be. Also, changes in acceleration and deceleration parameter settings seem to have an effect on the multiplication factor. However, clear relations between changes in microscopic parameter settings and mesoscopic reaction times when using fixed headways were not found. Therefore, mesoscopic simulation results should be interpreted with care and further research is required on the relations between microscopic and mesoscopic parameter settings.

In general, mesoscopic simulations could be used to obtain relatively similar results as found in microscopic simulation. However, it is very important to be aware of the differences in simulation results that can be found as a result of the simplifications to allow mesoscopic modelling. Generally, traffic flow patterns of microscopic and mesoscopic simulations seem to be relatively similar. However, microscopic simulations are more accurate in describing the severity of traffic flow effects caused by increasing penetration rates of (C)ACC. Furthermore, the effects of changes in market penetration rates of (C)ACC vehicle types on traffic flow characteristics are smaller and less clear when using mesoscopic simulations. Subsequently, the total amount of lane changes found in mesoscopic simulation was significantly lower than in microscopic simulation as a result of the network lay-out and simplifications to allow mesoscopic simulation. However, it is expected that differences in the total number of lane changes could be significantly reduced by selecting the 'penalize slow lanes' and 'penalize shared lanes' options, which were not selected in performing this research. Also, the total number of lane changes resulting from mesoscopic modelling increase when section lengths reduce, because the mesoscopic simulator only takes into account the moment and location (i.e. lane) at which a vehicle enters and leaves the road sections. Additionally, adding some spread over mesoscopic reaction times might also increase the number of lane changes found in mesoscopic simulation. The current network lay-out and mesoscopic

simulation parameter settings are unsuitable to evaluate effects of (C)ACC on lane-changing using mesoscopic simulation. Therefore, it could be concluded that mesoscopic simulations could be used as indications on the effects of (C)ACC on average speed, density and delay time, but differences between different penetration rates found in mesoscopic simulation are not as clear as in microscopic simulation. Accordingly, for detailed analyses of traffic flow effects of different market penetration rates of (C)ACC it is advised to use microscopic simulations.

Recommendations

Current ACC systems need to be improved in order to have a positive effect on traffic flow. In general, the reaction time and time headway settings of these systems should minimally be at certain threshold values, before the effects on traffic flow could be considered positive. Therefore, the maximum reaction time of these systems should be as low as 0.4 seconds and the maximum time headway should be decreased to 1.6 seconds and the mean time headway to approximately 1.2 seconds. Additionally, it is very important that ACC systems are able to detect vehicles on adjacent lanes and merging vehicles, in order to prevent severe braking actions to adjust to the desired time headway. Additionally, it is important that the ACC and CACC systems are able to work at full speed range.

In this research, the assumption was made that all vehicles were able to send speed information to CACC equipped vehicles, which is currently not possible yet. Therefore, it is advised that when the market penetration rates of CACC systems increase, all manually driven and ACC vehicles should be equipped with vehicle-awareness devices that can transmit speed and location information to CACC systems. This could be achieved by installing a DSRC radio that frequently broadcasts a message with speed and location data, which provides the advantage that vehicles equipped with CACC are always able to efficiently make use of the CACC system (Shladover, Su, & Lu, 2012).

When looking at average traffic flow conditions on the network, the following recommendations can be made:

- The market penetration rate of ACC systems with mean time headways near 1.6 seconds and a reaction time of 0.8 seconds, that are not able to detect vehicles on adjacent lanes should not be increased, because this will result in negative effects on traffic flow and an increase in delay time;
- When ACC vehicles are able to detect vehicles on adjacent lanes and reaction times decrease to 0.4 seconds and the mean time headway is still 1.6 seconds, the effects of ACC on traffic flow could be either positive or negative, depending on the bottleneck types, traffic demand and time of day. Therefore, it might be useful to start promoting ACC systems if the ACC systems have these specifications. However, further decreasing the mean time headway would provide better results;
- If the following distances are decreased towards mean time headways of 1.2 seconds, positive effects on traffic flow are predominantly found. Therefore, it can be advised to heavily promote the purchase and use of ACC systems, that have these system specifications, because a significant positive effect on traffic flow can be achieved;
- A positive effect on traffic flow is expected as results of the introduction of CACC systems. Therefore, the development of these systems is very important and should be supported. However, the improvements on traffic flow will be more significant if all vehicles are able to communicate with the CACC vehicles, which could be achieved by installing vehicles awareness devices, such as a DSRC radio in non-CACC vehicles (Shladover et al., 2012).

Additionally, at road sections where extreme or severe braking actions are a source of congestion, it is always advisable to use ACC and CACC systems, because these vehicles apply lower deceleration rates and have a stabilizing effect on traffic flow, leading to decreases of congestion. It was found that all types of (C)ACC systems had positive effects, because these systems apply some smoother and less severe braking actions.

At road sections with a reduction in the number of lanes that could become a capacity bottleneck, it is not advisable to keep ACC systems activated, because this leads to a capacity decrease as a result of relatively large headway settings. Therefore, it is advised to deactivate ACC systems near road sections with a lane drop. For very advanced ACC and CACC systems, no significant effects were found.

Similarly, it is advisable to deactivate (simple) ACC systems near on-ramps, because these systems have negative effects on traffic flow as a result of braking actions to adjust the time headway with merging vehicles. However, a positive effect was found with respect to very advanced ACC and CACC systems, because these systems stabilize traffic disturbances as a result of lane changes. Therefore, these systems should be kept active near on-ramps.

Simple ACC systems should be deactivated at weaving sections, because these systems generally have a negative effect on traffic flow at weaving sections, as a result of relative large following distances applied by ACC systems. At weaving sections with limited lengths or connections with limited capacity, the effects of (C)ACC are generally negative, which means that it is advised to deactivate these systems at these types of weaving sections. However, for weaving sections that are not restricted by limited lengths of the weaving section or limited capacities of connections, the effects of increasing penetration rates of sophisticated (C)ACC systems are generally positive. Therefore, it is advised to activate more sophisticated types of (C)ACC at weaving sections where there are no significant restrictions of the length of the weaving section or capacity of connections. At this type of weaving sections, disturbances are mainly caused by lane-changing behavior. Additionally, for road sections at capacity or in congestion, it is advisable to activate (C)ACC, because these systems have a homogenizing effect on traffic and seem to increase traffic safety.

To model (C)ACC systems more accurately in the current microscopic simulation in Aimsun, the following recommendations are presented:

- Split reaction times in separate reaction times for longitudinal and lateral driving behavior;
- Add a lane-changing willingness (or laziness) parameter to model the (un)desire to change lanes or overtake, depending on the vehicle class;
- Include the possibility of activation and deactivation of (C)ACC systems (at certain road sections);
- Include the possibility of applying a constant time gap policy for intelligent vehicles, which is not restricted by the V_b component of the current car-following model;
- In order to improve the accuracy of modelling (C)ACC even more, improved car-following models or platforms should be considered to enable the possibility to look more vehicles ahead and model interaction between vehicles.

Furthermore, the following recommendations for mesoscopic modelling of intelligent vehicles are made:

- Conduct further research to gain more insight in the relations between microscopic parameter settings and mesoscopic reaction times, especially when using fixed headway settings;
- Model lane changes more accurately by reducing the lengths of road sections and selecting the 'penalize slow lanes' and 'penalize shared lanes' options.

The following recommendations on simulation output and indicators to describe the effects of increasing market penetration rates of (C)ACC are presented:

- Include an indicator that provides the average number of lane changes per vehicle type over the whole network in order to gain insight in the lane-changing behavior of specific vehicle types;
- Add indicators to assess effects on traffic safety.

Managementsamenvatting

Achtergrond

Adaptive Cruise Control (ACC) is een geavanceerde versie van cruise control welke in staat is om automatisch een bepaalde ingestelde snelheid vast te houden en de snelheid van een directe voorganger te detecteren en snelheid aan te passen op basis van de locatie en snelheid van deze voorganger. Cooperative Adaptive Cruise Control (CACC) is een verdere ontwikkeling van ACC, waar communicatie tussen meerdere voertuigen mogelijk is. Dit stelt CACC voertuigen in staat om snelheidsinformatie te sturen en ontvangen, wat vloeiendere en snellere reacties oplevert dan ACC.

Deze systemen nemen een deel van de rijtaken over, wat betekent dat het rijgedrag van bestuurders en voertuigen op de weg beïnvloed wordt. Dit kan een significant effect hebben op de verkeersdoorstroming. Dit onderzoek is uitgevoerd om de effecten van ACC en CACC op realistische verkeerssituaties met meerdere knelpunten te bepalen.

Een brede variëteit aan literatuur die effecten van (C)ACC op verkeersstromen of prestaties bestuderen, is beschikbaar. Echter is het onderwerp nog niet goed begrepen, omdat resultaten verschillen van significante toenames tot significante verminderingen (Milanés & Shladover, 2014). Daarnaast ontbreken gedetailleerde studies naar de effecten van (C)ACC op relatief grootschalige netwerken, omdat de meeste microscopische studies gericht zijn op een enkel knelpunt of karakteristieke verkeerssituatie. Daarom kan deze studie van toegevoegde waarde zijn voor dit onderzoeksveld en extra inzicht geven in dit onderwerp.

Onderzoeksmethode

Het hoofddoel van deze thesis is om *inzicht te krijgen in de effecten van (verschillende penetratiegraden van) ACC en CACC op verkeersprestatie in realistische verkeerssituaties op de snelweg, zoals situaties met meerdere knelpunten en op weefvakken*. Om dit doel te bereiken, is de volgende onderzoeksvraag opgesteld: *‘Wat zijn de effecten van (Cooperative) Adaptive Cruise Control op verkeersstromen in realistische verkeerssituaties met meerdere knelpunten?’*

De onderzoeksvraag wordt beantwoord met behulp van een relatief simpele onderzoeksopzet. Eerst is een literatuuronderzoek uitgevoerd om inzicht in het onderwerp te krijgen en overeenkomsten en verschillen te vinden tussen verschillende literatuur bronnen. Ook zijn sommige microscopische simulatie studies gebruikt als referentie voor de parameters om (C)ACC rijgedrag te beschrijven. Vervolgens zijn microscopische verkeerssimulaties met (C)ACC scenario's uitgevoerd om inzicht te krijgen in effecten van (C)ACC op verkeersstroom. Ook is de mogelijkheid onderzocht om microscopische simulatieresultaten na te bootsen met mesoscopische simulatie, wat veel sneller is, maar versimpeld. Daarna zijn de resultaten geanalyseerd, vergeleken en beoordeeld, waarna conclusies zijn getrokken en aanbevelingen gegeven.

Simulatieprogramma en onderzoeksnetwerk

Het verkeerssimulatieprogramma Aimsun werd gebruikt voor het simuleren van effecten van (C)ACC in realistische verkeerssituaties op de snelweg. Zowel de micro- als mesoscopische simulator van Aimsun is gebruikt. De microscopische gedragsmodellen gebruiken bepaalde simulatiestappen waarop alle data van een voertuig in het netwerk worden berekend. Het longitudinale voertuig-volg model is een ontwikkeling van het Gipps voertuig-volg model (Gipps, 1981, 1986b). De mesoscopische simulator berekent enkel de tijdstippen waarop een voertuig de wegsectie binnentreedt of verlaat en kan gezien worden als simplificatie van het microscopische simulatiemodel.

Om de effecten van (C)ACC op verkeersstromen in realistische verkeerssituaties te beoordelen is gebruik gemaakt van een realistisch netwerk. Het simulatie netwerk bestaat uit de A15, aan de zuidzijde van de Ring Rotterdam met knooppunten Ridderkerk, Vaanplein en Benelux, waar file voorkomt op dagelijkse

basis. Typische filebeelden van Google (2016) en detector data van 2014 en 2016 (National Data Warehouse for traffic information, 2014, 2016) zijn gebruikt om het netwerk en het referentiescenario te kalibreren zodat het een realistische verkeerssituatie nabootst. Voor microscopische kalibratie, is de reactietijd voor trucks en auto's op 0.8 seconden gezet. In mesoscopische kalibratie is de mesoscopische reactietijd van de auto gezet op 1.2 seconden, wat overeenkomt met de vuistregel om microscopische reactietijden om te rekenen naar mesoscopische reactietijden ($R_{meso} = 1.5 * R_{micro}$). Voor trucks is de mesoscopische reactietijd op 1.6 seconden gezet om te compenseren voor verschillen in versnelling en remcapaciteiten. De microscopische simulatiestap is gezet op 0.2 seconden. De auto en truck hebben geen vaste volgafstanden gedefinieerd, omdat de volgafstanden toegepast door handmatige bestuurders verschillen met betrekking tot verwachte versnellings- en vertragingparameters en actuele snelheden. De gekalibreerde filebeelden in micro- en mesoscopische simulatie toonden voldoende realistische patronen. Echter kon een van de file fronten niet getoond worden in mesoscopische simulaties als gevolg van de gedefinieerde grenswaarden en de versimpelingen om mesoscopisch modelleren mogelijk te maken.

Modelleren van (C)ACC rijgedrag en simulatie scenario's

In dit onderzoek werd het rijgedrag van alle voertuigklassen beschreven door het empirische voertuig-volg model van Gipps (Gipps, 1981, 1986b), ontworpen om menselijk rijgedrag te modelleren. Dit voertuig-volg model is een zogenaamd veilige afstand model dat verzekert dat het volggedrag van voertuigen in de simulatie botsingvrij is. Om (C)ACC rijgedrag te modelleren zijn de beschikbare parameters in het Gipps voertuig-volg model op zo een manier gemanipuleerd dat (C)ACC rijgedrag gerepresenteerd wordt.

Omdat voertuigen met geactiveerde (C)ACC systemen ander rijgedrag tonen dan menselijke bestuurders is het belangrijk dit rijgedrag realistisch te modelleren. Ten eerste passen deze (C)ACC systemen een ingestelde snelheid toe als er geen beperking is met betrekking tot de snelheid van een voorganger. Als de volgafstand te klein wordt volgens de ingestelde volgafstand, zal het systeem lagere snelheden dan de ingestelde snelheid hanteren en de voorganger volgen met ongeveer dezelfde snelheid. Daarnaast gaf Gorter (2015) aan dat ACC gebruikers minder rijstrookwisselingen toepassen en geneigd zijn in dezelfde rijstrook, links of rechts, te blijven rijden. Hetzelfde onderzoek gaf aan dat ACC gebruikers meer bewust zijn van snelheidslimieten en iets lagere snelheden toepassen dan bestuurders. Om deze eigenschappen te modelleren zijn minimale (bruto) volgtijden ingesteld, om minimale volgafstand van (C)ACC systemen in te stellen. De snelheidsacceptatie parameter, die maximale snelheid met betrekking tot snelheidslimieten beschrijft, was lager gezet dan voor handmatige bestuurders, om te compenseren voor het meer bewust zijn van snelheidslimieten. Daarnaast rapporteerden de meeste studies dat vertragingen en versnellingen toegepast door (C)ACC voertuigen meestal lager zijn dan deze van menselijke bestuurders. Daarom zijn de maximale acceleratie, maximale remvertraging en normale remvertraging licht gereduceerd voor alle (C)ACC types. De gemodelleerde (C)ACC systemen moeten werken binnen het volledige snelheidsbereik, omdat in dit onderzoek is aangenomen dat de systemen altijd actief zijn tijdens het rijden. Een verdere beschrijving van de microscopische parameter instellingen om (C)ACC rijgedrag te simuleren is gegeven in *Table 2*, nadat de simulatie scenario's die in dit onderzoek gebruikt worden, besproken zijn.

De simulatie scenario's bestaan uit twee componenten. Zowel de (C)ACC types als de penetratiegraden worden gedifferentieerd. De penetratiegraden verschillen van 0% tot 50% van alle auto's (dus niet trucks) met stappen van 10%. Met betrekking tot (C)ACC voertuig types zijn sommige parameters veranderd om het rijgedrag na te bootsen. De gebruikte (C)ACC types in dit onderzoek zijn onderverdeeld in ACC, nieuwere ACC, verbeterde ACC en CACC. De term ACC is gebruikt om voertuigen met ACC systemen van dit moment te modelleren. Veel van deze systemen hebben een relatief korte reactietijd voor longitudinaal volggedrag, hoewel er wat sensor vertraging is. De meeste huidige ACC systemen niet in staat om voertuigen op naastgelegen rijstroken te detecteren. Dit betekent dat er traag gereageerd wordt op ritsende voertuigen. Om dit effect te compenseren, is de reactietijd gelijk gezet aan die van menselijke bestuurders met een (bruto) volgtijd van 1.6 seconden. De nieuwere ACC voertuigen kunnen voertuigen

op naastgelegen rijstroken detecteren en hebben verlaagde reactietijden van 0.4 seconden. De verbeterde ACC types worden gezien als verdere ontwikkeling van ACC technologie, waarbij kortere volgafstanden gebruikt worden. Voor CACC voertuigen zijn de reactietijden en volgtijden nog lager, onder de aanname dat alle voertuigen kunnen communiceren met CACC voertuigen. *Table 2* geeft een overzicht van de voertuigtypen inbegrepen in de simulaties. Voor menselijke bestuurders zijn geen vaste volgtijden gezet, maar test simulaties toonden aan dat (bruto) volgtijden van ongeveer 1.0 seconde werden toegepast door twee gelijke bestuurders in onbeperkte omstandigheden op de snelweg. In alle scenario's zijn de simulatiestappen op 0.2 seconden gezet, wat het mogelijk maakt om scenario's te vergelijken.

Table 2 - Overzicht van (C)ACC voertuigtypen en belangrijkste microscopische parameter instellingen

	Reactietijd [s]	Gemiddelde volgtijd [s]	Gemiddelde maximale versnelling [m/s ²]	Gemiddelde normale vertraging [m/s ²]	Gemiddelde maximale vertraging [m/s ²]
Auto	0.8	- (\approx 1.0)	2.8	-3.5	-7
ACC	0.8	1.6	2.5	-2.5	-6
Nieuwere ACC	0.4	1.6	2.5	-2.5	-6
Verbeterde ACC	0.4	1.2	2.5	-2.5	-6
CACC	0.2	0.8	2.5	-2.5	-6

Microscopische simulatieresultaten

Gemiddelde snelheden over het netwerk nemen af voor toenemende penetratiegraden van ACC. Ook nemen gemiddelde dichtheden en verliestijd over het netwerk toe voor toenemende penetratiegraden van ACC, wat negatieve effecten op verkeersstroming aangeeft. Voor de 40% en 50% ACC scenario's werden significante verslechtingen in vervoersprestatie gevonden, wat lijkt dat de capaciteitsgrenzen op lokale knelpunten bereikt zijn bij deze penetratiegraden. Algemeen gezien resulteert de introductie van ACC in verslechtingen in verkeersstromen. Daarnaast neemt het totale aantal rijstrookwisselingen af voor toenemende penetratiegraden van ACC.

Met betrekking tot nieuwere ACC is een kleine verslechting gevonden op vroege momenten van de simulatie als gevolg van toenemende penetratiegraden, wat uitgelegd kan worden door de lagere snelheidsacceptatie parameter voor (C)ACC systemen. Op een bepaald moment in tijd wordt een kleine verbetering in gemiddelde snelheid verkregen in verhouding met het referentiescenario zonder ACC voertuigen. Deze toename kan al behaald worden met een 10% penetratiegraad van nieuwere ACC, waar de file significant is afgenomen op lokale knelpunten. Verdere toenames in penetratiegraad leiden tot kleine veranderingen in gemiddelde snelheid. Daarnaast nemen dichtheden toe in de vroege avondspits als de penetratiegraden van nieuwere ACC toenemen, omdat de snelheidsacceptatie lager is wat resulteert in langere reistijden. Na 17:30, als de file begint op te lossen, nemen gemiddelde dichtheden af voor toenemende penetratiegraden nieuwere ACC. Gemiddelde verliestijd neemt af als gevolg van het introduceren van nieuwere ACC. Een 10% penetratie verlaagt de vertragingstijd substantieel in vergelijking met het referentiescenario, terwijl kleine vooruitgangen geboekt worden tot 30% penetratie. Tussen 30% en 50% penetratie nieuwere ACC worden weer substantiële verbeteringen gevonden als gevolg van verbeteringen op lokale knelpunten in het netwerk.

Voor de verbeterde versie van ACC zijn de resultaten redelijk gelijk aan de resultaten van nieuwere ACC. De kleine verschillen zijn dat sommige effecten eerder of op lagere penetratiegraden behaald worden, wat kleine verdere verbeteringen aangeeft in vergelijking met nieuwere ACC systemen.

Wanneer de simulatieresultaten van CACC scenario's geanalyseerd werden, werd gevonden dat de verbeteringen het grootst waren bij deze voertuigtypen. Gemiddelde snelheden nemen toe en dichtheden nemen af bij toenemende penetratiegraden van CACC vanaf het begin van de file tot het eind van de simulatie. De vertragingstijd is significant kleiner voor alle toenemende percentages CACC, hoewel de verbeteringen kleiner worden vanaf 30% en hoger in vergelijking met 10% en 20% CACC scenario's.

Dit toont aan dat de meeste congestie op lokale knelpunten al is opgelost bij penetratiegraden van 30%, onder de aanname dat alle voertuigen kunnen communiceren met ACC voertuigen. De verbeteringen tussen de 40% en 50% CACC scenario's zijn erg klein, wat aangeeft dat er waarschijnlijk geen verdere verbeteringen meer behaald worden voor hoge penetratiegraden. Echter is het erg belangrijk om te realiseren dat resultaten minder optimistisch zijn als communicatiemogelijkheden van individuele voertuigen in acht genomen worden.

Op knelpunten waar extreme remvertragingen toegepast worden, hebben alle (C)ACC voertuigtypen een positief effect. Dit effect komt door de lagere vertragingparameters en verlaagde reactietijden, wat betekent dat ACC en CACC voertuigen een dempend effect heeft op de hevige remvertragingen die worden toegepast. Dit leidt tot een stabilisatie van het verkeer en een afname van de congestie.

Als een capaciteitsknelpunt, zoals een rijstrookvermindering werd geanalyseerd, werd gevonden dat ACC en nieuwere ACC systemen een afname in verkeersprestatie teweegbrengt. Dit komt doordat de potentieel haalbare wegcapaciteit afneemt als gevolg van de langere volgafstanden die toegepast worden door ACC systemen. Daardoor neemt de theoretische capaciteit af, wat resulteert in een toename van file op capaciteitsknelpunten. Dit effect werd niet gevonden voor verbeterde ACC en CACC voertuigen, wat aangeeft dat deze voertuigen in staat zijn om kortere of gelijke volgafstanden toe te passen in vergelijking met handmatige bestuurders, die resulteert in gelijke of positieve effecten.

Wanneer snelwegopritten als potentieel knelpunt beschouwd worden, vertonen ACC en nieuwere ACC negatieve effecten als gevolg van relatief grote volgafstanden. Voor verbeterde ACC werden geen verschillen gevonden met het referentiescenario, wat aanduidt dat bruto volgafstanden minstens zo klein als 1.2 seconden moeten zijn om een filetoename, veroorzaakt door toenemende penetratiegraden van ACC, bij snelwegopritten te voorkomen. Met betrekking tot CACC voertuigen werden positieve effecten gevonden die veroorzaakt worden door afnames in de zwaarte en gevolgen van remacties als gevolg van invoegende voertuigen, wat een dempend en stabiliserend effect van CACC systemen aangeeft.

Met betrekking tot weefvakken zijn de effecten van ACC over het algemeen negatief als gevolg van de langere volgafstanden van ACC voertuigen die resulteren in afnamen in potentiële capaciteit. Voor alle andere (C)ACC types zijn zowel positieve als negatieve effecten gevonden. Het lijkt erop dat deze effecten vooral veroorzaakt worden door de lay-out en kenmerken van de beschouwde weefvakken. Op weefvakken van beperkte lengte of weefvakken met verbindingen met een beperkte capaciteit zijn de effecten van (C)ACC over het algemeen negatief. Voor normale weefvakken, die niet beperkt zijn door verbindingen met een beperkte capaciteit of korte lengte van de weefvakken, zijn de effecten van toenemende penetratiegraden van (C)ACC over het algemeen positief.

Daarnaast is gevonden dat het verhogen van de penetratiegraad van (C)ACC een homogeniserend effect heeft op snelheids-, dichtheid- en verkeersstroomverschillen tussen rijstroken op wegen op of nabij maximale capaciteit. Dit toont aan dat (C)ACC systemen verkeer kunnen homogeniseren op wegen nabij maximum capaciteit of in congestie. Dit effect is alleen gevonden voor wegen nabij maximum capaciteit.

Bovendien zijn de gemiddelde aantallen rijstrookwisselingen per voertuigtype onderzocht, waarbij werd gevonden dat ACC gebruikers inderdaad minder rijstrookwisselingen toepassen dan menselijke bestuurders. Echter waren de gemiddelde aantallen rijstrookwisselingen voor gebruikers van nieuwere ACC, verbeterde ACC en CACC gemiddeld genomen hoger dan menselijke bestuurders. Dit zou niet moeten kunnen volgens Gorter (2015). Dit effect kan echter uitgelegd worden door de verlaagde reactietijden, zodat de minimale accepteerbare invoegruimte in het rijstrookwisselmodel afneemt. Daarom leidt een afname in reactietijd tot een toename in het gemiddelde aantal rijstrookwisselingen in simulaties.

Hoewel microscopische simulaties geloofwaardige en acceptabele resultaten opleveren om de effecten van (C)ACC op verkeersstroming te bepalen, is de microscopische simulator niet volledig in staat om alle kenmerken en specificaties van (C)ACC te modelleren. Ten eerste worden minimum volgafstanden niet altijd toegepast door de simulator, omdat deze soms overreden wordt door de V_b component van het voertuig-volg model, die leidt tot onrealistisch rijgedrag. Dit is een van de gevolgen van het toepassen van een veilige afstand voertuig-volg model. Daarnaast is het op dit moment niet mogelijk om het aan- en uitschakelen van deze systemen te modelleren. Ook moet op een aanvullende manier invloed uitgeoefend kunnen worden op rijstrookwisselgedrag, om (C)ACC gebruikers die minder vaak wisselen van rijstrook te modelleren. De huidige reactietijd geldt voor longitudinaal en lateraal rijgedrag, terwijl huidige ACC systemen sneller reageren in longitudinale richting, maar trager of niet op voertuigen in laterale richting. Een ander effect wat nog niet mogelijk is in microscopische simulaties in Aimsun, is dat CACC systemen meerdere soorten rijgedrag toepassen, omdat deze systemen functioneren als ACC als de voorganger niet kan communiceren en als CACC als de voorganger dit wel kan. Omdat in dit onderzoek is aangenomen dat alle voertuigen kunnen communiceren met CACC systemen, zijn de resultaten van CACC scenario's positiever dan in studies waar communicatiemogelijkheden tussen voertuigen wel in acht zijn genomen als variabele voertuigkenmerken.

Mesoscopische simulatieresultaten

In het onderzoek naar de mogelijkheid om gelijke resultaten als gevonden in microscopische simulaties te verkrijgen met mesoscopische simulatie werd gevonden dat de algemene vuistregel om microscopische reactietijden te vertalen naar mesoscopische reactietijden ($R_{meso} = 1.5 * R_{micro}$) geen bevredigende resultaten opleverden wanneer vaste volgafstanden ingesteld werden in microscopische simulaties. De vermenigvuldigingsfactoren die de beste passing tussen microscopische en mesoscopische resultaten opleverde, waren verschillen voor elk type (C)ACC. De microscopische reactietijd en bruto volgtijd parameters lijken de meest significante invloed te hebben op de benodigde vermenigvuldigingsfactor om microscopische reactietijden om te zetten naar mesoscopische reactietijden. Over het algemeen lijkt het dat hoe meer beperkend (microscopische) bruto volgtijden zijn in relatie tot microscopische reactietijden, hoe hoger de vermenigvuldigingsfactor moet zijn. Ook de veranderingen in versnelling en vertraging lijken een invloed te hebben op de vermenigvuldigingsfactor. Echter zijn er nog geen duidelijke verbanden gevonden tussen microscopische parameter instellingen waarbij vaste volgafstanden ingesteld werden en mesoscopische reactietijden in microscopische simulaties. Mesoscopische simulatie resultaten moeten dus zorgvuldig geïnterpreteerd worden. Verder onderzoek naar de verbanden tussen microscopische parameter instellingen waarbij vaste volgtijden gebruikt worden en mesoscopische reactietijden, is nodig.

Mesoscopische simulaties kunnen over het algemeen gebruikt worden om vergelijkbare resultaten te verkrijgen als in microscopische simulatie. Het is echter van belang om bewust te zijn van de verschillen in simulatieresultaten als gevolg van versimpelingen om mesoscopisch modelleren mogelijk te maken. Veelal lijken verkeerspatronen uit microscopische en mesoscopische simulaties op elkaar. Microscopische simulaties zijn echter nauwkeuriger in het beschrijven van de zwaarte van verkeerseffecten die een gevolg zijn van toenemende penetratiegraden van (C)ACC. Bovendien zijn de effecten van verschillende penetratiegraden van (C)ACC op verkeerskenmerken kleiner en onduidelijker wanneer mesoscopische simulaties gebruikt worden. Ook zijn het totaal aantal rijstrookwisselingen gevonden in mesoscopische simulaties veel lager dan in microscopische simulatie, als gevolg van netwerk lay-out en versimpelingen om mesoscopisch simuleren mogelijk te maken. Echter is te verwachten dat de verschillen in het aantal rijstrookwisselingen substantieel gereduceerd kan worden als de 'penalize slow lanes' en 'penalize shared lanes' opties, die niet gebruikt zijn in dit onderzoek, geselecteerd worden. Het aantal rijstrookwisselingen in mesoscopische simulatie zal ook toenemen als sectielengtes afnemen, omdat de mesoscopische simulator alleen de tijd en locatie (rijstrook) dat een voertuig een sectie binnentreedt en verlaat, berekend. Ook zal het toevoegen van spreiding over mesoscopische reactietijden het aantal rijstrookwisselingen

kunnen verhogen. Het huidige netwerk en de mesoscopische parameter instellingen zijn ongeschikt om de effecten van (C)ACC op rijstrookwisselgedrag te evalueren. Mesoscopische simulaties kunnen gebruikt worden als indicatie voor de effecten van (C)ACC op gemiddelde snelheid, dichtheid en vertragingstijd, maar verschillen tussen penetratiegraden zijn in mesoscopische simulaties minder duidelijk dan in microscopische simulaties. Dienovereenkomstig worden microscopische simulaties geadviseerd voor gedetailleerde analyses van verkeerseffecten van toenemende penetratiegraden van (C)ACC.

Aanbevelingen

Huidige ACC systemen moeten verbeterd worden om een positief effect te hebben op verkeersstromen. Algemeen gezien moeten de reactietijd en (bruto) volgtijd instellingen van deze systemen minimaal bepaalde grenswaarden hebben om positieve effecten op te leveren. De maximale reactietijd van deze systemen moet minimaal 0.4 seconden zijn, terwijl de maximale (bruto) volgtijd 1.6 seconden mag zijn met een gemiddelde (bruto) volgtijd ongeveer 1.2 seconden. Daarnaast is het van belang dat deze systemen in staat zijn om voertuigen op naastgelegen rijstroken, invoegende of ritsende voertuigen te detecteren, zodat sterke remacties om de volgfstand aan te passe voorkomen kunnen worden. Ook is het van belang dat ACC en CACC systemen werken over het volledige snelheidsbereik.

In dit onderzoek is de aanname gemaakt dat alle voertuigen in staat waren om snelheidsinformatie te verzenden naar CACC uitgeruste voertuigen, wat op dit moment nog niet mogelijk is. Om deze reden wordt aangeraden om alle handmatig bestuurde voertuigen uit te rusten met apparaten die snelheids- en locatie informatie kunnen verzenden naar CACC systemen als CACC penetratiegraden toenemen. Dit kan door DSRC radio's te installeren, die regelmatig een bericht met snelheid en locatie data uitzenden, wat het voordeel heeft dat alle voertuigen met CACC effectief gebruik kunnen maken van de CACC systemen (Shladover et al., 2012).

Na een analyse van de gemiddelde verkeerscondities op het netwerk in alle gesimuleerde scenario's, worden de volgende aanbevelingen gedaan:

- De penetratiegraad van ACC systemen met (bruto) volgtijden nabij 1.6 seconden en reactietijden van 0.8 seconden, die geen voertuigen op naastgelegen rijstroken detecteren, mag niet verhoogd worden, omdat dit resulteert in negatieve verkeerseffecten en een toename in vertragingstijd;
- Wanneer ACC voertuigen in staat zijn voertuigen op naastgelegen rijstroken te detecteren, reactietijden dalen tot 0.4 seconden en de volgtijd nog 1.6 seconden is, kunnen de effecten van ACC zowel positief als negatief zijn, afhankelijk van knelpunt types, verkeersaanbod en tijdstip. Het kan zinvol zijn om ACC systemen te promoten als deze specificaties bereikt worden. Echter worden betere resultaten verkregen als de (bruto) volgtijd afneemt;
- Als gemiddelde (bruto) volgtijden verlaagd worden tot 1.2 seconden, worden vooral positieve verkeerseffecten gevonden. Zodoende wordt geadviseerd om de aankoop en het gebruik van ACC systemen te promoten als deze specificaties behaald worden, omdat een aanzienlijk positief effect op verkeersstromen behaald kan worden;
- Een positief verkeerseffect wordt verwacht als gevolg van de introductie van CACC systemen. Zodoende is verdere ontwikkeling van deze systemen erg belangrijk en moet deze ondersteund worden. De verbeteringen in verkeersdoorstroming zullen groter zijn als alle voertuigen kunnen communiceren met CACC voertuigen, wat behaald kan worden door het installeren van voertuigbewustzijns apparaten, zoals DSRC-radio's, in niet-ACC voertuigen (Shladover et al., 2012).

Daarnaast wordt geadviseerd om altijd gebruik te maken van (C)ACC systemen op wegsecties waar sterke en extreme remacties een bron van congestie zijn, omdat deze voertuigen lagere remvertragingen toepassen en een stabiliserend effect op verkeer hebben dat resulteert in een afname van congestie. Alle (C)ACC systemen toonden een positief effect omdat deze systemen wat vloeiendere en minder sterke remacties toepassen.

Op wegvakken met rijstrookverminderingen die een capaciteitsknelpunt kunnen worden, is het niet aan te raden om ACC systemen geactiveerd te houden, omdat dit leidt tot afnamen in capaciteit als gevolg van de relatief grote volgstanden. Zodoende wordt geadviseerd ACC systemen te deactiveren op en nabij wegen met rijstrookverminderingen. Voor erg geavanceerde types van ACC en CACC systemen werden geen substantiële effecten gevonden.

Eveneens wordt aanbevolen om (simpele) ACC systemen uit te zetten nabij snelwegopritten, omdat deze systemen hier negatieve verkeerseffecten hebben door remacties om de volgafstand aan te passen op invoegende voertuigen. Voor geavanceerde ACC en CACC systemen werd een positief effect gevonden, omdat deze systemen verstoringen veroorzaakt door rijstrookwisselingen stabiliseren. Zodoende wordt geadviseerd deze systemen ingeschakeld te houden nabij snelwegopritten.

Simpele ACC systemen moeten uitgeschakeld worden op weefvakken, omdat deze systemen over het algemeen een negatief verkeerseffect hebben op weefvakken, als gevolg van relatief grote volgafstanden die toegepast worden door ACC systemen. Op weefvakken met beperkte lengte of verbindingen met beperkte capaciteit zijn de effecten van (C)ACC over het algemeen negatief, waardoor geadviseerd wordt om deze systemen te deactiveren op deze weefvakken. Voor weefvakken die niet beperkt worden door beperkte lengtes of beperkte capaciteit van verbindingen, zijn de verkeerseffecten van toenemende penetratiegraden van geavanceerde (C)ACC systemen overwegend positief. Daardoor wordt geadviseerd om deze meer geavanceerde types van (C)ACC te activeren op weefvakken die niet beperkt worden door de lengte van het weefvak of capaciteit van verbindingen. Op dit type weefvakken worden verstoringen voornamelijk veroorzaakt door rijstrookwisselgedrag. Daarnaast wordt geadviseerd om (C)ACC te activeren op wegvakken nabij of op capaciteitslimieten, omdat deze systemen een homogeniserend effect hebben op verkeer, waardoor de verkeersveiligheid verhoogd lijkt te zijn.

Om (C)ACC systemen nauwkeuriger te modelleren in de huidige microscopische simulatie in Aimsun, worden de volgende aanbevelingen gepresenteerd:

- Splits reactietijden in gescheiden reactietijden voor longitudinaal en lateraal rijgedrag;
- Voeg een rijstrook-wissel bereidwilligheidsparameter toe om de (on)bereidheid om te wisselen van rijstrook of in te halen te modelleren, afhankelijk van het voertuigtype;
- Voeg de mogelijkheid toe (C)ACC systemen te activeren en deactiveren (op bepaalde wegen);
- Voeg de mogelijkheid toe om een constante volgtijd beleid voor intelligente voertuigen te modelleren, die niet beperkt wordt door de V_b component van het huidige voertuig-volg model;
- Om de nauwkeurigheid van het modelleren van (C)ACC verder te vergroten, moeten verbeterde voertuig-volg modellen of platforms overwogen worden zodat het mogelijk is om meer voertuigen vooruit te kijken en communicatie tussen voertuigen te modelleren.

Daarnaast worden de volgende aanbevelingen gedaan met betrekking tot het mesoscopisch modelleren van intelligente voertuigen:

- Voer verder onderzoek uit om meer inzicht te verkrijgen in de verbanden tussen microscopische parameter instellingen en mesoscopische reactietijden, vooral wanneer vaste volginstellingen worden gebruikt;
- Modelleer rijstrookwisselingen nauwkeuriger door de lengte van secties te verkleinen en de opties 'penalize slow lanes' en 'penalize shared lanes' te selecteren.

De volgende aanbevelingen met betrekking tot simulatie uitvoer en indicatoren om de verkeerseffecten van toenemende penetratiegraden te beschrijven, worden gepresenteerd:

- Voeg een indicator toe die het gemiddelde aantal rijstrookwisselingen per voertuigtype over het hele netwerk beschrijft om inzicht te geven in het rijstrookwisselgedrag van specifieke gebruikers;
- Voeg indicatoren toe om effecten op verkeersveiligheid te kunnen beoordelen.

Table of contents

Preface	I
Executive summary	II
Managementsamenvatting	IX
Table of contents	XVI
List of figures	XIX
List of tables.....	XXIV
1 Introduction.....	1
1.1 Context	1
1.2 Research objective & questions	2
1.2.1 Research objective	2
1.2.2 Research questions	3
1.3 Research methodology.....	3
1.3.1 Methods	3
1.3.2 Model choice.....	5
1.3.3 Research framework.....	5
1.4 Literature review	6
1.4.1 Purpose of ACC and CACC	6
1.4.2 Expected effect on traffic performance.....	7
1.4.3 Parameter specifications	13
1.5 Structure of the report.....	15
2 Traffic modelling in Aimsun	17
2.1 General introduction to Aimsun	17
2.2 Microscopic and mesoscopic simulation	17
2.3 Model parameters.....	18
2.3.1 Global modelling parameters.....	19
2.3.2 Local section parameters	19
2.3.3 Vehicle attributes	20
2.4 Microscopic behavioral models	21
2.4.1 Car-following model	22
2.4.2 Lane-changing model	23
2.5 Mesoscopic behavioral models	26
2.5.1 Car-following model	26
2.5.2 Lane-changing model	27
3 Calibration and validation.....	29
3.1 Network configuration	29
3.2 Preparatory work	30
3.3 Calibration process	31

3.3.1	Delivered mesoscopic model.....	33
3.3.2	Calibration of congestion patterns	33
3.3.3	OD matrix check & calibration	34
3.3.4	Fine-tuning of congestion patterns	37
3.3.5	Calibrated mesoscopic model	38
3.3.6	Microscopic calibration	44
3.3.7	Calibrated microscopic model	50
3.3.8	Validation check.....	55
4	Verification of ACC driving behavior	61
4.1	Modelling speed choice of ACC users	61
4.2	Modelling headway choices of ACC users	62
4.3	Modelling lane-changing behavior of ACC users	62
4.4	Modelling car-following behavior of ACC vehicles	63
4.5	Verification of ACC following behavior	64
4.5.1	Overview of parameter settings for ACC.....	64
4.5.2	Following scenario	66
4.5.3	Stop and go scenario.....	67
4.5.4	Emergency braking scenario	69
4.5.5	Cut-in scenario.....	70
4.5.6	Sensitivity analysis.....	72
5	Microscopic simulation scenarios and indicators	75
5.1	Scenarios.....	75
5.1.1	Types of (C)ACC systems	75
5.1.2	Simulation runs and random seeds	77
5.2	Indicators	78
5.2.1	Indicators at experiment level.....	78
5.2.2	Space-time diagrams.....	79
5.2.3	Indicators at section level	81
6	Microscopic simulation results	83
6.1	Average results at network level.....	83
6.1.1	Average influences of ACC	83
6.1.2	Average influences of newer ACC.....	86
6.1.3	Average influences of improved ACC.....	88
6.1.4	Average influences of CACC.....	91
6.2	Space-time diagrams of bottleneck locations.....	94
6.2.1	Detector set 1	94
6.2.2	Detector set 2	97
6.2.3	Detector set 3	99

6.2.4	Detector set 4	102
6.2.5	Detector set 5	104
6.2.6	Detector set 6	107
6.2.7	Detector set 7	109
6.2.8	Detector set 8	111
6.2.9	Detector set 9	113
6.2.10	Detector set 10	115
6.2.11	Overview of effects of ACC and CACC per bottleneck type	117
6.3	Results at section level	120
6.3.1	Lane changes per vehicle type	120
6.3.2	Speed differences between lanes	121
6.3.3	Density differences between lanes	122
6.3.4	Flow differences between lanes	123
7	Mesoscopic simulation	125
7.1	Mesoscopic input parameters	125
7.1.1	Mesoscopic reaction times for ACC scenarios	126
7.1.2	Mesoscopic reaction times for newer ACC scenarios	127
7.1.3	Mesoscopic reaction times for improved ACC scenarios	128
7.1.4	Mesoscopic reaction times for CACC scenarios	129
7.2	Mesoscopic averages at experiment level	131
7.2.1	Mesoscopic average simulation results for ACC scenarios	131
7.2.2	Mesoscopic average simulation results for newer ACC scenarios	133
7.2.3	Mesoscopic average simulation results for improved ACC scenarios	135
7.2.4	Mesoscopic average simulation results for CACC scenarios	137
7.3	Review of mesoscopic simulation results	139
8	Conclusions and recommendations	143
8.1	Conclusions	143
8.2	Recommendations	146
8.2.1	Recommendations for improvement and further research	146
8.2.2	Recommendations with respect to ACC and CACC systems	147
8.2.3	Recommendations with respect to traffic flow	148
8.2.4	Recommended improvements for traffic modelling in Aimsun	149
8.3	Reflection	150
	Bibliography	153
	Appendix A - Validation check	157

List of figures

Figure 1 - Levels of driving automation (SAE International, 2014).....	1
Figure 2 - Research framework.....	6
Figure 3 - Aimsun model of the Rotterdam area (RHDHV).....	29
Figure 4 - Research network in Aimsun.....	30
Figure 5 - Overview of preparatory work.....	30
Figure 6 - Calibration process.....	32
Figure 7 - Congestion patterns before dynamic matrix calibration procedure: Google (2016) for a random day (top) vs. simulation (bottom) at 17:00.....	34
Figure 8 - Section 645267 in Aimsun.....	35
Figure 9 - Dynamic network calibration link locations (Vaanplein - Ridderkerk).....	36
Figure 10 - Result of dynamic matrix calibration for section 108188.....	36
Figure 11 - Congestion patterns from simulation (top) vs. Google (2016) (bottom) for time period of 17:30-17:45.....	38
Figure 12 - DUE output summary.....	39
Figure 13 - DUE relative gaps per time period.....	40
Figure 14 - Congestion patterns from Google (2016) (left) and mesoscopic simulation (right) from 15:45 - 16:00.....	40
Figure 15 - Congestion patterns from Google (2016) (left) and mesoscopic simulation (right) from 16:00 - 16:15.....	41
Figure 16 - Congestion patterns from Google (2016) (left) and mesoscopic simulation (right) from 16:15 - 16:30.....	41
Figure 17 - Congestion patterns from Google (2016) (left) and mesoscopic simulation (right) from 16:30 - 16:45.....	41
Figure 18 - Congestion patterns from Google (2016) (left) and mesoscopic simulation (right) from 16:45 - 17:00.....	41
Figure 19 - Congestion patterns from Google (2016) (left) and mesoscopic simulation (right) from 17:00 - 17:15.....	42
Figure 20 - Congestion patterns from Google (2016) (left) and mesoscopic simulation (right) from 17:15 - 17:30.....	42
Figure 21 - Congestion patterns from Google (2016) (left) and mesoscopic simulation (right) from 17:30 - 17:45.....	42
Figure 22 - Congestion patterns from Google (2016) (left) and mesoscopic simulation (right) from 17:45 - 18:00.....	42
Figure 23 - Congestion patterns from Google (2016) (left) and mesoscopic simulation (right) from 18:00 - 18:15.....	43
Figure 24 - Congestion patterns from Google (2016) (left) and mesoscopic simulation (right) from 18:15 - 18:30.....	43
Figure 25 - Congestion patterns from Google (2016) (left) and mesoscopic simulation (right) from 18:30 - 18:45.....	43
Figure 26 - Congestion patterns from Google (2016) (left) and mesoscopic simulation (right) from 18:45 - 19:00.....	43
Figure 27 - Section parameters for microscopic simulation.....	45
Figure 28 - Turn parameters for microscopic simulation.....	46
Figure 29 - Parameters at experiment level for microscopic simulation.....	46
Figure 30 - Example of undesired node connections.....	47
Figure 31 - Infrastructure changes: node (left) and shoulder (right).....	47
Figure 32 - Conflicting node connection paths.....	48

Figure 33 - Traffic congestion pattern at start of congestion (16:30) at junction Vaanplein (Google, 2016)	49
Figure 34 - Merging and lane drop at the section where congestion starts at junction Vaanplein.....	49
Figure 35 - Traffic congestion pattern at start of congestion (16:30) at junction Ridderkerk (Google, 2016)	50
.....	
Figure 36 - Congestion patterns from Google (2016) (left) and microscopic simulation (right) from 15:45 - 16:00.....	51
Figure 37 - Congestion patterns from Google (2016) (left) and microscopic simulation (right) from 16:00 - 16:15.....	51
Figure 38 - Congestion patterns from Google (2016) (left) and microscopic simulation (right) from 16:15 - 16:30.....	51
Figure 39 - Congestion patterns from Google (2016) (left) and microscopic simulation (right) from 16:30 - 16:45.....	52
Figure 40 - Congestion patterns from Google (2016) (left) and microscopic simulation (right) from 16:45 - 17:00.....	52
Figure 41 - Congestion patterns from Google (2016) (left) and microscopic simulation (right) from 17:00 - 17:15.....	52
Figure 42 - Congestion patterns from Google (2016) (left) and microscopic simulation (right) from 17:15 - 17:30.....	52
Figure 43 - Congestion patterns from Google (2016) (left) and microscopic simulation (right) from 17:30 - 17:45.....	53
Figure 44 - Congestion patterns from Google (2016) (left) and microscopic simulation (right) from 17:45 - 18:00.....	53
Figure 45 - Congestion patterns from Google (2016) (left) and microscopic simulation (right) from 18:00 - 18:15.....	53
Figure 46 - Congestion patterns from Google (2016) (left) and microscopic simulation (right) from 18:15 - 18:30.....	53
Figure 47 - Congestion patterns from Google (2016) (left) and microscopic simulation (right) from 18:30 - 18:45.....	54
Figure 48 - Congestion patterns from Google (2016) (left) and microscopic simulation (right) from 18:45 - 19:00.....	54
Figure 49 - Loop detector locations for validation check.....	56
Figure 50 - Comparison of simulation flow results with traffic data.....	57
Figure 51 - Comparison of simulation speed results with traffic data.....	59
Figure 52 - General parameter settings for Car (top) and ACC (bottom).....	64
Figure 53 - Microscopic parameter settings for Car (top) and ACC (bottom).....	65
Figure 54 - Dynamic model parameter settings for Car (top) and ACC (bottom).....	65
Figure 55 - Speed plot for following scenario.....	66
Figure 56 - Acceleration plot for following scenario.....	67
Figure 57 - Speed plot for the stop and go scenario.....	68
Figure 58 - Acceleration plot for the stop and go scenario.....	68
Figure 59 - Comparison of actual simulated speed with the car-following model speed components.....	68
Figure 60 - Headway between vehicles in stop and go scenario.....	69
Figure 61 - Speed plot for the emergency braking scenario.....	70
Figure 62 - Acceleration plot for the emergency braking scenario.....	70
Figure 63 - Overview of the cut-in scenario.....	71
Figure 64 - Overview of merging vehicles (cut-in scenario).....	71
Figure 65 - Speed plot for the cut-in scenario.....	71
Figure 66 - Acceleration plot for vehicle 2 and 3 in the cut-in scenario.....	72
Figure 67 - Acceleration plot for vehicle 4 and 5 in the cut-in scenario.....	72

Figure 68 - Speed plot for sensitivity analysis	73
Figure 69 - Acceleration plot for sensitivity analysis.....	74
Figure 70 - Detector set locations and numbering at junction Ridderkerk	80
Figure 71 - Detector set locations and numbering at junction Vaanplein.....	80
Figure 72 - Detector set locations and numbering west from junction Vaanplein	80
Figure 73 - Detector set locations and numbering near junction Benelux	80
Figure 74 - Overview of average speeds over time in the ACC scenarios	83
Figure 75 - Overview of average densities over time in the ACC scenarios	84
Figure 76 - Overview of average delay time in the ACC scenarios.....	85
Figure 77 - Overview of total number of lane changes in the ACC scenarios	85
Figure 78 - Overview of average speeds over time in the newer ACC scenarios.....	86
Figure 79 - Overview of average densities over time in the newer ACC scenarios	87
Figure 80 - Overview of average delay time in the newer ACC scenarios.....	87
Figure 81 - Overview of the total number of lane changes in the newer ACC scenarios.....	88
Figure 82 - Overview of average speeds over time in the improved ACC scenarios.....	89
Figure 83 - Overview of average densities over time in the improved ACC scenarios	89
Figure 84 - Overview of average delay time in the improved ACC scenarios.....	90
Figure 85 - Overview of the total number of lane changes in the improved ACC scenarios	91
Figure 86 - Overview of average speeds over time in the CACC scenarios	92
Figure 87 - Overview of average densities over time in the CACC scenarios	92
Figure 88 - Overview of average delay time in the CACC scenarios	93
Figure 89 - Overview of the total number of lane changes in the CACC scenarios.....	94
Figure 90 - Space-time diagrams for ACC scenarios at detector set 1	95
Figure 91 - Space-time diagrams for newer ACC scenarios at detector set 1	95
Figure 92 - Space-time diagrams for improved ACC scenarios at detector set 1	96
Figure 93 - Space-time diagrams for CACC scenarios at detector set 1	97
Figure 94 - Space-time diagrams for ACC scenarios at detector set 2.....	97
Figure 95 - Space-time diagrams for newer ACC scenarios at detector set 2.....	98
Figure 96 - Space-time diagrams for improved ACC scenarios at detector set 2.....	98
Figure 97 - Space-time diagrams for CACC scenarios at detector set 2	99
Figure 98 - Space-time diagrams for ACC scenarios at detector set 3.....	100
Figure 99 - Space-time diagrams for newer ACC scenarios at detector set 3.....	100
Figure 100 - Space-time diagrams for improved ACC scenarios at detector set 3.....	101
Figure 101 - Space-time diagrams for CACC scenarios at detector set 3	101
Figure 102 - Space-time diagrams for ACC scenarios at detector set 4.....	102
Figure 103 - Space-time diagrams for newer ACC scenarios at detector set 4.....	103
Figure 104 - Space-time diagrams for improved ACC scenarios at detector set 4.....	103
Figure 105 - Space-time diagrams for CACC scenarios at detector set 4	104
Figure 106 - Space-time diagrams for ACC scenarios at detector set 5.....	105
Figure 107 - Space-time diagrams for newer ACC scenarios at detector set 5.....	105
Figure 108 - Space-time diagrams for improved ACC scenarios at detector set 5	106
Figure 109 - Space-time diagrams for CACC scenarios at detector set 5	106
Figure 110 - Space-time diagrams for ACC scenarios at detector set 6.....	107
Figure 111 - Space-time diagrams for newer ACC scenarios at detector set 6.....	107
Figure 112 - Space-time diagrams for improved ACC scenarios at detector set 6.....	108
Figure 113 - Space-time diagrams for CACC scenarios at detector set 6	108
Figure 114 - Space-time diagrams for ACC scenarios at detector set 7	109
Figure 115 - Space-time diagrams for newer ACC scenarios at detector set 7.....	109
Figure 116 - Space-time diagrams for improved ACC scenarios at detector set 7.....	110

Figure 117 - Space-time diagrams for CACC scenarios at detector set 7	110
Figure 118 - Space-time diagrams for ACC scenarios at detector set 8.....	111
Figure 119 - Space-time diagrams for newer ACC scenarios at detector set 8.....	112
Figure 120 - Space-time diagrams for improved ACC scenarios at detector set 8.....	112
Figure 121 - Space-time diagrams for CACC scenarios at detector set 8	113
Figure 122 - Space-time diagrams for ACC scenarios at detector set 9.....	113
Figure 123 - Space-time diagrams for newer ACC scenarios at detector set 9.....	114
Figure 124 - Space-time diagrams for improved ACC scenarios at detector set 9.....	114
Figure 125 - Space-time diagrams for CACC scenarios at detector set 9	115
Figure 126 - Space-time diagrams for ACC scenarios at detector set 10.....	115
Figure 127 - Space-time diagrams for newer ACC scenarios at detector set 10.....	116
Figure 128 - Space-time diagrams for improved ACC scenarios at detector set 10.....	116
Figure 129 - Space-time diagrams for CACC scenarios at detector set 10	117
Figure 130 - Average number of lane changes of ACC (green) and car (blue) on six selected road sections	120
Figure 131 - Average number of lane changes of improved ACC (green) and car (blue) on six selected road sections	121
Figure 132 - Speed differences between lanes for reference and 50% improved ACC scenario on section 108866.....	122
Figure 133 - Density differences between lanes for reference and 50% improved ACC scenario on section 108866.....	123
Figure 134 - Flow differences between lanes for reference and 50% improved ACC scenario on section 108866.....	124
Figure 135 - Comparisons of speed, density, delay time and total number of lane changes for the microscopic and mesoscopic reference and 50% ACC scenarios.....	126
Figure 136 - Comparisons of speed, density, delay time and total number of lane changes for the microscopic and mesoscopic reference and 50% newer ACC scenarios.....	128
Figure 137 - Comparisons of speed, density, delay time and total number of lane changes for the microscopic and mesoscopic reference and 50% improved ACC scenarios.....	129
Figure 138 - Comparisons of speed, density, delay time and total number of lane changes for the microscopic and mesoscopic reference and 50% CACC scenarios	130
Figure 139 - Overview of average speeds over time resulting from mesoscopic simulation of ACC scenarios	131
Figure 140 - Overview of average densities over time resulting from mesoscopic simulation of ACC scenarios	132
Figure 141 - Overview of average delay time resulting from mesoscopic simulation of ACC scenarios..	133
Figure 142 - Overview of speed over time resulting from mesoscopic simulation of newer ACC scenarios	133
Figure 143 - Overview of density over time resulting from mesoscopic simulation of newer ACC scenarios	134
Figure 144 - Overview of average delay time resulting from mesoscopic simulation of newer ACC scenarios	135
Figure 145 - Overview of speed over time resulting from mesoscopic simulation of improved ACC scenarios	135
Figure 146 - Overview of density over time resulting from mesoscopic simulation of improved ACC scenarios	136
Figure 147 - Overview of average delay time resulting from mesoscopic simulation of improved ACC scenarios	137
Figure 148 - Overview of speed over time resulting from mesoscopic simulation of CACC scenarios	137

Figure 149 - Overview of density over time resulting from mesoscopic simulation of CACC scenarios...	138
Figure 150 - Overview of average delay time resulting from mesoscopic simulation of CACC scenarios	139
Figure 151 - Loop detector locations	157
Figure 152 - Flows per 15 minutes for detector location 1	158
Figure 153 - Speeds per 15 minutes for detector location 1	159
Figure 154 - Flows per 15 minutes for detector location 2	160
Figure 155 - Speeds per 15 minutes for detector location 2	161
Figure 156 - Flows per 15 minutes for detector location 3	161
Figure 157 - Speeds per 15 minutes for detector location 3	162
Figure 158 - Flows per 15 minutes for detector location 4	163
Figure 159 - Speeds per 15 minutes for detector location 4	164
Figure 160 - Flows per 15 minutes for detector location 5	164
Figure 161 - Speeds per 15 minutes for detector location 5	165
Figure 162 - Flows per 15 minutes for detector location 6	166
Figure 163 - Speeds per 15 minutes for detector location 6	166

List of tables

Table 1 - Overview of (C)ACC vehicle types and main microscopic parameter settings	IV
Table 2 - Overzicht van (C)ACC voertuigtypen en belangrijkste microscopische parameter instellingen ...	XI
Table 3 - Different model parameter settings in literature	13
Table 4 - Simulation flow data vs. traffic counts at link 645267	35
Table 5 - Simulation flows compared with traffic counts in vehicles per hour after dynamic matrix calibration	37
Table 6 - Coefficients of determination [R ²] for comparisons of simulation flows with traffic data	56
Table 7 - Coefficients of determination [R ²] for comparisons of simulation speeds with traffic data	58
Table 8 - Road sections of following scenario	66
Table 9 - Road sections in stop and go scenario	67
Table 10 - Road sections in emergency braking scenario	69
Table 11 - Overview of scenarios for sensitivity analysis	73
Table 12 - Overview of (C)ACC system types used for simulation and the most important parameters	76
Table 13 - Random seeds per simulation run, used in all simulation scenarios	78
Table 14 - Overview of effects of (C)ACC on bottlenecks with extreme braking	118
Table 15 - Overview of effects of (C)ACC on bottlenecks with a lane drop	118
Table 16 - Overview of effects of (C)ACC on on-ramp bottlenecks	119
Table 17 - Overview of effects of (C)ACC on weaving sections	119
Table 18 - Average speed differences between lanes on section 108866 at capacity	122
Table 19 - Average density differences between lanes on section 108866 at capacity	123
Table 20 - Average flow differences between lanes on section 108866 at capacity	124
Table 21 - Corresponding coefficients of determination for comparison between microscopic and mesoscopic simulation results of ACC scenarios	126
Table 22 - Corresponding coefficients of determination for comparison between microscopic and mesoscopic simulation results of newer ACC scenarios	128
Table 23 - Corresponding coefficients of determination for comparison between microscopic and mesoscopic simulation results of improved ACC scenarios	129
Table 24 - Corresponding coefficients of determination for comparison between microscopic and mesoscopic simulation results of CACC scenarios	131
Table 25 - Overview of microscopic and mesoscopic reaction time and compensations	141
Table 26 - Coefficients of determination [R ²] for the flows at detector location 1	158
Table 27 - Coefficients of determination [R ²] for the speeds at detector location 1	159
Table 28 - Coefficients of determination [R ²] for the flows at detector location 2	160
Table 29 - Coefficients of determination [R ²] for the speeds at detector location 2	161
Table 30 - Coefficients of determination [R ²] for the flows at detector location 3	162
Table 31 - Coefficients of determination [R ²] for the speeds at detector location 3	162
Table 32 - Coefficients of determination [R ²] for the flows at detector location 4	163
Table 33 - Coefficients of determination [R ²] for the speeds at detector location 4	164
Table 34 - Coefficients of determination [R ²] for the flows at detector location 5	165
Table 35 - Coefficients of determination [R ²] for the speeds at detector location 5	165
Table 36 - Coefficients of determination [R ²] for the flows at detector location 6	166
Table 37 - Coefficients of determination [R ²] for the speeds at detector location 6	167

1 Introduction

Before conducting the research, the topic and reason for starting the research should be clear. Also, the way in which the research will be performed should be transparent. First, the context of the research and why this research is conducted will be explained. Subsequently, the research objective and research questions will be described. Afterwards, the research methodology is discussed, after which a literature review is provided and the structure of the report is discussed.

1.1 Context

In the Netherlands, traffic volume is increasing every year. This increase in traffic constantly confronts the society with problems. Results of the increase in road traffic are a congested traffic network and a negative influence on safety, air pollution and fuel and energy consumption. To reduce the consequences of this increase in road traffic, different solution strategies can be used. Building new infrastructure and improving safety policies, traffic management measures, roadside infrastructure, latest technologies and traffic education can contribute to solving these problems. Building new infrastructure is often not an option anymore due to high costs and dense environments. New technologies could lead to system innovations, which are expected to contribute to the problems in the long term (Vits, Hodac, Mossé, & Jaaskelainen, 2002).

There are many technological developments in the automotive industry. An important notice is that there are many technological developments on the control mechanisms of vehicles. Until now, cars were driven manually by their drivers. However, more and more vehicles with automated (driver assistance) systems are available. These automated vehicles can drive at a road all by itself. Sometimes, the partly automated vehicle is not capable of handling all driving modes. SAE International (2014) described six levels of automation (from 0 to 5), as shown in *Figure 1*. Automated vehicles are located in level 4 or 5. However, fully automated vehicles are not available on the commercial market yet. Currently, numerous Advanced Driver Assistance Systems (ADAS) are available and implemented into vehicles. These systems are aimed at supporting the driver of the vehicle with the driving task. It is noticeable that the focus is shifting from a driver who controls and takes decisions, to a vehicle that is increasingly capable of executing driving tasks on its own. These ADAS can be considered as the first step towards high and full automation as described by the SAE levels of automation in *Figure 1*. Examples of ADAS are various types of cruise control, park assist systems, collision warning-systems and lane-keeping systems.

SAE level	Name	Narrative Definition	Execution of Steering and Acceleration/Deceleration	Monitoring of Driving Environment	Fallback Performance of Dynamic Driving Task	System Capability (Driving Modes)
Human driver monitors the driving environment						
0	No Automation	the full-time performance by the human driver of all aspects of the dynamic driving task, even when enhanced by warning or intervention systems	Human driver	Human driver	Human driver	n/a
1	Driver Assistance	the driving mode-specific execution by a driver assistance system of either steering or acceleration/deceleration using information about the driving environment and with the expectation that the human driver perform all remaining aspects of the dynamic driving task	Human driver and system	Human driver	Human driver	Some driving modes
2	Partial Automation	the driving mode-specific execution by one or more driver assistance systems of both steering and acceleration/deceleration using information about the driving environment and with the expectation that the human driver perform all remaining aspects of the dynamic driving task	System	Human driver	Human driver	Some driving modes
Automated driving system ("system") monitors the driving environment						
3	Conditional Automation	the driving mode-specific performance by an automated driving system of all aspects of the dynamic driving task with the expectation that the human driver will respond appropriately to a request to intervene	System	System	Human driver	Some driving modes
4	High Automation	the driving mode-specific performance by an automated driving system of all aspects of the dynamic driving task, even if a human driver does not respond appropriately to a request to intervene	System	System	System	Some driving modes
5	Full Automation	the full-time performance by an automated driving system of all aspects of the dynamic driving task under all roadway and environmental conditions that can be managed by a human driver	System	System	System	All driving modes

Figure 1 - Levels of driving automation (SAE International, 2014)

One of the interesting research directions within ADAS is cruise control. Adaptive Cruise Control (ACC) has been introduced by the automotive industry. Adaptive Cruise Control is an extension of the conventional cruise control. An ACC system functions like a conventional cruise control, but is also able to detect the speed of the preceding vehicle using a radar or laser and adapting its own speed accordingly. When a preceding vehicle changes speed, the ACC system acts upon the speed of the preceding vehicle, the target speed and the desired headway defined. ACC is designed to relieve the driver from some driving tasks by increasing comfort, safety and convenience. Cooperative Adaptive Cruise Control (CACC) is a further development of ACC that adds vehicle-to-vehicle communication to gather more and better information about the vehicles it is following. ACC systems can only look one vehicle ahead, while CACC systems can communicate with multiple vehicles ahead within communication range. Using this information, CACC vehicles will be able to detect and anticipate on problems further ahead, by responding in a fast, safe, natural and smooth manner. ACC and CACC systems only control the longitudinal driving task, meaning that the driver still has to control the lateral driving tasks. Both CACC and ACC systems are located in SAE level 1 (*Figure 1*).

Since (Cooperative) Adaptive Cruise Control ((C)ACC) systems change the car-following behavior of vehicles, they are expected to have an effect on traffic safety and traffic flow efficiency. It is important to gain insight in the traffic flow effects of (C)ACC early in the development, because if problems or deteriorations are found, measures could be taken accordingly before these systems are widely spread (van Arem, van Driel, & Visser, 2006). In addition, studying the effects of (C)ACC might also contribute to improving and developing ACC and CACC systems to support future advances.

A wide variety of literature that study the effects of ACC and/or CACC on traffic flow is available. However, the topic is not yet well understood, since results differ from substantial increases to substantial decreases (Milanés & Shladover, 2014). Especially, research is lacking on the traffic flow effects of (C)ACC on traffic situations with multiple bottlenecks and weaving sections. Generally speaking, the effects of ACC systems are still uncertain, while CACC systems are expected to yield benefits in traffic safety and traffic flow efficiency.

For ACC and CACC systems, a theoretical trade-off exists between maximizing safety and maximizing traffic flow throughput (Alkim, Schuurman, & Tampere, 2000). The trade-off exists because the shorter the headway between two consecutive vehicles at a given speed, the more dangerous the situation becomes, since the time to react upon speed changes of preceding vehicles is reduced. However, throughput and capacities increase if headways are reduced. The (C)ACC systems are expected to increase both aspects, but the extent of this improvement is still unknown due to the facts that there will still be mixed traffic and merging processes on highways.

It becomes clear that it is necessary to gain insight in the traffic flow effects of ACC and CACC on highways in the Netherlands. When the influences of (C)ACC are depicted, this might give insight for the further implementation of ACC and CACC systems, user acceptance and legislation of these systems. Also, the results from this research might be used as an advice to policy makers.

1.2 Research objective & questions

This section describes the research objective and research questions.

1.2.1 Research objective

An increase in market penetration rates of (C)ACC has the potential to have a significant effect on traffic flow performance. However, the extent of these effects in realistic traffic situations is still uncertain. Therefore, the main objective of this thesis is to gain insight in the effects of (different market penetration

rates of) ACC and CACC on traffic flow performance in realistic traffic situations on the highway, such as traffic situations with multiple bottlenecks and at weaving sections.

Until now, only little is known about the traffic flow effects of (C)ACC on a large-size network. One of the reasons for this fact is that representing (C)ACC driving behavior at large-scale networks is complicated, since behavioral models often have to be simplified due to computational reasons. Therefore, there is a desire to abstract the results found on a microscopic scale into a model at a mesoscopic scale, in order to assess the traffic effects of (C)ACC at networks of larger sizes. However, it is questionable whether a sufficient level of detail can be achieved to realistically describe (C)ACC driving behavior on a large-scale network. A side objective of this research is to inventory whether it is possible to represent (C)ACC driving behavior pragmatically, but sufficiently realistic in a mesoscopic simulation. The reason for choosing the method of traffic simulation is discussed in section 1.3.

Concluding, this thesis consists of several objectives, described in this section. First, the effects of (C)ACC on traffic flow performance in realistic traffic situations should be investigated. Next, the results can be used in order to inventory the possibility to implement (C)ACC driving behavior into a larger-scale model. Subsequently, the limitations of the simulation models, behavioral models and results from the study should be inventoried to provide recommendation on further research and development of both (C)ACC systems and traffic simulation tools.

1.2.2 Research questions

In order to achieve the research objective and provide a contribution to the field of research, several research questions were composed, subdivided in a main research question and sub research questions. The following main research question was composed to contribute to the solution of the research problem:

What are the effects of (Cooperative) Adaptive Cruise Control systems on traffic flow in realistic traffic situations with multiple bottlenecks?

In order to answer the main research question and to achieve the research objectives, several sub research questions are used. The following sub research questions are used in this research:

- What are the predicted effects of ACC and CACC in state-of-the-art literature?
- How to model ACC and CACC in microscopic simulation?
- What parameter settings are used for modelling ACC and CACC?
- Which indicators are used to assess the effects of ACC and CACC on traffic flow?
- What are the effects of ACC and CACC on traffic flow performance?
- What are the effects of ACC and CACC on traffic flow at characteristic bottleneck types?
- To what extent can traffic flow effects of (C)ACC be assessed using mesoscopic simulations?
- What aspects of modelling (C)ACC systems and modelling in Aimsun could be improved?
- What recommendations can be made for future use and development of (C)ACC systems?

1.3 Research methodology

This section describes the research methodology used in this research. First, the methods that will be used in this research are discussed, after which the model choice is discussed. Finally, the research framework is provided.

1.3.1 Methods

First, a literature study on the state-of-the-art of (modelling and assessing) ACC and CACC systems is executed. The literature study has multiple goals. First, the expected effects in literature will be studied. Next, the ways of modelling (C)ACC driver behavior are explored in literature, together with the input parameters. The literature study is used to gain insight into the topic and to decide what scenarios and

situations are interesting to reflect. The results from the literature study will serve as input for the following steps.

In order to gain insight in the effects of ACC and CACC on traffic flow at realistic traffic situations, multiple methods could be used, such as field studies, driver simulation tests and traffic simulations. In this research, the method of traffic simulation will be used, because of several reasons. First, performing simulation is a very safe way to assess traffic flow effects and does not lead to accidents or other troublesome situations in real life. Secondly, using simulation it is possible to define many different types of vehicles and person characteristics, which has the advantage that it is possible and easy to change market penetrations or driver characteristics, which will all have an influence on traffic flow. The third advantage of using traffic simulation is that it is possible to change many parameters and road configurations in order to gain insight in the effects of changing parameters and road configurations in a safe environment.

Performing field tests at complicated traffic situations with multiple bottlenecks could potentially become dangerous, which means that this method is not the best suited for this research. In order to assess the effects with a driver simulation, many different test persons are needed in order to draw a realistic conclusion about the expected effects, even while many of the test persons will have limited to no experience with ACC or CACC systems whatsoever. Performing driver simulations for many different scenarios is very time-consuming. Also, applying different market penetration rates in a field study and a driver simulation is relatively complicated, while this is easy in traffic simulation. Therefore, a traffic simulation tool seems to be best suited for this research.

The microscopic modelling approach is able to represent a heterogeneous traffic stream of ACC, CACC and manually driven vehicles (Kesting, Treiber, Schönhof, & Helbing, 2007). However, the models must capture the driving dynamics of ACC, CACC and humans in order to realistically estimate the traffic impacts. Since there are many different parameters available in a microscopic model, it is found that a microscopic model is often able to represent human, ACC and CACC driving behavior to a sufficiently realistic extent. However, the ACC and CACC driving behavior should be validated and verified. Different validation scenarios will be set up in order to assess whether the model represents realistic driving behavior for scenarios such as cut-in maneuvers, normal highway following, stop and go traffic and emergency braking maneuvers. Therefore, a microscopic simulation of multiple ACC and CACC scenarios will be conducted in order to assess the effects of ACC and CACC on a network with multiple bottlenecks. However, it should be noted that the results partly depend on the model assumptions and parameter settings.

In addition, knowledge about to what extent it is possible to incorporate (C)ACC driving behavior in a mesoscopic model is still lacking. When microscopic simulations are performed on large-size networks, the simulations are very time-consuming. Mesoscopic simulations are often used to assess effects on a large-size network with a relatively high level of detail. In a mesoscopic modelling approach, vehicles are still modelled as an individual entity, but their behavioral models, and thus the model calculations, are simplified in comparison with the microscopic modelling approach. In order to assess whether it is possible to incorporate the (C)ACC driving behavior into a mesoscopic model, a quick-scan into the possibilities will be performed. However, the main goal and focus of this research is aimed at the microscopic model. The quick-scan into the mesoscopic model is primarily performed to provide recommendations for future use.

Finally, the results obtained in the simulations have to be compared and assessed. Many different indicators such as average total time spent in the network, capacities, densities, and flows, number of lane changes, speeds and vehicle loss hours can be used. After the analysis of results, conclusions and recommendations will be given, based on the information and results found in this research.

1.3.2 Model choice

In order to make a suitable choice between different simulation tools available, some criteria are needed. Therefore, the following list of criteria has been defined:

- The simulation model should be able to perform microscopic and mesoscopic simulations;
- The simulation model should be able to vary link and user class settings;
- It should be possible to model different types of driving behavior;
- The model should be suitable to test different assumptions of ADAS on driver behavior and vehicle dynamics;
- The model should be capable of assessing impacts on traffic flow;
- The model should contain a lane change model and a longitudinal model to describe longitudinal and lateral driving behavior.

Aimsun (Transport Simulation Systems, 2015) is one of the simulation models that fulfills these criteria. Aimsun also has some additional benefits. First, the simulation model is available at Royal HaskoningDHV (RHDHV). Secondly, there is a significant amount of experience with Aimsun at RHDHV. Thirdly, the complete Rotterdam road network is available and calibrated in Aimsun, which means that the network to use in this research can be depicted and calibrated relatively easily. Lastly, many different performance indicators, such as total time spent, speeds and delay times are already implemented in Aimsun, which helps the analysis of results.

Based on the fulfilled criteria and the additional benefits, Aimsun was chosen as a suitable simulation model for this research. Other options were also available. However, Aimsun had some attractive additional benefits, which made Aimsun the preferred choice.

1.3.3 Research framework

Figure 2 provides an overview of the research framework. The research framework contains the methods as described in section 1.3.1 and some additional components of the research, such as the introduction, problem definition and conclusions. Also, some additional important components of the microscopic modelling parts are referred to in the framework.

To start with the research, it is important to have an introduction into the research topic. Additionally, it is also important to gain skills needed to use the chosen simulation program. Subsequently, the problem should be defined and explained in the problem definition. In this process, the main and sub research questions are defined. Then, different sources of literature will be used and reviewed in order to gain more insight into the topic and to pinpoint clear or missing conclusions.

Subsequently, the core of the research is the microscopic modelling of different types of (C)ACC to analyze the effects of these vehicles on traffic flow in realistic traffic situations with multiple bottlenecks. This will be done using various scenarios. In some cases, it is important to establish more scenarios after analysis, because additional results might be needed to draw clear conclusions. This relation is indicated with dotted feedback loops in *Figure 2*. Next to microscopic modelling, a quick scan into mesoscopic modelling will be performed in order to check whether it is possible to represent similar results using mesoscopic simulations. Feedback loops are also added for this procedure, because this will probably be a process of trial and error.

Consecutively, the results found in both types of simulation will be compared and assessed. In this process, some of the hypotheses drawn from the literature review can be tested. When the comparison and assessment is finished, the most important conclusions and recommendations will be given to describe the most important results found in this research.

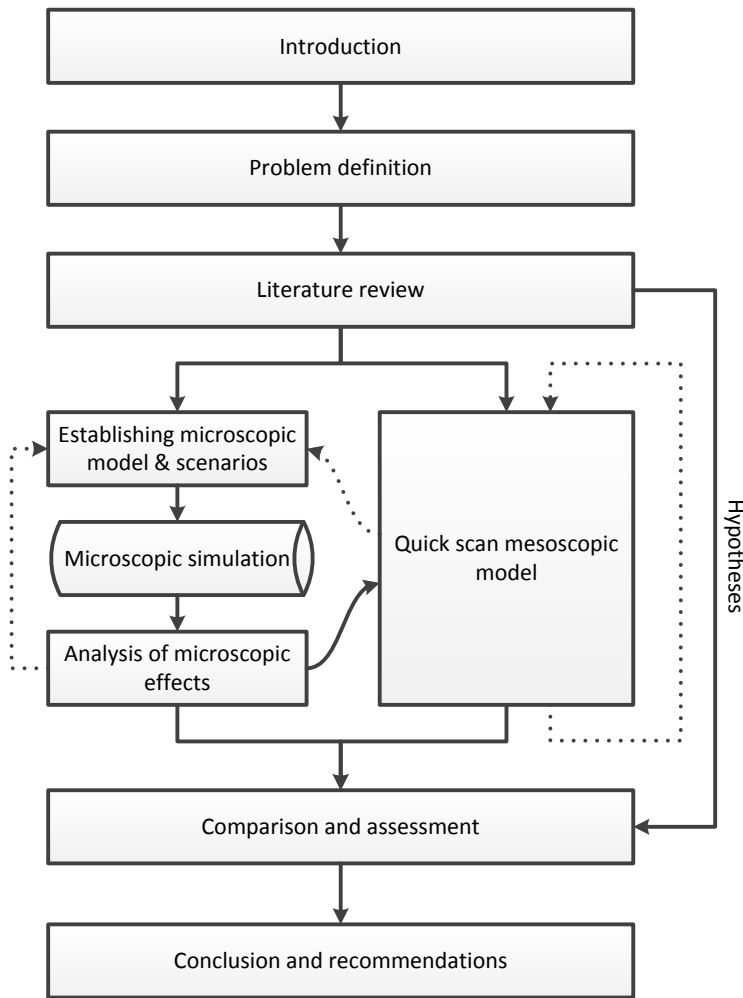


Figure 2 - Research framework

1.4 Literature review

Many researchers study or studied this topic, which means that there is plenty of information available on this topic. The available literature might be useful in the light of this research. Therefore, a literature review is conducted.

The literature review is divided into different subcomponents. First, the purpose of (C)ACC is reviewed. Then, the expected effects of (C)ACC are elaborated upon. Also, a small overview of the parameter specifications used in some of the literature that studies the effects of (C)ACC on traffic has been provided, in order to get an insight in parameter settings that could be used in this research.

1.4.1 Purpose of ACC and CACC

According to Pamela Labuhn and William Chundrlik, who are considered to be one of the early adopters of Adaptive Cruise Control technology, ACC is designed as an aid for the driving tasks, but will also have a positive influence on traffic flow and safety (Labuhn & Chundrlik, 1995). Additionally, ACC was one of the first steps towards automated vehicles.

Car manufacturers that sell cars are usually more focused on the aesthetics of a vehicle than on the (safety) systems installed in a vehicle. Also, the aesthetics of a vehicle are important features of television commercials. It is only recently that commercials also mention the systems available in a vehicle. Mostly,

the benefits in terms of comfort are mentioned by car manufacturers and in the commercials, since comfort is an important aspect when buying or selecting a new car. However, car manufacturers do not focus on the effects on traffic flow, since they are not interested in traffic performances in terms of travel time and flow, while this is an aspect that is valuable to car drivers. Additionally, car manufacturers briefly reflect upon the effects on traffic safety, which also is an important aspect for car drivers.

Currently, there still is a large disclaimer on ACC systems, because many instruction manuals state that it is important to drive attentively. In addition, the driver is still responsible for the driving task, which means that the driver should always be prepared to overrule the system. Current legislation clearly states that the driver in the vehicle is still responsible, indicating that the driver has to be attentive when the ACC system is activated. Summarizing, car manufacturers want drivers to be more relaxed and comfortable by offering ACC systems, but the responsibility for the complete driving task is still by the driver of the vehicle.

Cooperative Adaptive Cruise Control systems are not commercially available nowadays. Currently, there are several studies, tests and technological developments going on in the field of CACC. Since communication is added to CACC, these systems are expected to have (more) positive effects on traffic safety, comfort, traffic flow and the environment. However, it should be noted that the additional gains of CACC can probably only be reached at relatively high penetration rates, since the CACC systems can only provide additional gains if communication is possible between other vehicles.

1.4.2 Expected effect on traffic performance

This subsection describes the expected effects of (C)ACC on traffic performance. This section is divided into different subsections. The expected effects in terms of behavior, environment, safety and traffic flow are discussed accordingly. Please note that there is some overlap and interaction between the sub-topics, which means that some of the topics might be touched upon in multiple subsections.

1.4.2.1 Behavior

Generally speaking, (C)ACC systems are designed for enhancing comfort and lead to more constant car-following behavior. In Gorter (2015) and Bianchi Piccinini, Rodrigues, Leitão, & Simões (2015) it was found that ACC users indeed report an increase in driver comfort. Driving with an activated ACC system leads to a calmer driving style (Gorter, 2015; van Twuijver & Pol, 2004), which is argued by some of the ACC users due to the sometimes sudden and unexpected accelerations and decelerations they experienced if vehicles merge in front. It was found that drivers with a calmer driving style like ACC more (Gorter, 2015), which seems plausible due to the relatively relaxed driving style of ACC. A driver with an aggressive driving style is less likely to be willing to use an ACC system. This idea is supported by the driving simulator tests and questionnaires by Hoedemaeker & Brookhuis (1998), who found that drivers with an aggressive driving style are less prone to use ACC, since this system is designed for comfort and most systems do not allow for sportive driving styles. However, some car brands, like Tesla, do allow for generally more sportive driving in ACC systems. Also, the national platoon test 2016 at 16 March 2016 at the A2 in the Netherlands showed that ACC systems of different car brands are tuned differently. For example, Tesla shows a relatively sportive ACC driving behavior, while Volvo shows a more relaxed and comfortable driving style. Many different researches stated that (C)ACC must be customizable (Gorter, 2015; van Twuijver & Pol, 2004; Viti, Hoogendoorn, Alkim, & Bootsma, 2008) to select a personally preferred driving style. However, this customization should mainly be in the headway settings, already incorporated in many ACC systems.

ACC systems still have some limitations caused by limitations in the devices (radar, sonar or camera) or the maximum braking capacity, which might cause critical situations. These limitations are often described in the user manual. However, according to Mehlenbacher, Wogalter, & Laughery (2002), a significant percentage of drivers do not read the manual, while those who do read the manual, read approximately

50% of the manual. It is advised for ACC users to prepare before using ACC, in order to know about the capabilities and limitations of the system. However, drivers tend to start using ACC without properly investigating the risks and limitations. Also, it was found that users who do have experience with the ACC system tend to appreciate it more (Alkim, Bootsma, & Looman, 2007; Bianchi Piccinini et al., 2015; Gorter, 2015), which seems plausible, since these drivers are aware of the risks of using these systems.

The majority of ACC users receives some kind of information on the system and is able to use it wisely, since they are more aware of the risks and limitations. However, it was found that a significant amount of users have a too high level of trust in the ACC system (Gorter, 2015). This group often consists of users that did not receive any instructions and are overestimating the capabilities of the ACC system. A similar pattern was found in Bianchi Piccinini et al. (2015). As a consequence of the overestimation of the ACC system capabilities, these users tend to have a reduced level of focus and an increase in secondary activities, which results in larger response times. This behavioral pattern can be extremely dangerous in critical situations, where there is a risk of collision during driving with ACC. However, it should be noted that even experienced users have a higher response time during ACC driving than during manual driving, which can be explained by the extra time needed to react to ACC system changes. Additionally, this increase in response time is higher for unexperienced users.

The use of ACC systems results in a decrease in the amount of lane changes (Gorter, 2015; van Twuijver & Pol, 2004). This can be explained by the fact that the ACC system makes sure the car is following his predecessor, which means that drivers are more likely to keep following the same vehicle and stick to the same lane. In a study by van Twuijver & Pol (2004) it was found that ACC users tend to drive more on the right lane. However, in the field study of Gorter (2015) it was found that there are two different groups. Some drivers tend to use the left lane more often, while others tend to use the right lane more often. In the researchers opinion it is more likely that the left lane is used more frequently by ACC users, which is also support by Hoedemaeker & Brookhuis (1998). The conclusion that ACC is often used in the left lane could also be a consequence of the fact that the system is more frequently used in free flow conditions, but is very often deactivated in slow and dense traffic conditions (Pauwelussen & Feenstra, 2010). Additionally, it was found that ACC users tend to go to the left lane at an earlier moment in time when trying to overtake a vehicle, to prevent braking for a preceding vehicle (Alkim et al., 2007; Gorter, 2015). It is reasonable to believe that ACC users tend to minimize (strong) braking reactions. However, Gorter (2015) notes that drivers with a more defensive driving style are more prone to use ACC systems, which would suggest that these systems will be used more frequently on the slower right lanes.

There are various motives to overrule the ACC system. In order to get a feeling for the reasons to switch off the ACC system (Pauwelussen & Feenstra, 2010), the most common motives are explained below:

- **Speed adaptation prior to a lane change:** Just before switching a lane, the driver decides to take over control in order to change speed in such a way that is not supported by the system;
- **Speed adaptation to avoid overtaking on the wrong lane:** To avoid illegal overtaking in the right lane, the driver might choose to disengage the ACC system. However, some of the newest ACC systems already prohibit overtaking at a right lane and change their speed accordingly. During the national platoon test it was found that Mercedes cannot overtake on a right lane, because it also checks and acts upon the speed of a vehicle in the left adjacent lane;
- **Overruling due to defensive or offensive driving behavior:** ACC systems might be overruled for braking or accelerating to create a gap for a merging vehicle or to overtake a merging vehicle. This behavior depends on the type of driver. Some drivers have an offensive driving style, while other drivers drive defensively;
- **Reaching the system support boundaries in a safety-critical situation:** It might be necessary to overrule the ACC system in order to prevent a collision. This is due to the fact that ACC systems are constrained in speed and acceleration.

Until now, CACC systems are not commercially available yet, which means that the behavioral effects of CACC are uncertain. Since CACC is an improved version of ACC, it is expected that the CACC systems will have a reduced amount of limitations and boundaries. Therefore, it is likely to believe that behavioral impacts of CACC will be more positive. However, if the trust of drivers will become too high, some drivers might not be alert and unable to safely take over control of the vehicle in safety-critical situations.

1.4.2.2 Environment

It is expected that (C)ACC systems have a positive influence on speed variances of vehicles, because these systems will reduce the variance of accelerations, resulting in more constant speeds. Even though ACC systems are designed for enhancing driver comfort, Marsden, McDonald, & Brackstone (2001) found reductions in acceleration variances of 44% to 52% due to ACC performances, which delivers potential benefits in both traffic safety and environmental impacts.

In a field operational test with 20 ACC vehicles in the Netherlands in 2006, effects on environment were also found. When it is assumed that the fleet of 20 ACC vehicles is representative of all drivers in their surroundings, a 3% reduction in fuel consumption and a decrease of associated emissions up to 10% were found (Viti et al., 2008). No negative effects on throughput were found in this study. Unfortunately, a clear explanation on the reductions in fuel and associated emissions is lacking in this study.

It is expected that CACC systems will increase the environmental gains of ACC even more, since CACC systems enable the possibility to drive at shorter headways, which reduces the air drag. Reductions in air drag result in a reduction of fuel consumption and associated emissions, if a similar driving style is assumed. Additionally, the applicability of platooning will be enlarged by the introduction of CACC, which will have a positive effect on environment.

In a study on the effects of autonomous heavy-duty vehicle (HDV) platooning in mixed traffic, Deng & Ma (2015) found positive effects on the environment. Their simulation results showed that autonomous platooning of HDV can gain substantial fuel saving when HDV penetration rates are higher than 40%. Generally, the positive impacts on overall traffic are also preserved in this case. Another interesting feature Deng & Ma (2015) observed was that fuel savings of (unequipped) passenger cars can also be achieved, which proves benefits of HDV platoons to overall fuel consumption. These benefits can be explained by the fact that passenger cars will have to overtake HDV vehicles less frequently when HDV platooning rate increases, since the HDV are driving as a block or coupled (with a maximum of 3 trucks in a platoon) and only require a single overtaking action instead of three separate overtaking actions. This line of reasoning is easy to understand and straight forward. However, a missing component is that HDV vehicles might have to speed up over a certain period of time in order to start platooning (Liang, Mårtensson, & Johansson, 2013), which might have a substantially negative effect on the environment.

If (C)ACC systems manage to reduce congestion, a reduction in fuel consumption will also be achieved, because speed and acceleration variances will decrease. However, if there is an increase in congestion, the effects on environment will probably become negative, due to an increase in acceleration and deceleration movements in congested traffic. Smoother driving will reduce the air drag coefficient, resulting in positive effects on environment (Barth, Boriboonsomsin, & Wu, 2014). In general, based on air drag reductions, energy savings of 10% up to 15% can be achieved in platooning scenarios with a separation distance of roughly 4 meters (Browand, McArthur, & Radovich, 2004). However, this study does not take into account the consequences of speeding up to catch up with a platoon.

1.4.2.3 Safety

Regarding (C)ACC systems there is a theoretical trade-off between maximizing safety and maximizing throughput, because short headways result in increases in capacity but a decrease in time to react upon

disturbances (Alkim et al., 2000). For (C)ACC systems, both increases and decreases in traffic safety were found.

Normally, ACC systems are claimed to result in a reduction in front-end collisions (Gorter, 2015; van Twuijver & Pol, 2004). However, this seems true for simple car-following behavior without very strong decelerations and drivers with knowledge of the system that are attentive and ready to take over control in a critical situation. Front-end collisions were not witnessed in the field study of Gorter (2015), because the drivers overruled the ACC system in such safety-critical situations. It is of vital importance that drivers are aware of the limitations of the system and are ready to overrule the system in case of critical situations. Currently, most ACC systems are not capable of detecting merging vehicles and vehicles on adjacent lanes, such that the driver often takes over control in traffic situations like overtaking, merging and weaving in order to prevent a collision (Klunder, Li, & Minderhoud, 2009; Pauwelussen & Feenstra, 2010). Therefore, the driver still has to be attentive during driving and should be aware of surrounding vehicles in order to be able to prevent collisions in these situations. It is reported that it is likely that drivers overrule the system in cut-in situations (Viti et al., 2008). Also, the allowable accelerations and decelerations of some ACC (and probably future (C)ACC) systems are bounded, indicating that the systems might have to be overruled in case of safety-critical situations, such as an emergency stop with strong braking.

It was found that ACC leads to more constant speed in all traffic conditions. In congested and capacity conditions, ACC was found to perform less strong braking actions (3-10 km/h/s decrease in speed) in comparison with human driving, meaning that these systems outperform the human driver in these dense traffic conditions with respect to prevention of shockwaves and collisions (Gorter, 2015). Additionally, Kikuchi, Uno, & Tanaka (2003) reported that ACC vehicles help to regain stability more quickly and promote safety to both ACC and non-ACC vehicles. In free flow traffic, strong braking actions were found more often in comparison with human drivers, which can be explained by the larger desired headways of ACC systems and the braking reactions of the ACC systems to (merging) vehicles within a distance shorter than the desired headway (Gorter, 2015). This behavior might be unsafe in some situations, because the human driver following an ACC vehicle might not expect the vehicle to brake. Therefore, it is important to stay alert, also when (C)ACC is activated. All car brands also indicate that the driver is still responsible and that your hands have to be on the steering wheel during driving. This indicates that current ACC systems are not collision and risk free yet.

The Time To Collision (TTC) was found to reduce when ACC is activated (Bianchi Piccinini et al., 2015). In this study, the participants had to react upon a stationary vehicle when they were driving on a highway. As a consequence of limitations in many ACC systems, the ACC systems are not able to react to stationary vehicles, meaning that the drivers have to react to stationary vehicles by themselves. A lower TTC represents a higher possibility of collisions. The decrease in TTC was especially found for experienced users of ACC, which can be explained by their excessive trust in the system. It should be noted that although the TTC decreases when activating ACC, there is a homogenizing effect of ACC, which is an effect of ACC that makes traffic safer.

Various studies have showed that ACC is string unstable, which means that disturbances are amplified upstream. String instability can be seen as an unwanted feature of traffic. However, human driving is also string unstable (Milanés & Shladover, 2014). CACC systems will have string stability, since the delays are minimized because of the communication added to these systems (Milanés & Shladover, 2014; van Arem et al., 2006). A positive effect on traffic safety is expected for CACC systems. Although, both ACC and CACC system will still have to be able to perform in situations with mixed traffic. An important notion by van Arem et al. (2006) is that if communication between vehicles is restricted to longitudinal control, the system has a negative effect on traffic safety in merging situations, as was also found in some ACC field tests and experienced by ACC users or testers. Other vehicles could be prevented from merging when the

distance between consecutive CACC vehicles is considered as an unsafe gap to perform a lane change, which probably leads to an increase in safety when CACC market penetrations increase. On the other hand, vehicles equipped with communication devices might be able to notify each other that they want to perform a merging action, so that a safe gap can be created by the platooning vehicles.

A field test showed that ACC users are more aware of speed limits and deliberately adjust the set speed to the maximum section speed (Gorter, 2015), which has a positive effect on traffic safety. Similar effects were found by Alkim et al. (2007) and van Twuijver & Pol (2004). This seems a clear characteristic of driving with ACC, since the same patterns were found for these systems.

1.4.2.4 Traffic flow

A wide variety of literature that study the effect of (C)ACC on traffic flow and traffic performance is available. However, the topic is not yet well understood, since results differ from substantial increases to substantial decreases (Milanés & Shladover, 2014). A reason for the differing results are the approaches and assumptions taken in every research and the differing time gap settings, road configurations, traffic demands, car following models and performance indicators used to assess the effects. There is only little research on realistic traffic situations at road sections with recurrent congestion. Especially, research is lacking on the effects of (C)ACC on traffic situations with multiple bottlenecks and weaving sections with recurrent congestion. Generally speaking, the effect of ACC systems is still uncertain, while CACC systems are expected to yield benefits in traffic flow, safety and efficiency.

String stability is also a component of traffic flow. String stability was also discussed in the subsection on safety and will not be discussed again, since string stability is not the focus of this research. The conclusion was that human driving and ACC driving show string unstable behavior, while CACC driving shows string stability. If traffic is string stable, this has a positive influence on the traffic flow.

The study of Gorter (2015) revealed that using ACC leads to more constant or homogeneous speeds. This has a positive effect on traffic flow stability, since the number of disturbances will be reduced when speeds are more constant. The same research also reports an increased, but more constant headway for ACC driving. An increased headway results in reduced capacities, while more constant headways positively result in more stable and smoother traffic. One of the main disadvantages of ACC systems is that these systems only take the direct preceding vehicle into account, while human drivers anticipate multiple vehicles ahead and in adjacent lanes, which can also be seen as one of the reasons for the differences in headways. Gorter (2015) also found a reduction in the number of lane changes when comparing ACC driving with human driving. This effect is expected to be positive, since perturbations in reality are often a result of lane changes. Ahn & Cassidy (2007) even found that all shockwaves at their studied highway were a result of lane changes. However, since the traffic demand was not set at a critical value or near capacity conditions, a lane change is the most likely reason for the occurrence of congestion.

The effects of (C)ACC on throughput and capacity are studied extensively. Currently, the effects of ACC are still uncertain, since both positive (Davis, 2004; Kesting, Treiber, Schönhof, & Helbing, 2008) and negative (Marsden et al., 2001; Milanés & Shladover, 2014) results were found in literature. Nevertheless, Kerner & Klenov (2003) might describe the occurrence of positive and negative results more effectively by stating that wide moving jams can be suppressed by ACC vehicles leading to more stabilized traffic flow, while at certain parameters and percentages of ACC, traffic flow could be influenced negatively and ACC functionality could lead to traffic breakdown and congestion occurrence at bottleneck locations. Strikingly, more recent simulation studies on ACC increasingly report that ACC will have a negative or only a small impact on traffic throughput, performance and capacity (Milanés & Shladover, 2014; Shladover et al., 2012; van Arem et al., 2006; VanderWerf, Shladover, Miller, & Kourjanskaia, 2002). With respect to CACC, mainly positive effects are found (Milanés & Shladover, 2014; van Arem et al., 2006).

In the study of Kesting et al. (2008) it was found that a 25% market penetration rate of ACC could solve all congestion. Even a 5% penetration rate showed significant improvements in traffic flow for their specific peak-period and traffic scenario. However, these improvements appear to be results of the variable speed limit and driving strategy they adopt, based on an infrastructure controller, rather than to the car-following behavior of ACC systems. The direct impacts of the ACC system on capacity were not considered. As reported by Shladover et al. (2012), there is a maximum allowed braking and acceleration rate for ACC vehicles. In their review, Shladover et al. (2012) also states that the studies by Kesting (Kesting, Treiber, & Helbing, 2010; Kesting, Treiber, Schönhof, & Helbing, 2007; Kesting et al., 2008; Kesting, Treiber, Schönhof, Kranke, & Helbing, 2007) ignore this problem and instead assume a braking rate that is higher than any real system can brake and is even double as high as the rate allowed by the ISO15622.

Most studies were based on permanent bottlenecks such as on-ramps, off-ramps, lane drops, sags or uphill and downhill gradients. In Papacharalampous et al. (2015) it was proved that (C)ACC systems improve traffic flow at sags. Both ACC and CACC show a reduction in delay time. When a traffic state adaptive (C)ACC system is used, the improvements are significantly larger. This shows the same results as the studies of Kesting. An important component of the traffic state adaptive algorithms is that the desired speed is increased when driving out of congestion, in order to be able to resolve congestion as fast as possible, which has a positive effect on the cumulated total time spent inside the network.

A study by Wang, Daamen, Hoogendoorn, & van Arem (2015) focussed on temporary bottlenecks, which are often results of accidents, roadworks or temporary changes in roadway regulations, such as variable speed limits. These bottlenecks are well-known for creating stop-and-go waves or wide moving jams, where the jam head and tail move in the upstream direction. This type of jam is highly related to deceleration and acceleration behaviors. It was found that (C)ACC systems were able to reduce the effects of these wide moving jams, and thus improve traffic flow performance. However, practical traffic situations with geometric inhomogeneities of the road, such as on- and off-ramps were not included in this research, while traffic flow effects of (C)ACC systems might differ between different types of congested states. Furthermore, Bose & Ioannou (2003) found that during stop-and-go traffic conditions, the presence of (semi-)automated vehicles results in shorter average delay in comparison with a fully manual traffic mix.

Results of Shladover et al. (2012) show that ACC systems are unlikely to yield any significant change in highway capacity, since headways are slightly larger than in human driving, even though ACC systems homogenize speeds and speed disturbances. In contrast, CACC has the potential to significantly increase highway capacity when it reaches medium to high market penetration rates, due to the increased dynamic responses and shorter headways applied. Their results show a maximum capacity of approximately 4000 vehicles per hour per lane at 100% CACC market penetration rate. The capacity benefits of CACC can be accelerated at lower market penetration rates by installing vehicle awareness devices in non-CACC vehicles in order to send information to the CACC equipped vehicles and serve as lead vehicles for CACC vehicles. Without using vehicle awareness devices in non-CACC vehicles, there is a quadratic relation between the CACC penetration rate and lane capacity, while this shape becomes linear if non-CACC vehicles are equipped with vehicle awareness devices. Additionally, small increases in capacity can be obtained when ACC penetration rates range from 0 to 50%, while decreases in capacity were found for penetration rates above 70% approximately. This effect is explained by the homogenizing effects on speed and larger headways of ACC compared to human driving. VanderWerf et al. (2002) found similar effects. This study also reviewed the effect of increasing ACC headway settings. An increase in headway obviously leads to reductions in capacity. However, this effect becomes larger at higher penetration rates.

It can be concluded that CACC is able to improve traffic flow characteristics. However, low penetration rates of CACC (< 40%) were found to have no effect on traffic flow throughput (van Arem et al., 2006), while other studies report improvements in traffic flow at only 5% market penetration rates (Wang et al.,

2015). Also, a reduction in shockwaves was found in this research. High penetration rates of above 60% were found to have benefits on traffic stability and throughput. However, it should be noted that the level of improvement relies heavily on the local traffic conditions. Especially in high traffic volumes, the situation improves, as results of reduced headway settings and improved string stability.

Some results indicate that while CACC is likely to improve traffic flow, ACC systems might even cause bigger traffic jams than human driving behavior, which is not in line with the large majority of literature (Milanés & Shladover, 2014; Shladover et al., 2012). Milanés & Shladover (2014) represented real vehicle data obtained by field tests, to describe (C)ACC driving behavior. Their simulations show that all CACC vehicles follow each other without amplifying disturbances, as was also found in their field study. This indicates increases in highway capacities and traffic flow stability. A scenario of five consecutive ACC vehicles, with a front vehicle braking from 30 to 26 m/s at a deceleration rate of 1 m/s², showed that the last vehicle had to brake to 20 m/s, indicating string instability as results of amplified disturbances. At high penetration rates, string instability might lead to reductions in highway capacity. In a scenario with mixed ACC and CACC vehicles, the unstable behavior of ACC vehicles was clearly shown, although the remaining CACC vehicles were able to reduce oscillations, providing benefits in traffic flow and stability.

1.4.3 Parameter specifications

In many literature studies, the effects of (C)ACC are analyzed by traffic simulations. Many different parameter settings were found in these studies. This section describes some settings used in literature and briefly reflects upon differences. The parameter settings from literature might be used as a reference for simulation input and are primarily included in this literature review to serve as a source of information for defining the (C)ACC driving behavior later. *Table 3* shows some parameter settings used in literature.

Table 3 - Different model parameter settings in literature

Literature	Type	Desired time gaps [s]	Comfortable acceleration [m/s ²]	Comfortable deceleration [m/s ²]	Minimum clearance [m]	Maximum deceleration [m/s ²]
van Arem et al. (2006)	ACC	1.4	2	-3	2	-3
	CACC	0.5	2	-3	2	-3
Shladover et al. (2012)	Human	1.64 (±10%)				
	ACC	2.2 (31.3%) 1.6 (18.5%) 1.1 (50.4%)	2	-2		-2
	CACC	1.1 (12%) 0.9 (7%) 0.7 (24%) 0.6 (57%)	2	-2		-2
Milanés & Shladover (2014)	ACC	1.1	1	-2	0	-2.8
	CACC	0.6	1	-2	0	-2.8
VanderWerf et al. (2002)	Human	1.1 + 0.15 σ				
	ACC	1.4				0.3g
	CACC	0.5 or 1.4				0.3g
Davis (2004)	ACC	1.0(Headway)				
Milanés & Shladover (2015)	ACC	1.1 1.6 2.2				-2.5
	CACC	0.6 0.9 1.1				-2.5
Deng & Ma (2015)	CACC	0.5	2	-3	2	

Schakel, van Arem, & Netten (2010)	AACC, CACC	1.2 ± 0.15 1.2 ± 0.30 (Headway)		-5		-5
Kesting, Treiber, Schönhof, & Helbing (2007)	ACC	1.5 (Car) 2.0 (Truck)	1.4 (Car) 0.7 (Truck)	-2	2	
Kesting, Treiber, Schönhof, Kranke, et al. (2007)	ACC	1.5	1.0	-2	2	
Bianchi Piccinini et al. (2015)		1 (Headway) 1.5 2.0 2.5	1	-3		-8.8
Pauwelussen & Feenstra (2010)	ACC	1 (Headway) 1.4 1.8 2.2 2.6 3.0		-3		-8
van Driel & van Arem (2010)	Congestion assistant	0.8 & 1.0 (stop&go traffic)	3 1.5	-5 -3		-5
Klunder et al. (2009)	ACC	1 (Headway) 1.4 1.8 2.2 2.6 3.0	3	-3		-5
Schakel & van Arem (2014)	ACC		2	-2.09		
Mullakkal-Babu, Wang, Van Arem, & Happee (2016)	ACC	1.2	1.5		3	-8

Table 3 clearly illustrates that many different (maximum) acceleration, deceleration, gap and headway parameter settings were considered in the studies on this topic. However, the choices for these parameter settings might have a significant influence on the effects of (C)ACC on traffic flow and performance found in these studies. This overview might serve as a reference when defining the inputs for the model in this research.

Additionally, it should be noted that some data from field test with ACC systems is available. This data might also be used for defining driving behavior when driving with activated (C)ACC systems more accurately, although most field test only gather results from a small mix of (C)ACC vehicles, which might not give a representative view on the variance between (C)ACC systems.

The comfortable acceleration of an ACC vehicle is often limited to acceleration rates of approximately 2 to 3 m/s², while comfortable deceleration has a value of approximately 2 or 3 m/s². The minimum clearance between vehicles in jam conditions was often found to be approximately 2 to 3 meters in the considered literature in *Table 3*. The maximum decelerations of (C)ACC vehicles differ significantly. Some studies report maximum decelerations of only 2 m/s² due to vehicle limitations, while others report maximum decelerations of 8 m/s². The headways for ACC vehicles vary from 1 to 3 seconds, with a mean of approximately 1.5 seconds. The headways of CACC were varied from approximately 0.6 to 1.2 seconds, with a mean of approximately 0.8 second. These different parameter settings might also be used as reference for this study. However, a clear explanation on which assumptions were taken and why specific parameters are selected, should be included.

1.5 Structure of the report

The structure of this report is described in this subsection. Traffic modelling in Aimsun is described in chapter 2, where a global description on the simulator, parameters and behavioral models is provided. Chapter 3 discusses the network and calibration procedure where the mesoscopic and microscopic models are calibrated. The calibrated models form the starting point of this research. A verification of ACC driving behavior is included in chapter 4, which justifies the input parameters of ACC vehicles on the basis of some characteristic driving scenarios. Chapter 5 elaborates upon the microscopic simulation scenarios and indicators used to define the effects of (C)ACC on traffic flow. Subsequently, microscopic simulation results are provided and discussed in chapter 6. An exploration on the possibilities to represent the same results and effects using mesoscopic simulation is included in chapter 7. Chapter 8 provides an overview of conclusions and recommendations, where the most important conclusions and recommendations with respect to traffic effects of (C)ACC and traffic modelling in Aimsun are presented.

2 Traffic modelling in Aimsun

Before starting simulations in Aimsun and stepping into more detail with respect to the simulation results, it is important to get a feeling for how Aimsun works and what methods can be used. This chapter will start with a general introduction to Aimsun, after which the most important features of the mesoscopic and microscopic simulation approach in Aimsun will be discussed. Subsequently, the most important parameters will be explained. Afterwards, the (most important) behavioral models for both the mesoscopic and microscopic approach will be described.

2.1 General introduction to Aimsun

Aimsun is a traffic simulation program that allows three types of dynamic simulations: a microscopic simulator, mesoscopic simulator and a hybrid simulator. These simulators can handle different traffic networks and can be used to test traffic control measures, management policies and implementations of intelligent transport systems.

The microscopic and mesoscopic simulator follow different approaches, while the hybrid simulator is a combination of both approaches, which means that a part of the network, where a high level of detail is required, could be handled microscopically, while the rest of the network could be handled using a mesoscopic approach.

In general, the required input data for simulation consists of a simulation scenario and a set of parameters to define the experiment. The simulation scenario is a combination of a network description, traffic control plans, traffic demand data and public transport plans. The traffic control plans and public transport plans are optional, while the network descriptions and traffic demand data are required for running a simulation. There are two types of simulation parameters, which can be divided into parameters that describe the experiment (e.g. simulation time) and variable parameters to calibrate the models and describe traffic behavior, at section level (e.g. lane-changing cooperation) or vehicle level (e.g. reaction time).

2.2 Microscopic and mesoscopic simulation

There are some fundamental differences between the microscopic and mesoscopic simulator in Aimsun. A description of the most important differences between the modelling types is given in this section. The information on the microscopic and mesoscopic modelling approaches originates from the Aimsun user manual (Transport Simulation Systems, 2014).

In the microscopic simulation approach, the behavior of each vehicle that travels through the network is modelled continuously throughout the simulation period, according to several behavioral models. The state changes are split into short, fixed time intervals called simulation steps. This system offers highly detailed modelling of the traffic network and can distinguish different vehicle types and drivers. The speed and location of the vehicle inside the network are calculated for every simulation step within the simulation period. Additionally, other elements, such as traffic signals and entrance points are modelled with state changes discretely at specific points in simulation time. The microscopic simulator is also able to handle these changes. The microscopic simulator combines the event scheduling approach with activity scanning.

The mesoscopic simulation approach also models the vehicle as an individual entity. However, the mesoscopic simulation approach is based on a discrete-event simulation, where each node works as a queue server for the input sections. The simulation time changes at different points in time and does not use (fixed) simulation steps. The points in time at which changes occur, are when an event is defined. Each event is defined as an instantaneous occurrence, which changes system states. The different types of events are vehicle generation, vehicle system entrance, vehicle node movements and changes in traffic

lights, statistics and traffic demand. All these events have a time and priority, which are used to sort the event list. In this type of simulation, the times at which a vehicle enters or leaves a node or section are calculated and added to the event list, while the speeds and locations at any point in time between the entrance and exit moment is not calculated and stored. For example, average section speeds are calculated by taking the length of a section divided by the vehicles section time.

Another main difference between the microscopic and mesoscopic approach is the description of vehicle movement and dynamics throughout the network. The microscopic model is able to represent driving behavior with a high level of detail. For the mesoscopic approach, the behavioral models are simplified in order to have a simulation event oriented. The mesoscopic approach has simplified behavior with a slight loss of realism. Also, many variables to describe driving behavior in microscopic models are not available in the mesoscopic models. In comparison with the microscopic model, the mesoscopic model has a slight loss of realism, but benefits from a reduction of computational efforts. This means that mesoscopic simulations are more suitable for large-size networks, since the mesoscopic simulators require less computational efforts, meaning that a lower amount of time and data is used.

Additionally, there are some minor differences between the microscopic and mesoscopic approach. The microscopic simulator is able to simulate vehicles and pedestrians at the same time, by using an embedded simulator engine called Legion, while this is not possible for the mesoscopic simulator. Also, the mesoscopic network loading translates the Aimsun network to a directed graph. As a consequence of this, having different maximum speeds at lane level is not supported, which means that the default section speed is used. In a microscopic network, maximum allowable speeds could be varied per lane. In addition, the microscopic simulation provides an animation, which shows the vehicles driving over the network, while this is not provided for the mesoscopic simulations.

Next to the differences between the simulation approaches, there are many modules and concepts that are similar or shared, such as the vehicle entrance process, network geometry, traffic demand data and control plans.

2.3 Model parameters

This subsection describes the most important parameters used in Aimsun. Basically, these parameters are used to describe simulation preferences or driving behavior of simulated vehicles.

Depending on the characteristics of the traffic that should be modelled, parameters can be set. According to the level at which the parameters are defined, the parameters are grouped into three categories:

- **Global modelling parameters:** Generally, this category consists of general parameter settings applied to all vehicle types and the whole network;
- **Local section parameters:** These parameters are related to different road sections and turnings. However, it should be noted that these parameters also affect vehicle type behavior. The local section parameters are applied locally to the vehicles driving on the respective road section or turning, but are changed when the vehicle enters a new section;
- **Vehicle attributes:** These parameters are applied at the level of a vehicle type. For these parameters, the mean, deviation, minimum and maximum values can be given for the attributes of each of the different vehicle types modelled. Then, each vehicle's characteristic is sampled from a truncated normal distribution.

The most relevant parameters for describing driving behavior will be discussed per category. In the following subsections it is also indicated whether the parameters are available in the microscopic and/or mesoscopic modelling approach.

2.3.1 Global modelling parameters

The global network parameters are defined for the entire network, simulation and each vehicle type. The most relevant global network parameters are:

- **Simulation step (micro):** This parameter defines the update interval of the microscopic simulation at which the states are updated. The simulation step should be set at a relatively low value, in order to obtain results with a higher level of detail. Lower values of the simulation step results in a higher level of detail and an increase in computation time;
- **Driver's reaction time (micro/meso):** The time a driver takes to react upon speed changes of the preceding vehicle. This value is used in the car-following model and the lane-changing model. Driver's reaction time can be fixed, which means that the parameters are the same for each vehicle type. If this parameter is set to variable, the driver's reaction times can be set for every type of vehicle by defining a discrete probability function. The driver's reaction time for microscopic and mesoscopic simulation have a slightly different meaning, since the reaction time in mesoscopic simulation should also incorporate the influences of acceleration and deceleration, which is taken into account separately in a microscopic simulation. In general, the relation between the different types of simulation is: $R_{meso} = 1.5 * R_{micro}$;
- **Reaction time at stop (micro):** The time it takes for a vehicle at standstill to react to an acceleration of the leading vehicle. This parameter could also be set to fixed or variable, as discussed before;
- **Reaction time at traffic light (micro/meso):** This parameter defines the time it takes for the first vehicle stopped at a traffic light to react upon a green light. Again, this parameter could be set to fixed or variable;
- **Two-lane car following model (micro):** It is an option to activate a two-lane car following model, in which the (desired) speed in a lane is adjusted based on speeds in adjacent lanes. If this option is used, a maximum speed difference between lanes should be given as input before starting the simulation. The parameters used for this model are the maximum number of vehicles to be considered, maximum distance, maximum speed difference and maximum speed difference at on ramp;
- **Queue speeds (micro):** The speeds at which a vehicle enters and leaves the queue. Note that this is a global parameter, which is not variable for different vehicle types;
- **Lane-changing model (micro/meso):** Both types of simulation use a different lane-changing model. However, both types make use of distance zones, which will be explained later in this report. The microscopic lane-changing model has a higher level of detail.

2.3.2 Local section parameters

The local section parameters contain many of the same parameters from the global network parameters section, but the difference is that the local section parameters are only applied to the specific road section selected. Although certain local parameters might affect vehicle behavior, they are related to road sections or turnings and are not defined on a vehicle type level, meaning that all vehicle types will use the same local section parameters. When vehicles leave the road section, the local section parameters change to the settings of the parameters for the newly entered section. The most relevant section parameters are discussed below:

- **Section maximum speed (micro/meso):** Describes the maximum allowable speed on a road section;
- **Lane-changing cooperation (micro):** The percentage of cooperation of upstream vehicles to create a large enough gap to merge and change lanes;

- **Additional reaction time at stop (micro):** Correction of the global parameter setting due to section or node characteristics;
- **Additional reaction time at traffic light (micro):** Correction of the global parameter setting due to section or node characteristics;
- **Side lane parameters (micro):** There are two side lane parameters that are used in case of an on-ramp or lane drop. The first one is the side lane cooperation distance, which defines the length from the end of the on-ramp or lane drop over which vehicles of side lanes are willing to cooperate to create a large enough gap to change lanes. Subsequently, the side lane merging distance sets the distance from which vehicles are allowed to merge onto the main road;
- **Jam density (meso):** The jam density denotes the capacity of a link. When the link reaches the jam density, it is assumed the link is full and no new vehicles can enter the link, until vehicles leave the link. This is used to indirectly model capacities in a mesoscopic model, because the jam density is a part of the definition of the fundamental diagram;
- **Reaction time factor (meso):** Local parameter for the global vehicle reaction time, to provide more flexibility in the calibration process. The standard reaction time is multiplied by the defined reaction time factor on section level;
- **Lane selection model (meso):** It is an option to penalize shared lanes and slow lanes to penalize a lane shared by multiple turnings and to model slow vehicles on slow lanes and fast vehicles on fast lanes;
- **Lane speed limits (micro):** It is also possible to model speed limits in a specific lane or to set dedicated lanes, for certain types of traffic or different speeds;
- **Increasing acceleration (micro):** It is possible to select no, medium or high increases in acceleration to improve queue discharge or to compensate for the effect of slopes, which were not taken into account in the current network, since the original model is a mesoscopic model;
- **Braking intensity (micro):** It is possible to select no, high or extreme braking intensities to influence the lane-changing behavior or to compensate for the effect of slopes, which were not taken into account in the current network;
- **Imprudent lane-changing (micro):** It is possible to select a tick box for imprudent lane-changing, which means that some vehicles might merge into non-safe gaps that are smaller compared to the normal gaps. However, it should be noted that the simulation models are constructed to be safe at any time and case;
- **Turning parameters (micro):** Several parameters used to define driving behavior on turnings can be altered, such as turning speed, distance zones (micro), distance zone variability (meso) and additional waiting times before losing a turn. In this research, the turning speeds and distance zones are important for defining lane-changing behavior at weaving sections.

2.3.3 Vehicle attributes

These parameters are defined per vehicle type. The mean values, as well as the deviations, maximum and minimum values can be given. The characteristics of a vehicle are sampled from a truncated normal distribution. Several relevant vehicle attributes are discussed below:

- **Length (micro/meso):** This parameter refers to the length of a vehicle. This parameter is used for graphical and modelling purposes. Vehicle length has an influence on the car-following behavior. This parameter is also used to draw the size of vehicles and visualize the vehicles in an animated microscopic simulation;
- **Width (micro):** This parameter relates to the width of a vehicle, but is only used for graphical purposes;
- **Maximum desired speed (micro/meso):** The maximum speed that this vehicle type would like to travel at any point in the network. Usually, this parameter is set to the desired speed of users of this vehicle type on the freeway;

- **Speed acceptance (micro/meso):** This parameter relates to the degree of acceptance of speed limits. The maximum desired speed of a vehicle at any point inside the network is either the maximum desired speed of that vehicle or the speed acceptance multiplied with the maximum speed on the specific road section the vehicle is driving;
- **Clearance (micro/meso):** This parameter refers to the distance between the own vehicle and preceding vehicle at standstill. This parameter has a direct influence on the car-following behavior and critical density;
- **Maximum give-way time (micro/meso):** When a vehicle has been at a standstill for more than the give-way time (in seconds), it will become more aggressive and will reduce the acceptance margins. However, this parameter will hardly have any influence in this study, since the research network mainly consists of highways;
- **Guidance acceptance (micro/meso):** This parameter defines the level of compliance of this vehicle type with guidance instructions;
- **Maximum acceleration (micro):** This parameter defines the maximum acceleration a vehicle can achieve under any conditions, which has a significant effect on the driving behavior;
- **Normal deceleration (micro):** This parameter reflects the maximum deceleration a vehicle driver wishes to use in normal conditions. This parameter is also important for describing driving behavior;
- **Maximum deceleration (micro):** The most severe braking rate that a vehicle type can apply. This is a physical vehicle property;
- **Sensitivity factor (micro):** The sensitivity factor in the deceleration component of the car-following model. This parameter basically defines the estimation of the (desired) deceleration of the preceding vehicle;
- **Gap (micro):** Setting this parameter ensures a minimum (time) headway between the leader and follower. Please note the difference between gap and headway, since the gap is the distance from the rear bumper of the leading vehicle towards the front bumper of the preceding vehicles, while the headway defines the distance between the front bumpers of both vehicles. In the vehicle attributes and manual (Transport Simulation Systems, 2014), this parameter is described as a gap. While some simulation tests have proven that this parameter actually defines the headway between 2 consecutive vehicles. This was found in a simulation of a homogeneous road section with a homogeneous maximum speed, where all simulated vehicles had the same parameters, including a gap setting of 1.4 seconds. The headways were computed at different points on the test network by storing detector data. The detector data proved that the headways between the consecutive vehicles were 1.4 seconds. Note that this indicates that improper terminology was used and that the vehicle parameter gap, is actually an headway;
- **Staying in overtaking lane (micro):** A tick-box could be selected to define vehicles that stay in a fast lane instead of recovering to a slower lane;
- **Imprudent lane-changing (micro):** A tick-box could be selected to define vehicles that will apply a lane change in a non-safe gap;
- **Experiment defaults (micro/meso):** The experiment defaults regarding the reaction times for both microscopic and mesoscopic simulation could be selected. However, these parameters are defined and overruled in the global modelling parameters of a scenario. Thus, the parameters defined in the global modelling parameters are decisive.

2.4 Microscopic behavioral models

This section will describe the most important behavioral models for microscopic simulations in Aimsun. First, the car-following model will be explained, after which the lane-changing model will be discussed. The information used to discuss all these models was deduced from the Aimsun manual (Transport Simulation Systems, 2014).

2.4.1 Car-following model

The car-following model implemented in Aimsun is a development of the empirical Gipps model (Gipps, 1981, 1986b), in which the model parameters are not global, but determined by local parameters depending on the type of driver, vehicle class, roadside geometry, speed limits and some more. The Gipps model was constructed empirically to represent human driving behavior.

It is important to note that the car-following model of Gipps can be categorized as a safety distance or collision avoidance model (Brackstone & McDonald, 1999), which means that the car-following model will always adapt speeds of following vehicles in such a way that collisions will be avoided, based on maximum desired acceleration and deceleration rates. Therefore, it is not possible to draw conclusions on increases or decreases in the frequencies of collisions. In reality, collisions and accidents occur on a frequent basis.

The car-following model is based on acceleration and deceleration as main components. The acceleration component represents the will to reach a certain desired speed. The deceleration component is representing the restriction on reaching the desired speed due to driving speeds of preceding vehicles. The longitudinal car-following behavior is explained in the text below.

The speed to which a vehicle can accelerate at maximum during a time period is defined by:

$$V_a(n, t + T) = V(n, t) + 2.5 a(n) T \left(1 - \frac{V(n, t)}{V^*(n)}\right) \sqrt{0.025 + \frac{V(n, t)}{V^*(n)}}$$

Where:

- $V(n, t)$ is the speed of vehicle n at time t;
- $a(n)$ is the maximum acceleration for vehicle n;
- T is the reaction time;
- $V^*(n)$ is the desired speed of vehicle n at the specific road section.

Note that the desired speed of a vehicle at a specific road section equals the minimum of the maximum desired speed of the respective vehicle and the speed acceptance of that vehicle multiplied with the maximum section speed.

The maximum speed the vehicle can reach during the same time interval is also restricted due to its own characteristics and the limitations imposed by the presence of a leading vehicle (n-1). The maximum speed as a consequence of this constraint is given by:

$$V_b(n, t + T) = d(n) T + \sqrt{d(n)^2 T^2 - d(n) \left[2\{x(n-1, t) - s(n-1) - x(n, t)\} - V(n, t) T - \frac{V(n-1, t)^2}{d'(n-1)} \right]}$$

Where:

- $d(n)$ is the maximum deceleration desired of vehicle n (< 0);
- $x(n-1, t)$ is the position of the preceding vehicle (n-1) at time t;
- $s(n-1)$ is the effective length of the preceding vehicle (n-1);
- $x(n, t)$ is the position of vehicle n at time t;
- $V(n-1, t)$ is the speed of vehicle (n-1) at time t;
- $d'(n-1)$ is an estimation of the preceding vehicle (n-1) desired deceleration.

The estimation of the preceding vehicle (n-1) desired deceleration is determined by:

$$d'(n - 1) = \alpha * d(n - 1)$$

Where:

α represents the sensitivity factor. When $\alpha < 1$, the deceleration of the leader is underestimated, while $\alpha > 1$ means that the deceleration of the leading vehicle is overestimated;
 $d(n - 1)$ is the actual desired deceleration of the lead vehicle.

The speed of vehicle n during time interval (t, t+T) is defined by:

$$V(n, t + T) = \min\{V_a(n, t + T), V_b(n, t + T)\}$$

Additionally, there is a constraint on the minimum headway, which is applied by:

$$\text{If } x(n - 1, t + T) - [x(n, t) + V(n, t + T) * T] < V(n, t + T) * \text{MinHW}(n)$$

$$\text{Then } V(n, t + T) = (x(n - 1, t + T) - x(n, t)) / (\text{MinHW}(n) + T)$$

Where:

$x(n - 1, t + T)$ is the position of the preceding vehicle at time $t + T$;
 $\text{MinHW}(n)$ is the minimum headway of vehicle n with respect to the preceding vehicle;
 $x(n, t)$ is the position of vehicle n at time t.

In the formula above, it is important to note that the minimum headway is actually compensated to a minimum time gap, since the goal is to prevent head to tail collisions. Subsequently, the new position of the vehicle is given by:

$$x(n, t + T) = x(n, t) + V(n, t + T) * T$$

It should be noted that it is also possible to select a two-lane car-following model, which adapts the desired speed in a lane based on the speed in adjacent lanes. If this is the case, this influence is taken into account in the $V^*(n)$ component in the formula for deciding the speed to which a vehicle can accelerate at maximum during a time period (represented by: $V_a(n, t + T)$).

2.4.2 Lane-changing model

The model for lane-changing is also considered as a development of the Gipps lane-changing model (Gipps, 1986a, 1986b). The lane-changing model can be considered as a decision process, in which the necessity of the lane change, the desirability of the lane change and the feasibility conditions for the lane change are taken into consideration. There are many different components of the lane-changing model, which will be discussed in subsections.

2.4.2.1 Decision model

The decision model makes an approximation of the behavior of the driver by asking the following questions:

- **Is it necessary to change lanes?** The answer of this question depends on the turning feasibility in the current lane, the distance to the next turning and the traffic conditions in the current lane. These traffic conditions are calculated in speed and queue length. If a driver is driving slower than its desired speed, the driver would try to overtake. While drivers travelling at desired speeds tend to retrieve back to the slower lane. If the answer to this question is yes, there are two more questions to be answered;
- **Is it desirable to change lanes?** For answering this question, it is checked whether there will be any improvements in traffic conditions as a results of changing lanes, measured in terms of speed

- and distance. If either the speed of the new lane is fast enough or the queue is short enough, a lane change is desirable;
- **Is it possible to change lanes?** In order to answer this question, it should be verified that there is a safe gap to make a lane change. The braking imposed by the lane-changing vehicle to the new downstream and upstream vehicle is calculated. When braking/acceleration ratios are found to be within acceptable margins, it is possible to change lanes.

The previous text did only explain the very basics of the lane-changing model. However, there are some important components and calculations used for answering these lane-changing questions. The lane-changing model contains the following elements in microscopic simulation: Lane-changing zones calculation, target lanes calculation, vehicle behavior considering the target lanes, gap acceptance model and the target gap and cooperation. The following subsections will elaborate upon the elements incorporated in the lane-changing model.

2.4.2.2 Lane-changing zones calculation

Three different lane-changing zones are considered to represent the driving behavior in the lane-changing process more accurately. There are three different lane-changing zones, where every zone has a different motivation for applying lane changes:

- **Lane-changing zone 1:** In this zone, the decisions to change lanes are dominantly governed by the traffic conditions on the respective lanes. Several parameters, such as desired speed, the speed of the leading vehicle in the current and destination lane, are used to measure the improvement the driver will get from applying a change of lanes;
- **Lane-changing zone 2:** Basically, this zone could be seen as an intermediate zone between lane-changing zones 1 and 3. This zone is used for vehicles that are not driving in a valid lane yet, but will be changing lanes toward the valid lane if a safe gap is available. Valid lanes are lanes where it is possible to make the desired turning movement. In this zone, drivers tend to get closer to the valid lanes from which the turn is allowed and will be looking for a gap by trying to adapt to possible gaps downstream or adjacent;
- **Lane-changing zone 3:** This zone could be considered as some kind of critical lane-changing zone. In this zone, vehicles are forced to reach their valid lane, which means that they are looking for gaps and will reduce speed if necessary. If there are no safe possible gaps, these vehicles could even come to a complete stop in order to make it possible to change lanes.

In a microscopic simulation, these lane-changing zones are calculated by using the distance zones, defined in the turning and the distance zone variability. Distance zone 1 and distance zone 2 could differ per turning. In general, distance zone 1 is set in the range near 600 meters, while distance zone 2 is set in the range near 100 meters. The distance from the turn to the value of distance zone 2 in front of the turning belongs to lane-changing zone 3. The range between distance zone 1 and 2 in front a turn is part of lane-changing zone 2. While all points that are further upstream of the turning than the distance zone 1 setting, belong to lane-changing zone 3. The distance zone variability has been set to 40%, which means that there is a 40% distribution over the distance zones for all vehicles using a uniform distribution. When a distance zone is set to 100 meters, values for separate vehicles could range between 80 to 120 meters ($100 \pm 20\%$). When the distance zones are set to 100 and 600 meters, the first 100 meters are within distance zone 3. The next 500 meters (i.e. 600-100) belong to distance zone 2, while every location further upstream belongs to distance zone 1.

2.4.2.3 Target lanes calculation and corresponding vehicle behavior

By now, each vehicle should have a perception of the distance zones, which means that the lane-changing process can start by calculating the valid target lanes (or valid lanes, as these were called in the previous subsections) according the current traffic conditions and the feasible lanes for reaching the

turning according to the path plan. The output of the calculation consists of two sets. There is one set of valid lanes for lane-changing zone 3 (TL3) and one set for lane-changing zone 2 (TL2).

The vehicle will compute the type of behavior according to the current lane and the valid target lanes. At this moment, multiple if-then loops are used to define the behavior. The following paragraphs will describe the logic behind the corresponding vehicle behavior.

If the current lane of the vehicle is not within the set of valid target lanes as defined by zone 3 (TL3), the lane-changing behavior is defined by zone 3. If the current lane of the vehicle is within the set of valid lanes determined by zone 3, but outside the set of valid lanes determined by zone 2, the vehicle behavior is defined by zone 2. If the vehicle is currently driving in a lane that is within both sets, the lane-changing behavior is defined by zone 1. In general, if a vehicle is in a valid lane as determined by zone 2 and 3, the behavior is modelled as zone 1.

The general idea behind this logic is that every vehicle attempts to reach a valid lane, defined by either zone 2 or 3. Once the current lane of the vehicle is inside the set of valid lanes, the behavior will be determined by lane-changing zone 1.

2.4.2.4 Gap acceptance model

The gap acceptance model describes which gaps are acceptable to apply a lane change. The gap model follows the logic of the model as presented by Gipps (Gipps, 1986a, 1986b). The gap acceptance model has full consistency with the car-following model, which is a requirement in order to avoid artificial breakdowns during simulation. The gap acceptance model is defined as follows:

$$V_n(t + \tau_n) = b_n \tau_n + \sqrt{(b_n \tau_n)^2 - b_n \left[2(x_l(t) - x_n(t) - l_l - s_n) - V_n(t) \tau_n - \frac{V_l(t)^2}{b_l} \right]}$$

$$Gap(t) = (x_l(t) - x_n(t) - l_l - s_n) = \frac{V_l^2(t)}{2b_l} - \frac{V_n^2(t + \tau_n)}{2b_n} + (0.5V_n(t) + V_n(t + \tau_n))\tau_n$$

Where:

$V_n(t + \tau_n)$ is the maximum safe speed for vehicle n with respect to the leading vehicle at time $(t + \tau_n)$;

$V_n(t)$ is the speed of vehicle n at time t;

b_n is the maximum desired braking rate vehicle n would like to apply;

τ_n is the time step between consecutive calculations of speed and position (time step);

$x_l(t)$ is the position of the leading vehicle at time t;

$x_n(t)$ is the position of vehicle n at time t;

l_l is the length of the leading vehicle;

s_n is the minimum spacing in front of vehicle n at standstill;

$V_l(t)$ is the speed of the leading vehicle at time t;

b_l is an estimate of the maximum desired braking rate the leading vehicle would like to apply;

$Gap(t)$ is the minimum gap according to the gap acceptance model.

It should be noted that the Gipps car following model is stable in the sense that there is no need to use decelerations above the maximum desired deceleration (Transport Simulation Systems, 2014), which equals to αb_n , where b_n is the maximum desired deceleration for vehicle n and α refers to an aggressiveness parameter, which is set to 1 by default. It should be noted that the only exception is when the minimum headway constraint is severely exceeded or when artificial tricks are used. As a result of the model stability, the constraint to the minimum speed achievable becomes:

$$V_n(t + \tau_n) \geq \text{Max}(V_n(t) + \alpha b_n \tau_n; 0)$$

Applying this constraint to the gap function gives the following:

$$\text{Gap}(t) \geq \frac{V_l^2(t)}{2b_l} + 0.5 V_n(t) \tau_n + \text{Max} \left[0, -\frac{V_n^2(t)}{2b_n} + (1 - 0.5\alpha)\alpha b_n \tau_n^2 + (1 - \alpha) V_n(t)\tau_n \right]$$

However, another constraint should be applied, because the model should be crash free, which will be the case if the gap remains positive all over the deceleration process. This results in:

$$\text{Gap}(t) \geq \text{Max} \left[\frac{V_l^2(t)}{2b_l} + 0.5 V_n(t) \tau_n + \text{Max} \left[0, -\frac{V_n^2(t)}{2b_n} + (1 - 0.5\alpha)\alpha b_n \tau_n^2 + (1 - \alpha) V_n(t)\tau_n \right], 0 \right]$$

This is the condition that has to be fulfilled to fulfill the Gipps car-following model after changing lanes. Applying this formula ensures that there is a safe and positive gap with a new leader after the vehicle has changed lanes. Thus, the gap is acceptable if the gaps are positive, the computed speeds are positive and the decelerations found are smaller than αb_n .

The gap equation is applicable to upstream and downstream gaps. However, one should pay attention to what vehicle is defined as leading vehicle. In the following formula, the subscripts up and DW are used for either the respective upstream or downstream vehicle to be taken into consideration to apply the lane change. The following formulas show the gap equations in case of an upstream and downstream gap:

$$\text{Gap}_{up}(t) \geq \text{Max} \left[\frac{V_n^2(t)}{2b_n} + 0.5 V_{up}(t) \tau_{up} + \text{Max} \left[0, -\frac{V_{up}^2(t)}{2b_{up}} + (1 - 0.5\alpha_{up})\alpha_{up} b_{up} \tau_{up}^2 + (1 - \alpha_{up}) V_{up}(t)\tau_{up} \right], 0 \right]$$

$$\text{Gap}_{DW}(t) \geq \text{Max} \left[\frac{V_{DW}^2(t)}{2b_{DW}} + 0.5 V_n(t) \tau_n + \text{Max} \left[0, -\frac{V_n^2(t)}{2b_n} + (1 - 0.5\alpha_{DW})\alpha_{DW} b_n \tau_n^2 + (1 - \alpha_{DW}) V_n(t)\tau_n \right], 0 \right]$$

2.4.2.5 Target gap and cooperation

One of the section parameters defines the degree of cooperation between vehicles, which defines to what extent drivers are willing to help creating safe gaps for other vehicles, so these vehicles can change lanes. The cooperating vehicle could adapt the speed at which it is driving, which will make it easier for the vehicles that would like to change lanes.

2.5 Mesoscopic behavioral models

This section will describe the most important behavioral models in the mesoscopic simulation model. First, the car-following model will be explained, after which the lane-changing model will be discussed briefly. It is important to note that the mesoscopic behavioral models are simplifications of the microscopic models.

2.5.1 Car-following model

The mesoscopic car-following model in Aimsun is a simplification of the microscopic car-following model of Gipps (Gipps, 1981, 1986b). In the mesoscopic model, the maximum accelerations and decelerations of the vehicles are not taken into consideration, which means that all vehicles reach their desired speeds instantaneously. The car-following model is described by:

$$x(n, t) = \min[x(n, t - R) + VR, x(n - 1, t - R) - L]$$

Where:

$x(n, t)$ is the location of vehicle n at time t ;

R is the reaction time;

V is the maximum speed;

L is the effective length (vehicle length + minimum distance between vehicles).

Where the maximum speed is defined by the maximum desired speed of the vehicle or the speed limit at the considered road section multiplied with the speed acceptance of the respective vehicle. This definition of maximum speed is similar to the microscopic definition.

The car-following model is written to give the time at which vehicles exit the road section, meaning that the algorithm is inverted from speed to time. Hence, this ensures that the formula can be used in an event-based simulation. The first term of the car-following algorithm checks that the vehicle is not driving above maximum desired speed, while the second term is used to avoid collisions with preceding vehicles. This car-following model produces a triangular flow-density diagram, which can be described by:

$$Q(k) = \min\left(Vk, \frac{1}{R}(1 - Lk)\right)$$

Where:

$Q(k)$ is the flow;

k is the density.

The first term in the formula represents the free flow branch of the (triangular) fundamental diagram, while the second term represents the congested branch of the fundamental diagram. Additionally, from this equation it becomes clear that the flow is zero for $k=0$ and $k=1/L$, which represents the jam density. The propagation of the jam wave in upstream direction has a slope of $-L/R$. The maximum flow (theoretical section capacity) and critical density at a section could be computed and are given by:

$$Q_{max} = \frac{1}{R + \frac{1}{Vk_{jam}}}$$

$$k_{crit} = \frac{1}{VR + \frac{1}{k_{jam}}}$$

Where:

k_{jam} is the jam density of the section;

V is the maximum speed;

R is the reaction in a section ($R = R_{experiment} * R_{factor}$), which corresponds to the reaction time defined at experiment level multiplied by the reaction time factor at section level.

2.5.2 Lane-changing model

The mesoscopic lane-changing model is a simplification of the microscopic model, but is structured in a similar manner. First, the default lane and permitted section departure lanes are calculated. Then, the valid lanes are calculated, based on the look-ahead distance and look-ahead distance variability defined.

Subsequently, the next departure lane, based on the current lane and a set of valid lanes, is calculated using a discrete choice model based on a utility based logit function. The exact algorithm and weights of

the components are unknown. It is known that the lane-changing model is based on penalties. The different components that influence the utility function are known.

The first component is the density of a lane. A higher density applies a higher penalty to the utility function for changing towards this lane. The second component is the number of lane changes required to reach the considered lane. The higher the number of lane changes required, the higher the penalization. Additionally, penalties could be applied if the considered lane is a slow or shared lane. This could be done by selecting the tick boxes at section level. A lane is shared if the lane is used for two or more turnings.

3 Calibration and validation

The calibration and validation steps used for this research are discussed in this chapter. The chapter starts with the network configuration, which introduces the research network used in this study. Subsequently, an elaboration on the preparatory work is given, which was conducted before starting this research. Subsequently, the calibration process and the steps conducted within this calibration process are explained. A validation check on the calibrated microscopic and mesoscopic simulation results have been added to the calibration process to check the validity of the calibrated simulation results.

3.1 Network configuration

Regarding the network configuration, it is required to select a network with multiple bottlenecks in order to investigate the effects of ACC and CACC in realistic traffic situations. Congestion is often found at large highway junctions, which usually consist of multiple weaving sections, on- and off-ramps. Therefore, highway junctions are interesting locations to investigate the effects of ACC and CACC. Additionally, research on highways seems to be of more value in comparison with lower level road types.

There is a network available of the city and surroundings of Rotterdam, which was developed for a project at RHDHV and commissioned by the Port of Rotterdam. This network was calibrated for mesoscopic simulations in this project and is considered to be a sufficiently realistic presentation of reality. An impression of this network is shown in *Figure 3*, where dark grey lines refer to road sections that are inside the model, while light grey lines refer to road sections that are not included in the model. The red square indicates the subnetwork used in this study.



Figure 3 - Aimsun model of the Rotterdam area (RHDHV)

Subsequently, a cut-out was taken from the Rotterdam area network in order to receive the subnetwork. *Figure 4* shows the subnetwork, used for this study, in Aimsun. The black lines refer to road sections or links, the dotted green line shows the network boundaries and the circles with a blue dot inside refer to the centroids or in- and output locations of the network.

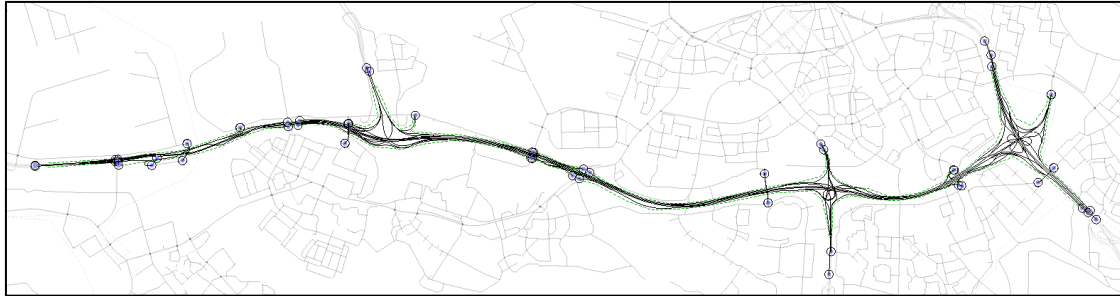


Figure 4 - Research network in Aimsun

The research network consists of a road stretch of the A15 and contains three large junctions (Ridderkerk, Vaanplein and Benelux, from East to West). All these junctions are well-known locations for congestion, which occurs on a regular basis. This road section is of vital importance for the Port of Rotterdam, since a large share of port-related traffic uses this road section as part of their route between the port of Rotterdam and the hinterland.

3.2 Preparatory work

The research network and corresponding traffic demand is a cut-out of a network and traffic demand model that has already been calibrated. This section explains the preparatory work that was performed (by others) before the research network and corresponding traffic demand model was delivered to start this study. Hence, the preparatory work is not part of this research, but is essential for the understanding of the model and the data used to establish the traffic demand matrices. An overview of the preparatory work is given in Figure 5.

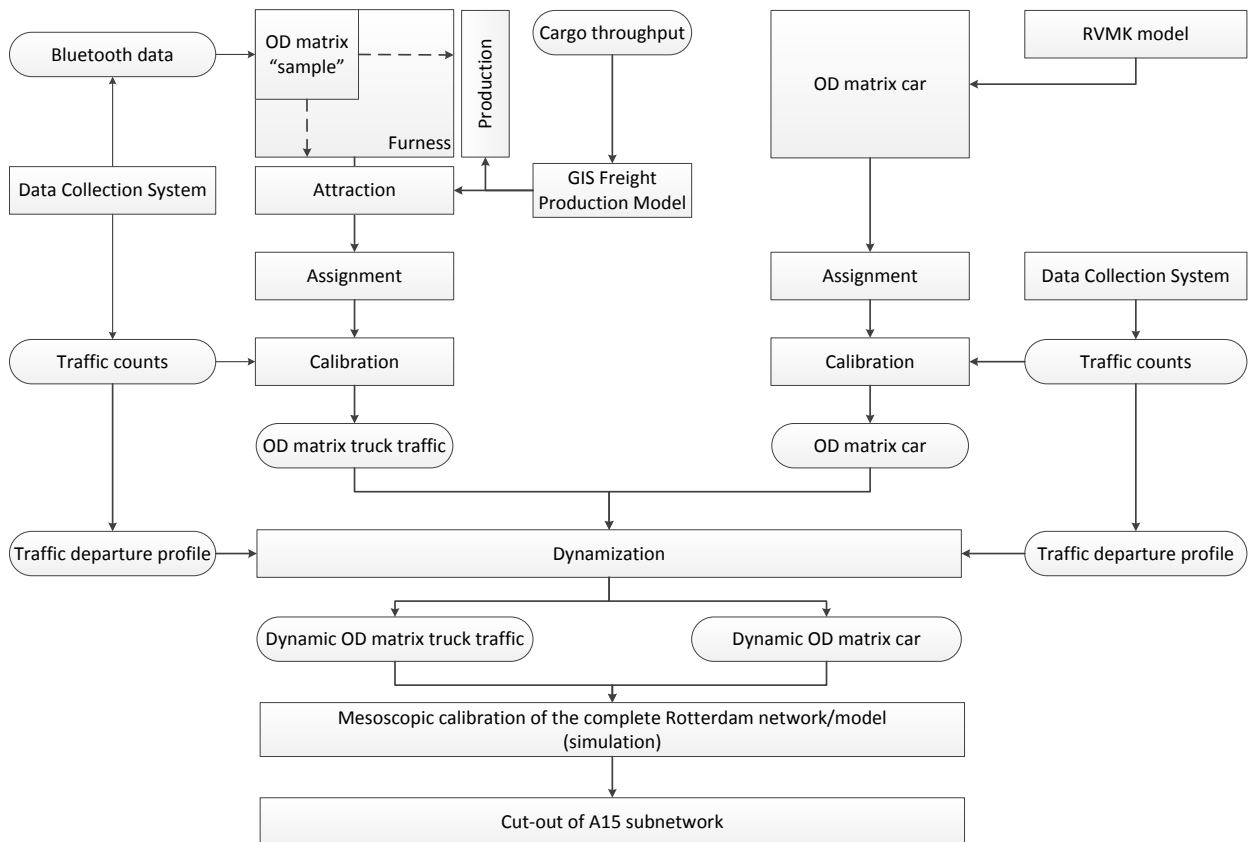


Figure 5 - Overview of preparatory work

Figure 5 shows the generation of the truck OD-matrices on the left side, while the generation of the car OD-matrices is shown at the other side of the figure.

The OD-matrix for truck traffic was derived from different sources of data. The traffic production and attraction has been calculated based on cargo throughput, using a freight production model. The distribution of truck traffic over the origin and destinations was determined from Bluetooth data. The OD-matrix was depicted by applying a Furness-method, after which this matrix has been assigned in Aimsun and calibrated, based on hourly truck traffic flows, resulting in a calibrated OD matrix for truck traffic.

The car OD-matrix was directly imported from the RVMK model. RVMK is a Dutch name for regional traffic and environment map (Regionale Verkeers- en MilieuKaart), where different scenarios of current and future traffic flows are simulated to determine the effects on environment. This matrix has been assigned and calibrated, based on hourly traffic flows, which resulted in a calibrated OD-matrix for car traffic.

Subsequently, the OD-matrices for cars and trucks were made dynamic, which divided the matrices into multiple matrices with time intervals of 15 minutes. This dynamization has been performed based on traffic departure profiles that were depicted from traffic counts. This dynamization procedure resulted in dynamic OD matrices for cars and trucks over time.

Again, these matrices were assigned to Aimsun using mesoscopic simulation and calibrated on typical congestion patterns. These matrices were cut out for the subnetwork that only contains a part of the A15. Additionally, the corresponding traffic demand over this road stretch was depicted and added to the simulation model of the research network. This was the starting point of this research.

3.3 Calibration process

For this research, an additional calibration process is required, since this will be the basis for assessing the effects of ACC and CACC. The calibration process is divided into different steps. It is important to have an insight into the logic of the calibration procedure. The calibration process is discussed here.

Many different approaches can be used with respect to the calibration process. However, it is important to keep the research objective in mind. For this research, it is important to make sure that the reference scenario provides an accurate representation of the congestion found on the network in reality. Therefore, typical traffic patterns from Google (2016) are considered to be a good source of information, because these traffic patterns gives a quick and fairly accurate view on the location and length of congestion over time.

A practical procedure for the calibration of microscopic traffic simulation models was designed by Hourdakis, Michalopoulos, & Kottommannil (2003). Their calibration procedure was primarily developed for freeways. Their calibration is performed based on two main stages of traffic volume and traffic speed and an optional stage to fine-tune the model for the specific purpose of simulation. Also, Madi (2016) performed a calibration based on vehicle dynamics, traffic volume and traffic speeds. For this research, the vehicle dynamics of the car are considered to be calibrated before, since these were depicted from standard mesoscopic and microscopic templates used at RHDHV.

In addition, Jha et al. (2004) performs a validation after calibration. In this study, new data that was not used for the calibration was used to perform a validation check on travel times. However, other types of data such as traffic flows, traffic speeds or congestion lengths could also be used.

The calibration process used and designed for this research is shown in *Figure 6*, which gives an overview of the calibration process and the different steps involved. This calibration procedure is mainly based on traffic flows and traffic speeds, as described by Hourdakis et al. (2003).

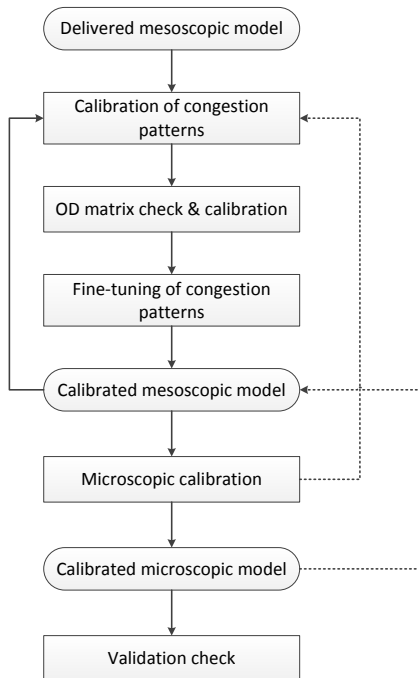


Figure 6 - Calibration process

First, the delivered mesoscopic model as discussed in section 3.2 is used as a starting point. At this stage, the base year for the OD-matrix and network has to be chosen, as well as some initial simulation settings.

Next, the mesoscopic model will be calibrated, based on typical congestion patterns from Google (2016). This step is mainly based on traffic speed. Then, the OD-matrix should be checked and calibrated to resemble representative traffic volumes, which will be done by comparing simulation flows with traffic counts. Afterwards, some fine-tuning of the congestion patterns is probably necessary and should be conducted. When this part is finished, the mesoscopic model has been calibrated. However, when it is found that the model has not been calibrated to a sufficient level, these calibration steps should be performed again, which has been visualized by a feedback loop in *Figure 6*.

It was chosen to start with calibrating the mesoscopic model, which is a clear step, since the original model was a mesoscopic model as well. However, a significant part of this study is based on the microscopic model, which means that the microscopic model should be calibrated after the mesoscopic model. The path assignment from mesoscopic simulation is saved and used as input for the microscopic simulation, which results in comparable path assignments.

Subsequently, the microscopic simulation should be calibrated, based on the same congestion patterns. It might be possible that small changes to the network are necessary, which could theoretically lead to changes in the mesoscopic model. In *Figure 6*, a dotted feedback loop has been included to show this effect.

When the microscopic calibration has been completed, a calibrated microscopic model has been obtained. However, the path assignments from the mesoscopic model were used as input for the microscopic model, which means that the mesoscopic simulation might have to be ran again, to update the path assignments that serve as input for the microscopic model. Again, this has been visualized using a dotted feedback loop in *Figure 6*.

When the calibration is completed, a validation check will be performed, based on traffic flow and speed data from loop detectors. As discussed by (Jha et al., 2004), it is important that the validation data was not used for performing the calibration. In order to read the loop detector data, an application (Dataack) was used.

All the different steps from *Figure 6* are discussed in more detail in the following subsections.

3.3.1 Delivered mesoscopic model

Initially, OD-matrices were available for three different base years (2014, 2020 and 2030). The delivered model contained an OD-matrix for the year 2020 of the evening peak period. The OD-matrix of 2020 was chosen, because this matrix was considered to fit the current traffic situation best, since the influences of the extended A4 are incorporated in these OD-matrices, which is not the case in the OD-matrices of 2014. The OD-matrix contains data of an evening peak from 14:00 up and to including 19:30, which is divided in blocks of 15 minutes. The OD-matrix of 2020 was deducted by using the calibrated 2014 matrix and increasing the traffic by approximately one percent per year, with the exception of some origins and destinations with higher or lower growth percentages. After some test simulation runs, it was quickly found that the traffic demand was approximately 5% higher than the available traffic counts of 2014. Thus, it was decided to distract 5% from this OD-matrix, which quickly improved the results.

The (expected) network lay-outs of 2014, 2020 and 2030 were also available to choose. In this case, the network lay-out of 2014 was chosen, since this network resembles the current network to a very high extent. In the 2020 network, additional lanes are available at several points in the network, which is not the case on the actual network nowadays. Therefore, the network of 2014 is the best choice.

Subsequently, some mesoscopic parameters have to be defined in order to be able to run mesoscopic simulations. The most important parameter for mesoscopic simulation are the jam density and reaction time factor, which are both set at the level of a road section. The jam density defines the capacity of a link. When a lane reaches the jam density, no more vehicles can enter the lane until vehicles leave. The reaction time factor is a local section parameter for the global vehicle reaction time. The default jam density was set to 160 vehicles per kilometer, which can be considered as an achievable jam density on highways and roads in general. In mesoscopic models at RHDHV, the mesoscopic reaction time is usually set to 1.2 seconds for cars and 1.6 seconds for trucks. The reaction time factor is a section parameter, which describes the multiplication factor of the default reaction time as a section characteristic. The reaction time factor usually ranges from a minimum of 0.7 to a maximum of 1.2 seconds. Some sections had an initial reaction time factor below 0.7 or above 1.2, which is quite extreme and therefore not desirable. These extreme values are fixed at 0.7 or 1.2, in order to make sure that all links have a realistic reaction time factor between 0.7 and 1.2.

With respect to the lane-changing parameters at experiment level, the look-ahead distance variability has been set to a default value of 80% which corresponds to a look-ahead distance for vehicles that varies between 600 and 1400 meters for a mean look-ahead distance of 1000 meters.

3.3.2 Calibration of congestion patterns

A stochastic (one-shot) simulation was ran in order to check the congestion patterns, based on a typical traffic pattern as defined by Google (2016), which is based on the speed reduction of an average vehicle on a road section in comparison with the maximum speed on this section. The simulation results were computed in the simulation run and can be compared by using a view mode, which produces the same type of results as the Google (2016) typical traffic plots. The simulation results were not representing the typical congestion patterns to a sufficient extent, which meant that some model parameters had to be changed multiple times. The biggest problem was that the congestion was not always found on the right

locations. Therefore, the sections reaction time factors were changed in order to get the congestion on the right locations. The logic of changing the reaction time factors is as follows: an increase in the reaction time factor leads to an increase of congestion severity and duration on the upstream link, which might cause or increase spillback of congestion. A decrease in the reaction time factor leads to a decrease of congestion severity and duration on the upstream link, which might prevent or decrease the spillback of congestion. However, applying this logic did not lead to satisfactory results yet. The congestion patterns obtained from simulation still significantly differ from the congestion patterns found by Google (2016).

Figure 7 shows the comparison of the congestion patterns in reality and found in simulation. The percentages show the speed reduction in terms of average vehicle speed with respect to the section maximum speed. Sections highlighted in yellow have a speed reduction between 10 to 25%. Links highlighted in yellow are not really congested, but could be close to capacity conditions.

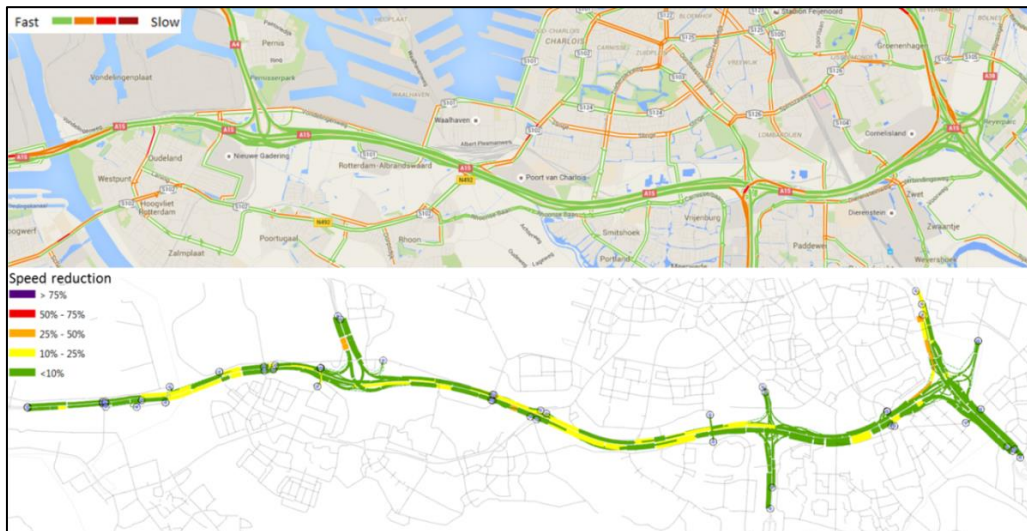


Figure 7 - Congestion patterns before dynamic matrix calibration procedure: Google (2016) for a random day (top) vs. simulation (bottom) at 17:00

3.3.3 OD matrix check & calibration

The flows obtained by the simulation were compared with the actual traffic flows of 2014 recorded by National Data Warehouse (NDW) for traffic information (National Data Warehouse for traffic information, 2014). The simulation results differed from the recorded traffic flow data. The traffic counts of 2014 were used, because average yearly traffic counts for 2016 were not available yet and the traffic counts of 2015 were insignificant due to road maintenance that was conducted during this year at multiple locations in the network. Some adaptations to the OD-matrices were required. Therefore, the vehicle flows at some critical links were compared with traffic counts from these links. It was found that some of the link flows significantly differed with the traffic data (National Data Warehouse for traffic information, 2014). As an example, the data and location of link 645267 (in Aimsun) at this step of the calibration is shown in Table 4 and Figure 8. Link 645267 is the link that defines the input flow from the north of junction Ridderkerk. Table 4 points out that there are significant differences between the flows found in simulation and the traffic counts. The large deviations at the start and end of the simulation period occur, because some time is needed to fill and clear the network. Values in Table 4 are in vehicles per hour, while the time periods are divided into blocks of 15 minutes.

To indicate how the model fits the traffic data, the R^2 statistic is used. The coefficient of determination [R^2] is a statistic that gives information about the goodness of fit of a model. An R^2 of 1 indicates that the model fits the data perfectly, while a R^2 of 0 indicates no fit between model and data. Values of R^2 range from 0

to 1 and represent the proportion of the variance in the measured data that can be explained by the model. Higher values indicate less error variance. In general, R^2 values above 50% are considered to be acceptable (Moriassi et al., 2007), although this depends on the type of study that is conducted. *Table 4* shows that the R^2 value is 0.036, which means that only 3.6% of the variability in the simulation results can be explained by the traffic data. In order to improve the goodness of fit of the flows, adaptations to the OD-matrices have to be made, which directly influences the number of vehicles driving over the network. In addition, this also directly influences the traffic flow conditions and could either increase or decrease the amount and severity of congestion.

Table 4 - Simulation flow data vs. traffic counts at link 645267

Time	Before: Flow [veh/h]	Counts [veh/h]
14:15:00	2432	6440
14:30:00	7248	6677
14:45:00	8236	7030
15:00:00	9156	7462
15:15:00	9292	7922
15:30:00	9512	8357
15:45:00	10156	8724
16:00:00	6228	9015
16:15:00	5576	9231
16:30:00	7188	9372
16:45:00	6484	9436
17:00:00	5132	9406
17:15:00	4780	9262
17:30:00	6028	8984
17:45:00	6892	8563
18:00:00	6300	8030
18:15:00	5072	7426
18:30:00	5288	6793
18:45:00	6124	6169
19:00:00	6744	5574
19:15:00	4716	5027
19:30:00	5936	4543
	R^2	0.036



Figure 8 - Section 645267 in Aimsun

A dynamic matrix calibration was performed to increase the goodness of fit of simulation flows with the traffic counts. A dynamic matrix calibration is a method used for calibrating simulation traffic demand. The dynamic network calibration automatically calibrates the flows resulting from simulation towards the traffic counts given as input for the selected road sections.

First, the simulation results were scanned for critical road sections where congestion should occur, while the simulation does not show congestion. As a result, five different road sections were selected to start with the dynamic network procedure. Almost all these road sections did not show signs of congestion in the previous simulation, while the congestion patterns showed that congestion should occur. These links were all located at or near the junction Vaanplein or Ridderkerk (*Figure 9*). The sections near junction Ridderkerk were chosen to make sure that the input into the network is realistic, while the sections near junction Vaanplein are primarily chosen in order to create realistic traffic patterns.

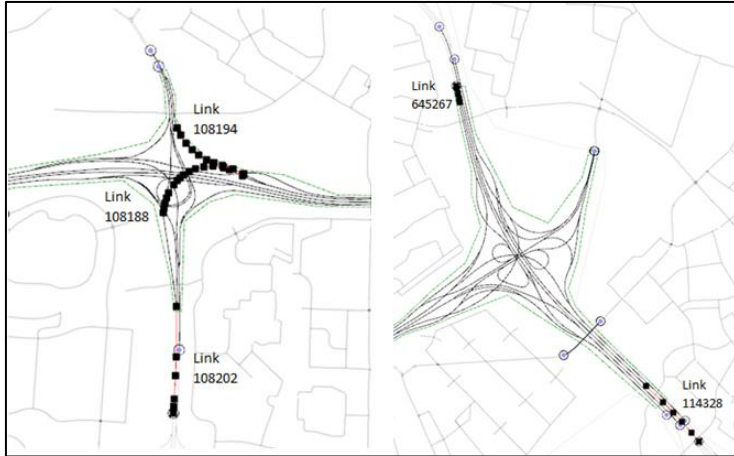


Figure 9 - Dynamic network calibration link locations (Vaanplein - Ridderkerk)

In order to perform the dynamic matrix calibration, a traffic departure profile with 15 minute intervals was interpolated from traffic count data. A spline-function was used, which interpolates the traffic counts per periods of 15 minutes according to the underlying hourly count values (National Data Warehouse for traffic information, 2014). The dynamic matrix calibration was performed for the five locations shown in *Figure 9*.

The dynamic matrix calibration resulted in changes in the OD-matrices. For all sections on which the dynamic matrix calibration was performed, the coefficients of determination [R^2], improved towards values of approximately 0.75 or higher. For example, the R^2 improved to a value of 0.76 for section 108188. The first and last time steps were excluded when calculating the R^2 , because these are part of the warm-up and cooldown period of simulation. At these time steps, large differences are found between calibration counts and simulation flows. *Figure 10* shows the improvement in goodness of fit for this section.

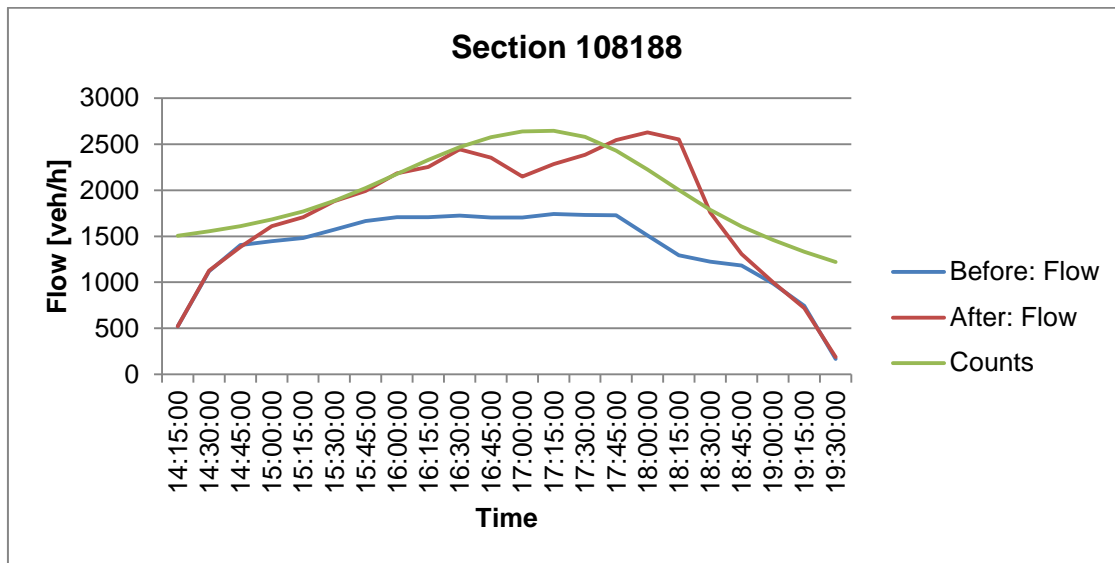


Figure 10 - Result of dynamic matrix calibration for section 108188

After the dynamic matrix calibration, the traffic flows departing from the western entrance point of the network were found to be too high. The OD-matrices for 2020 were chosen, where an increase in activities at Maasvlakte 2, located west of the research network, have led to a significant increase in traffic production and attraction. The amount of traffic entering the network from the western locations was slightly decreased to make sure that the distribution of traffic over the network fits the traffic data better.

After applying changes to the OD-matrices, the goodness of fit of the simulation flows will be determined. In general, R^2 -values of above 0.5 are considered to be acceptable, although this statistic is oversensitive to high extreme values (outliers) and insensitive to additive and proportional differences between model prediction and measured data (Moriassi et al., 2007). Generally, a R^2 of 0.75 or higher is considered to be satisfactory for this study, because this indicates that the standard deviation of the errors is exactly one-half of the standard deviation of the dependent variable, which means that 50% of the standard deviation is explained by the model (Nau, 2016). Lower values of this statistic can be accepted if the deviation can be explained. Time series models might provide disappointing results, since the predictive power is derived from its own history, differences and time-dependent or seasonal adjustments (Nau, 2016). *Table 5* shows the vehicle flows resulting from simulation and the calibration counts used for the dynamic network calibration and the corresponding R^2 statistics for goodness of fit. Note that the first and last time steps were excluded for calculating the coefficient of determination to exclude warm-up and cooldown periods and extreme outliers.

Table 5 - Simulation flows compared with traffic counts in vehicles per hour after dynamic matrix calibration

Time	Section 108188		Section 108194		Section 108202		Section 114328		Section 645267	
	Sim.: Flow	Counts	Sim.: Flow	Counts	Sim.: Flow	Counts	Sim.: Flow	Counts	Sim.: Flow	Counts
14:15:00	524	1504	200	600	1528	3230	1568	3540	2440	6440
14:30:00	1128	1553	404	612	3228	3384	3476	3553	7284	6677
14:45:00	1384	1611	444	614	4240	3578	3652	3576	8244	7030
15:00:00	1608	1681	540	612	4028	3814	3624	3623	7944	7462
15:15:00	1708	1771	624	614	4024	4092	3720	3713	7912	7922
15:30:00	1880	1884	604	629	4436	4412	3880	3864	8336	8357
15:45:00	1992	2023	652	661	4788	4770	4108	4083	8752	8724
16:00:00	2184	2176	720	704	5024	5141	4332	4338	9000	9015
16:15:00	2252	2329	756	746	5344	5496	4588	4587	9216	9231
16:30:00	2444	2467	796	776	5752	5804	4788	4787	9352	9372
16:45:00	2352	2575	784	787	5676	6035	4940	4905	9456	9436
17:00:00	2148	2639	796	781	5832	6156	4960	4941	9496	9406
17:15:00	2284	2645	664	763	5860	6132	4912	4902	9360	9262
17:30:00	2384	2577	716	739	5760	5928	4812	4796	9148	8984
17:45:00	2544	2429	712	713	5656	5530	4608	4632	8168	8563
18:00:00	2628	2226	780	685	5532	4998	4412	4418	8032	8030
18:15:00	2552	2001	704	655	5352	4413	4156	4162	7416	7426
18:30:00	1760	1786	628	623	3856	3854	3844	3873	6816	6793
18:45:00	1308	1606	484	588	3332	3385	3936	3561	6200	6169
19:00:00	1000	1459	384	549	2860	3002	3980	3242	5604	5574
19:15:00	720	1333	200	509	2004	2687	1832	2931	4376	5027
19:30:00	188	1219	44	465	568	2419	44	2646	432	4543
R^2	0.758		0.779		0.898		0.812		0.931	

From *Table 5* can be concluded that all five sections have R^2 values of above 0.75, which is considered as satisfactory. No further explanation is required for accepting these statistics. However, it should be noted that these simulation flows were obtained by a single simulation run, whereas other simulation runs could provide slightly different flows caused by different random seeds.

3.3.4 Fine-tuning of congestion patterns

The traffic demand over the research network was changed by performing the dynamic matrix calibration, which resulted in changes in traffic and congestion patterns. A simulation was ran and proved that the congestion patterns were improved. Although, the congestion patterns from simulation did not resemble the typical congestion patterns as shown by Google (2016) to a satisfactory extent yet. Therefore, further fine-tuning had to be performed.

To represent the typical traffic patterns, additional changes to reaction time factors for the problematic sections were required. After some small changes, the congestion pattern resembles the typical congestion patterns as shown by Google (2016) to a satisfactory extent. *Figure 11* indicates that the congestion patterns look similar. However, at junction Vaanplein, two small congestion fronts from the south spilled back to the north and west are not found in the simulation results. It was impossible to include the congestion front that should spill back to the west in the simulation, since the source of this congestion is located outside the boundaries of the research network. For the congestion that should spill back to the north, the reaction time factor should have to be set too high (>1.2) to include this congestion. Another factor is that this congestion partly occurs due to a lane drop in the downstream road section, where lane-changing behavior plays an important role and is a cause of congestion. However, lane-changing behavior is simplified in a mesoscopic simulation, which is an explanation of not being able to simulate this congestion. The remaining congestion fronts are incorporated in the simulation.

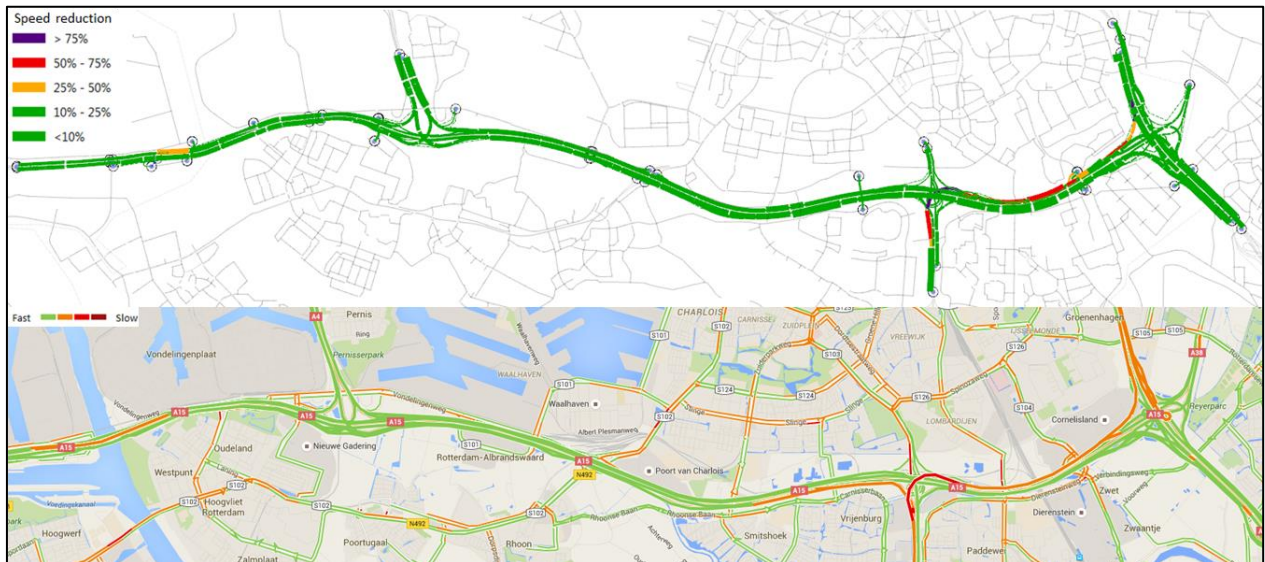


Figure 11 - Congestion patterns from simulation (top) vs. Google (2016) (bottom) for time period of 17:30-17:45

3.3.5 Calibrated mesoscopic model

After completing the previous steps, the mesoscopic model is calibrated. All changes made were based on a one-shot mesoscopic experiment with only one random seed used. In order to improve the sensitivity of the simulation and calibration, a mesoscopic simulation, based on a DUE assignment was used. The DUE results as well as the resulting congestion patterns are discussed in this subsection. The congestion patterns are compared with the Google (2016) patterns to evaluate the fit of congestion patterns. A brief reflection on the comparison of traffic patterns is provided.

3.3.5.1 DUE results

The mesoscopic simulation based on a DUE assignment was used in order to find and define the proportion of vehicles over sub paths and sections. Subsequently, this path assignment plan is stored and will be selected as input for all further simulations and scenarios, to minimize differences in path assignment and division of traffic over the network between different (future) scenarios.

The simulation using DUE assignment was equipped with a stopping criteria of a maximum of 30 iterations or a relative gap (Rgap) of 0.5% or lower between subsequent iterations. The DUE assignment was based on a weighted method of successive averages (MSA), capable of yielding converging solutions relatively fast. The relative gap function determines whether the solution reached, can be interpreted in terms of a

DUE, in the sense that the actual travel time of travelers departing at the same time are equal and minimal (Transport Simulation Systems, 2014). Smaller relative gap refer to smaller deviations between iterations.

The simulation required 20 iterations to fulfill the relative gap criteria. In *Figure 12*, the DUE output summary is shown. It can be found that the number of vehicles waiting to enter, inside and outside the network do not differ significantly from iteration 9 and onwards (from 13 is visible in the figure). The table related to (computation) time shows what process took what amount of time. The dynamic network loading took the most time in any iteration, while the calculation of shortest paths, method of successive averages and relative gap took a negligible amount of time. From *Figure 12* could be found that the total simulation time for a single DUE mesoscopic simulation was approximately 750 seconds, which is approximately 12.5 minutes.

Execution Data		Relative Gap		
Vehicles per Iteration				
	Waiting to Enter	Inside	Outside	
20	0	42	227940	
19	0	42	227940	
18	0	42	227940	
17	0	42	227940	
16	0	42	227940	
15	0	42	227940	
14	0	42	227940	
13	0	42	227940	
Time (seconds)				
	DNL	SP	MSA	RGap
20	64.491	0	0	0
19	35.692	0.063	0	0
18	35.663	0	0	0
17	35.351	0.03	0	0
16	35.475	0.093	0	0
15	35.413	0.047	0	0
14	35.382	0.061	0	0
13	35.6	0.078	0	0
Global Time (seconds)				
Total	Mean DNL	Mean SP	Mean MSA	Mean RGap
752.705	37.5752	0.05925	0.0008	0

Figure 12 - DUE output summary

The relative gap is calculated per time period and iteration. How the relative gap is evolving, is shown in *Figure 13*. The relative gaps of all time periods are below 0.5% for the 20th iteration, which shows that the stopping or convergence criteria have been reached. From the figure, it becomes clear that the relative gaps for the time periods indicated in (dark) blue are converging faster than the other time periods, because the dark blue lines refer to the early time periods (14:00-15:00) where the simulation takes some time to fill the network with vehicles. The red lines refer to the late time periods of the simulation (19:00-19:30), where some time is needed to flush or clear the network of the last vehicles inside. The largest oscillations are found for the time periods that are considered to experience some congestion (approximately 16:45-18:00) and the last time periods to make sure that the network gets cleared again. The largest relative gap at iteration 20 is found for the time period between 19:15 and 19:30, with a relative gap of slightly below 0.5%. The relative gap is reduced quite effectively, since only 20 iterations are required to meet the stopping criteria.

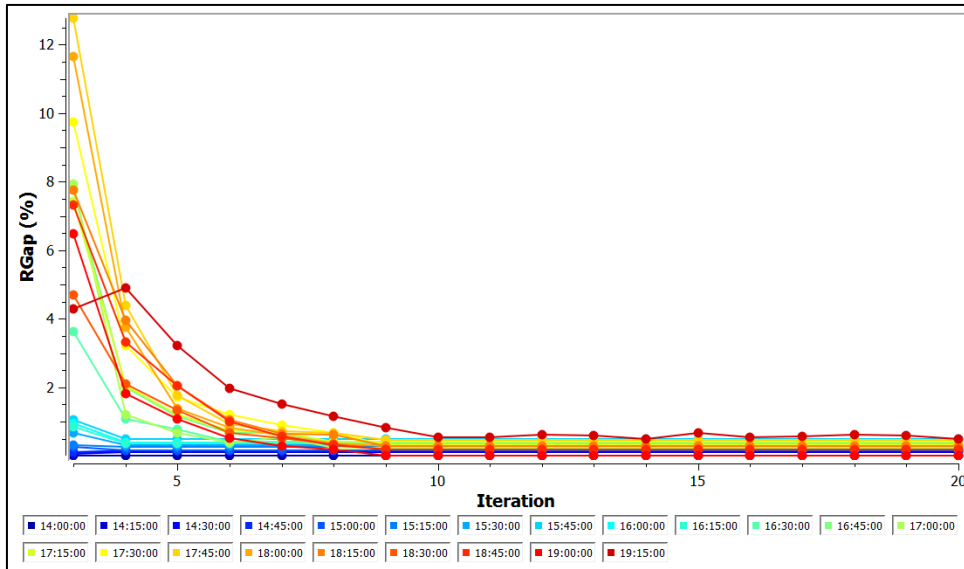


Figure 13 - DUE relative gaps per time period

3.3.5.2 Congestion patterns

The congestion patterns from the mesoscopic DUE simulation are compared with the typical congestion patterns of a typical evening peak period from Google (2016). The congestion patterns from simulation and data will be shown for time periods from 15:45 up and to including 19:00. Please note that the time period from 15:45 to 16:00 from simulation is compared with the Google (2016) congestion pattern of 16:00. These congestion patterns are used to check whether the congestion occurs at similar locations and time periods. It was chosen to use typical Thursday traffic data, since Mondays, Tuesdays and Thursdays are considered as normative days regarding traffic congestion in the Netherlands.

The dynamic speed reductions from mesoscopic simulation and Google (2016) are compared in Figure 14 up and to including Figure 26. The speed reductions are considered as the difference between the average speed of the vehicles in a certain time period and the section maximum speed, divided by the section maximum speed. The color scale used to visualize the speed reductions in Aimsun is expected to be comparable to the one used by Google (2016). However, the exact values for the color scale used by Google (2016) are unknown. To provide a clear picture, it was chosen to only show the junctions of Vaanplein and Ridderkerk in the figures, since these are the locations where serious congestion occurs. Only limited congestion is found at other locations in the research network. It should be noted that the calibration was also performed for the other locations. For reasons of clarity, it was chosen to limit the figure sizes and only include the congestion patterns for the junctions Vaanplein and Ridderkerk.

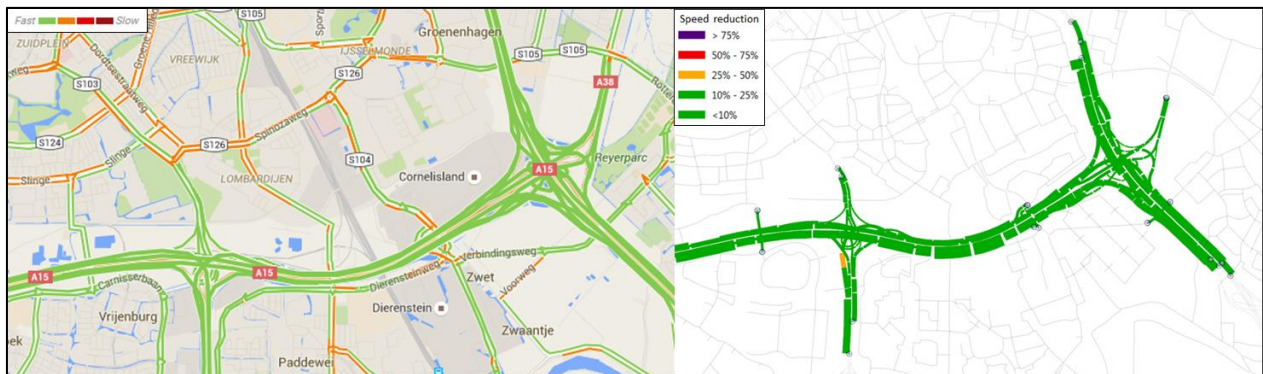


Figure 14 - Congestion patterns from Google (2016) (left) and mesoscopic simulation (right) from 15:45 - 16:00

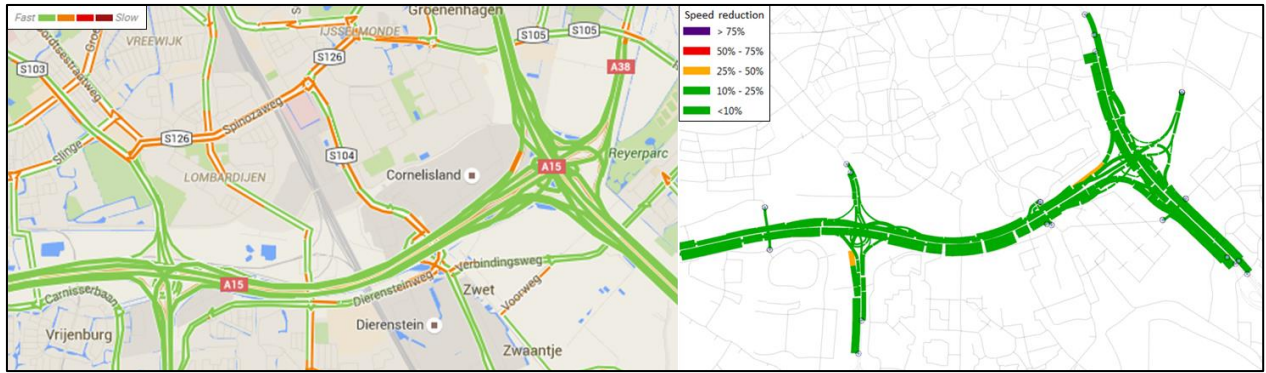


Figure 15 - Congestion patterns from Google (2016) (left) and mesoscopic simulation (right) from 16:00 - 16:15

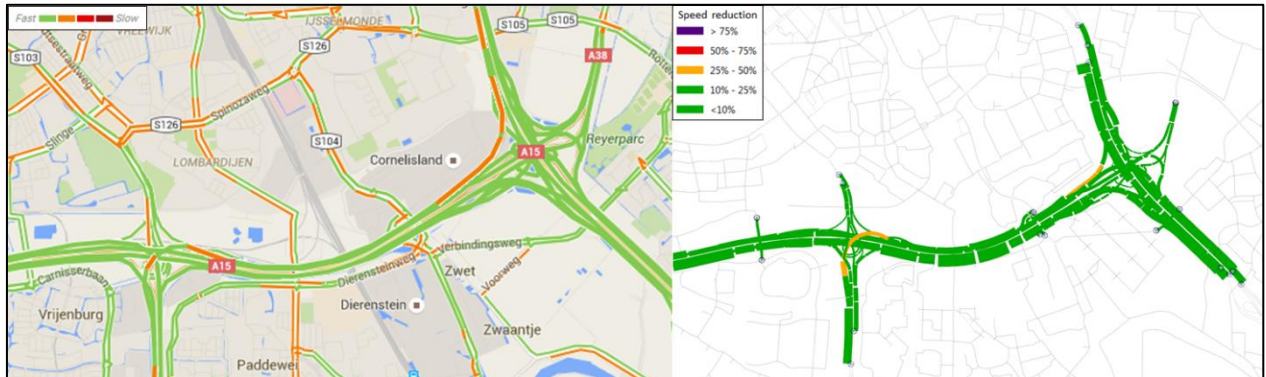


Figure 16 - Congestion patterns from Google (2016) (left) and mesoscopic simulation (right) from 16:15 - 16:30

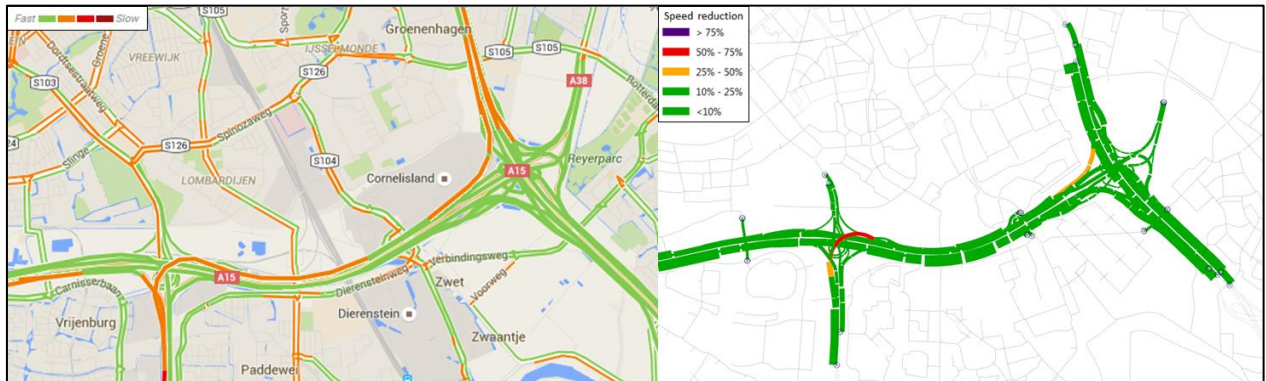


Figure 17 - Congestion patterns from Google (2016) (left) and mesoscopic simulation (right) from 16:30 - 16:45

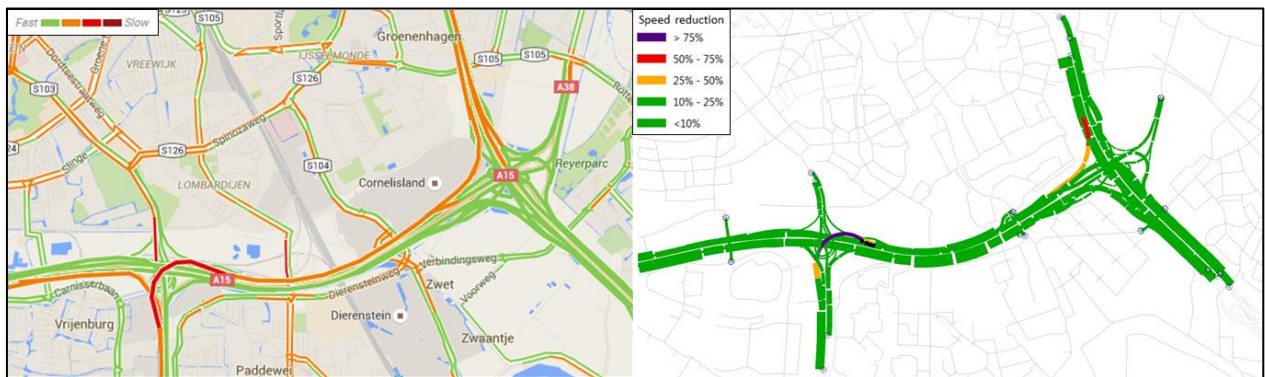


Figure 18 - Congestion patterns from Google (2016) (left) and mesoscopic simulation (right) from 16:45 - 17:00

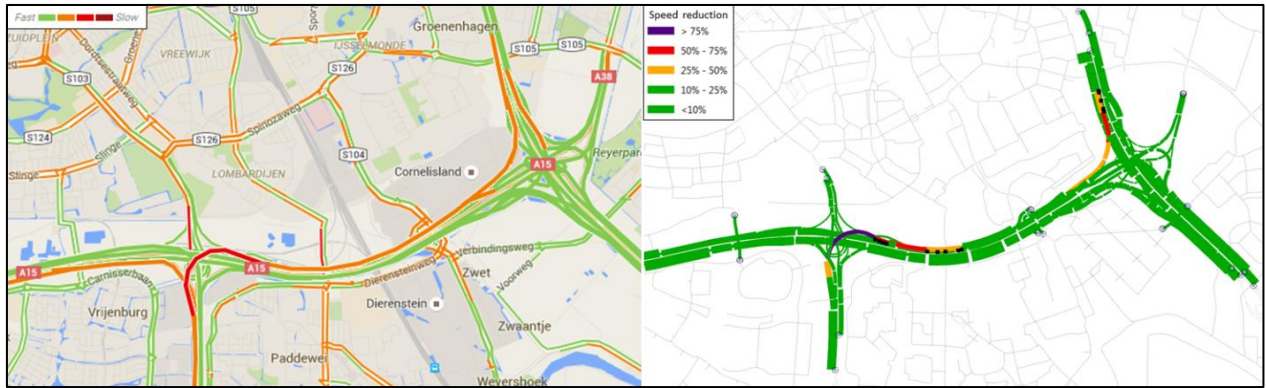


Figure 19 - Congestion patterns from Google (2016) (left) and mesoscopic simulation (right) from 17:00 - 17:15

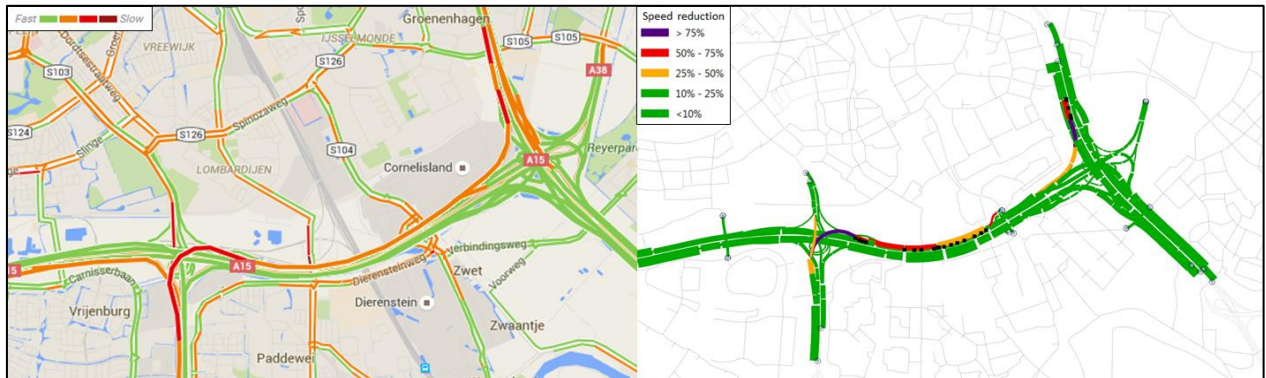


Figure 20 - Congestion patterns from Google (2016) (left) and mesoscopic simulation (right) from 17:15 - 17:30

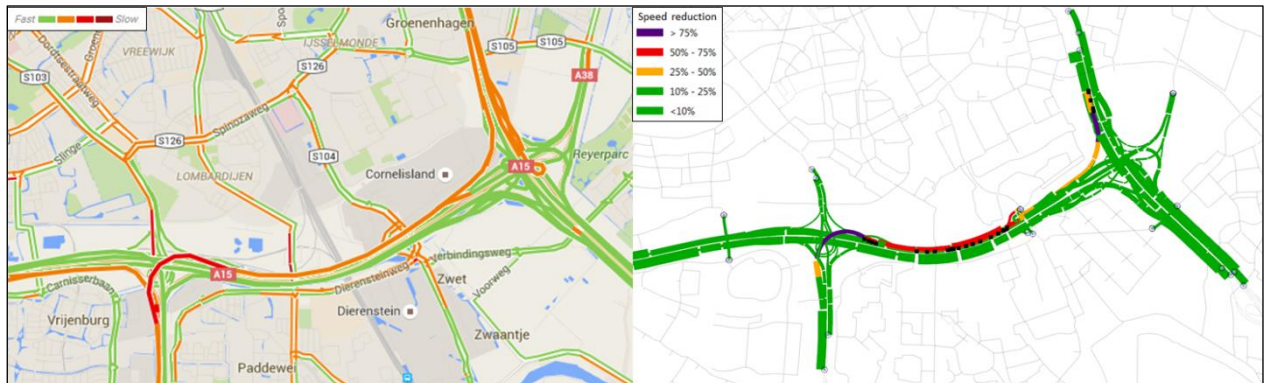


Figure 21 - Congestion patterns from Google (2016) (left) and mesoscopic simulation (right) from 17:30 - 17:45

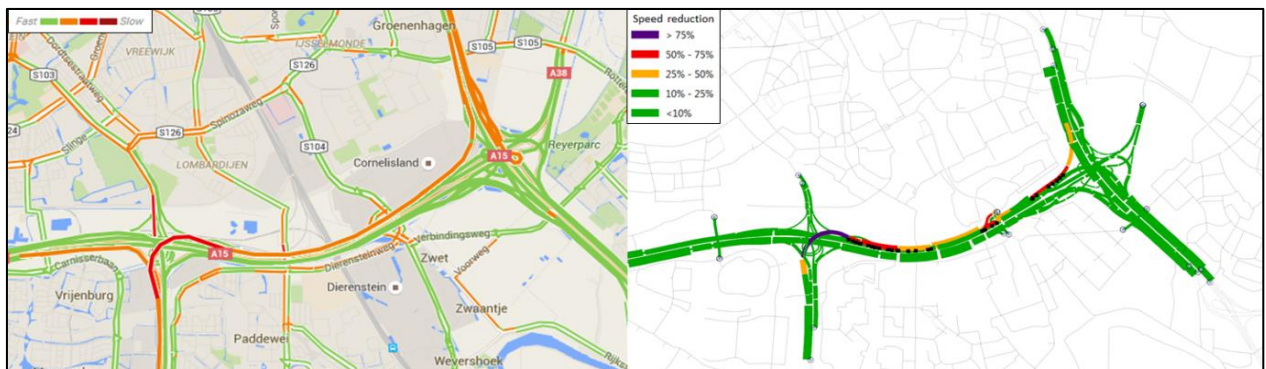


Figure 22 - Congestion patterns from Google (2016) (left) and mesoscopic simulation (right) from 17:45 - 18:00

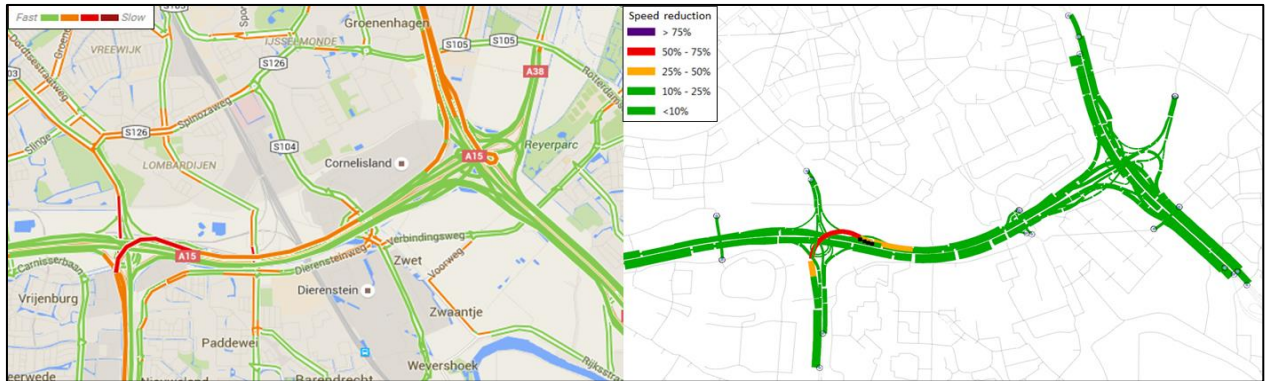


Figure 23 - Congestion patterns from Google (2016) (left) and mesoscopic simulation (right) from 18:00 - 18:15

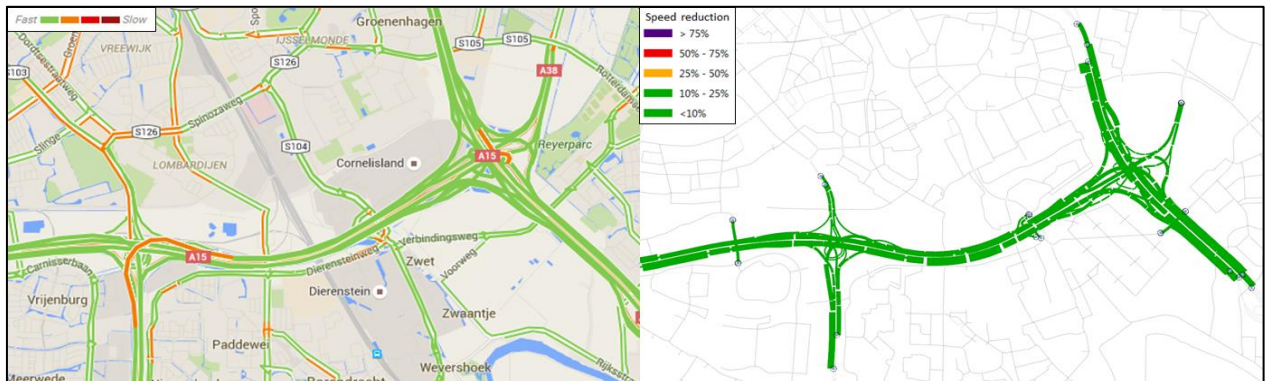


Figure 24 - Congestion patterns from Google (2016) (left) and mesoscopic simulation (right) from 18:15 - 18:30

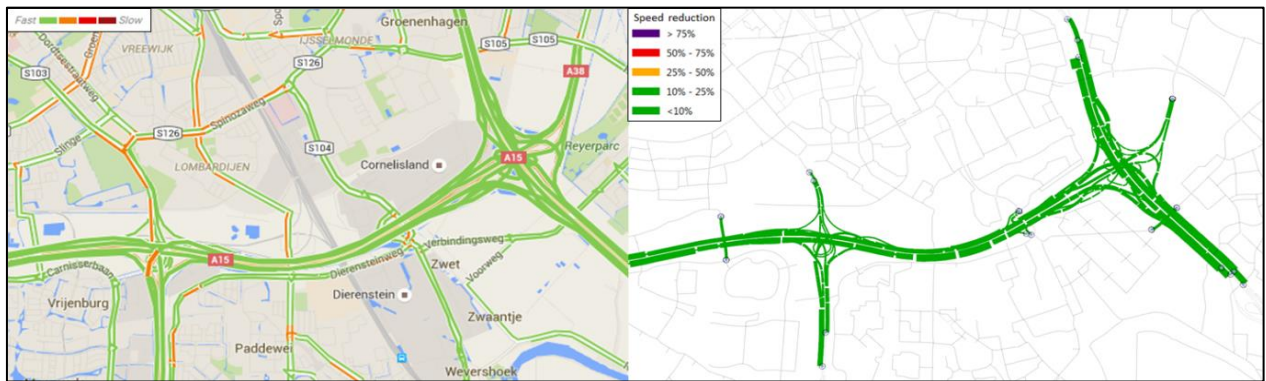


Figure 25 - Congestion patterns from Google (2016) (left) and mesoscopic simulation (right) from 18:30 - 18:45

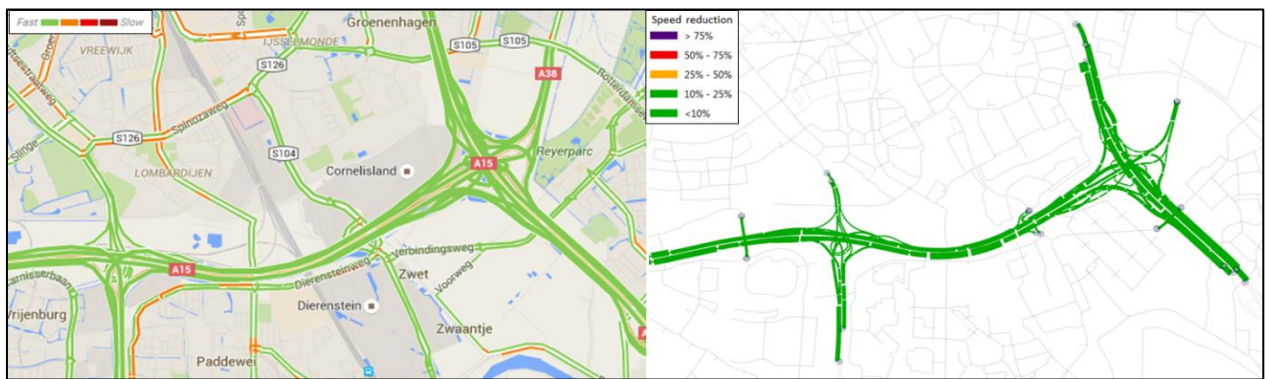


Figure 26 - Congestion patterns from Google (2016) (left) and mesoscopic simulation (right) from 18:45 - 19:00

Generally speaking, the mesoscopic simulation results represent the traffic patterns relatively well. The actual traffic patterns show some more congestion fronts. However, the triggers of these congestion fronts are often located outside of the network used for this research and could not be modelled properly. The congestion starting from the north of junction Ridderkerk and spilling back over the A16 at Ridderkerk is expected to occur due to the bottleneck of the Brienoord Bridge. The other congestion front that is not modelled in the simulation is the congestion front which is triggered just south outside the research network at junction Vaanplein, spilling back in western direction from junction Vaanplein. The other important sources of congestion are included in the simulation results.

When looking at the starting times of congestion, similar propagation patterns are found. At the first time periods, *Figure 14* and *Figure 15* show that the congestion in simulation starts a bit earlier. However, from 16:15 to 16:45 (*Figure 16*, *Figure 17*) and onwards, the congestion in the Google (2016) traffic patterns propagates faster. The starting times of congestion are found to be at approximately the same times. Also, the propagation of the congestion becomes more severe in the simulation and typical traffic patterns at approximately the same time periods.

After a while, the congestion fronts are connected in the Google (2016) traffic plots (*Figure 18* to *Figure 22*), which breaks apart in two different jam fronts at later time periods (*Figure 23*). As stated, the congestion in the simulation propagates slightly slower, since both congestion fronts are still propagating in *Figure 18* and *Figure 19*. The congestion fronts in simulation do not get connected, but are located very close to each other in *Figure 20*, *Figure 21* and *Figure 22*. However, the speed reductions found in simulation at these congestion fronts are more severe (more red/purple). Concluding, it could be stated that the traffic patterns found in this situation are similar. There is only a limited difference found in terms of speed reduction severity and spillback, while the overall congestion pattern is very similar. These small differences can be accepted in terms of calibration.

When the times of the relief of congestion are compared, it is found that the congestion starts resolving slightly faster in the simulation patterns. In *Figure 23*, the congestion at Ridderkerk has been solved in the simulation model, while the typical traffic patterns still show some congestion. The congestion in the typical traffic patterns is resolved one time period later in *Figure 24*. In the mesoscopic simulation, the congestion near Vaanplein is resolved in *Figure 24*. In the typical traffic patterns, the congestion is also solved slightly later (*Figure 25* or *Figure 26*).

Additionally, some congestion is found near the Botlek area (at the western part of the network), which is not shown in the congestion pattern figures. Both the simulation and typical traffic patterns show a very similar congestion pattern and severity at this location.

In general, the mesoscopic simulation results show a very similar congestion pattern when compared with the Google (2016) typical traffic patterns. The start and end of congestion are found to be at approximately equal time periods. Also, the length and severity of congestion are similar. Therefore, it can be concluded that the simulation is a reasonable representation of reality. It should also be noted that the traffic demands were found to be similar to the traffic data used. Also, the simulation input parameters and values (e.g. jam densities) are characteristic values. After this analysis, the mesoscopic model has been calibrated and does represent the real life situation to a sufficiently realistic extent.

3.3.6 Microscopic calibration

In this subsection, the microscopic calibration procedure is discussed. First, an overview of the most important parameters is given in order to gain insight into the logic of calibration. Additionally, some examples of compatibility problems found when switching from a mesoscopic to a microscopic simulation

will be given. The solutions to these problems are briefly discussed. Subsequently, choices made to calibrate the congestion patterns at critical points in the network are elaborated upon.

In order to calibrate the network using a microscopic simulation, many different parameters have to be set and adapted. Since this network was calibrated for a mesoscopic simulation, the microscopic settings still had to be adapted based on representative values. A standard microscopic template of RHDHV was used for the initial settings. This template mainly defined the section settings per road type. However, many different adaptations are still required in order to calibrate the model microscopically.

3.3.6.1 Calibration parameters

Generally speaking, there are three types of parameters that are important to calibrate the microscopic simulation. These types are section parameters, turn parameters and behavioral model parameters that can be defined at experiment level. Additionally, physical changes to the network also have an effect on the simulation results and could be included in this subsection. However, physical changes to the network are not desirable, unless compatibility problems between mesoscopic and microscopic simulations will be found (discussed in subsection 3.3.6.2).

Section parameters (lane-changing and side lane cooperation): The default lane-changing cooperation is set to 80% and the aggressiveness is set to 0%. The side lane cooperation distance has been set to the whole lane, while the merging distance is normally set to default, which refers to a lane change on a lane drop at approximately 5 seconds before the lane drop. However, to decrease the congestion on the lane of the lane drop, this value could be set manually, based on a distance over which merging is allowed. The queue discharge and two-way two-lane overtaking model have been set as defined in *Figure 27*. In some special cases it might be necessary to set the braking intensity to high or extreme in order to create congestion. On the other hand, an increasing acceleration of medium or high could be selected to increase queue discharge and solve the congestion at an earlier moment in time.

The screenshot shows a 'Micro' settings panel with the following sections and values:

- Lane Changing:**
 - Cooperation: 80,00 %
 - Aggressiveness: 0,00 %
 - Braking Intensity: Normal
 - Imprudent Lane Changing
- Side Lane:**
 - Cooperation Distance: Whole Lane
 - Merging Distance: 500,00 m
 - Merge: First Vehicle On is First Vehicle Off
- Queue Discharge:**
 - Increasing Acceleration: None
 - Additional Reaction Time at Stop: 0,00 sec
 - Additional Reaction Time at Traffic Light: 0,00 sec
- Two-Way Two-Lane Overtaking Model:**
 - Mirror Section: None
 - Visibility Distance: 300,00 m
 - Visibility Factor: 1,50
- HCM Settings (Category: None):**
 - Weaving
 - Merge / Diverge Starting Point
 - Consider Two-lane Car-following Model

Figure 27 - Section parameters for microscopic simulation

Turn parameters (Distance zones and give way model): These settings are different among different road types. The give way model parameters are the same for all road types, but are not very relevant on highways. The waiting time before losing turn and the yellow box speed are not used within this simulation, because these are used on intersections. The distance zones are very important in this simulation, because these parameters refer to the distances before the end of the weaving sections at which the vehicles would like to change lanes if an appropriate gap is available (distance zone 1) and the distance towards the end of the weaving section at which the vehicles have to merge, even in smaller gaps (distance zone 2), as explained in subsection 2.4.2. An example of the turn parameters has been provided in *Figure 28*. The distance zones displayed in this figure are the default for highways with maximum speeds of 120 km/h. Specific changes to these distance zones might be required to ensure that drivers will tend to change lanes at an earlier or later stage.

Microscopic Model			
Distance Zone 1:	666,67 m	Additional Waiting Time Before Losing Turn:	0,00 sec
Distance Zone 2:	100,00 m	Yellow Box Speed:	10,00 km/h
Give-way Model			
Initial Safety Margin:	3,00 sec	Final Safety Margin:	1,00 sec
Initial Give-way Time Factor:	1,00	Final Give-way Time Factor:	2,00
Visibility to Give Way:	25,00 m	Visibility along Main Stream:	20,00 m

Figure 28 - Turn parameters for microscopic simulation

Experiment level parameters: At experiment level, there are some parameters with respect to behavioral models. Since slopes are not included in this research, the slope model is irrelevant. The two-way two-lane overtaking model is not used and irrelevant. The queue speeds are set to the default values as displayed in Figure 29. The two-lane car-following model can be selected per road section. The two-lane car-following model has a maximum (relative) speed difference of 20 kilometers per hour at regular lanes and 50 km/h at on-ramps.

Car Following			
<input checked="" type="checkbox"/> Two-lane Car-following Model			
Number of Vehicles:	4	Maximum Speed Difference:	20,00 km/h
Maximum Distance:	100,00 m	Maximum Speed Difference on Ramp:	50,00 km/h
		Speed Difference Setting:	Relative
<input type="checkbox"/> Apply Slope Model			
Lane Changing			
Distance Zone Variability:	40 %		
<input type="checkbox"/> Two-way Two-lane Overtaking Model			
Delay Time Threshold:	60,00 sec	Number of Simultaneous Overtakings Allowed:	1
Minimum Speed Difference Threshold:	10,00 km/h	Delay Between Simultaneous Overtakings:	10,00 sec
Maximum Speed Difference Threshold:	35,00 km/h	Sensitivity Factor for Reduced Car Following:	0,65
Maximum Rank:	2	Overtaking Speed Enhancement Factor:	1,10
Remaining Travel Time Threshold:	0,00 sec	Speed Difference Threshold for Enhanced Overtaking Speed:	15,00 km/h
Queue Speeds			
Queue Entry Speed:	1,00 m/s	Queue Exit Speed:	4,00 m/s

Figure 29 - Parameters at experiment level for microscopic simulation

3.3.6.2 Compatibility problems

After some test runs it was found that there were some network compatibility problems when switching from mesoscopic to microscopic simulation. These problems occur because the microscopic simulator follows every vehicle at every time step, while the mesoscopic simulator only calculates the points in time of entering and leaving the section. Basically all of these compatibility problems can be associated with the prevention of undesired travel behavior or to prevent collisions, which could almost occur due to small flaws in network lay-out or definitions. The compatibility problems and the solutions to these problems are discussed in this subsection. Three types of problems are discussed: undesired node connections, infrastructural changes and conflicting node connection paths.

Node connections: Some of the connections inside the node were defined incorrectly. The connections inside the node define from which lane it is possible to enter downstream lanes. Figure 30 shows an example of undesired node connections, where a 4-lane road splits up into two different two-lane roads. The initial mesoscopic settings made it possible to drive into the two-lane sections from the 3 closest lanes. This resulted in congestion in the microscopic model, because many vehicles change lanes at the node in order to reach their desired road section, which is considered as undesired behavior. The intersecting flows at the node cause severe congestion on upstream road sections.

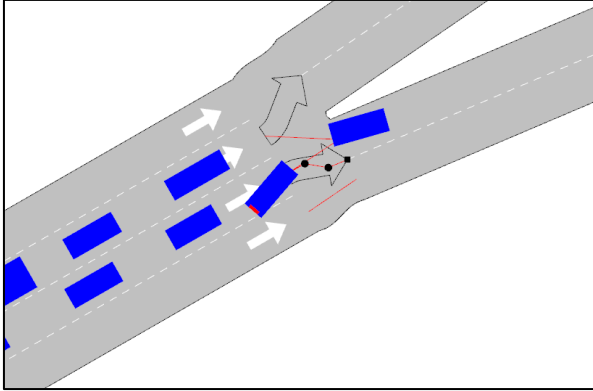


Figure 30 - Example of undesired node connections

The simple solution to this problem is to remove the undesired connector, which means that it should only be possible to enter the two downstream lanes via the two corresponding lanes of the upstream sections. This problem was found at approximately 45 intersections within the research network.

Infrastructure changes: In order to model a lane drop, one could use a node (left) or a shoulder (right) as shown in *Figure 31*. It was found that using a node results in more unstable microscopic behavior. As a result, these types of nodes have to be changed to shoulders at critical locations. However, this is only necessary when the number of lanes decrease in the downstream direction. If an extra lane is added, differences are negligible. This problem was found at multiple points in the network. In approximately 15 cases, nodes had to be changed to shoulders in order to prevent unstable microscopic simulation results.

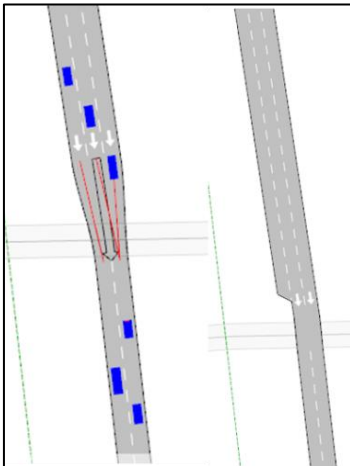


Figure 31 - Infrastructure changes: node (left) and shoulder (right)

Conflicting node connection paths: Another problem was found during simulation, which is displayed in *Figure 32*. In the figure, a four-lane upstream road section is displayed with two two-lane downstream sections and a node between those sections. The connections inside the node are set to the corresponding lanes. However, the connection paths of the middle lanes are slightly curved and touch upon each other, which results in a possibility of collision. The simulator recognizes the danger of possible collisions and will prevent collisions by alternately giving way to vehicles from the middle right and middle left lane. In *Figure 32*, the vehicle in the middle right lane is braking to wait for the truck on the middle left lane to pass and prevent collision. These undesired situations result in heavy congestion, because the combined capacity of two lanes will basically be reduced to a single lane capacity.

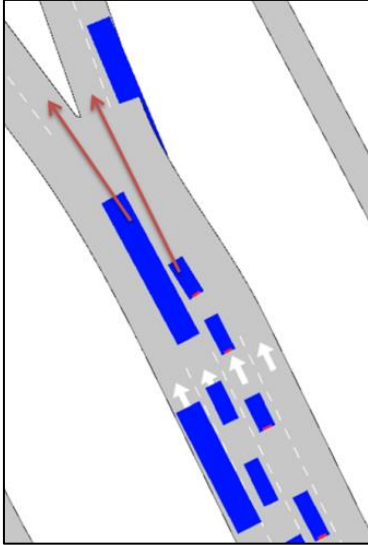


Figure 32 - Conflicting node connection paths

The solutions to this problem are to slightly change the locations of the starting points of the downstream sections or change the connection path inside the node. Very small changes are sufficient to prevent these problems of conflicting paths inside the node. This problem had to be changed at approximately 20 locations inside the research network.

3.3.6.3 Calibration of congestion patterns

Subsequently, fine-tuning of the congestion patterns is required by changing the distance zones, cooperation distances and side lane merging distances in most of the cases. At this stage, the majority of changes are with respect to improving lane-changing behavior at specific road sections. Often, the lane-changing behavior was improper in the sense that vehicles started changing lanes too far from or close to their destination lanes. These problems could be solved by changing the distance zones. The distance zones are set to higher values if the vehicles have to change lanes further away from the node or lower if they should change lanes at a later stage (i.e. closer to the node).

Subsequently, serious congestion occurred at some weaving sections and lane drops, because the vehicles at these road sections did not help each other enough to make the lane-changing processes run smoothly. In order to improve these situations, the cooperation rate at these sections was increased. This resulted in simulation results, which did show congestion on the most important congestion locations, but the length, severity, spillback and duration of congestion was not found satisfactory yet. Therefore, additional attention should have to be paid to the most important congestion locations inside the network. The congestion fronts will be discussed for the junctions (Ridderkerk and Vaanplein) at which the congestion starts occurring.

3.3.6.3.1 Junction Vaanplein

At this junction, the congestion propagates in two different directions. According to *Figure 33*, the congestion starts at the point where the two flows from the north and east towards the south join each other. Additionally, it is important to be aware that there is a lane drop approximately 200 meters downstream from the merging point, as shown in *Figure 34*. This results in a relatively high number of lane changes that should be performed in order to handle the traffic flow. At the initial settings, the congestion did only spill back towards the north (on-ramp), but not to the east, while the spillback to the east is quite severe in reality.

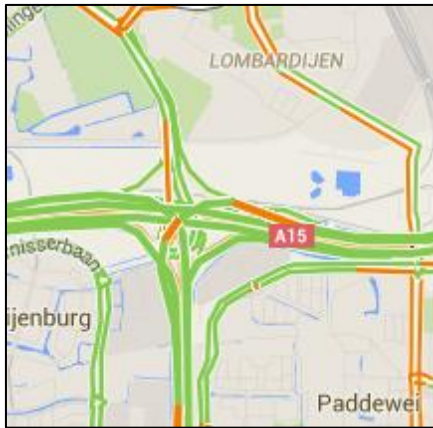


Figure 33 - Traffic congestion pattern at start of congestion (16:30) at junction Vaanplein (Google, 2016)

Numerous changes to parameter settings were made in order to calibrate the congestion patterns on this point in the network. First, the merging distance of the on-ramp has been set to 50 meters, which is relatively low. However, many drivers tend to use the full on-ramp at this location, which can be modelled by setting the merging distance at a relatively low value. After this change, the severity of the congestion was not represented to a satisfactory extent yet. Also, the congestion only had limited spillback towards the east. Therefore, the two-lane car-following model was used in order to make sure that the speed differences between lanes will not get extreme. The study of Munoz & Daganzo (2002) justifies the parameter of maximum speed difference between lanes, set to 20km/h for normal lanes, because the speed differences between lanes found in their study are approximately 20km/h. The maximum speed difference for an on-ramp was set to 50km/h, which was also found for an off-ramp by Munoz & Daganzo (2002).

These parameter settings did increase the amount of congestion. However, the severity of congestion should still be increased in order to represent the congestion patterns as found by Google (2016). The possible additional reason for the occurrence of congestion is due to slopes. Since the original model was a mesoscopic model, the slopes are not included in the simulation, while slopes could have a significant effect on driving behavior (Papacharalampous et al., 2015). It is possible to fill in the slopes at every single road section, but this is very time-consuming. Therefore, all the slopes are modelled to be zero. Since the slope of this road section is negative in reality and seems to have a quite important impact on the occurrence of congestion, this effect is compensated by increasing the braking intensity in simulation. This could be justified, because drivers tend to brake harder when they know that there is a downhill slope. The braking intensity was set to extreme to represent the correct severity of congestion.

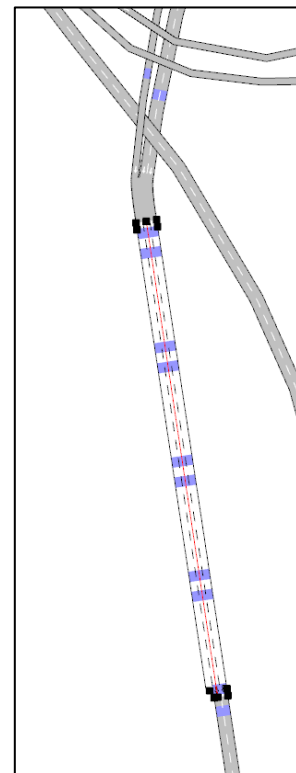


Figure 34 - Merging and lane drop at the section where congestion starts at junction Vaanplein

3.3.6.3.2 Junction Ridderkerk

At this junction, the congestion occurs at the connection from the north to the west. The simulation results showed some congestion, but the length, duration and severity was not incorporated to a satisfactory extent. Therefore, a more detailed approach is needed in order to improve the results.

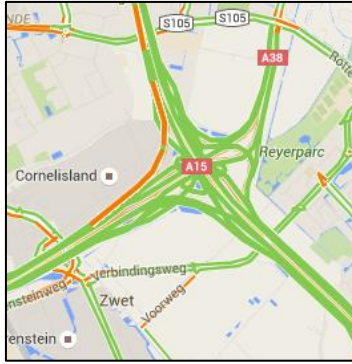


Figure 35 - Traffic congestion pattern at start of congestion (16:30) at junction Ridderkerk (Google, 2016)

From Figure 35, the location and start of congestion is shown. The congestion starts at a short distance upstream from off-ramp Barendrecht. In front of this off-ramp, there is a weaving section of approximately 450 meters. The traffic signs at the road sections just upstream of this weaving section indicate the destinations of the lanes. In this case, it is reasonable to assume that many of the drivers tend to change lanes at an early stage, because they are already informed about the destination lanes by the traffic signs and would like to be on their destination lane at an early stage. Also, the congestion pattern plots show that the congestion starts at this weaving section.

To incorporate this behavior of changing lanes at an early stage, the distance zones for both destination lanes have to be set higher than the default parameter settings. For both directions (straight ahead and off-ramp) the distance zones have been set to 700 (DZ1) and 500 (DZ2) meters. This means that all vehicles are forced to change lanes from 400-600 meters in front of the node and onwards, while the length of the weaving section is approximately 550 meters. Doing so, it is expected that congestion starts occurring due to the early lane-changing behavior of the vehicles. After doing some test runs, it turned out that these parameter settings give proper congestion patterns, with a similar time and propagation pattern to the congestion patterns found by Google (2016).

Additionally, the two-lane car following model has been selected to use at these road sections, since this ensures that the speed differences between lanes cannot be too high. The study of Munoz & Daganzo (2002) justifies the parameter of maximum speed difference between lanes, which is set to 20km/h, because the speed differences between lanes found in their study are approximately 20km/h.

3.3.7 Calibrated microscopic model

Until now, the microscopic calibration is only based on a single simulation run, without changing the random seeds or taking averages of multiple simulation runs. To decrease the sensitivity for random seeds, an average of 10 simulation runs with simulation steps of 0.8 seconds will be used to assess the calibrated microscopic model. First, a small check was required to find out whether the average does not significantly deviate from the single simulation run used for the calibration. The average of 10 different simulation runs was very similar to the single simulation run used for the calibration, which meant that no additional parameter changes were required to influence the sensitivity between simulation runs.

Subsequently, the congestion patterns resulting from microscopic simulation are compared with the Google (2016) patterns to give some conclusions on the goodness of fit. The simulation results are compared with the typical congestion patterns of a typical Thursday evening peak period from Google (2016). Similar to subsection 3.3.5.2, the congestion patterns from microscopic simulation and typical traffic patterns will be shown for time periods from 15:45 up and to including 19:00. The time period from 15:45 to 16:00 from simulation is compared with the Google (2016) congestion pattern of 16:00. These congestion patterns are used to check whether the congestion occurs at similar locations.

The dynamic speed reductions from microscopic simulation and Google (2016) are compared in *Figure 36* up and to including *Figure 48*. The speed reductions are considered as the difference between the average speed of the vehicles and the section maximum speed within a certain time period, divided by the section maximum speed. The color scale used to visualize the speed reductions in Aimsun is expected to be comparable to the one used by Google (2016). However, the exact values for the color scale used by Google (2016) are unknown. To provide a clear figure and overview, only the junctions of Vaanplein and Ridderkerk are shown, since these locations are the locations where serious congestion occurs. Only limited congestion occurs at other locations in the research network. Also, these locations have been calibrated to represent similar congestion patterns. However, for reasons of clarity, it was chosen to only include the congestion patterns for the junctions Vaanplein and Ridderkerk.

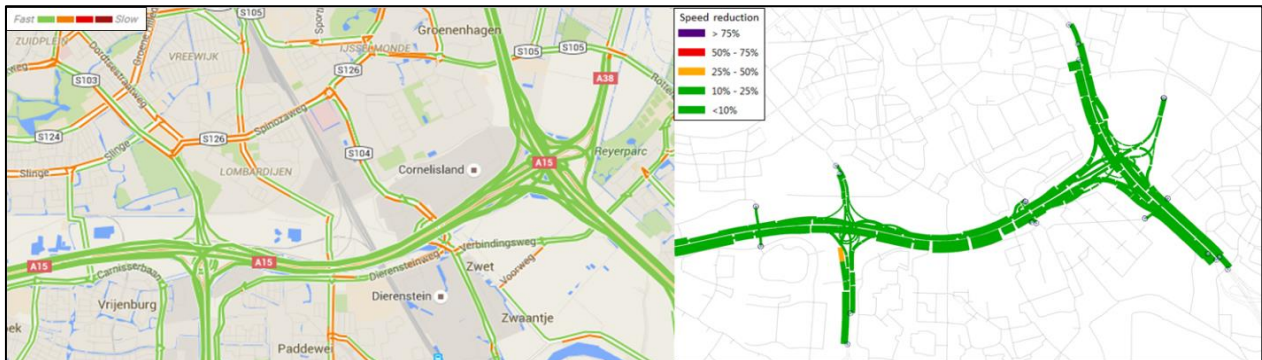


Figure 36 - Congestion patterns from Google (2016) (left) and microscopic simulation (right) from 15:45 - 16:00

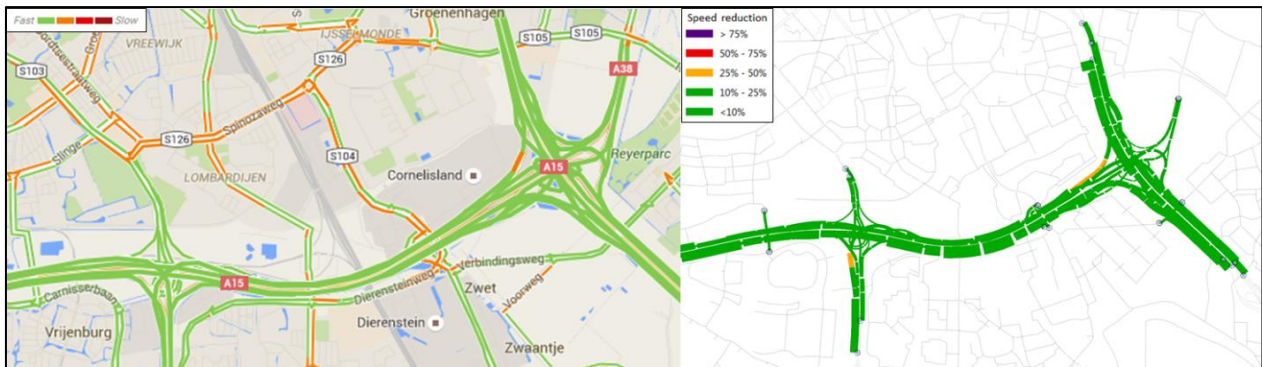


Figure 37 - Congestion patterns from Google (2016) (left) and microscopic simulation (right) from 16:00 - 16:15

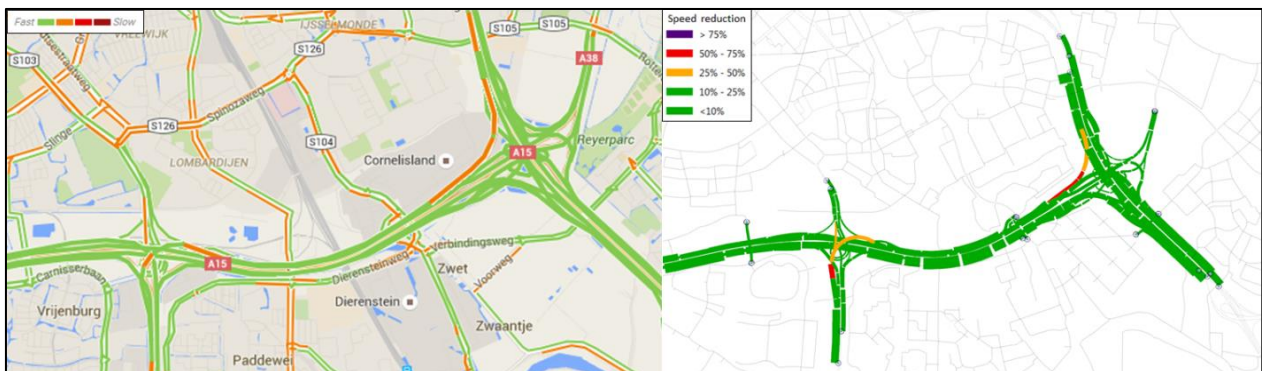


Figure 38 - Congestion patterns from Google (2016) (left) and microscopic simulation (right) from 16:15 - 16:30

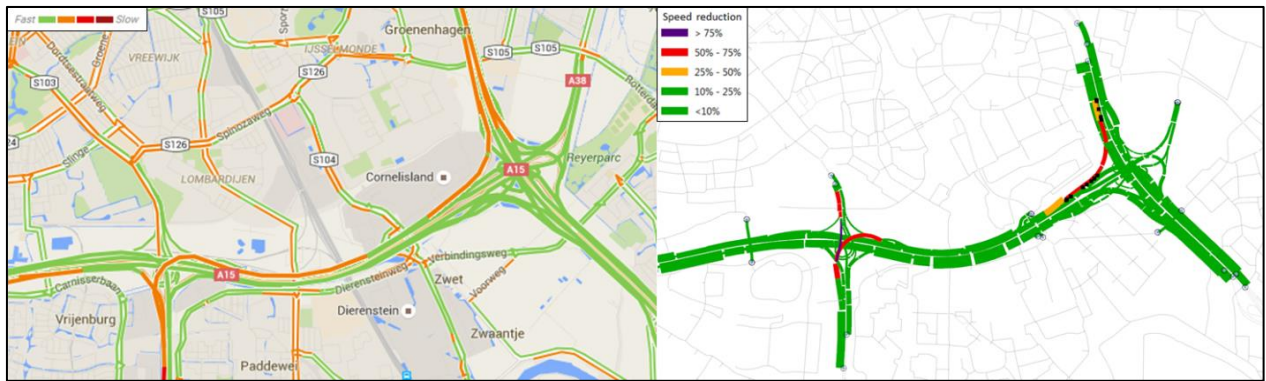


Figure 39 - Congestion patterns from Google (2016) (left) and microscopic simulation (right) from 16:30 - 16:45

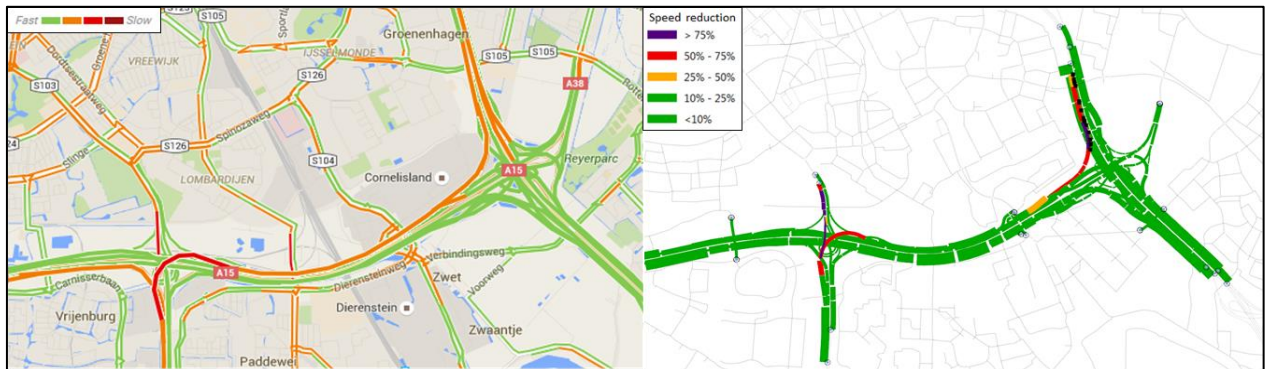


Figure 40 - Congestion patterns from Google (2016) (left) and microscopic simulation (right) from 16:45 - 17:00

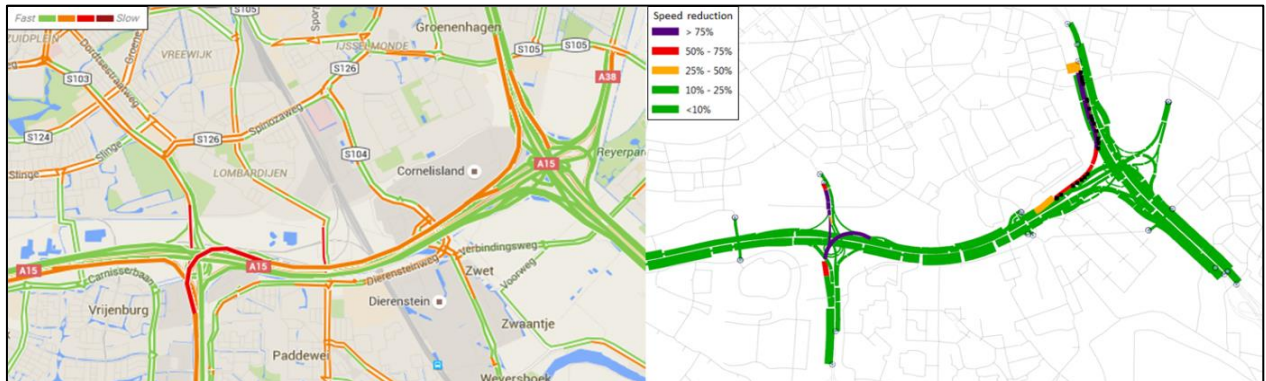


Figure 41 - Congestion patterns from Google (2016) (left) and microscopic simulation (right) from 17:00 - 17:15

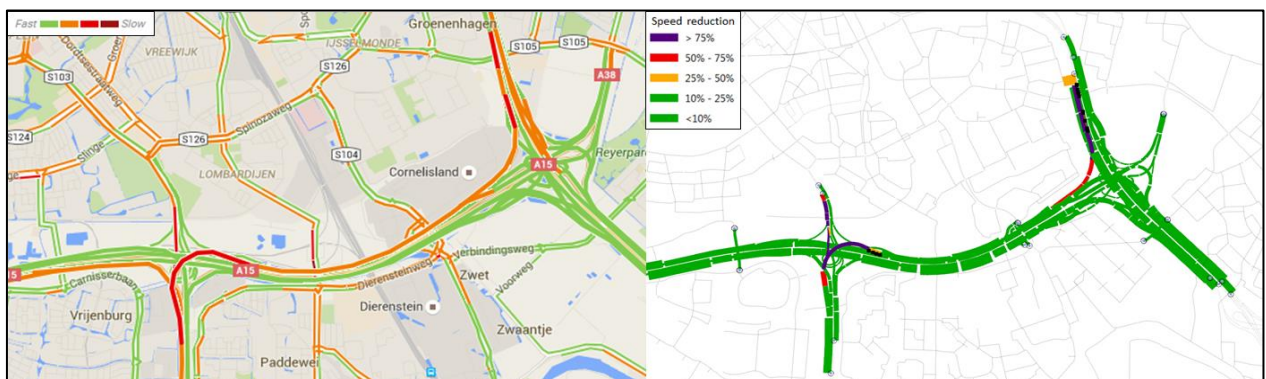


Figure 42 - Congestion patterns from Google (2016) (left) and microscopic simulation (right) from 17:15 - 17:30

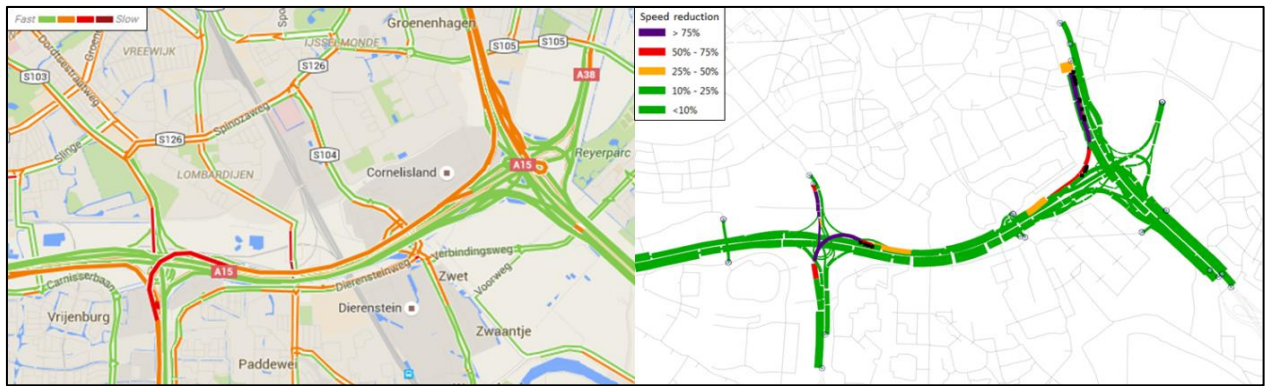


Figure 43 - Congestion patterns from Google (2016) (left) and microscopic simulation (right) from 17:30 - 17:45

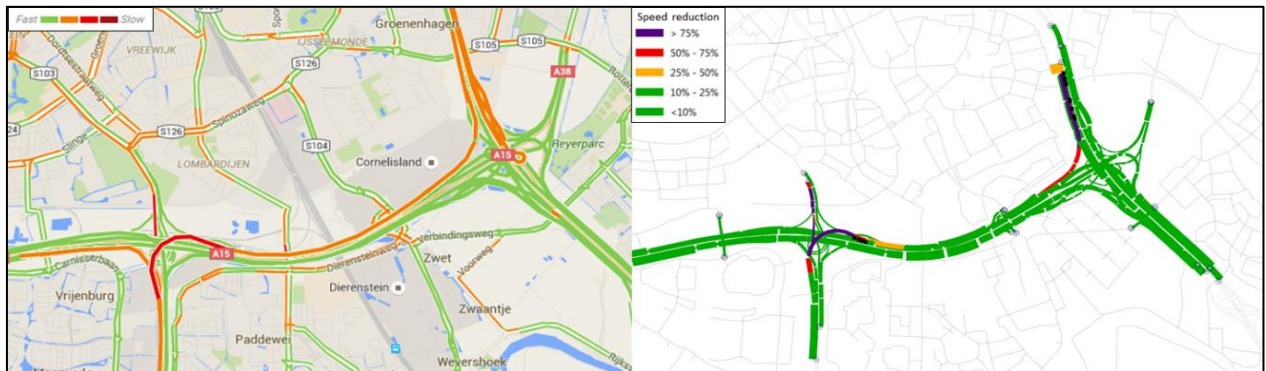


Figure 44 - Congestion patterns from Google (2016) (left) and microscopic simulation (right) from 17:45 - 18:00

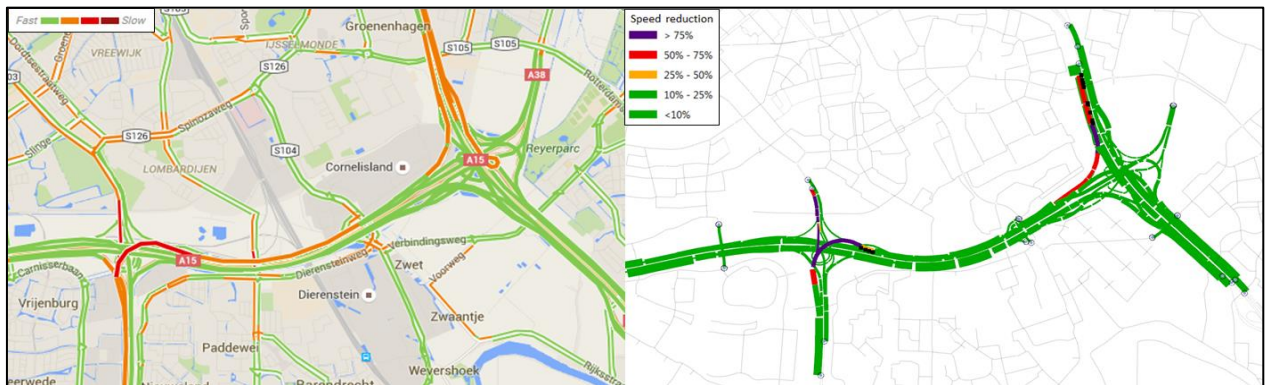


Figure 45 - Congestion patterns from Google (2016) (left) and microscopic simulation (right) from 18:00 - 18:15

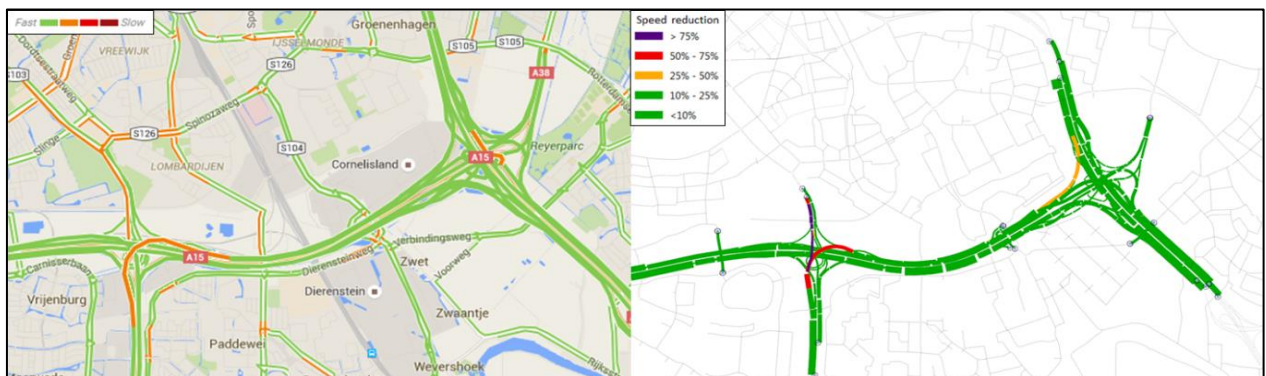


Figure 46 - Congestion patterns from Google (2016) (left) and microscopic simulation (right) from 18:15 - 18:30

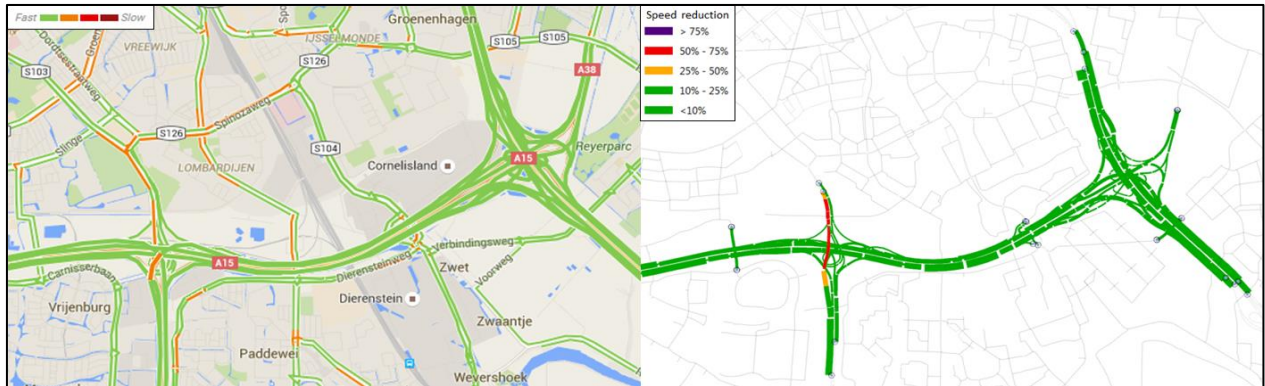


Figure 47 - Congestion patterns from Google (2016) (left) and microscopic simulation (right) from 18:30 - 18:45

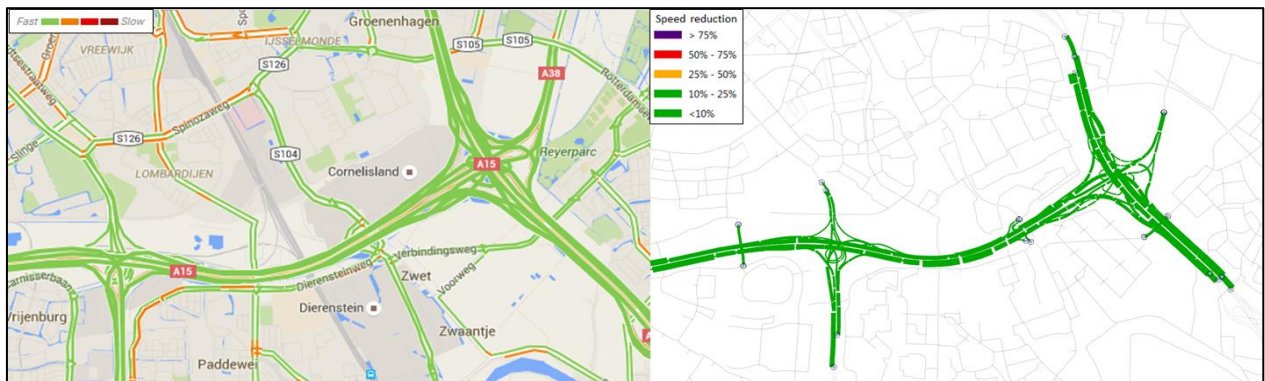


Figure 48 - Congestion patterns from Google (2016) (left) and microscopic simulation (right) from 18:45 - 19:00

In general, the microscopic simulation model represents the typical traffic patterns sufficiently. The most important congestion fronts are included in the simulation results. The typical traffic patterns might show a few more (small) congestion fronts. However, these congestion fronts are triggered by locations outside the research network and are not modelled in this research.

Regarding the start of congestion, the microscopic simulation results are very similar to the typical traffic patterns. At the first time periods, *Figure 36* and *Figure 37* show that the congestion at Ridderkerk starts somewhat earlier in the simulation results. However, this congestion front becomes more severe in *Figure 38*, for both the Google (2016) congestion patterns and microscopic simulation results. Regarding the start of congestion at Vaanplein, both the simulation results and typical traffic patterns indicate a time period of 16:00 to 16:15 (*Figure 37*) or 16:15 to 16:30 (*Figure 38*).

Subsequently, the congestion propagates relatively fast after the start of congestion, which could be found from *Figure 38*. The congestion fronts are connected in the Google (2016) traffic plots from *Figure 40* to *Figure 44*, which breaks apart in two different congestion fronts from 18:00 to 18:15 (*Figure 45*). In the microscopic simulation congestion patterns, these fronts do not get connected. However, the severity of the speed reductions seems to be larger. Also, the congestion is propagated in these time periods, which could be considered as similar behavior. Overall, the congestion images from microscopic simulation and Google (2016) are similar.

In the typical traffic patterns of Google (2016), junction Ridderkerk is free of congestion from *Figure 46* and onwards. For the microscopic simulation results this is the case from *Figure 47* and onwards. At junction Vaanplein, the congestion that propagated in the eastern direction is relieved in *Figure 47* for both plots, while the congestion that propagated in the northern direction is still found. This congestion is relieved in *Figure 48* for both plots.

Additionally, some congestion is found near the Botlek area (at the western part of the research network), which is not shown in the congestion pattern figures. Both the simulation results and typical traffic patterns show a very similar pattern and severity. The start and end of congestions are found to be at approximately the same time periods. Also, the length and severity of congestion are relatively similar for the simulation results and typical traffic patterns. Therefore, it can be concluded that the simulation is a sufficiently realistic representation of reality. The most important difference between the microscopic and mesoscopic congestion patterns is that the microscopic simulation results clearly show the congestion front from junction Vaanplein propagating to the north, while this severity of congestion was not found in mesoscopic simulation results. After this analysis, the microscopic model has been calibrated and does represent the real life situation to a sufficiently realistic extent. Additionally, the microscopic and mesoscopic simulation results show a high degree of similarity.

At a later stage, when running the different scenarios to compute the simulation results, it was found that the reaction time at stop and traffic light, as defined in the vehicle parameters is rounded down to a multiple of the simulation steps. This means that the defined reaction time at stop of 1.35s was simulated as 0.8s, while this should not be true. If simulation steps of 0.4 seconds would have been used, the reaction time at stop would be simulated as 1.2 seconds, which is significantly closer to 1.35. This would have resulted in some more spillback and thus an increase in congestion length in microscopic simulation. In this case, the simulation results were even expected to fit the data better as it did right now. However, this effect was not compensated for, because it would be a time-consuming process, while the results are expected to improve and seem to fit the data to a sufficient extent already.

3.3.8 Validation check

A validation check will be performed to check whether simulation results are in line with actual detector data, not used in the calibration procedure, since the calibration procedures have been based on traffic counts of 2014 and typical congestion pattern plots from Google (2016). To perform the validation check, loop detector data in terms of speed and flow is used. Loop detector data was collected by the National Data Warehouse for traffic information (2016). The application Dataack, developed by Royal HaskoningDHV and PathMobility, was used to read the data. This application stores detector data and is used to visualize patterns in detector data. In this case, speed and flow plots over some detectors were used to store the speeds and flows from 14:15 to 19:30 for 15 minute time intervals. The data is compared with the corresponding speed and flows at road sections on some critical locations in the network. For flow comparisons, the first and last time periods (i.e. warmup and cooldown period) are excluded.

The critical locations where the simulation results and NDW data are compared are locations where congestion occurs or where the traffic is put on the network. Again, these locations are chosen to be at the junctions Vaanplein and Ridderkerk. In this case, loop detector data of 2016 will be used to validate the simulation results. Data of 2016 is used, which is in line with the congestion patterns displayed by Google (2016) and this data is expected to show the effect of the extended A4, which was completed at the end of 2015. First, an average of the available loop detector data from the 1st of January 2016 until the 31st of March 2016 is used. This average is computed for weekdays, where public holidays are filtered. Secondly, loop detector data of a representative day, with a quite significant amount of congestion will be used. The reason for this is that the average congestion patterns are often smaller than representative congestion patterns, because some days might be free of congestion. February 29, 2016 was found to show a representative amount of congestion and was chosen as representative day to compare with. Additionally, the calibration has been performed such that serious congestion has been found. This means that in some cases the simulation results are expected to fit the representative day better than an average weekday.

To indicate the model fit with the traffic data, the R^2 statistic is used. The coefficient of determination [R^2] is a statistic that gives information about the goodness of fit of a model. A R^2 of 1 indicates that the model fits

the data perfectly, while a R^2 of 0 indicates that the model does not fit the data at all. Values of R^2 range from 0 to 1 and represent the proportion of the variance in the measured data that can be explained by the model. Higher values indicate less error variance. In general, R^2 values above 50% are considered to be acceptable (Moriasi et al., 2007), although this is very dependent on the type of study that is conducted. Additionally, this statistic is oversensitive to high extreme values (outliers) and insensitive to additive and proportional differences between model prediction and measured data (Moriasi et al., 2007). Generally speaking, a R^2 of 0.75 or higher is considered satisfactory for this study, since this indicates that the standard deviation of the errors is exactly one-half of the standard deviation of the dependent variable, which means that at least 50% of the standard deviation is explained by the model (Nau, 2016). Lower unsatisfying values of this statistic need further investigation. If the differences can be explained, lower R^2 -values could still be accepted.

Whenever possible, microscopic and mesoscopic speed and flow simulation results are compared with the average weekday, representative day and calibration counts. The coefficient of determination is depicted for any of these combinations. The chosen locations are at locations where congestion occurs or where traffic enters the network. Since the calibration procedure has aimed at the two junctions (Ridderkerk and Vaanplein) where congestion occurs, these junctions are chosen to check the validity. The detector locations are displayed and numbered in *Figure 49*. More detectors could be used to check the validity of simulation results, but this is not desired in terms of computational efforts. These six detector locations were chosen, because these detectors are located inside regions where significant congestion occurs.

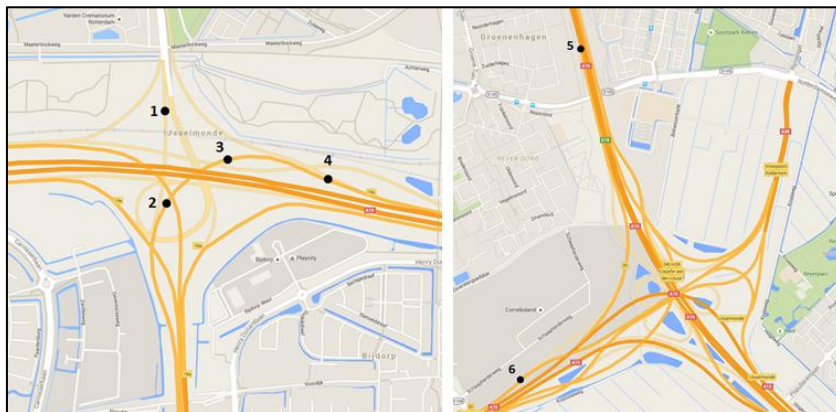


Figure 49 - Loop detector locations for validation check

3.3.8.1 Flows

In this section, the R^2 -values of the flow data and results of simulation are reported and reflected upon. For all analyses on flow, the first and last time periods are filtered out in calculating the coefficient of determination, since some time is needed to fill and flush the network in simulation, which means that the first and last time periods will deviate significantly from the traffic data. In Appendix A, flow and speed plots are shown per detector location. Additionally, an elaboration on the flow plots is concluded per detector location in this appendix.

Table 6 - Coefficients of determination [R^2] for comparisons of simulation flows with traffic data

Detector location	1		2		3		4		5		6	
	Micro	Meso	Micro	Meso	Micro	Meso	Micro	Meso	Micro	Meso	Micro	Meso
Average weekday	0.219	0.671	0.807	0.697	0.817	0.709	0.733	0.815	0.824	0.818	0.784	0.852
Representative day	0.005	0.069	0.407	0.299	0.313	0.200	0.449	0.266	0.143	0.175	0.278	0.332
Calibration counts	0.121	0.795	0.777	0.685	0.777	0.685			0.920	0.934		

In *Table 6*, the coefficients of determination [R^2] are shown for the simulation flows in comparison with the traffic data and calibration counts. Cells with R^2 -values above 0.75 are indicated in green. For detector locations 5 and 6, the simulation flows, both mesoscopic and microscopic, contain R^2 -values above 0.75 in comparison with the average weekday flow. These flows are directly validated micro- and mesoscopic.

For detector locations 2 and 3 (*Appendix A, Figure 154 and Figure 156*), mesoscopic simulation flows could not be validated directly. However, when looking at the flow patterns from simulation, it is found that the calibration counts are similar until 16:30, after which a similar flow pattern as the representative weekday is found. Although, the peak is slightly shifted in time, which results in decreasing values of R^2 . Additionally, these links need quite some time to be filled and flushed, which takes more than one time period for these locations and also contributes to decreasing values of R^2 due to outliers. Nevertheless, the mesoscopic simulation results show a comparable flow pattern if the calibration counts and representative weekday are considered at different time periods. The deviations can be explained, meaning that these flow patterns could be accepted in terms of validation.

For detector location 4 (*Appendix A, Figure 158*), the microscopic simulation flows do not have a R^2 -value above 0.75, which means that further explanation is required. The microscopic simulation flow results at detector location 4 resemble the flow patterns of the average weekday until 18:00, but are constantly found to be approximately 500 vehicles per hour lower. From 18:00 and onwards, the same peak as the representative weekday is found, albeit slightly less severe. When comparing with the representative weekday, a very similar pattern is found between 16:30 and 19:30. Therefore, the microscopic simulation flows are also validated, because the patterns are similar to a combination of the average and representative day taken into account, although the peaks in flows are shifted in time. Additionally, the last time periods contribute to a decrease in R^2 , because the flows are already very low at these locations, in order to flush the network.

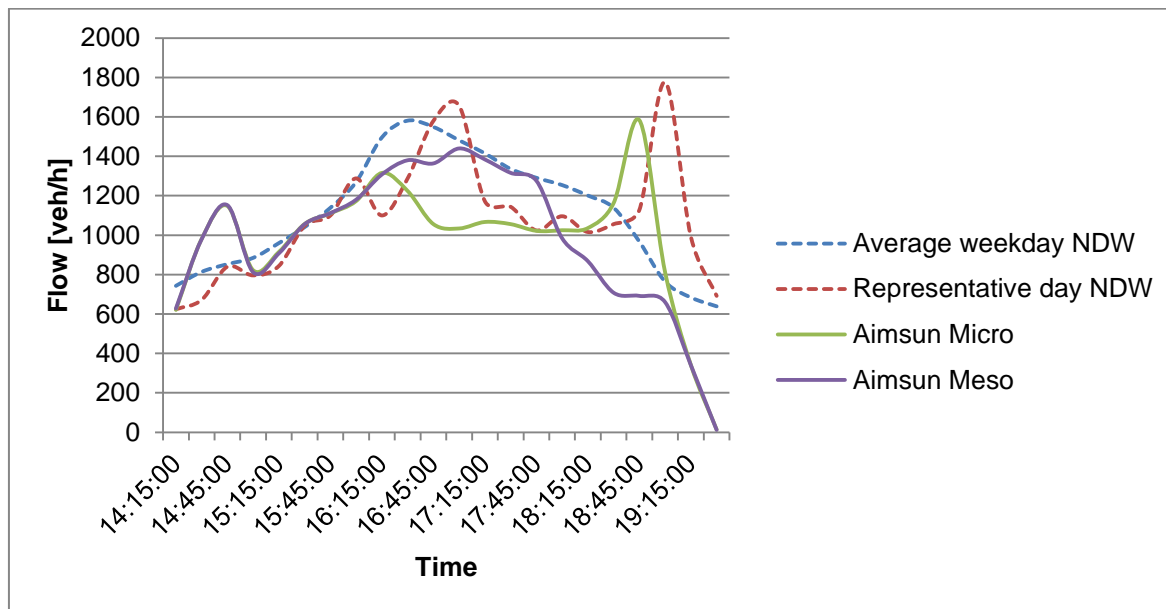


Figure 50 - Comparison of simulation flow results with traffic data

For the mesoscopic simulation results for detector 1, the simulation results are within the acceptable margin with respect to the calibration counts. Additionally, the mesoscopic simulation flows resemble the pattern of the average weekday, except for some outliers. The microscopic simulation flows show very low R^2 -value and require some attention. However, if the flow over time at detector location 1 is compared with

the flow pattern at the representative weekday (*Figure 50*), it is found that the pattern is very similar. Both the microscopic simulation flows and representative day flows show two serious peaks. However, the peaks in the microscopic simulation results are somewhat shifted in time and are found at earlier time periods. The microscopic flows peak at approximately 16:15 and 18:45, while the peaks for the representative day are found at approximately 17:00 and 19:00. Since these peaks are found for different time periods, these differences contribute to decreasing values of R^2 , since extreme outliers are found in these occasions. In terms of validation, the combination of the microscopic flows and representative day flows is accepted, because the patterns are very similar, but slightly shifted in time. However, due to the similar pattern, the simulation results can be accepted in terms of validation.

3.3.8.2 Speeds

In this section, the R^2 -values of the speeds from detector data and results of simulation are reported and reflected upon. For the analyses on speed, the first and last time periods do not have to be filtered out, since these points will show free flow speeds, which are also expected to be found in the detector data. In Appendix A, speed plots are shown per detector location. Additionally, an elaboration on the flow and speed plots is concluded per detector location in this Appendix. Additionally, the same approach was used to validate the speed over time found in the simulations. Again, the coefficients of determination are given with respect to the average weekday and representative day. The results are given in *Table 7*. In *Table 7*, cells with R^2 -values above the limit of 0.75 are indicated in green.

Table 7 - Coefficients of determination [R^2] for comparisons of simulation speeds with traffic data

Detector location	1		2		3		4		5		6	
	Micro	Meso	Micro	Meso	Micro	Meso	Micro	Meso	Micro	Meso	Micro	Meso
Average weekday	0.809	0.238	0.840	0.798	0.863	0.817	0.766	0.902	0.660	0.286	0.464	0.430
Representative day	0.853	0.151	0.911	0.970	0.933	0.956	0.493	0.714	0.764	0.177	0.476	0.349

It becomes clear that detector 2, 3 and 4 all have green cells, for both micro- and mesoscopic simulation results, which means that these speeds are considered to fit the data sufficiently and are validated directly.

The microscopic speed results at detector location 1 could also be justified, because the coefficients of determination are above 0.75 for both the average weekday and representative day. However, the mesoscopic speed results are relatively far off, because this location does not suffer serious congestion in the mesoscopic simulation, while the average and representative weekday show more congestion (*Appendix A, Figure 153*). It is expected that this congestion front is caused by lane-changing behavior of drivers, which is simplified for a mesoscopic simulation. Therefore, the severity of congestion at this location could not be included sufficiently in the mesoscopic simulation, within the calibration boundaries defined. However, since the reason for this problem is known, this flaw is still accepted in terms of validation, because the mesoscopic simulation does show some congestion in a comparable pattern, albeit that the severity and duration of congestion is significantly lower.

The microscopic speeds for detector location 5 could also be accepted directly, because the R^2 for the representative day is above 0.75. The mesoscopic flow results are relatively far off from the limit. This could be explained by the fact that the congestion is not spilled back towards this location in the mesoscopic simulation, while congestion (i.e. speed reductions) was found in the microscopic results and representative day data (*Appendix A, Figure 161*). The speed differences between the mesoscopic speeds from simulation and the speeds at an average weekday are very close to each other, since the maximum speed difference is found to be only 12 km/h. This maximum speed difference is low, which means that these results are also accepted in terms of validation. The corresponding R^2 -value for the

combination of the mesoscopic speeds and average day is low, because the averages are close to each other, which implies that all deviations contribute significantly to decreasing values of R^2 .

At detector location 6, the coefficients of determination are too low as well. This location can be considered as the approximate head or source of congestion. The representative day shows serious congestion, while the average weekday does only show mild congestion. The microscopic simulation reports speeds that are somewhat reduced from the start of simulation, while the mesoscopic shows some congestion, but only for a limited time period (*Figure 51*). The expected reason for the relatively poor fit is that the detector is located at a single place, while the simulation results are obtained as an average speed over a road section, which influence the results. Most of the congestion in the simulation is shown just upstream of this road section, which means that congestion is not shown for the simulation results. If the microscopic and mesoscopic speed results are compared with the speeds found for the average weekday, the simulation results seem to have a relatively good fit with the average weekday. However, the mesoscopic simulation shows a shorter decrease in speed, while the microscopic simulation shows a longer decrease in speed. Additionally, the speed differences are all below 20 km/h, which allows that these speed patterns are also accepted in terms of validation. Concluding, it could be stated that in most cases, there is at least one coefficient of determination that falls within the limits. When this is not true, the differences can be explained by clear reasons.

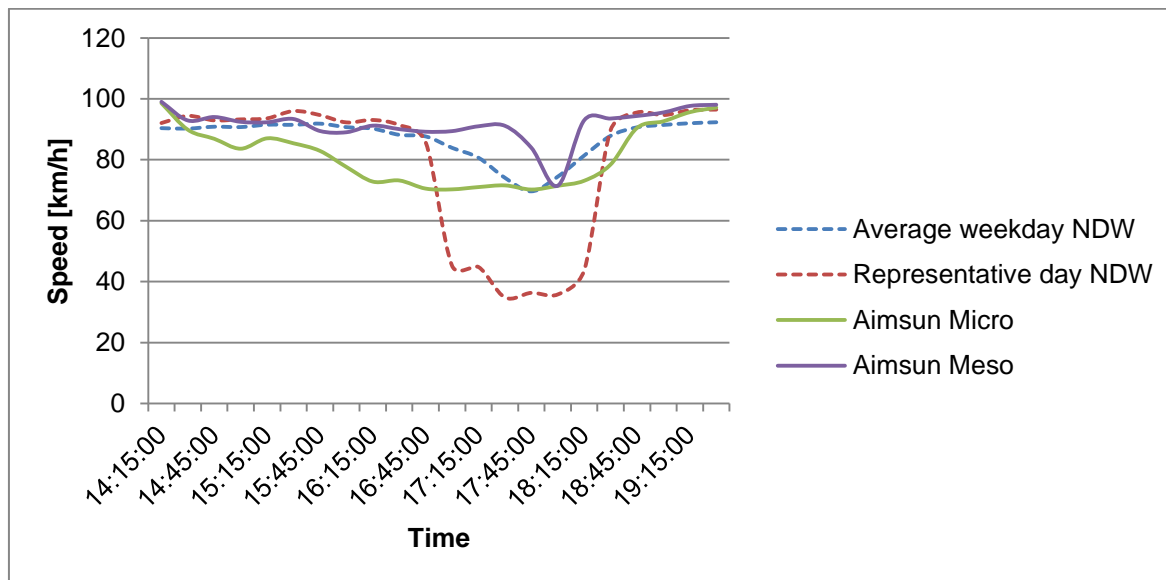


Figure 51 - Comparison of simulation speed results with traffic data

4 Verification of ACC driving behavior

Since modelling the driving behavior of ACC vehicles/drivers is of vital importance in this research, a verification of ACC driving behavior is included to assess whether the ACC vehicles defined in the simulation perform realistic and representative behavior. Since this study is on the effect of ACC and CACC vehicles upon traffic flow, the driving behavior of ACC vehicles should be defined properly.

Firstly, the car-following model implemented in Aimsun, as discussed in chapter 2, will be used to describe ACC and CACC driving behavior. It is of vital importance to realize that this means that a car-following model to describe human driving behavior has been manipulated in such a way that it is able to represent ACC or CACC driving behavior. Thus, no separate car-following model is used to describe driving behavior of intelligent vehicles. This also implies that the same lane-changing and car-following models are used to model ACC driving behavior with different parameters in comparison with human drivers in Aimsun. Secondly, the parameter settings used as input for defining the ACC behavior have to be sufficiently realistic and representative for ACC vehicles. The parameters used in similar literature studies, displayed in *Table 3* can help to find realistic parameter settings. Thirdly, since the simulation is performed for a whole network where congestion occurs and vehicles could come to a standstill, the ACC vehicles have to be capable of working safely at full speed range. In order to make sure that ACC systems work properly in typical driving situations, a study by Mullakkal-Babu et al. (2016) will be used as a reference to ensure that the controller can function at full speed ranges in typical driving situations defined.

This chapter contains information on how the speed choices of ACC users are modelled. Additionally, it is explained how the headway choices, lane-changing behavior and car following behavior of ACC users of ACC systems will be modelled. Then, typical driving scenarios (Mullakkal-Babu et al., 2016) are included to test whether the ACC vehicles behave according to the expectations and defined parameter settings.

4.1 Modelling speed choice of ACC users

Similar to conventional cruise control systems, the users of ACC systems have to select a set speed at which they wish to drive. If a set speed is selected, the system will automatically try to reach and maintain the set speed, if the constraints of the following distances to the leading vehicle are not exceeded.

In normal car driving, two different types of drivers could be distinguished. There are aggressive drivers who tend to drive at relatively high speeds and accept smaller merging gaps, while defensive drivers tend to drive at a lower speed and only change lanes when the gaps are safe. In his study on ACC in practice, Gorter (2015) found out that a similar pattern is observed between ACC users. Two groups are distinguished in this study. One group of ACC users decide to apply more car-following behavior, instead of overtaking slow vehicles. This behavior leads to an increase in the use of the right lane, where speeds are relatively lower. This group of ACC users could be considered as defensive ACC users. The other group of ACC users was found to choose to overtake other cars. This group of users tends to keep driving on the left lanes, to prevent braking actions to maintain a safe set following distance towards the preceding vehicle, executed by the ACC system when they return to a slower lane. This group of ACC users could be considered as aggressive ACC users. As a consequence, defensive ACC users often drive at lower speeds in comparison with aggressive ACC users.

The desired maximum speed an ACC user would like to use is not expected to differ much from the desired maximum speed this person would like to apply during driving in a normal vehicle. However, Gorter (2015) found that ACC drivers are more aware of the speed limits and do adapt to these speed limits more frequently. To account for this effect, the speed acceptance parameter of ACC users should be adapted. Therefore, the mean speed acceptance for ACC users has been set to 1.05, with a deviation of 0.05 and minimum and maximum of 1.00 and 1.15. Normal car drivers have a mean speed acceptance of

1.1, a minimum of 1.0 and a maximum of 1.2. This ensures that ACC users adapt their speeds to the speed limits more frequently. Additionally, the 0.05 deviation is used to differentiate between the defensive and aggressive ACC users.

4.2 Modelling headway choices of ACC users

Next to selecting a set speed, users of ACC systems have to manually select their desired gap when using the system. Most ACC systems provide some fixed gap settings to select. In most cases, ACC users can select at least three different time gap settings.

However, it should be noted that time gap and time headway are different concepts. In real ACC systems, user set their desired time gap, which is the net time headway (headway-speed/vehicle length of leader). However, time headway should be given in as a parameter in Aimsun. Please note that Aimsun uses improper terminology, because the term gap is used, while it actually represents headway in simulation.

Generally, time gap settings in literature were found to vary from a 1 second minimum to 3 seconds maximum (*Table 3*). Gap settings ranging from 1.1 to 2 seconds for ACC are commonly used in *Table 3*. In the literature studies considered in *Table 3*, both time headway and time gap are used. Time gaps are net time headways, where the length of the leading vehicle is abstracted from the time headway. Time gaps between 1.1 and 2 seconds are often found in literature, as well as time headway settings between 1.2 and 2.0 seconds are found in many studies. With a vehicle length of 4 meters and a driving speed of 100 kilometers per hour, a time gap of 1.1 seconds equals 1.244 seconds headway.

In Aimsun, some improper terminology is used, because the parameter is called gap, although it actually defines the time headway. In order to represent ACC driving behavior, it was chosen to set the mean time headway at 1.6 seconds in Aimsun, with a deviation of 0.2 seconds, a 1.4 seconds minimum and a 2 seconds maximum. The mean value of 1.6 seconds was chosen, because this is in the middle of 1.2 and 2.0 seconds, which is in line with settings used in literature. Additionally, the writer of this report estimated the time headway of the vehicles equipped with ACC vehicles the writer drove in to be approximately 1.5 to 2.0 seconds. The deviation of 0.2 seconds is used to account for differences between car brands and ACC systems, since some systems are known to use a more aggressive driving style (for example, Tesla) or more defensive driving style (like Volvo). The maximum headway of 2.0 seconds was based on the gap/headway ranges found in literature. The minimum headway of 1.4 seconds was chosen to partly compensate for the differences in terminology (gap/headway) and to simulate currently available ACC vehicles, which are estimated to apply headways between approximately 1.5 and 2.0 seconds.

4.3 Modelling lane-changing behavior of ACC users

In most current ACC systems, the driver is still fully responsible for the lane-changing behavior. However, there also are some cars (e.g. Tesla) that could change a lane on itself if the driver uses the direction indicator on the highway. However, this type of technology is still very sophisticated and is not taken into account for the first type of ACC in this research.

Regarding the lane-changing behavior, Gorter (2015) found out that ACC users change lanes less frequently. In his study on ACC in practice, Gorter (2015) found out that two groups can be distinguished. One group of ACC users decide to apply more car-following behavior, instead of overtaking slow vehicles. This behavior leads to an increase in the use of the right lane, where speeds are relatively lower. This group of ACC users could be considered as defensive ACC users. The other group of ACC users was found to choose to overtake other cars. This group of users tends to keep driving on the left lanes, to prevent braking actions to maintain a safe set following distance towards the preceding vehicle when returning to a slower lane. This group of ACC users could be considered as aggressive ACC users.

Additionally, more use of the right lane is also found by van Twuijver & Pol (2004) and Strand, Nilsson, Karlsson, & Nilsson (2011), while more use of the left lane is found by Rudin-Brown & Parker (2004).

There are no clear vehicle parameters that directly influence the lane-changing behavior in Aimsun. However, as discussed in section 2.4.2, the lane-changing behavior depends on factors such as the need, desire and possibility to change lanes, the target lanes or destination, braking rates and available gaps. To account for the reduction in the total number of lane changes by ACC users, different approaches are used. First, speeds at which ACC users will be driving are closer to the maximum speed due to the speed acceptance parameter as discussed before. Therefore, the average need and desire to perform an overtaking maneuver will reduce. Since ACC users have a time headway defined in the simulation, these users will also apply these headways in terms of lane-changing behavior. Therefore, the number of lane changes will also be reduced. Also, as indicated in *Table 3*, ACC systems often use lower acceleration and deceleration rates in comparison with human drivers. Therefore, the acceleration and deceleration rates used in simulation will be reduced too, which should lead to a further decrease in the amount of lane changes. The extent of reductions in acceleration and deceleration are discussed later in this chapter.

The parameter settings used to influence the lane-changing behavior of ACC users have been discussed. However, it is very important to note that the destinations and routes are very important contributions to the total number of lane changes applied, since several lane changes are needed to follow routes towards the destination. In addition, some lane changes also occur due to cooperation behavior, where one of the drivers switches lanes to make room to provide a safe gap for other vehicles.

4.4 Modelling car-following behavior of ACC vehicles

It is important to look at the whole car-following behavior of ACC vehicles, since there might be some significant differences in comparison with normal car drivers. How the car-following behavior of ACC vehicles is modelled is discussed in this subsection.

The car-following model in Aimsun is considered as a safe distance model, in which the vehicles will apply safe following distances at all times. ACC systems work by applying a constant time gap, whenever possible. To include this constant time gap policy in the simulation, a desired headway is defined. However, in some cases, larger headways will be found, because Aimsun automatically ensures safe following distances, which is different from how real ACC vehicles would respond, since these vehicles would simply adapt the set following distance with respect to the preceding vehicle.

The changes in following distances and lane-changing behavior have been discussed in the previous subsections. Summarizing, the speed acceptance parameter for ACC users is reduced. Additionally, the number of lane changes should be reduced as well, due to small changes in ACC parameters.

The clearances define the distance between two vehicles at standstill. In *Table 3*, the clearances used in literature are also provided. For most studies, the clearance for ACC systems was set to 2.0 meters. The same input was used for manual car drivers. In this study, the clearance was also set to 2.0 meters.

Additionally, many literature studies in *Table 3* show that ACC systems generally apply lower acceleration and deceleration rates. The most common values for maximum acceleration in *Table 3* are 2 and 3m/s². Therefore it was chosen to set the mean maximum acceleration at 2.5m/s². The deviation was set at 0.2m/s², similar to the settings for manual cars. Subsequently, the minimum and maximum acceleration was set at 2.1 and 2.9m/s². Comfortable decelerations in real life are taken into account in Aimsun by the normal deceleration. The most common values found for comfortable decelerations in literature (*Table 3*) are -2 and -3m/s². Therefore, the mean normal deceleration for ACC vehicles in Aimsun is set to -2.5m/s², with a minimum and maximum of -2 and -3m/s². The corresponding deviation was set at 0.25m/s².

Since the simulation is performed for a whole network where congestion occurs and vehicles could come to a standstill, the ACC vehicles have to be capable of working safely at full speed range. A study by Mullakkal-Babu et al. (2016) will be used as a reference to ensure that the controller works at full speed range. In studies, considering relatively high maximum decelerations or full range ACC systems, found in Table 3, maximum decelerations of -5 to -8m/s² are the most common values. Therefore, a mean maximum deceleration of -7m/s² for ACC vehicles was modelled in Aimsun, with minimum and maximum values of -5 and -8m/s² for this parameter. To ensure a relatively large spread of maximum decelerations, a deviation of 1 m/s² was used. In this way, the ACC systems are capable of working at full speed range.

The last important parameter that has a large influence on car-following behavior is the reaction time. For the ACC systems modelled at the start of this study, the reaction time is set to 0.8 seconds, just like the reaction time for manual car drivers. However, it is important to note that ACC systems are capable of reacting significantly faster to preceding vehicles. Only a small sensor delay is found and reaction times should be set lower if this and only this part of reaction time is taken into account. However, ACC systems respond very slowly to vehicles merging directly in front of them, which meant that these effects were compensated for and a reaction time of 0.8 was chosen. For the reaction time at stop and reaction time at traffic light, it is assumed that ACC users still have to accelerate by themselves after standstill.

4.5 Verification of ACC following behavior

A study by Mullakkal-Babu et al. (2016) will be used as a reference to ensure that the controller works at full speed range and is capable of dealing with typical traffic situations. Similar approaches and scenarios will be used to assess whether the vehicles are able to work at full speed range and are able to work safely and according to the input parameters in characteristic scenarios, such as a simple following scenario, stop and go scenario, emergency braking scenario and cut-in scenario. The parameters will be defined in a worst-case scenario, which means that all ACC systems with improved parameters are also expected to react in a safe manner. Additionally, a small sensitivity analysis is performed to check which parameters have a high or low influence in the car-following behavior of the vehicles. This sensitivity analysis could later be used to estimate the effects of improving ACC driving behavior parameters.

First, an overview of the parameter settings for ACC vehicles in comparison with the regular car is given. Subsequently, the characteristic driving scenarios and results are provided and reflected upon. Afterwards, a short sensitivity analysis is performed.

4.5.1 Overview of parameter settings for ACC

For the general user class settings, such as width, length and desired speed, the standard parameter values as used for 'normal' cars have been used, since these are not expected to change significantly. Although, the desired speed might slightly change, this effect is compensated in the speed acceptance parameters. For ACC users, the selection of speed is going hand in hand with the knowledge of the speed limit. A summary of these parameters is given in Figure 52. With respect to these settings, there are no differences between ACC vehicles and manual car drivers.

Car	Mean	Deviation	Minimum	Maximum
Length	4,05 m	0,50 m	3,00 m	5,00 m
Width	1,60 m	0,10 m	1,40 m	1,80 m
Max Desired Speed	115,00 km/h	10,00 km/h	100,00 km/h	130,00 km/h
ACC	Mean	Deviation	Minimum	Maximum
Length	4,05 m	0,50 m	3,00 m	5,00 m
Width	1,60 m	0,10 m	1,40 m	1,80 m
Max Desired Speed	115,00 km/h	10,00 km/h	100,00 km/h	130,00 km/h

Figure 52 - General parameter settings for Car (top) and ACC (bottom)

For the microscopic parameters, there are changes in parameter settings between car and ACC users. These differences are found in the acceleration/deceleration parameters, as well as in the headway settings. As discussed in the previous subsections, the accelerations and decelerations for ACC systems are slightly lower, although the maximum deceleration parameter might be more severe, because ACC systems need to work at full speed range. For ACC vehicles, a constant time gap policy should be used, while this is not the case for regular car users. An overview of the microscopic settings of ACC vehicles in comparison with the car parameters is provided in *Figure 53*. The dynamic model parameter settings for both vehicle types are provided in *Figure 54*, where it is found that there is a change in speed acceptance, because ACC users more frequently adapt to the speed limits.

Car				
	Mean	Deviation	Minimum	Maximum
Max Acceleration	2,80 m/s ²	0,20 m/s ²	2,40 m/s ²	3,20 m/s ²
Normal Deceleration	3,50 m/s ²	0,20 m/s ²	3,10 m/s ²	3,90 m/s ²
Max. Deceleration	7,00 m/s ²	0,40 m/s ²	6,20 m/s ²	7,80 m/s ²
Car-following Model				
	Mean	Deviation	Minimum	Maximum
Sensitivity Factor	1,00	0,00	1,00	1,00
Gap	0,00 secs	0,00 secs	0,00 secs	0,00 secs
Lane-changing Model				
<input type="checkbox"/> Staying in Overtaking Lane		<input type="checkbox"/> Imprudent Lane Changing		
Two-Way Overtaking Model				
	Mean	Deviation	Minimum	Maximum
Margin for Overtaking Manouever	5,00 secs	3,00 secs	1,00 secs	10,00 secs
ACC				
	Mean	Deviation	Minimum	Maximum
Max Acceleration	2,50 m/s ²	0,20 m/s ²	2,10 m/s ²	2,90 m/s ²
Normal Deceleration	2,50 m/s ²	0,25 m/s ²	2,00 m/s ²	3,00 m/s ²
Max. Deceleration	6,00 m/s ²	1,00 m/s ²	5,00 m/s ²	8,00 m/s ²
Car-following Model				
	Mean	Deviation	Minimum	Maximum
Sensitivity Factor	1,00	0,00	1,00	1,00
Gap	1,60 secs	0,20 secs	1,40 secs	2,00 secs
Lane-changing Model				
<input type="checkbox"/> Staying in Overtaking Lane		<input type="checkbox"/> Imprudent Lane Changing		
Two-Way Overtaking Model				
	Mean	Deviation	Minimum	Maximum
Margin for Overtaking Manouever	5,00 secs	3,00 secs	1,00 secs	10,00 secs

Figure 53 - Microscopic parameter settings for Car (top) and ACC (bottom)

Car				
	Mean	Deviation	Minimum	Maximum
Speed Acceptance	1,10	0,05	1,00	1,20
Clearance	2,00 m	0,20 m	1,60 m	2,40 m
Maximum Give Way Time	20,00 secs	2,00 secs	15,00 secs	25,00 secs
Guidance Acceptance	75,00 %	70,00 %	65,00 %	90,00 %
Value of Time	0,00 \$/h	0,00 \$/h	0,00 \$/h	0,00 \$/h
ACC				
	Mean	Deviation	Minimum	Maximum
Speed Acceptance	1,05	0,05	1,00	1,15
Clearance	2,00 m	0,20 m	1,60 m	2,40 m
Maximum Give Way Time	20,00 secs	2,00 secs	15,00 secs	25,00 secs
Guidance Acceptance	75,00 %	10,00 %	65,00 %	90,00 %
Value of Time	0,00 \$/h	0,00 \$/h	0,00 \$/h	0,00 \$/h

Figure 54 - Dynamic model parameter settings for Car (top) and ACC (bottom)

4.5.2 Following scenario

The following scenario consists of five consecutive road sections with differing maximum speeds, as shown in *Table 8*. This scenario checks whether the ACC vehicles follow the leader vehicles accordingly and respects the maximum section speed and parameter settings of the ACC vehicles. Several detectors were put on the network to check the headway between consecutive vehicles along the network. In this scenario, several ACC vehicles are put into the network as fast as possible.

Table 8 - Road sections of following scenario

Section	Maximum speed [km/h]	Length [m]
1	120	495
2	100	207
3	120	266
4	80	128
5	120	89

Three ACC vehicles are modelled in this scenario. The following vehicles have the lowest deceleration parameters as defined in the previous subsection, to simulate a worst case scenario where the following vehicle brakes at the lowest rate possible. However, the desired speeds of these following vehicles is set higher than the desired speed of the leading vehicle in order to get small headways. However, it should be noted that whenever the braking rate of the leading vehicle is higher than the following vehicle, the V_b component of the car-following model ensures a safe headway and might propose to drive at larger gaps. Additionally, the lowest headway possible of 1.4s has been used to ensure short following distances.

The speed and acceleration plots of three ACC vehicles against time are shown in *Figure 55* and *Figure 56*. From these figures it can be concluded that the following vehicles respond well to the leading vehicle. All vehicles show resembling speed and acceleration profiles. It is found that vehicle 2 and 3 need some time to drive at its' desired headway, since their speeds are higher at the start. Also, the decelerations and accelerations applied are very similar for all vehicles. One of the important conclusions is that the accelerations are between 2 and -1.5, which means that these are in the acceleration range as it was defined. When vehicle 1 leaves the simulation, the speed constraint for the following vehicle disappears, which results in higher accelerations. Additionally, small delays could be witnessed around second 40 to 45 in *Figure 56*. Real ACC systems also show small delays, so this delay is justified in this simple following scenario.

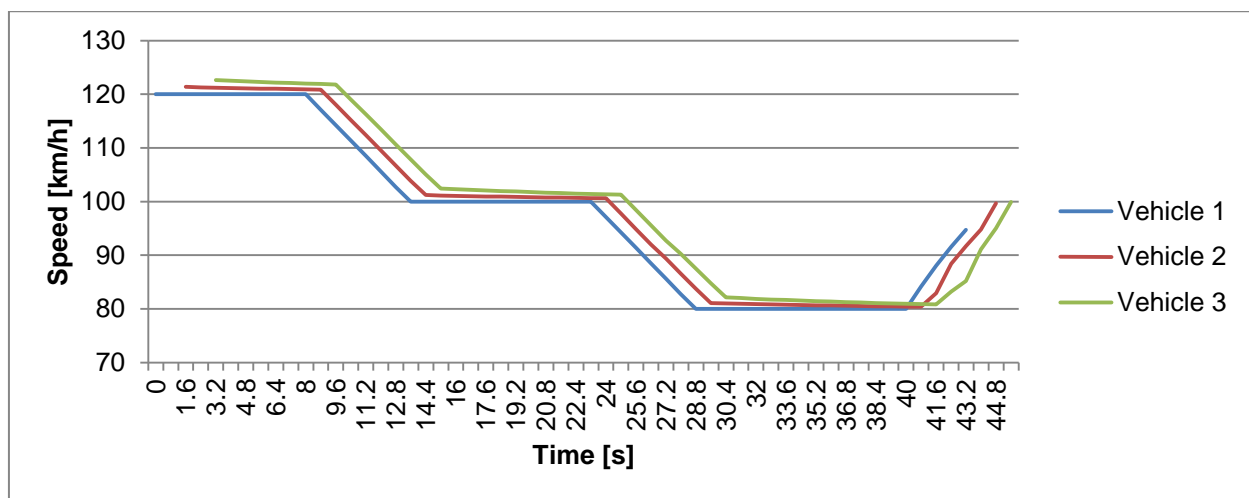


Figure 55 - Speed plot for following scenario

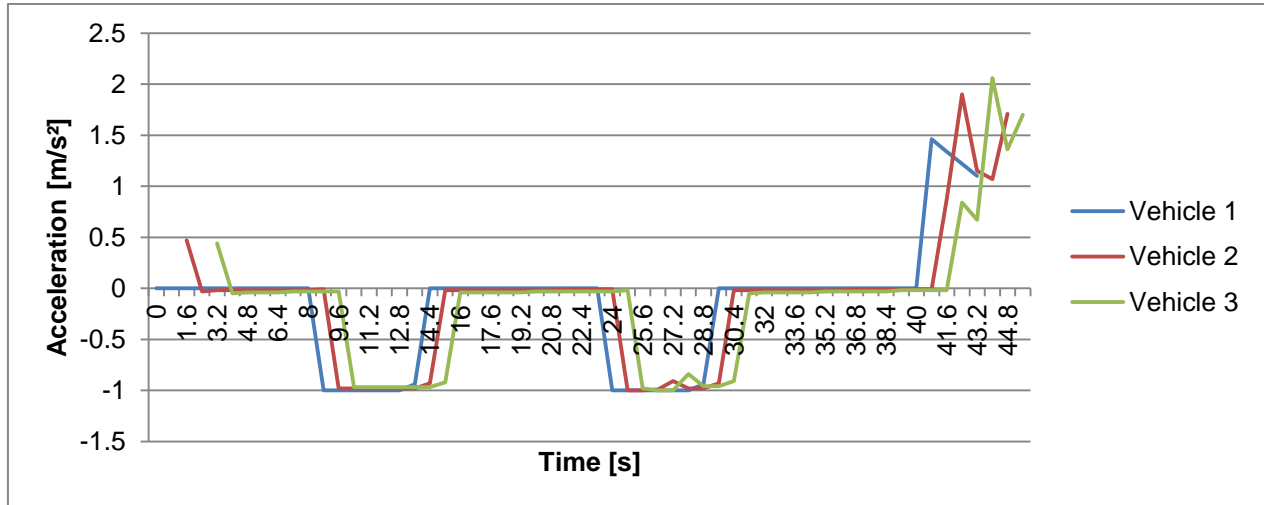


Figure 56 - Acceleration plot for following scenario

The ACC vehicles respond adequately to their leading vehicles, because they are adapting their speeds according to their predecessors speed and respect the section maximum speeds within the defined speed acceptance margin. The smallest headway found is 1.40 seconds, which is in line with the parameter settings. The headways generally range between 1.4 and 1.6 seconds along the entire network.

4.5.3 Stop and go scenario

The stop and go scenario consists of four subsequent road sections with relatively low maximum speeds (up to 50 km/h) to resemble a congested traffic situation with stop and go traffic. One of the road sections is closed for 2 minutes from the simulation start to create a temporary standstill for the vehicles. This scenario is used to see whether the following ACC vehicle is able to show realistic driving behavior at low speeds. Again, this scenario also checks whether the following vehicle behaves similar to the leading vehicle and applies the correct headway settings. A summary of the road sections is given in *Table 9*.

Table 9 - Road sections in stop and go scenario

Section	Maximum speed [km/h]	Length [m]	Lane closure [s]
1	20	87	
2	50	1066	
3	50	53	0-120
4	50	349	

Again, the following vehicle has a normal deceleration of 2 m/s² and a maximum deceleration of 5 m/s², which is the minimum defined in the parameter settings. The following vehicle has the maximum acceleration possible to decrease headways, while the leading vehicle has the minimum acceleration possible. The minimum headway of 1.4 seconds is applied to the vehicles.

The speed and acceleration plots of this scenario are provided in *Figure 57* and *Figure 58*. It can be found that vehicle 2 follows the same speed and acceleration behavior as the leading vehicle. However, there is a small drop in the speed profile of vehicle 2 near second 20 of the simulation. This drop could be explained by the two different speed components of the car-following model. In *Figure 59*, it can be verified that the vehicle speed is restricted by the V_b component for the majority of simulation. However, at the moment of this drop, the vehicle speed is restricted by the V_a component. Furthermore, the speed and acceleration behavior of the two vehicles is very similar. Because the following vehicle has a lower deceleration defined, the following vehicle brakes at a lower rate, but for a longer period of time.

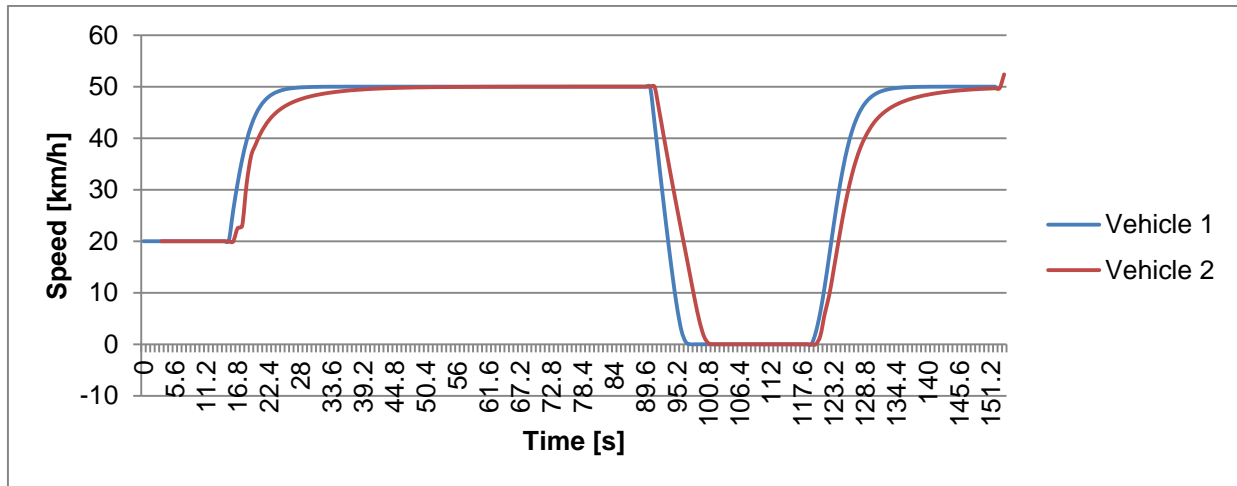


Figure 57 - Speed plot for the stop and go scenario

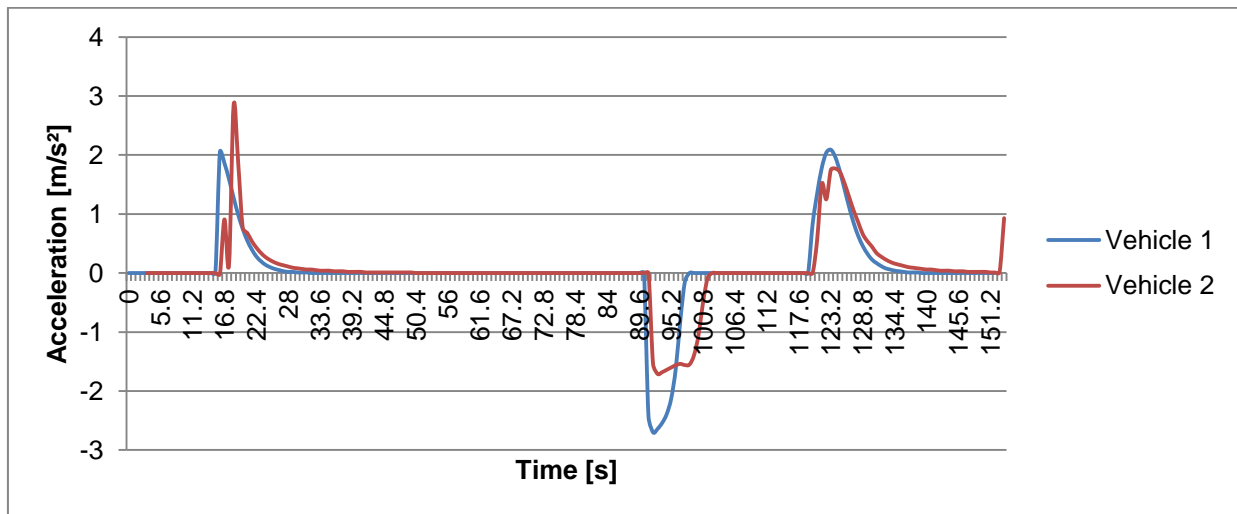


Figure 58 - Acceleration plot for the stop and go scenario

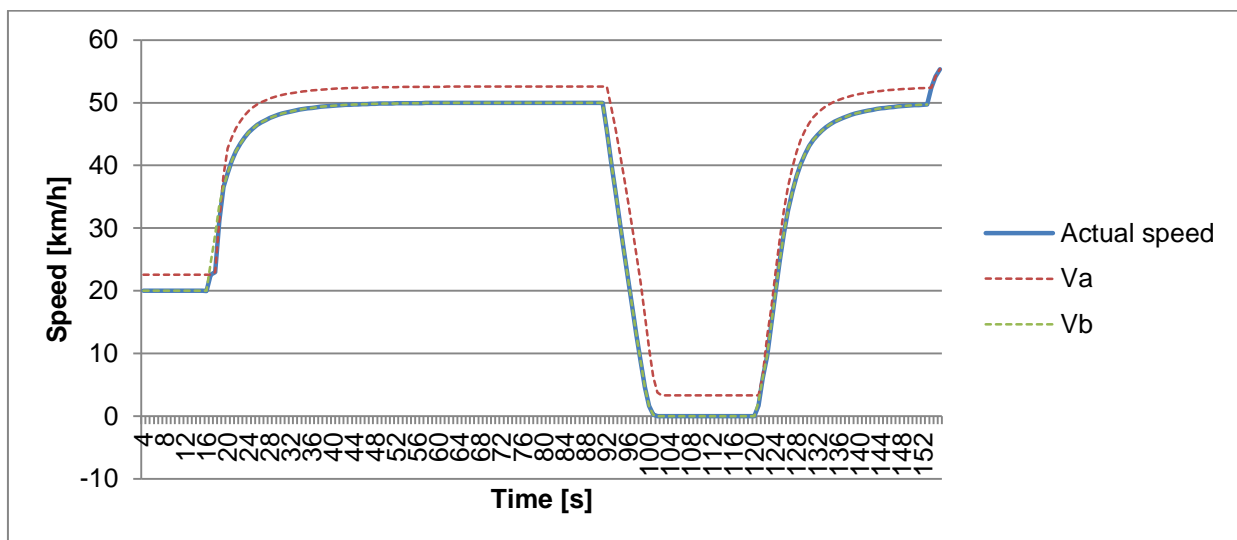


Figure 59 - Comparison of actual simulated speed with the car-following model speed components

Next, the headways between the vehicles have to be checked. An overview of the headways between the vehicles has been provided in *Figure 60*. From this overview, it can be concluded that the following vehicle is trying to drive at headways of approximately 2.7 seconds. This could be explained by the restriction of the V_b component of the car-following model, because the defined decelerations of the leading vehicle are more severe. The leading vehicle is accelerating after approximately 15 seconds, which results in a change in headway. Consecutively, the following vehicle comes closer, because it drives slightly faster as a result of the higher speed acceptance. During braking for the road closure, the headway shortly decreases (not really visible in the plot). When the vehicles start driving again, the headway is smaller early after driving away from standstill and starts increasing towards a safe headway of 2.7 seconds (restricted V_b component and not the minimum headway). The headway applied by Aimsun is larger than the headway parameter, due to the restrictions of the V_b component, which limits the speed due to differences in normal deceleration rates. This behavior is caused by the defined car-following model.

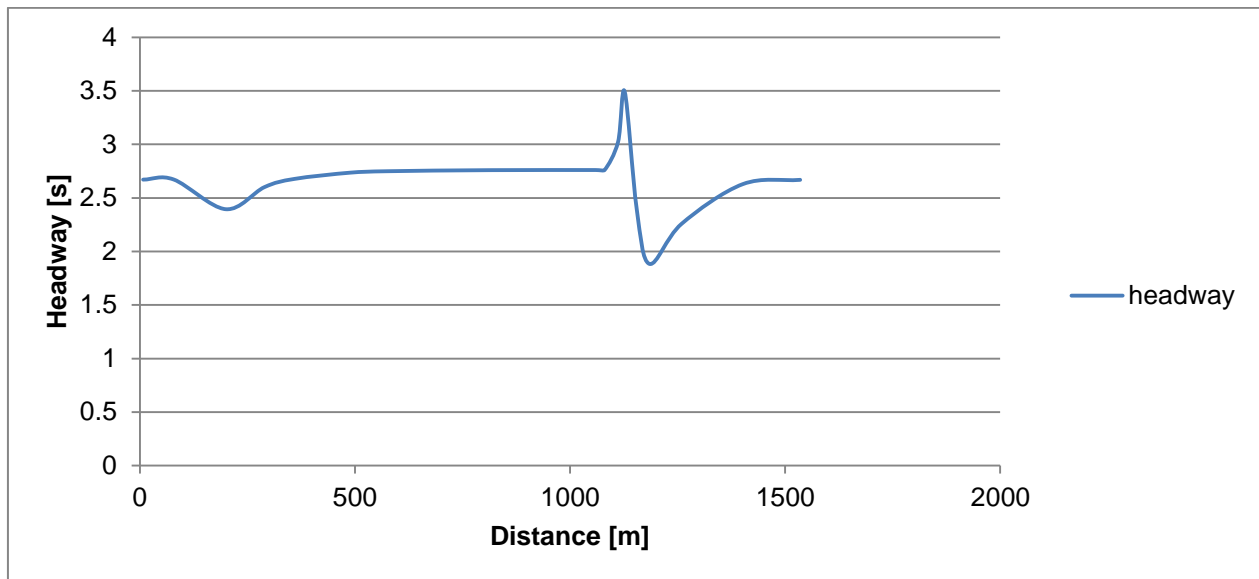


Figure 60 - Headway between vehicles in stop and go scenario

4.5.4 Emergency braking scenario

This scenario consists of two road sections with similar characteristics. The second road section is closed at the moment that a leading ACC vehicle is close, which means that this vehicle has to perform an emergency braking maneuver. Also, a following vehicle is used to assess whether this vehicle is able to respond to the emergency braking of the leading vehicle. This scenario is included to check whether the vehicles are able to respond to an emergency braking situation and to check whether the vehicles do not exceed the maximum accelerations or decelerations defined. In this scenario, several detectors are also used to see whether the vehicles behave according to the headway parameters. A summary of the road sections is included in *Table 10*. Again, the leader and follower both have the minimum deceleration rates possible of 2 m/s^2 for the normal deceleration and 5 m/s^2 for the maximum deceleration. The following vehicle has a higher speed acceptance in order to close gaps between vehicles. The desired headway of the following vehicle is set at 1.4 seconds.

Table 10 - Road sections in emergency braking scenario

Section	Maximum speed [km/h]	Length [m]	Road closure [s]
1	120	701	
2	120	253	from 13-53

The speed and acceleration plots (Figure 61 and Figure 62) show that the vehicles are able to brake to a full stop. Both vehicles do not exceed the maximum deceleration parameter (5 m/s²). At the start, the following vehicle is driving slightly faster in order to reach the desired headway. At the moment of emergency braking, the headway between the vehicles is approximately 1.6 seconds, which is relatively close to the desired headway of 1.4 seconds. After speeding up, the following vehicle starts adapting the headway to 1.4 seconds again. Additionally, both vehicles show very similar speed and acceleration plots, which means that the ACC vehicles handle this situation safely.

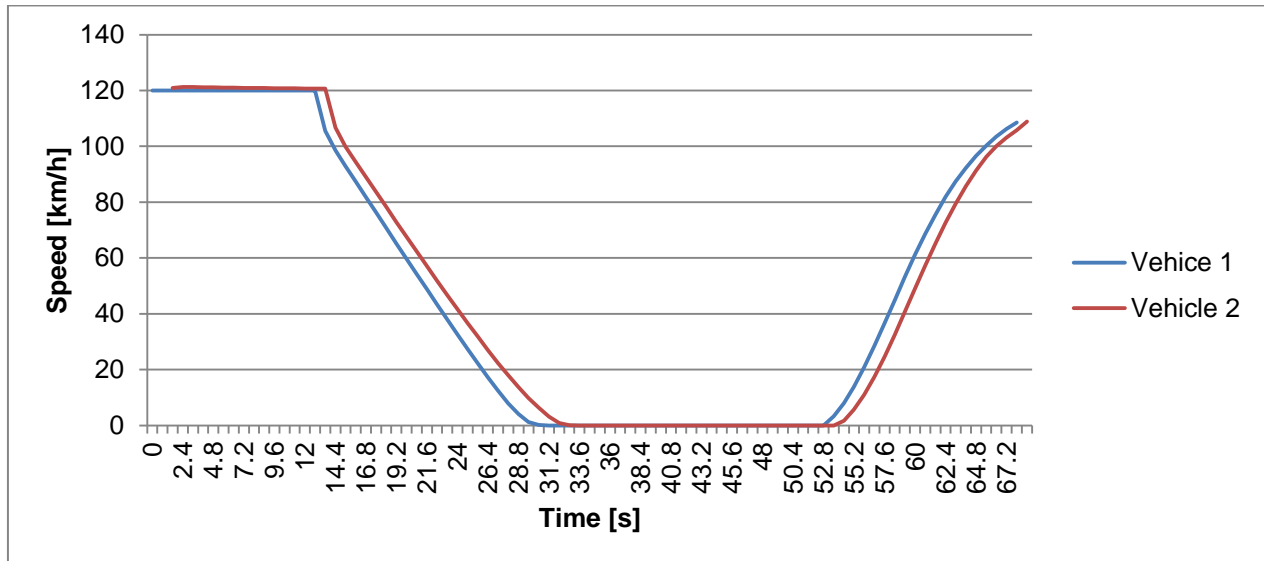


Figure 61 - Speed plot for the emergency braking scenario

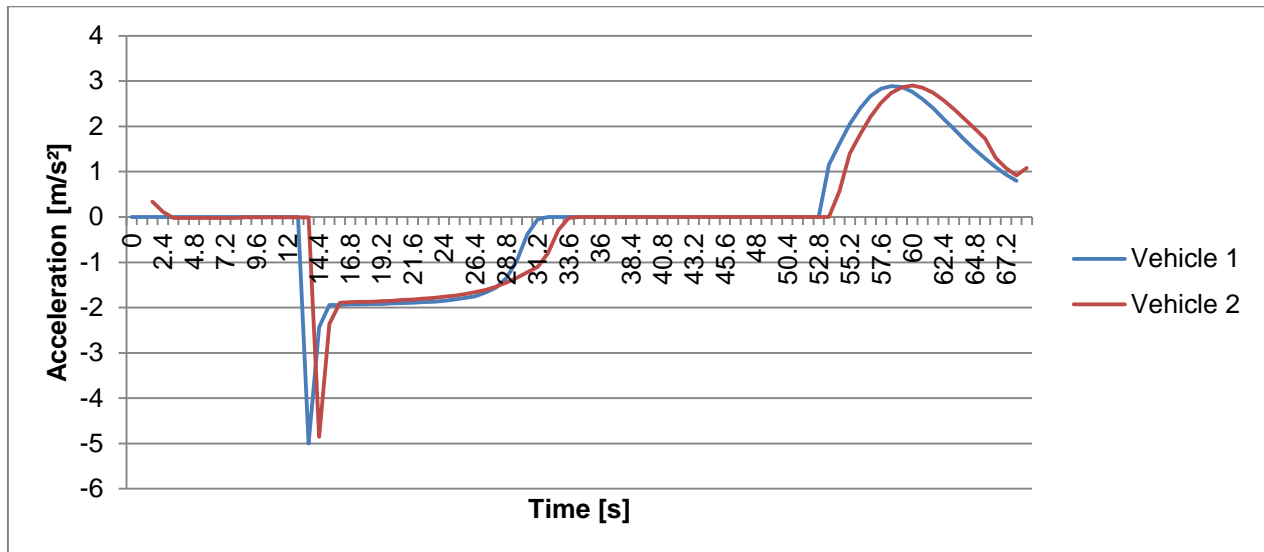


Figure 62 - Acceleration plot for the emergency braking scenario

4.5.5 Cut-in scenario

This scenario consists of a cut-in situation at an on-ramp. The main road has a maximum speed of 80 kilometers per hour. Five vehicles are simulated, of which two vehicles have to perform a cut-in maneuver. The first vehicle has a speed acceptance parameter of 1, while the value for the followers has been set to 1.05. The normal and maximum decelerations have been set at 2 and 5m/s² and the maximum acceleration of the following vehicles is set to 2.9m/s², while the leading vehicle has a maximum

acceleration of 2.1m/s^2 , so that gaps can be closed by the following vehicles. Additionally, the time headways of the following vehicles are set at the minimum of 1.4 seconds.

The test network is shown in *Figure 63*. An overview of the vehicle numbers and the merging situation is given in *Figure 64*. Vehicles 2 and 4 are the merging vehicles. These vehicles will merge, which results in short (undesired), temporary headways. This scenario checks whether the ACC vehicles are able to adapt their speeds to reach desired headways again. The purple detector just right of the leading vehicle in *Figure 64* will collect the headway data just after merging. Further downstream, multiple detectors collect headway data to find out how quickly the ACC vehicles are able to restore desired headways.



Figure 63 - Overview of the cut-in scenario



Figure 64 - Overview of merging vehicles (cut-in scenario)

A speed plot for all five vehicles is provided in *Figure 65*. Acceleration plots for vehicle 2 and 3 and vehicles 4 and 5 have been provided in *Figure 66* and *Figure 67*. The speed plot shows that the leading vehicle is able to drive a constant speed, while the other vehicles have to adapt speeds. It also shows that vehicle 2 and 3 and vehicle 4 and 5 adapt their speeds with a similar pattern, because vehicles 2 and 4 merge in front of vehicles 3 and 5. The headways at merging are 1.40 seconds for vehicle 2 and 0.84 seconds for vehicle 4, which means that these vehicles will adapt their speed in order to reach desired headways again. At approximately 63 meters from the merging location, the smallest headway found is 1.39 seconds, which could be considered as the minimum time headway parameter of 1.4 seconds. Approximately 111 meters after merging, the smallest headway found is 1.36 seconds, which shows that the headways stay relatively constant after a small distance to adapt the headway after merging. This behavior is considered to be realistic, since ACC vehicles will try to adapt the headway as soon as possible, when a merging vehicle is detected.

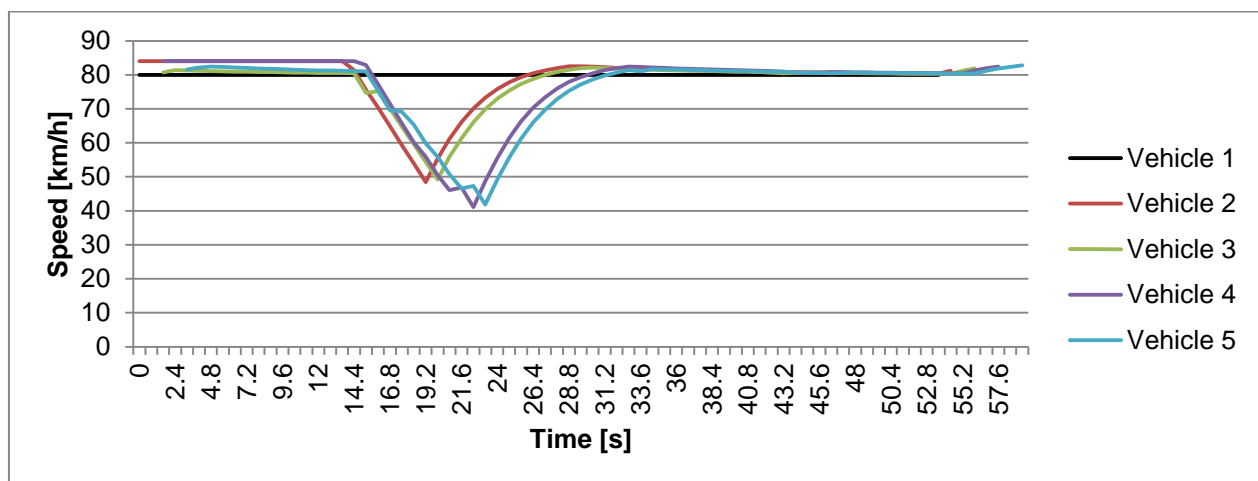


Figure 65 - Speed plot for the cut-in scenario

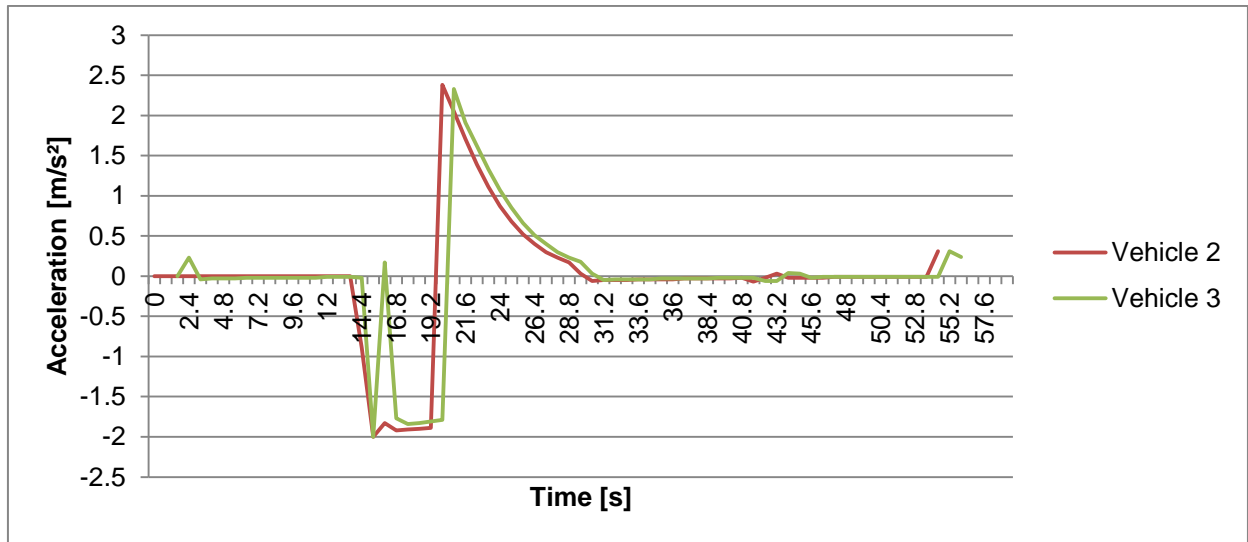


Figure 66 - Acceleration plot for vehicle 2 and 3 in the cut-in scenario

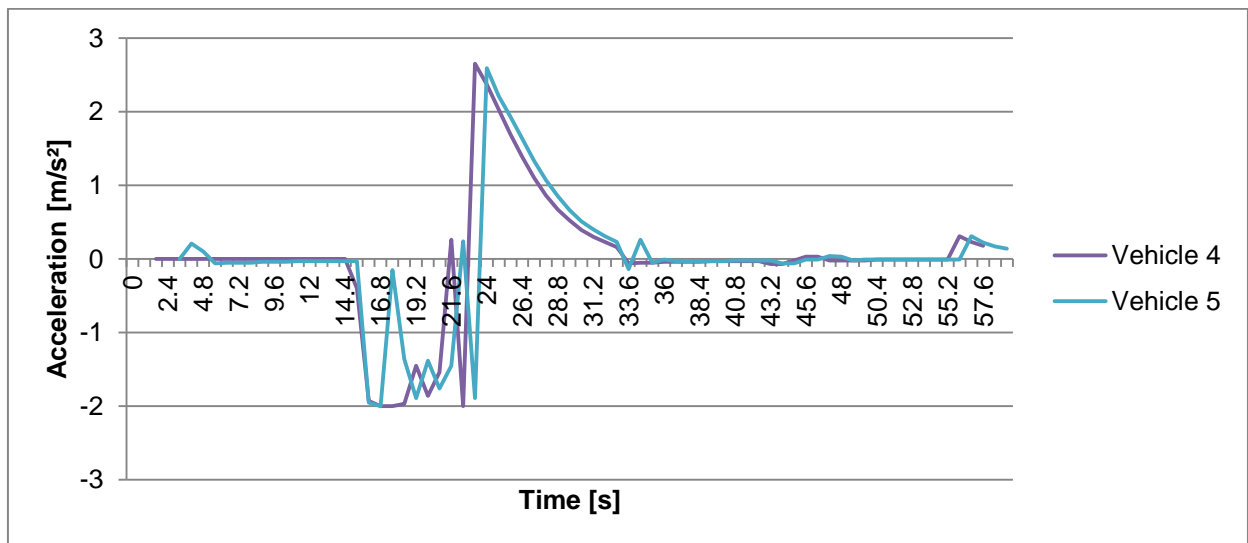


Figure 67 - Acceleration plot for vehicle 4 and 5 in the cut-in scenario

Vehicle 3 follows the accelerations of vehicle 2 relatively well (Figure 66) and the acceleration behavior of vehicle 3 looks fairly stable. Vehicle 5 needs more adjustments to reach its desired headway (Figure 67). Also, this acceleration behavior is less stable and more time is needed to adjust to the desired headway, which makes sense because vehicle 4 merges at a shorter headway than vehicle 2 did. This effect of decreasing stability can be explained by the increased number of speed variations, since vehicle 4 also has to adjust the headway to vehicle 3. Overall, the behavior of ACC systems in these scenarios is logical and as expected. Additionally, these results are in line with the expectations of the system and the results of Mullakkal-Babu et al. (2016). Therefore, the driving behavior of these ACC systems is accepted. Since the worst case scenarios were considered, all other combinations of ACC parameters are expected to be safe and representative for ACC vehicles.

4.5.6 Sensitivity analysis

The simple following scenario of subsection 4.5.2 has been used in order to gain insight in the sensitivity of the ACC driving behavior for some of the parameters. To test the sensitivity, the most important

parameters (headway, normal deceleration and reaction time parameters) of the following vehicles have been changed. *Table 11* provides an overview of the scenarios to perform the sensitivity analysis.

Table 11 - Overview of scenarios for sensitivity analysis

	Reference scenario	Reaction time scenario	Headway scenario	Deceleration scenario
Reaction time [s]	0.8	0.4	0.8	0.8
Headway [s]	1.4	1.4	1.0	1.4
Normal deceleration [m/s ²]	2	2	2	3

The speed and acceleration plots for these sensitivity scenarios are shown in *Figure 68* and *Figure 69*. The speed plot looks relatively similar for all scenarios. When the headway parameter was reduced, the speed profile follows the reference profile very well. The only difference is that the vehicle is put on the network at an earlier time step. Due to this reason, the speed of the following vehicle in the headway scenario is slightly lower at the early simulation steps, because the vehicle is driving closer to the leading vehicle from the start. The acceleration profiles of the headway scenario and the reference scenario are very similar, while the acceleration profiles of the vehicles in the two remaining scenarios show different patterns. The speed profiles of the reaction time and deceleration scenario show resembling patterns. This could probably be explained by their influences in the speed formulas of the car-following model, where both parameters have a similar influence in the V_b component of the car-following model. The acceleration plots show that the reaction time scenario and deceleration scenario show significantly more oscillations in acceleration. For the reaction time scenario, this pattern is found because vehicles can respond faster and are also able to change their speed at a shorter time frame. For the deceleration scenario, the deceleration of the following vehicle is significantly higher than the leading vehicle, which means that the restriction due to the V_b component of the car-following model is lowered and the vehicle is also able to drive at a shorter headway. However, when the headway is decreased due to this influence and the vehicle is able to apply more severe braking, the vehicle will try to reach the desired headway at every time step. However, if the leading vehicle is changing speed, this behavior might result in oscillations.

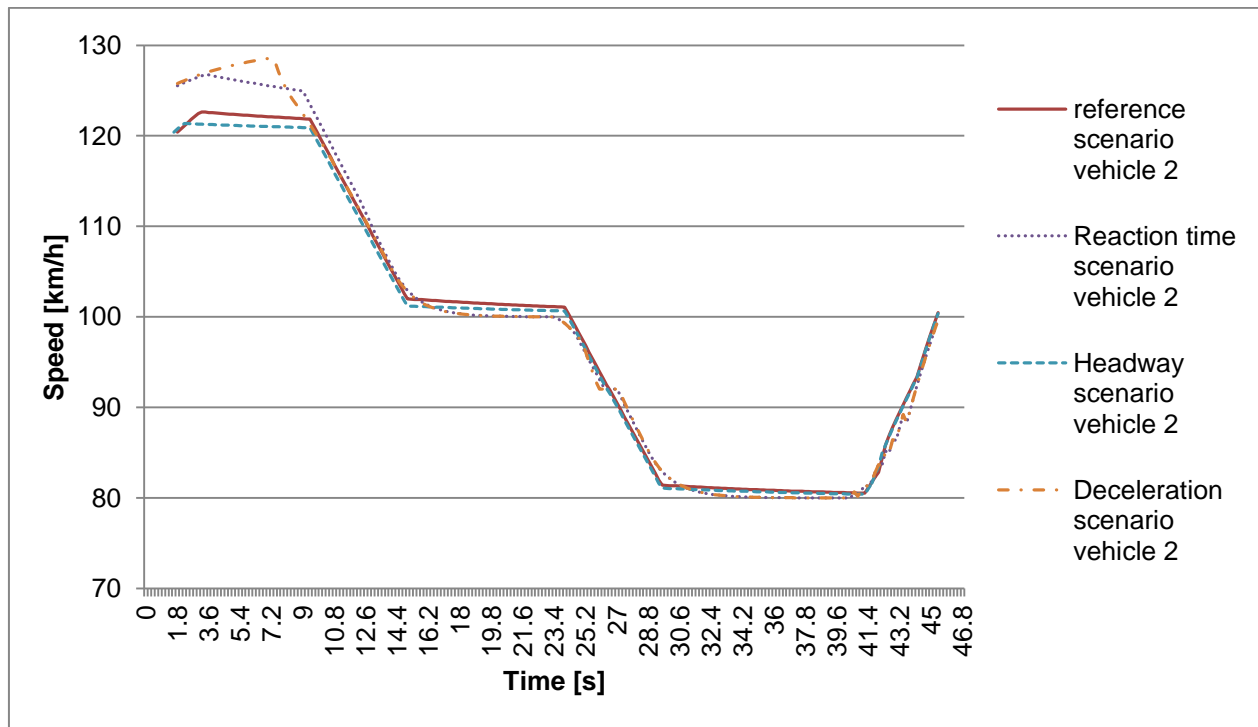


Figure 68 - Speed plot for sensitivity analysis

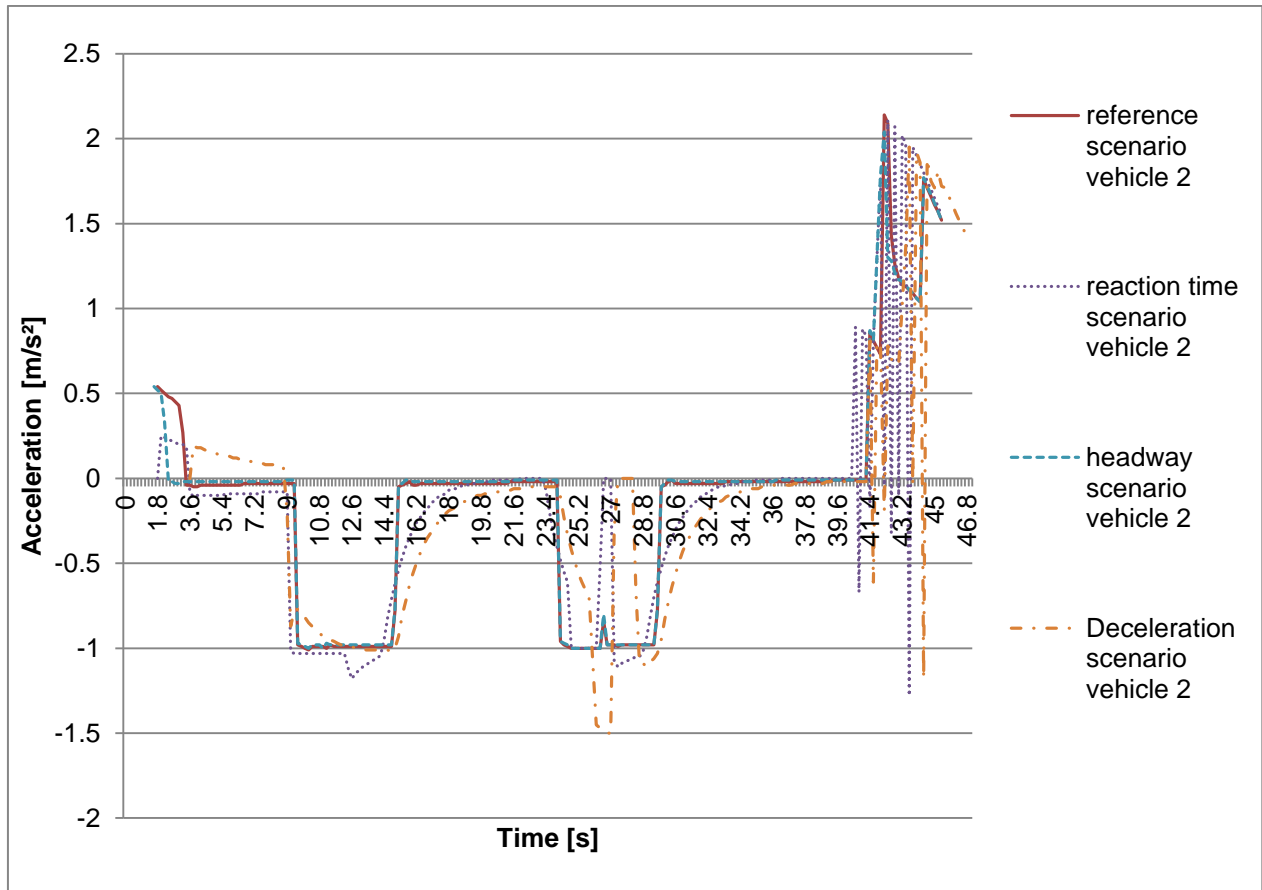


Figure 69 - Acceleration plot for sensitivity analysis

Concluding, it could be stated that the influences of changing the reaction time and decelerations have a bigger influence in comparison with changing the headway. However, it is important to note that the car-following behavior in this scenario is primarily restricted by the V_b component of the car-following model. The influence of the headway is only found at the moment of vehicle entrance and if the minimum headway constraint should be applied, which does not occur in this scenario. In cases of emergency braking and cut-in scenarios, a change in headway will have a higher impact, because the minimum headway constraints are more likely to occur in these situations and vehicles could merge into gaps, which temporarily reduces headways significantly.

5 Microscopic simulation scenarios and indicators

This chapter will discuss the simulations scenarios and indicators used for the microscopic simulations. First, the choices and assumptions made to create scenarios will be discussed in detail in this chapter. Subsequently, the indicators used to assess the effects of (C)ACC on traffic flow will be discussed.

5.1 Scenarios

To simulate ACC and CACC vehicle types, the available parameters inside the Gipps car-following model implemented in Aimsun (as discussed in chapter 2), are varied to describe differences in driving behavior. However, it is important to note that this car-following model was developed to describe human driver behavior and cannot be seen as a strict ACC or CACC controller model. In order to create different scenarios for simulation, two main components of these scenarios were varied.

On the one hand, the (C)ACC types were varied, in order to assess the results based on the parameters given in per vehicle type. It was chosen to simulate three types of ACC. Subsequently, some parameters were improved again to simulate a CACC vehicle type. The three types of ACC were chosen, because there still are significant differences between ACC systems, while vehicles equipped with ACC are already commercially available. Some different opinions on these ACC systems were used to create 3 types of ACC. Only one type of CACC was simulated, because it is currently impossible to model the communication with (multiple) vehicles ahead in the car-following model implemented in Aimsun. Additionally, CACC vehicles are not commercially available yet, which means that more time would be needed to increase the market penetration rates of vehicles with CACC systems.

On the other hand, the market penetration rates of the (C)ACC systems are important factors for creating scenarios. It is taken into account that the differences between consecutive penetration rates should be large enough to find differences in traffic flow performance. Also, the market penetration rates of these systems should be achievable in real traffic, where there always is a mix of traffic. The (C)ACC penetration rates are only applied to the vehicle class car. Additionally, the assumption is made that truck drivers will not use ACC or CACC. The OD-matrix for trucks is kept constant in all scenarios, meaning that the truck drivers are driving manually in each scenario. It was chosen to use a 50% (C)ACC penetration rate as a maximum, since higher penetration rates are not expected to be achieved in the near future. A reference scenario, in which there are no (C)ACC vehicles, is also used to compare the simulation results. The market penetration rates are varied with steps of 10%, meaning that six different penetration scenarios are considered, ranging from 0 to 50% (C)ACC per simulated type of (C)ACC. As an example, to describe a 20% ACC scenario, the OD matrix for cars is applied to the car class for 80%, while the same OD matrix is applied to ACC vehicles for 20% and the truck matrix is (always) applied for 100%.

The total of four (C)ACC types multiplied with the six different market penetration rates result in 24 scenarios to simulate. A further description of the types of (C)ACC simulated and the input parameters is given in the following subsections.

5.1.1 Types of (C)ACC systems

As discussed, four different types of (C)ACC systems will be defined and used for simulation, of which three can be considered as ACC systems and one as a CACC system. The parameters discussed in section 4.5.1 will be used as the basis for defining (C)ACC driving behavior. The parameters will be kept to the values described in section 4.5.1 unless different parameter settings are defined in this section. It is assumed that all vehicles equipped with ACC or CACC will drive with their system switched on at any point in time. Therefore, on- and off-switching of the system is not included.

The types of (C)ACC systems considered in this study are subdivided in ACC, newer ACC, improved ACC and CACC. As discussed, the driving behavior of these types is modelled by manipulating the Gipps car-

following model that is used to describe human driving behavior. The term ACC is used to describe vehicles with ACC systems that are currently found on the road. The newer ACC systems are considered to represent the newest vehicles with ACC currently available. The improved ACC type represents an improved version of ACC, which could become available in the (near) future. These three types are also used to make a comparison between the types and to find the effects of differences in reaction time and following distance on traffic flow. An overview of the types of (C)ACC systems is provided in *Table 12*. A description of the (C)ACC systems, parameter settings and the reason for selecting these values is given below. For the acceleration and deceleration parameters, many literature studies use lower acceleration and deceleration rates for (C)ACC systems in comparison with acceleration and deceleration rates that manual drivers use. These acceleration and deceleration rates of (C)ACC vehicles are assumed to be lower in comparison with the rates human drivers apply. All (C)ACC systems have similar acceleration and deceleration capabilities. For a more detailed description of the acceleration/deceleration rates used to describe (C)ACC vehicles, refer to Chapter 4. However, it is important to note that differences in normal decelerations are taken into account in the car-following model, which could apply larger following distances than the desired time headway as a result of differences in normal deceleration rates.

Table 12 - Overview of (C)ACC system types used for simulation and the most important parameters

	Reaction time [s]	Mean time headway [s]	Mean maximum acceleration [m/s ²]	Mean normal deceleration [m/s ²]	Mean maximum deceleration [m/s ²]
Car	0.8	- (\approx 1.0)	2.8	-3.5	-7
ACC	0.8	1.6	2.5	-2.5	-6
Newer ACC	0.4	1.6	2.5	-2.5	-6
Improved ACC	0.4	1.2	2.5	-2.5	-6
CACC	0.2	0.8	2.5	-2.5	-6

For ACC, the reaction time is set to 0.8 seconds, similar to human drivers. Currently, there still is a delay in reaction time of ACC systems due to sensor delay and the calculation of accelerations or decelerations of the leading vehicle. This delay is lower in comparison with human drivers in case of simple longitudinal driving behavior. However, if a vehicle is changing lanes, just in front of an average ACC vehicle, the ACC system needs a relatively long time before it is able to detect the merging vehicle. Therefore, the reaction time was set to 0.8 seconds to compensate for the described effects. The time headway settings used are similar to those described in section 4.5.1, which describes headway/gap settings for ACC vehicles that are often found in reality and used in literature. The mean time headway is set to 1.6 seconds. In comparison, the car user class has no defined headway settings, but applies headways of approximately 1.0 seconds in unrestricted situations. The reaction time should be a multiple of the simulation step. In order to have a safe and fair comparison between the different types of (C)ACC, the simulation step has to be set to 0.2 seconds to exclude differences in results caused by differences in simulation step.

The newer ACC systems currently available are able to detect vehicles on adjacent lanes. Additionally, these vehicles are also capable of detecting the direction indicators of merging vehicles and adapting the driving behavior as a result of flashing direction indicators. Therefore, the reaction time for reacting to merging vehicles is reduced, which means that the reaction time assumed for these vehicles is set to 0.4 seconds. However, the following distances of these vehicles are still relatively similar, which means that the mean time headway is set to 1.6 seconds. The simulation step has been set to 0.2 seconds.

The reaction time for the improved ACC is also fixed to 0.4 seconds, similar to the newer ACC. The improved ACC is assumed to be able to drive at shorter following distances on average. Therefore, the mean time headway is set to 1.2 seconds, which is in close correspondence with minimum headways or gaps (compensated) for ACC systems found in literature. The minimum and maximum time headways are set to 1.0 seconds and 1.6 seconds, while a 0.2 seconds deviation is applied. Again, the simulation step has been set to 0.2, which is in line with the other scenarios.

With respect to the reaction times at stop for ACC vehicles, it is assumed that all ACC users still have to accelerate by themselves, if the vehicles have come to a standstill. This means that the reaction time at stop should be set equal to human drivers (1.35 seconds). Note that the reaction time at stop is rounded down to 1.2 seconds in simulation, since it must be a multiple of the simulation step of 0.2 seconds.

For the CACC system, it is assumed that the vehicle equipped with CACC could always communicate with a preceding vehicle, which could be achieved by using so-called “vehicle awareness devices” as discussed by Shladover et al. (2012). This ensures that CACC vehicles are capable of responding at very short reaction times. Therefore, the reaction time has been set to 0.2 seconds. As a consequence, these vehicles are also able to drive at shorter headways. The mean headway was set to 0.8 seconds, with a 0.6 seconds minimum and a 1.2 seconds maximum. The deviation was set to 0.2 seconds to differentiate between different brands and user preferences. This mean time headway setting is in line with other literature studies, where time gaps of approximately 0.6 to 0.8 seconds are often used. Additionally, Bu, Tan, & Huang (2010) use time gap settings between 0.6 and 1.1 seconds in their study on a design and field test of CACC. Shladover et al. (2012) uses time gaps of 0.5 seconds to describe their CACC system. However, it is important to note that time gap is not exactly the same as time headway. Example given, when the vehicle length is 4 meters and all vehicles are driving at speeds of 100 km/h, a time gap of 0.6 seconds, refers to 0.744 seconds time headway.

The reaction time at stop for CACC vehicles could change, but the communication between vehicles can only take place if both vehicles have communication possibilities. However, this is not the case in mixed traffic. On the one hand, CACC vehicles might react faster, if the leading vehicle can send speed and acceleration information. Although, in cases when a leading vehicle is not able to communicate, the reaction times at stop of CACC systems will increase, due to the time needed to detect a slow object and filter the noise. Therefore, the reaction time at stop is not different from human reaction times at stop, since a decrease in reaction time at stop will be found when both leading and following vehicles are able to communicate, which is not always the case when there is mixed traffic. When the leading vehicle has no communication abilities, an increase in reaction time is expected, because radars are less accurate in detecting slow objects and may need more time to filter the noise and get a reasonable estimation of leader speed, shortly after a stop. In comparison, human drivers can anticipate by looking further downstream, which lowers reaction time. Some drivers might also be busy with doing something different and could react at a slower rate. Since the extents of these effects are unclear, it is assumed that the reaction times at stop for CACC and human drivers are similar. As an extra advantage, this would also ensure a clearer comparison with ACC systems.

5.1.2 Simulation runs and random seeds

Every simulation run uses a random seed, which is used to apply slight differences between simulation runs, in order to compensate for effects that could influence the traffic flow, such as weather or vehicle properties. Every random seed provides a unique result, meaning that it is not always safe to compare the simulation results of runs with different random seeds. Generally speaking, a different random seed should be considered as a different day, because no days are identical in terms of traffic flow.

Additionally, it is desired to use multiple random seeds in order to average out differences for extremely good or bad days (or random seeds). Therefore, it is chosen to use 10 simulation runs with different random seeds for every scenario and calculate the average over these 10 simulation runs. However, in order to compare all different scenarios, it is important to use the same random seeds for every penetration scenario. Therefore, the random seeds for all 10 runs were generated for one scenario and these random seeds were also used for all other scenarios. An overview of the random seeds is provided in *Table 13*.

Table 13 - Random seeds per simulation run, used in all simulation scenarios

Simulation run	1	2	3	4	5	6	7	8	9	10
Random seed	32261	32659	16440	23635	13046	28780	5593	26193	25632	26690

5.2 Indicators

This subsection will discuss the indicators used to assess the effects of ACC and CACC systems on traffic flow. Additionally, it is important to be aware of how these indicators are defined and on what level these indicators are defined to get a feeling for the effects on specific locations or network-wide effects.

Three types of indicators will be used to assess the effects of increasing market penetration rates of ACC and CACC. The first types of indicators are indicators at experiment level, which contains totals or averages over the entire network and simulation. Secondly, space-time diagrams are provided for 10 different road stretches that contain (possible) bottlenecks. These could be used to assess the effects on typical road stretches and bottlenecks. Additionally, six typical road sections were selected, where speed, flow and density data was computed per lane, as well as the average number of lane changes for cars, ACC and CACC vehicles. These statistics can be used to evaluate effects on lane level or between vehicle types. These statistics will only be included in the report if important and relevant results are found, to limit the size of the report and reported data.

5.2.1 Indicators at experiment level

All the indicators at experiment level contain total or average values over the detection intervals within the total simulation period. Most of these parameters are basic traffic indicators, such as flow, density, speed, input counts, travel time, delay time and distance travelled. For some of these indicators, there is a possibility to select the option of adding bands, which adds the standard deviation to the graphs at both sides of the mean. The statistical periods are 15 minute periods.

The indicators used to assess the effects of (C)ACC are: delay time, speed, density and the total number of lane changes. The standard deviation could only be showed for the delay time and speed indicators. The standard deviations were computed and found to be small. When displaying the results of the different simulation scenarios, the bands/standard deviations are not shown in the figures, for reasons of clarity. Definitions for the statistics delay time, speed, density and total number of lane changes are:

- **Delay time [s/km]:** Gives the average delay time per vehicle per kilometer. This average delay time is computed for a full journey and is calculated by taking the difference between the expected travel time (travel time under ideal conditions, so at maximum desired speeds) and the actual travel time. It is calculated over all vehicles exiting the network in the corresponding statistical period. First, the delay time is calculated per vehicle exiting the simulation in the corresponding statistical period. At the end of the statistical period, the delay times of all vehicles exiting the simulation within this statistical period is summed up and divided by the number of vehicles, which results in average delay time per vehicle;
- **Speed [km/h]:** Represents the average speed for all vehicles that have left the system. This is calculated using the mean journey speed for each vehicle when it leaves the network. All journey speeds obtained within a statistical period are added and divided by the number of vehicles leaving the network within this statistical period to obtain an average journey speed for all vehicles leaving the system in that statistical period;
- **Density [veh/km]:** This indicator gives the average number of vehicles per kilometer per lane over the whole network in a statistical period. The total length of lanes is taken into consideration, which means that this indicator actually is the average lane density;
- **Total number of lane changes [#]:** This indicator gives the total number of lane changes applied over the whole network. The statistics are computed per statistical period.

The delay time indicator gives an indication of the amount and severity of congestion as an average over the whole network. Higher delay times refer to deteriorations in overall traffic flow performance. Vehicle loss hours could be used as indicator, but the exact amount of vehicles slightly differs between different scenarios, which could lead to large differences in vehicle loss hours, making this indicator unsuitable to use for this research. Since the delay time is averaged over all vehicles, this problem is solved.

The speed over the whole network could be used to test the severity of congestion. However, since the journey speeds are averaged, a lot of information might be averaged out. Therefore, the differences between congested and uncongested periods could become relatively small. However, in combination with the delay time indicator, an insight in the amount and severity of congestion could be gained.

The density indicator reports the average lane density over the whole network. Basically, this indicates how many vehicles are on the network, or how busy it is on the network. This indicator is also expected to provide a rough indication of the severity of congestion in the statistical periods. However, also in this case, some information might be averaged out when averaging over an entire network.

The indicator on the total number of lane changes is used to check whether the amount of lane changes change for increasing market penetration rates of ACC or CACC. As Gorter (2015) indicated, ACC users apply lane changes less frequently in comparison with regular car drivers. Nevertheless, it would have been better if this indicator could be averaged over vehicle kilometers of a specific vehicle type. Unfortunately, this is currently not possible in Aimsun.

5.2.2 Space-time diagrams

Space-time diagrams give a good overview of the occurrence, severity and propagation pattern of congestion per location. Therefore, space-time diagrams were included to compare the influences of increasing market penetration rates of ACC and CACC at different (potential) bottlenecks in the network. In order to retrieve space-time diagrams from simulation, detector sets were added, consisting of detectors placed at approximately 50 meters distance from each other on the considered road segment. Sometimes, the distances between detectors are slightly larger than 50 meters, because the (often negligible) length of the nodes was not taken into consideration when placing these detectors.

Detector sets were added at road stretches where bottlenecks are expected or where congestion was found in reference scenarios. There were three important congestion fronts found in the calibration procedure where detectors were added from the start. Some other road stretches with potential bottlenecks were selected to add up to a total of 10 detector sets.

The detector set locations and detector set numbering are provided in *Figure 70*, *Figure 71*, *Figure 72* and *Figure 73*. In these figures, the driving directions are indicated with a black arrow. Additionally, these figures are ordered from the eastern (*Figure 70*) to the western (*Figure 73*) part of the research network.

Detector set 1 contains a weaving section where congestion might occur. Detector set 2 contains an on-ramp construction, which might cause congestion due to relatively high intensities and lane-changing behavior. Detector set locations 3, 4 and 5 contain detectors where congestion occurs, as discussed in the calibration chapter (Chapter 3). Detector set 6 contains a lane drop, which leads to a reduction in capacity and could lead to congestion due to high traffic intensities. Detector sets 7 and 8 both consists of road sections starting on the parallel stream, going to the main stream and back to the parallel stream, where weaving behavior between the main stream and parallel stream could cause congestion. More upstream road sections are taken into consideration for detector set 8, because serious spillback could be expected in this situation as a result of high traffic intensities. Detector set 9 contains a short on-ramp, which could cause congestion due to merging behavior. Lastly, detector set 10 contains two subsequent weaving

sections where congestion could occur due to lane-changing and weaving behavior at the first weaving section. Additionally, it should be noted that some detector sets are located very close to each other.

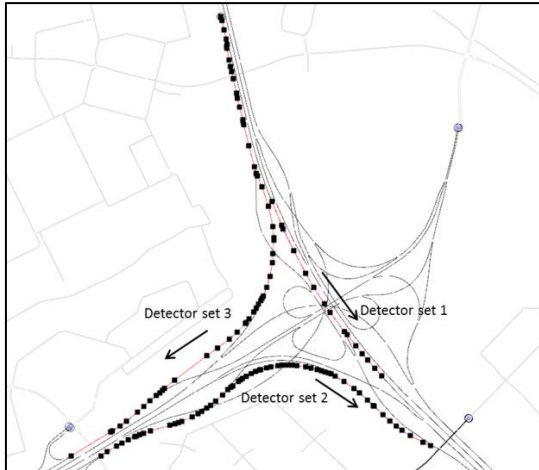


Figure 70 - Detector set locations and numbering at junction Ridderkerk

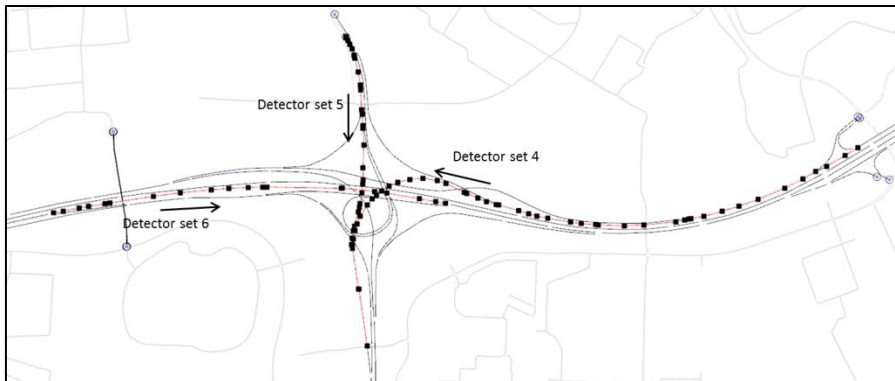


Figure 71 - Detector set locations and numbering at junction Vaanplein

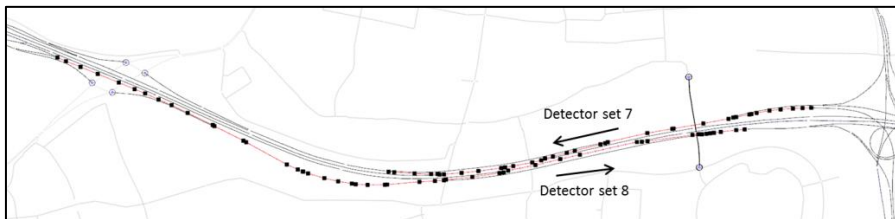


Figure 72 - Detector set locations and numbering west from junction Vaanplein



Figure 73 - Detector set locations and numbering near junction Benelux

5.2.3 Indicators at section level

The indicators at section level contain totals or average values for the total road section, as well as values per lane or vehicle type. In general, the same indicators that were available on experiment level are available at section level as well. It is often possible to add bands, which adds the standard deviation at both sides of the mean value. Once again, the corresponding statistical periods are 15 minutes.

The indicators at section level that were computed for this research are lane speeds, densities and flows to evaluate differences between lanes and to give an evaluation on the homogeneity pattern of traffic for the different scenarios. Additionally, the average number of lane changes for the car and ACC or CACC vehicle type will be provided to evaluate whether ACC users change lanes less frequently or not. The statistics are formulated as follows:

- **Speed [km/h]:** This indicator provides the average section journey speeds. First, these section speeds are calculated per vehicle. Then, these section speeds are averaged over the number of vehicles that have left the considered road section within the statistical period. Additionally, these speeds could also be divided per lane. The lane speed indicators are used in this research;
- **Density [veh/km]:** The section and lane density are calculated for every time step. Subsequently, the lane density is averaged over the statistical period;
- **Flow [veh/h]:** The section and lane flow are calculated at every time step, when vehicles are leaving the considered road section or lane. Subsequently, the lane density is averaged over the statistical period;
- **Number of lane changes [#veh]:** The amount of lane changes at the considered section is counted for every vehicle. Subsequently, all these lane changes per vehicle type are added up and averaged over the number of vehicles of this type to obtain an average number of lane changes on the section. Additionally, it is also possible to set the vehicle type to all, which results in an average number of lane changes for all vehicle types together.

As discussed, the speed, flow and densities at lane level could be used to reflect the (improve or decrease) in the homogeneity of traffic. The number of lane changes per vehicle type could be used to check whether ACC users change lanes less frequently in comparison with manual car drivers or not.

Since it would be too time-consuming to compute these statistics for every link in the network, six characteristic locations were chosen for which these statistics will be computed. A short overview of the sections and characteristics is given in the following text. Section 114328 contains a road section where free flow is found at any moment in simulation. This road sections consists of five lanes and a lane drop at the end. Section 42461 is a three lane weaving section at junction Ridderkerk, where congestion pops up. Section 108188 is a two-lane road section where spillback of congestion is found. Section 108866 consists of a two-lane road section at capacity, shortly downstream of a lane drop. Section 63512 consists of a four-lane road section with a lane reduction to three lanes, which could lead to congestion if the capacity limit is reached. Section 29033 is a weaving section with relatively low intensities, where no congestion is expected. Reflections on these indicators at section level will only be provided if these are relevant in the light of this research. The reasons for this decision are to limit the total size of the report, improve readability and to filter (insignificant) results from which no clear conclusions can be drawn.

6 Microscopic simulation results

This section describes the simulation results of the described scenarios. In this chapter, the simulation results will be discussed based on the indicators explained in section 5.2. First, indicators at experiment level will be analyzed per type of (C)ACC. These results are averaged over the whole network, but give a good indication of the influences of (C)ACC. Subsequently, the space-time diagrams of the 10 selected bottleneck locations are given per bottleneck location and type of (C)ACC. The space time diagrams are discussed per bottleneck location, where the different types of (C)ACC are discussed in subsections. This approach was chosen to provide a clear overview per location and to compare the different (C)ACC types with each other. Also, some interesting results found in the indicators at section level will be discussed.

6.1 Average results at network level

This subsection will discuss the simulation results at experiment level. The output from the simulations in Aimsun is used to analyze the effects of different types of ACC or CACC systems. However, it is important to note that information could be filtered out, since these results are averaged over the whole network. The different indicators will be discussed per type of ACC or CACC.

6.1.1 Average influences of ACC

This subsection describes the network-wide effects of increasing penetration rates of the ACC vehicle type in terms of speed, density, delay time and total number of lane changes.

6.1.1.1 Speed

The average speeds for different market penetration rates of ACC are shown in *Figure 74*. These average speeds refer to the average journey speed of vehicles that have completed their trip within a considered time period.

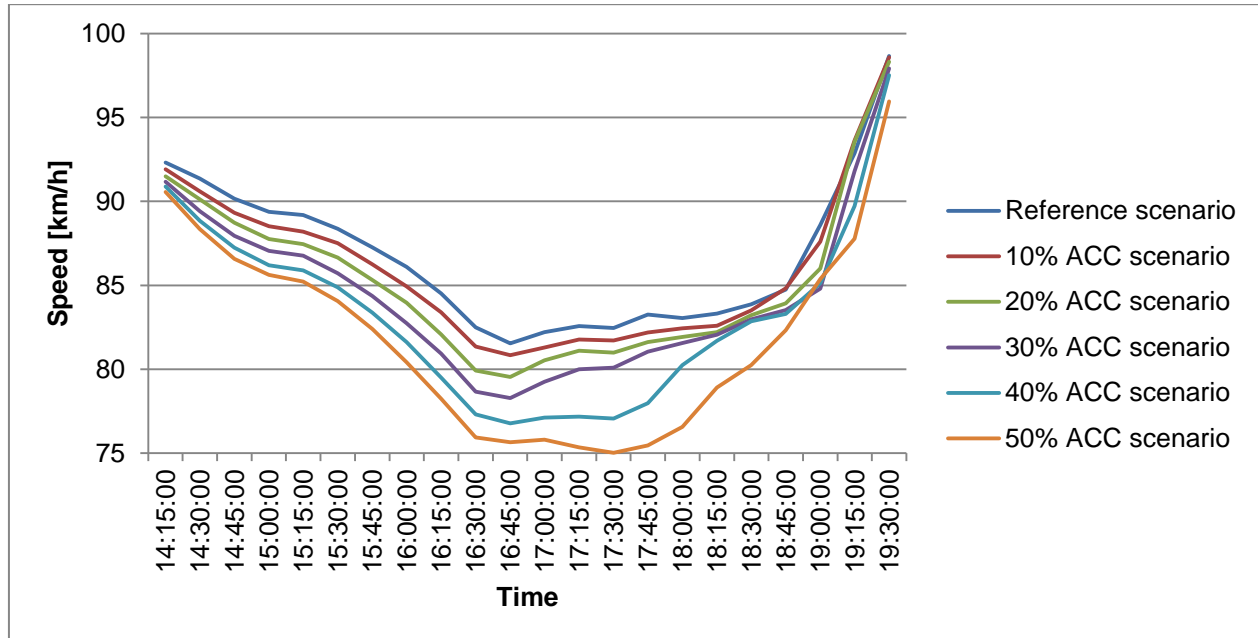


Figure 74 - Overview of average speeds over time in the ACC scenarios

It is found that the average journey speed decreases for increasing market penetration rates of ACC. This effect could be expected, because the speed acceptance parameter of ACC vehicles was set lower than the speed acceptance parameter of cars, which means that the average maximum desired speed of vehicles will also change as a result. From the start of simulation, a small linear decrease can be found for

market penetration rates between 0 and 30%. From 18:45 and onwards, the average speeds are very similar to each other. However, for the 40% and 50% ACC scenarios, the decrease in average speed is more severe, as a consequence of severe increases in congestion at local bottlenecks inside the network, where the capacity limit might be reached. These results support the finding that low penetration rates of ACC have no or only a small influence (van Arem et al., 2006; VanderWerf et al., 2002). Above 40%, a clear loss in terms of speed could be witnessed.

In general, the evening peak period in the Netherlands is considered between 16:00 and 19:00. In the graph, a clear drop in speed can be witnessed between 16:15 and 18:45, which can be considered as the period in which the most severe congestion is found.

6.1.1.2 Density

The average densities over the network are provided in *Figure 75*. These average densities refer to the average densities all over the network, which means that it only provides some information, since dense sections could be compensated by empty sections. However, it will indicate the amount of vehicles on the network and gives an indication of the amount of congestion. The warm-up and cooldown period to fill and flush the network are not shown in this graph. The representative speed in the graph refers to the speed of the reference scenario and is included to indicate the congestion period, where the speeds are reduced.

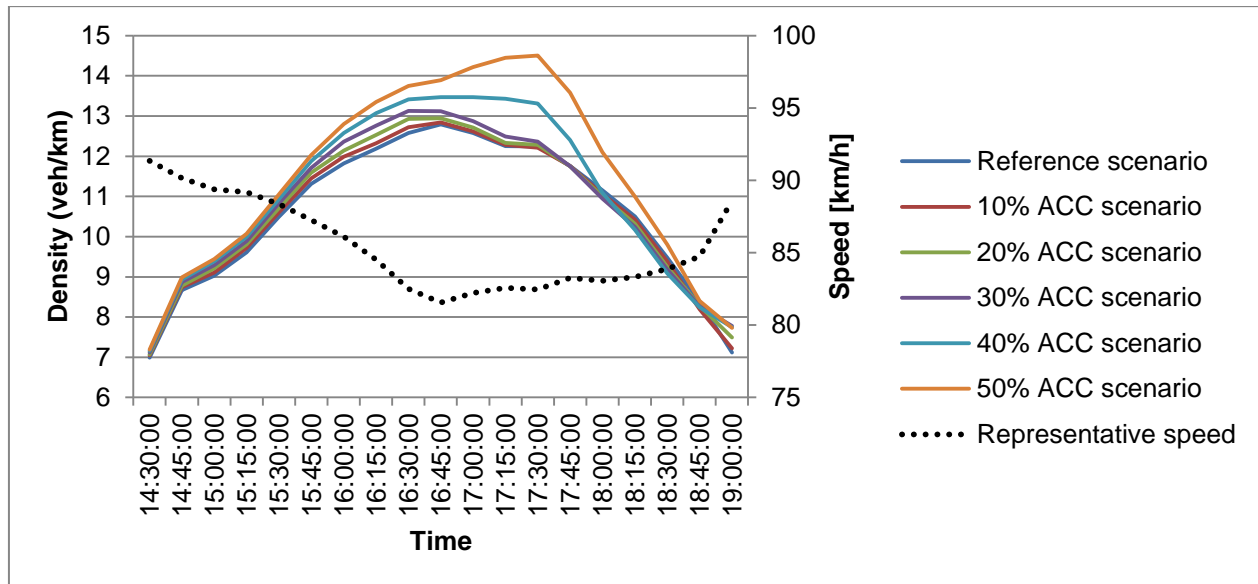


Figure 75 - Overview of average densities over time in the ACC scenarios

The average density slightly increases for increasing percentages of ACC. The changes between 0% and 30% are relatively small, which could be explained by the lower speed acceptance for ACC, which means that these vehicles will drive slightly slower and be on the network for a slightly longer period of time. Again, for the 40% and 50% ACC scenarios, the differences are more significant as a consequence of severe increases in congestion at local bottlenecks inside the network, where the capacity limits might be reached. These more significant differences are found within a period in which average speeds are reduced, indicating an increase in congestion. These findings support the finding that low penetration rates of ACC have no or only a small influence (van Arem et al., 2006; VanderWerf et al., 2002).

6.1.1.3 Delay time

The delay times for differing penetration rates of ACC are shown in *Figure 76*. These averages refer to delay time on a full journey and are calculated at the moment that the respective vehicle leaves the

network. The representative speed in the graph refers to the average speed in the reference scenario and is included to indicate the congestion period, where the speeds are reduced.

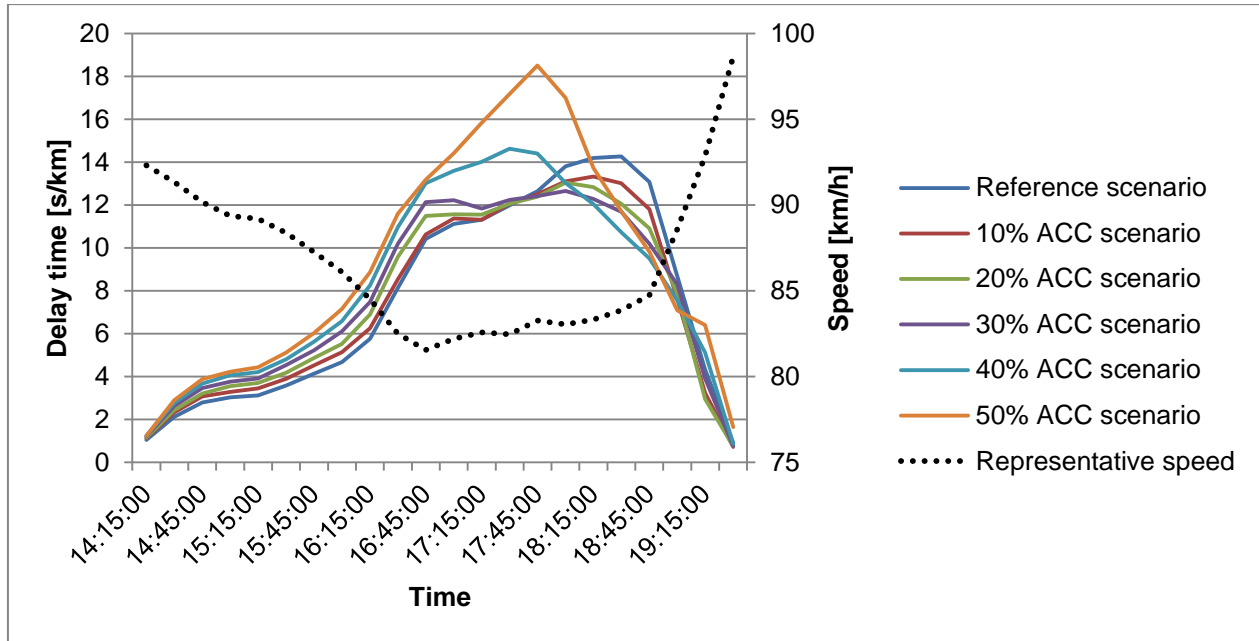


Figure 76 - Overview of average delay time in the ACC scenarios

Again, differences in delay time are relatively small from 0% to 30% ACC, while increases are found for the 40% and 50% ACC scenarios as a result of severe increases in congestion at local points in the network. The sharp increase in delay is very clear for the 50% ACC scenario, where the capacity limit is probably reached at multiple points in the network and severe increases in congestion are found. In combination with the representative speed, it shows that this delay is found in the congestion period. This supports the findings of VanderWerf et al. (2002) and van Arem et al. (2006) that at low penetration rates of ACC, there are no or only small impacts of ACC. VanderWerf et al. (2002) reports that a loss in traffic performance could be obtained above 60% ACC, however this loss is already found for 50% ACC here.

6.1.1.4 Total number of lane changes

The total number of lane changes for the different ACC scenarios are shown in Figure 77. The warm up and cooldown period have been excluded from the graph.

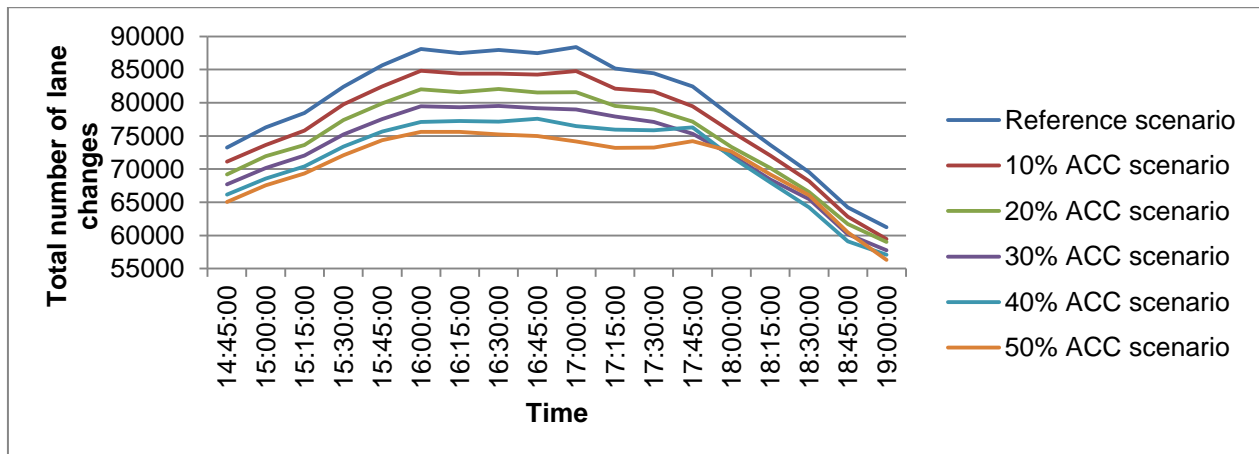


Figure 77 - Overview of total number of lane changes in the ACC scenarios

It could be found that the total number of lane changes decrease for increasing percentages of ACC, which seems that using ACC leads to reductions in lane changes, as indicated by Gorter (2015).

6.1.2 Average influences of newer ACC

This subsection describes the network-wide effects of increasing percentages of the newer ACC vehicle type in terms of speed, density, delay time and total number of lane changes.

6.1.2.1 Speed

The average journey speeds are displayed in *Figure 78*.

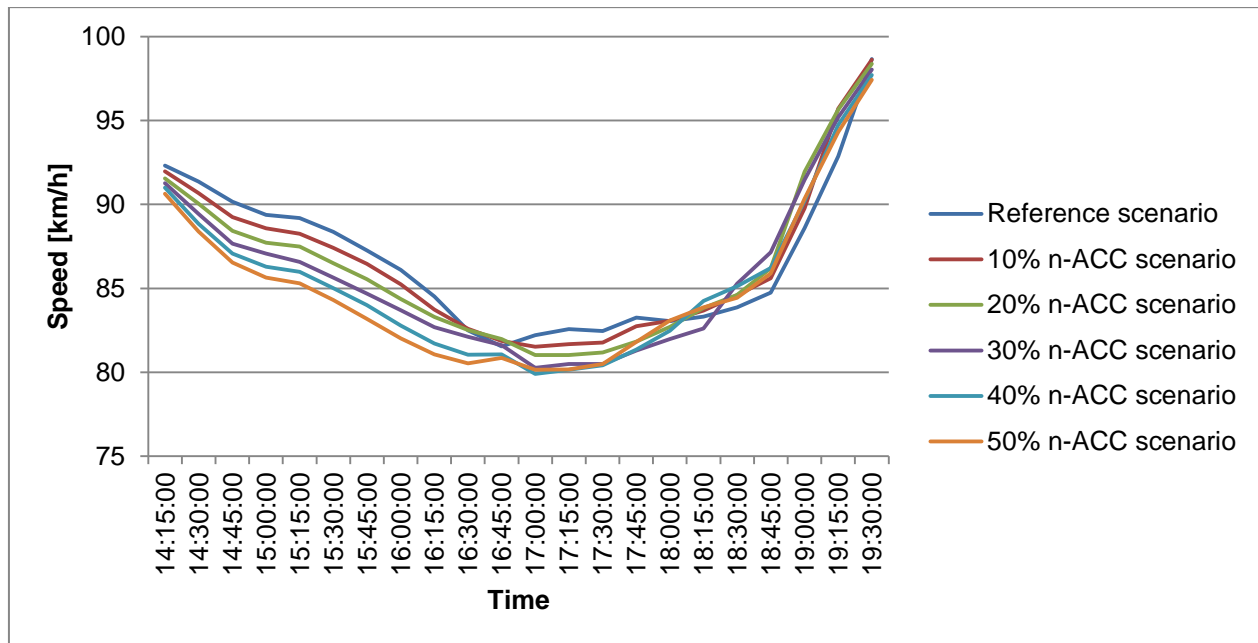


Figure 78 - Overview of average speeds over time in the newer ACC scenarios

At start, the average journey speed decreases for increasing market penetration rates of newer ACC, because of the lower speed acceptance parameters for ACC, resulting in lower maximum desired speeds and thus slightly lowers speeds in general. However, from 18:00 and onwards, the average speeds are relatively similar for all ACC penetration rates. Between 18:00 and 19:00, the average speeds for the reference scenario are slightly lower. Again, these findings support that there are no or only small effects as a result of ACC (van Arem et al., 2006; VanderWerf et al., 2002). When analyzing the drop in speed, the congestion is expected to be active between approximately 16:00 and 18:30. In contrast with the ACC scenarios (*Figure 74*), there is no severe reduction in average speed within the congested periods.

6.1.2.2 Density

The average densities over the network are provided in *Figure 79*. These average densities refer to the average densities all over the network, which means that it only provides some information, since dense sections could be compensated by empty sections. However, it will indicate the amount of vehicles on the network and gives an indication of the amount of congestion. The warm-up and cooldown period to fill and flush the network are not shown in this graph. The representative speed in the graph refers to the speed of the reference scenario and is included to indicate the congestion period, where the speeds are reduced.

At early time periods, average densities increase for increasing rates of newer ACC, which can be explained by the lower speed acceptance parameters for ACC, meaning that these vehicles will drive slightly slower and stay on the network slightly longer. For 40% and 50% ACC, the average densities peak

at approximately 16:00. However, after this time the average density stays constant until approximately 17:30. From 17:30 and onwards, the average densities of higher ACC percentages are lower. The average density of the reference scenario is the highest from 17:30 and onwards, which indicates that the congestion is resolved faster than in the scenarios with ACC. These results indicate that the congestion occurs slightly earlier for scenarios with newer ACC, but this comes with the advantage that the congestion is also resolved earlier. For all market penetration rates of newer ACC, the densities are very similar from 17:15 and onwards.

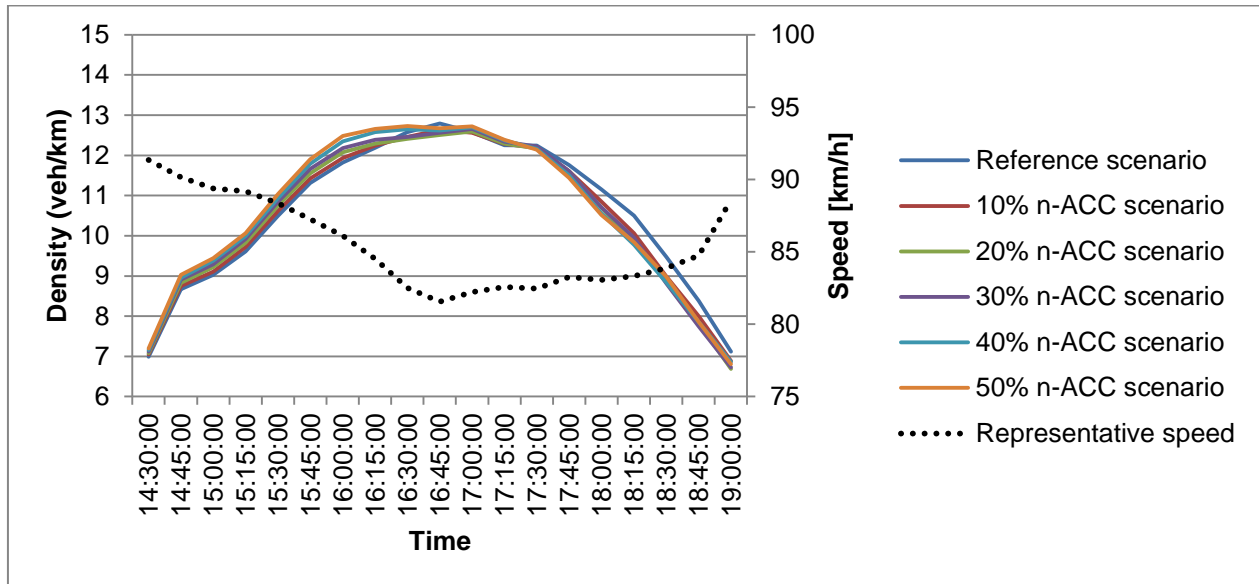


Figure 79 - Overview of average densities over time in the newer ACC scenarios

6.1.2.3 Delay time

The average delay times for increasing newer ACC market penetration rates are provided in Figure 80. The representative speed refers to the speed of the reference scenario, indicating congestion severity.

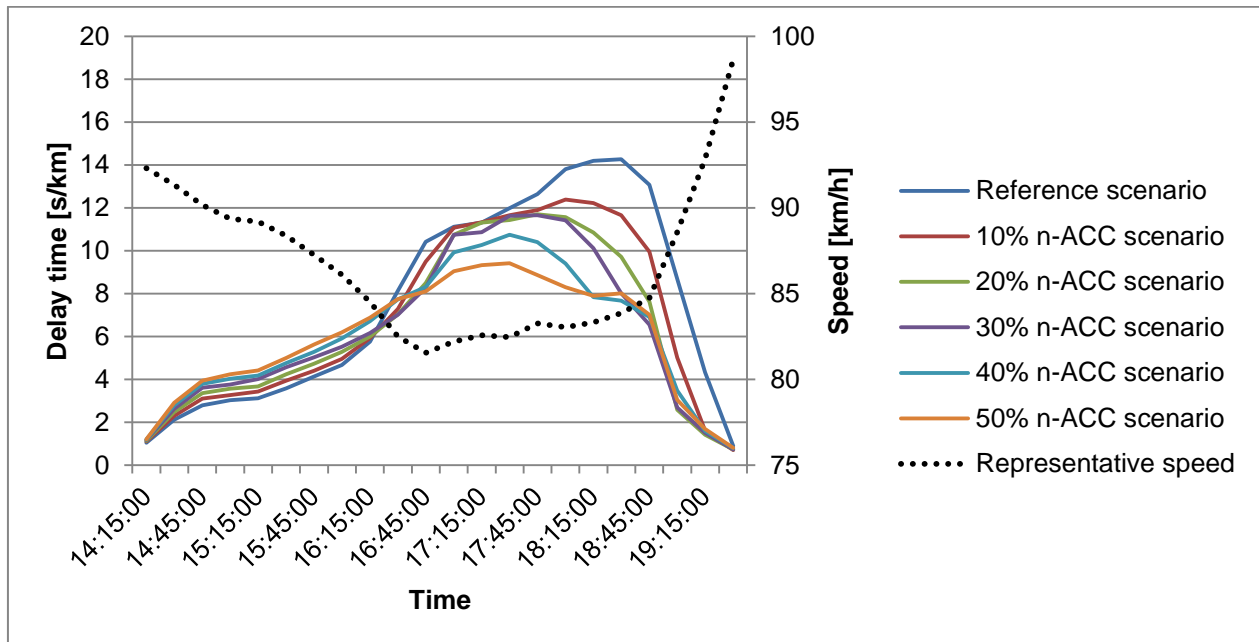


Figure 80 - Overview of average delay time in the newer ACC scenarios

At early time periods, the delay times increase for increasing penetration rates of newer ACC. From approximately 16:30 and onwards, the delay times are higher for lower penetration rates of newer ACC. From 16:30, the severe peak period starts, since the delay increases rapidly. The delay times of the reference scenario are highest. Subsequently, the 10%, 20% and 30% newer ACC scenarios have relatively similar delay times and follow the same pattern. For the 40% and 50% newer ACC market penetration rate, the delay times decrease further. These decreases in delay time are caused by decreases or relieves of congestion at specific bottleneck locations. In terms of congestion, low penetration rates of newer ACC seem to only have a small impact as VanderWerf et al. (2002) indicates. Contrary to his study, penetration rates of 40% already seem to have a significant influence on traffic flow and average delay times of vehicles.

6.1.2.4 Total number of lane changes

The total number of lane changes for the different newer ACC market penetration rates are provided in *Figure 81*. The warm up and cooldown period have not been included in the graph.

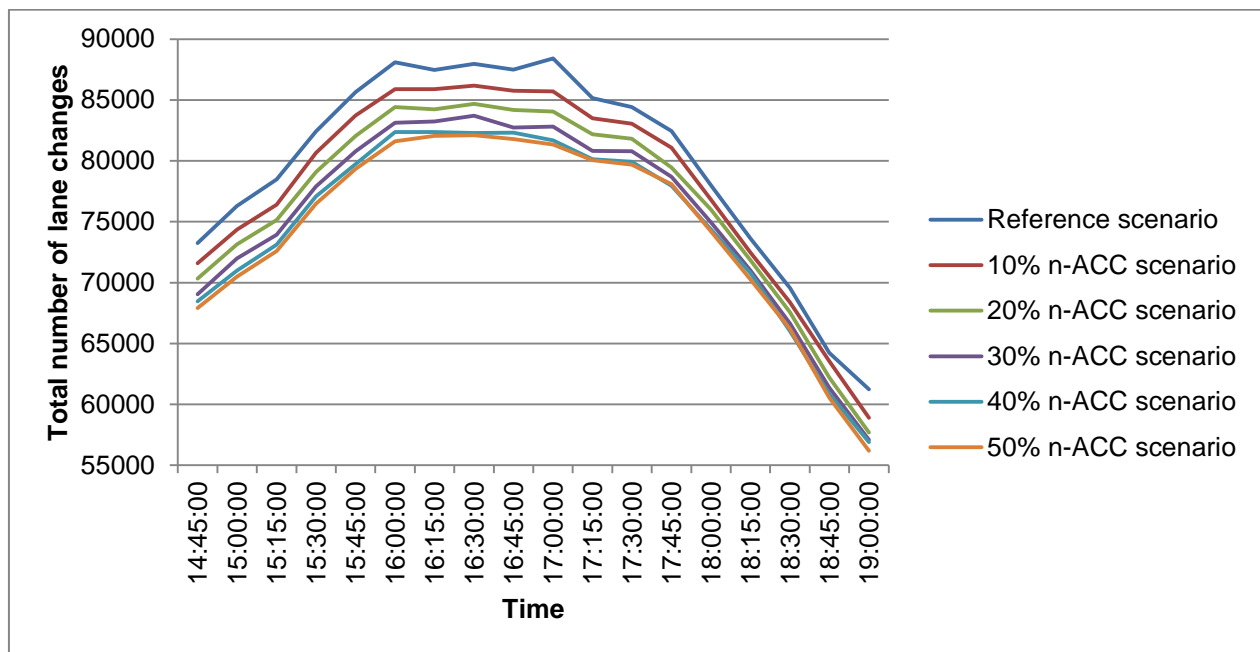


Figure 81 - Overview of the total number of lane changes in the newer ACC scenarios

The total number of lane changes decrease for increasing percentages of newer ACC, which indicates that newer ACC leads to a reduction in total number of lane changes, as indicated by Gorter (2015).

6.1.3 Average influences of improved ACC

The network-wide effects of improved ACC in terms of speed, density, delay time and total number of lane changes are described in this subsection.

6.1.3.1 Speed

Average journey speeds for the different market penetration rates of improved ACC are provided in *Figure 82*. At start, the average journey speed decreases for increasing market penetration rates of improved ACC, because of the lower speed acceptance parameters for ACC, which results in lower maximum desired speeds and slightly lower speeds in general. However, from 18:00 and onwards, the average speeds for higher improved ACC penetration rates are higher. Contrary to the newer ACC scenario (*Figure 78*), the gains in average speeds from 18:00 and onwards are higher for increasing penetration rates. For the reference and 10% improved ACC scenarios, the average speeds are much lower than for

the higher improved ACC penetration rates after 18:00. This indicates that low percentages of improved ACC already solve some congestion problems at local bottlenecks. This is in line with the study of Davis (2004), who claims that jams are suppressed with 20% ACC penetration with headways of 1 second.

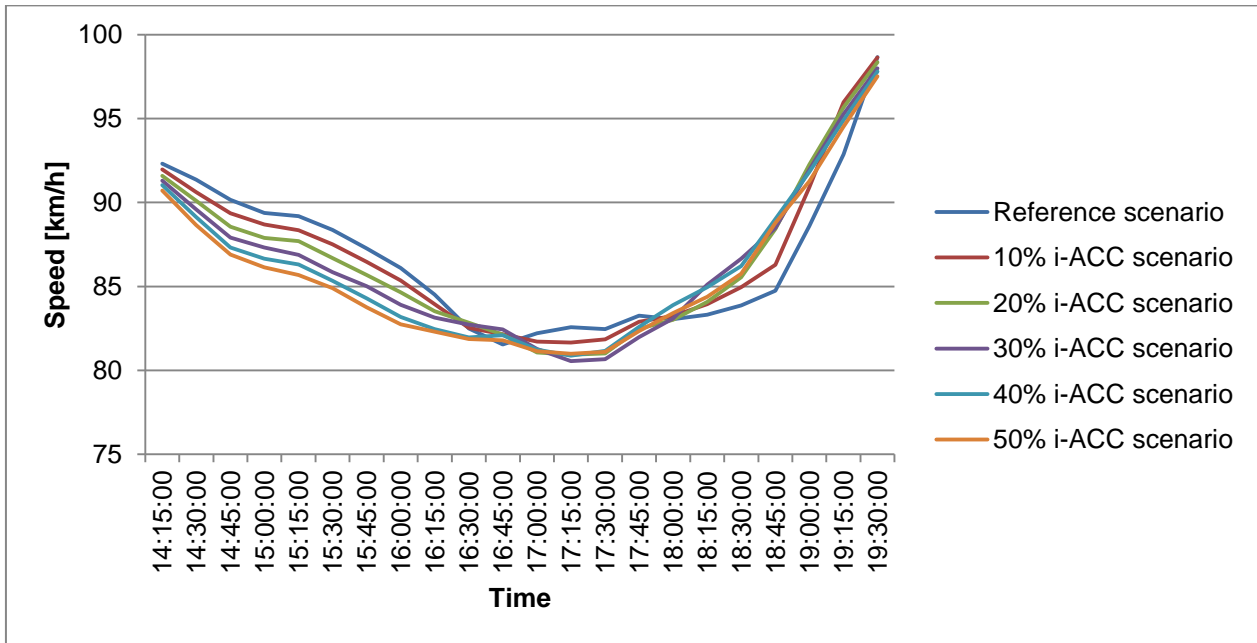


Figure 82 - Overview of average speeds over time in the improved ACC scenarios

6.1.3.2 Density

The average densities for the improved ACC scenarios are provided in *Figure 83*. It only provides some information, since dense sections could be compensated by empty sections. However, it will indicate the amount of vehicles on the network and gives an indication of the amount of congestion. The warm-up and cooldown period are excluded. The representative speed refers to the speed of the reference scenario and is included to indicate the peak period, where the speeds are reduced. The warm up and cool down periods are excluded from the graph to provide a better overview on the differences.

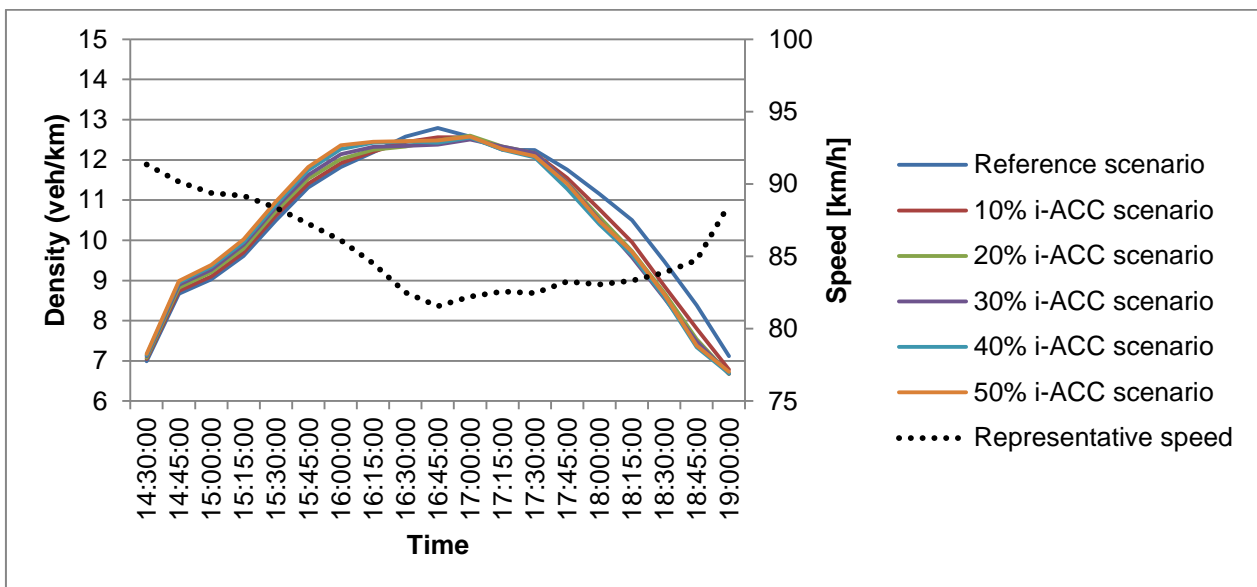


Figure 83 - Overview of average densities over time in the improved ACC scenarios

A very similar pattern as the newer ACC scenarios (*Figure 79*) could be observed. However, the differences between the reference scenario and other equipment scenarios is slightly bigger for the improved version of ACC. At early time periods, the average densities increase for increasing improved ACC percentages. For late time periods, the average densities decrease for increasing percentages of improved ACC.

6.1.3.3 Delay time

Figure 84 provides the average delay times for the improved ACC penetration scenarios. The representative speed refers to the speed of the reference scenario and indicates the peak period, where speeds are reduced.

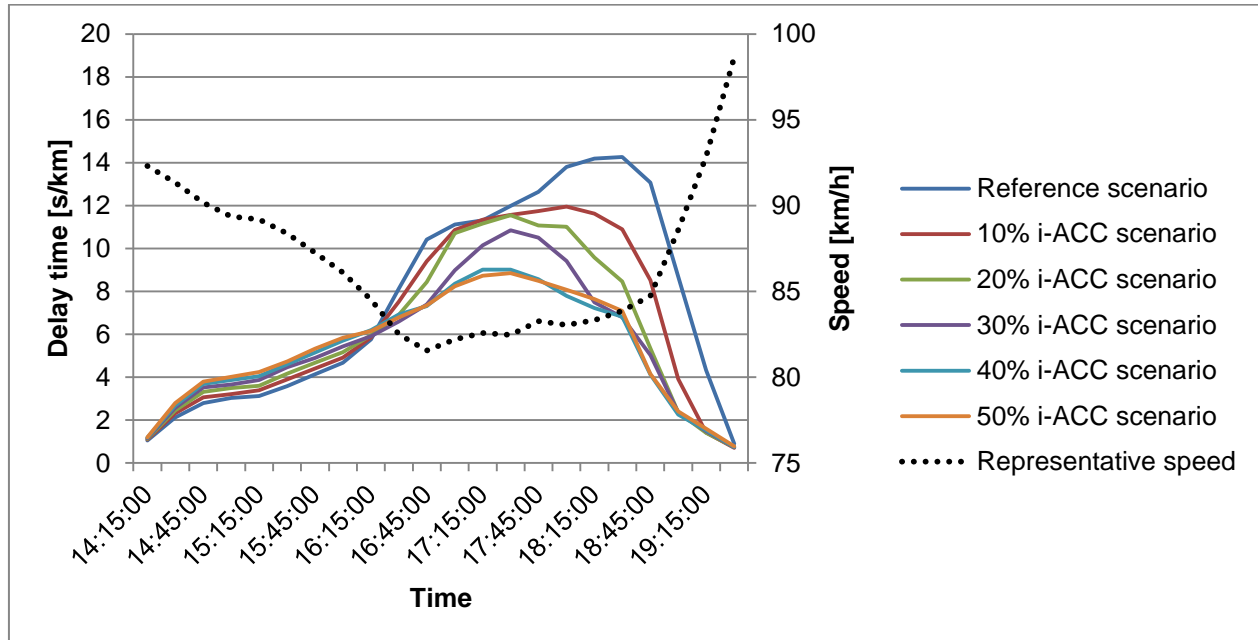


Figure 84 - Overview of average delay time in the improved ACC scenarios

Contrary to the ACC and newer ACC scenarios (*Figure 76* and *Figure 80*), a clearer and stepwise decrease in delay times is found for increasing rates of improved ACC. However, similar to the ACC and newer ACC scenarios, the delay times are increasing for increasing percentages of improved ACC in the early time periods, because of the lower speed acceptance parameters for ACC vehicles. Between 0% and 40% improved ACC, there are clear and significant improvements for increasing market penetration rates of improved ACC, due to increased traffic situations at local bottlenecks. However, between 40% and 50%, the differences are negligible, indicating that the gains for increasing the market penetration rates even further are limited. It is found that the decrease in delay time is exactly located within the period where congestion is found and speeds are lowered. This indicates that the improved ACC vehicles are able to relieve or solve congestion. This is in contrast with the studies of VanderWerf et al. (2002) and van Arem et al. (2006) who report that ACC will have no or small effects on traffic flow. However, as Davis (2004) indicated, ACC could also suppress traffic jams. Additionally, Kesting et al. (2008) indicates that ACC could be used to avoid congestion, although their study is mainly focused on applying adaptive driving strategies in combination with ACC. Also, the results found in their study are mainly achieved as a result of the adaptive driving strategies rather than due to ACC market penetration rates.

6.1.3.4 Total number of lane changes

The total number of lane changes for the improved ACC market penetration rates are provided in *Figure 85*. The warm up and cooldown period are excluded from the graph.

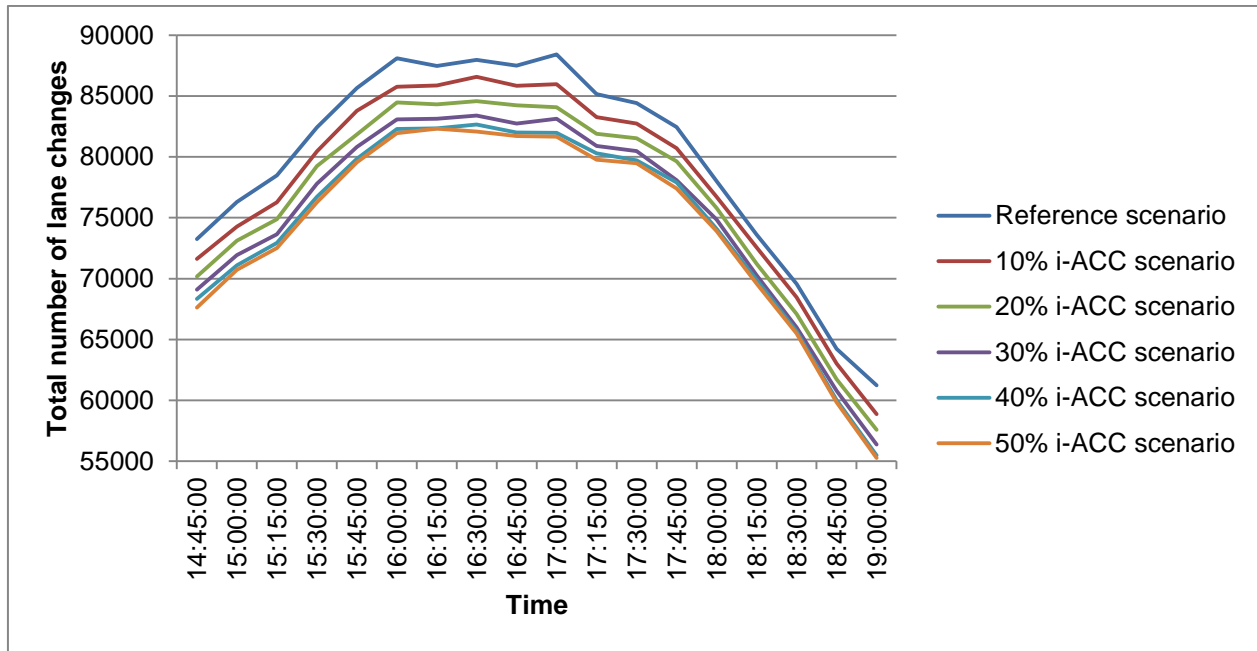


Figure 85 - Overview of the total number of lane changes in the improved ACC scenarios

Similar to the ACC and newer ACC scenarios (Figure 77 and Figure 81), the total number of lane changes reduces for increasing ACC penetration rates. However, from 30% improved ACC or more, the differences are negligible. In comparison with the ACC scenarios, the stepwise differences are smaller, which indicates that the improved ACC users simulated might change lanes more frequently than the (normal) ACC users simulated in Aimsun, as the reduced reaction times for improved ACC

6.1.4 Average influences of CACC

This subsection describes the network-wide effects of CACC with graphs given on average speed, density, delay time and the total number of lane changes from simulation. Additionally, it is important to note that for this study it was assumed that all other vehicles are also able to communicate with the CACC vehicles. Also, the users of the CACC vehicles still accelerate by themselves after standstill, meaning that the reaction times at stop for CACC users are equal to the reaction times at stop of all ACC users and manual car drivers.

6.1.4.1 Speed

Figure 86 provides the average journey speeds resulting from simulating the CACC scenarios with the given market penetration rates.

In the early time periods, the speeds for increasing percentages of CACC are lowered, as a result of smaller maximum desired speeds for CACC users, because this group of drivers is expected to adapt to the speed limits more frequently. This also results in lower free flow speeds on average, which explains the early decrease for increasing percentages of all ACC and CACC scenarios.

However, when the speeds drop, a transformation is found, which turns the order of speeds found for the CACC scenarios around. This means that speeds are higher for higher percentages of CACC, indicating that there is less congestion at local points in the network in scenarios with higher penetration rates of CACC. This effect is clearly observed at late time periods between 18:00 and 19:15, which especially indicates that the congestion is solved earlier for increasing penetration rates of CACC. Additionally, the gains in average speeds in comparison with the improved ACC scenarios (Figure 82) are clearly visible in the graph.

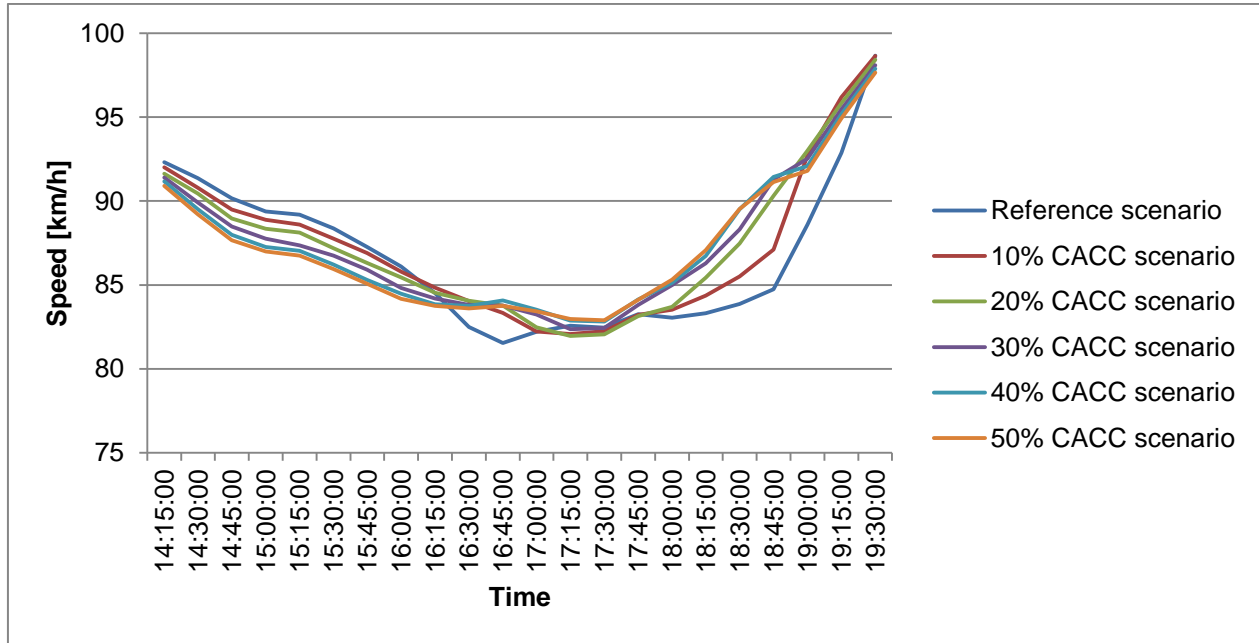


Figure 86 - Overview of average speeds over time in the CACC scenarios

6.1.4.2 Density

Figure 87 provides the average densities for scenarios with increasing CACC market penetration rates. This graph should be read with care, because dense sections could be compensated by empty sections. Nevertheless, this will provide some information on the amount of vehicles on the network and the severity of congestion. Also, the speed of the reference scenario has been included in the graph, which indicates the peaks of congestion. Also, the warm up and cooldown periods are excluded from the graph.

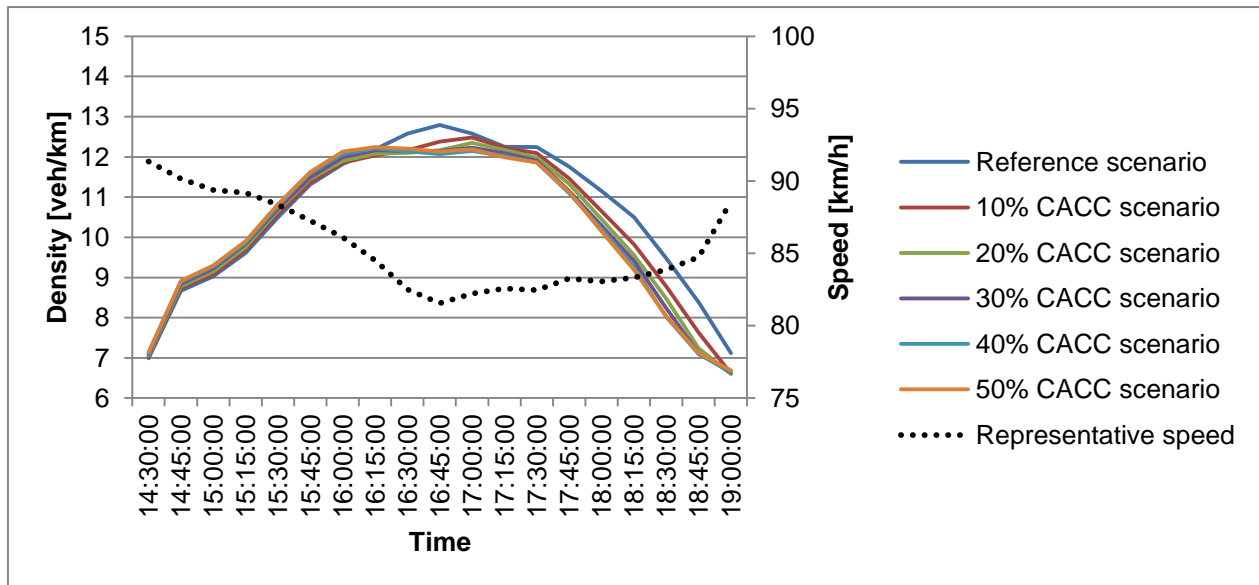


Figure 87 - Overview of average densities over time in the CACC scenarios

At early time periods, the average density slightly increases for increasing percentages of CACC, because of the lower speed acceptance parameters for CACC, meaning that these vehicles will drive slightly slower and stay on the network for a longer period of time. However, this pattern changes at approximately 16:15, where densities decrease for increasing rates of CACC, because congestion is resolved or prevented at

local bottlenecks. It should be noted that the difference between the reference and 10% CACC scenario is relatively big compared to differences between other subsequent percentages of CACC. This indicates that increases in terms of traffic flow can already be achieved at low penetration rates, which is in contradiction with the study by van Arem et al. (2006), where the driving behavior of CACC vehicles is dependent of the communication capabilities of the leading vehicle. However, this current study assumes that all vehicles will have the ability to send speed information to the CACC systems, which explains why the effects found in this study are more positive compared to the results found by van Arem et al. (2006). When so-called vehicle awareness devices are used to communicate with CACC vehicles, direct gains in terms of roadway capacity were found as a result of CACC market penetration (Shladover et al., 2012).

6.1.4.3 Delay time

Average delay times for the CACC scenarios are provided in *Figure 88*. The speeds of the reference scenario are also included in the graph in order to indicate the moments of congestion.

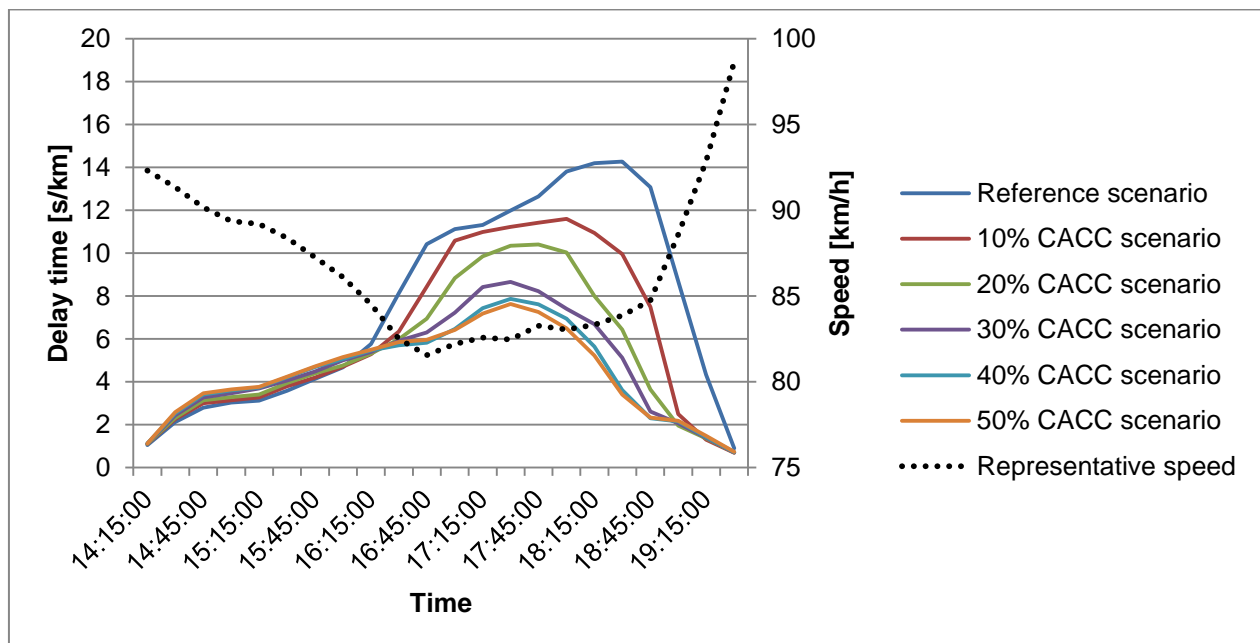


Figure 88 - Overview of average delay time in the CACC scenarios

Again, at early time periods, the delay times for scenarios with increasing market penetration rates of CACC are slightly higher, because CACC vehicles will drive at slightly lower speed as a result of the lower speed acceptance parameter. Similar to the improved ACC scenarios, a clear and stepwise decrease in delay times can be observed for increasing percentages of CACC. Between 40% and 50% CACC, the gains are very small, which indicates that the gains in terms of delay time stabilize for higher percentages of CACC, indicating that most congestion has been solved at 40% penetration. Additionally, the gains are mostly found for periods where congestion is likely to occur, which shows that increases in CACC penetration rates result in decreases of congestion. Also, gains are already found at low penetration rates of CACC. This contradicts with the results of a study on the impacts of CACC on traffic flows (van Arem et al., 2006). However, this difference can be explained by the assumption in this study that all vehicles are able to send speed information to the CACC systems. In another study that includes vehicle awareness devices that can also communicate with CACC vehicles, clear gains in terms of lane capacity are also found for low penetration rates of CACC, similar to the results found here (Shladover et al., 2012).

In comparison with the other ACC scenarios, the delay time of the 40% and 50% CACC market penetration scenarios is always lower than 8 seconds per kilometer on average, which means that the

average delays are decreasing for improved versions of ACC or CACC. This indicates that it is very useful to invest in research and further development of (cooperative) adaptive cruise control systems.

6.1.4.4 Total number of lane changes

Figure 89 shows the total number of lane changes for increasing percentages of CACC. The two first and last time periods are excluded, which can be considered as warm up and cooldown period of simulation.

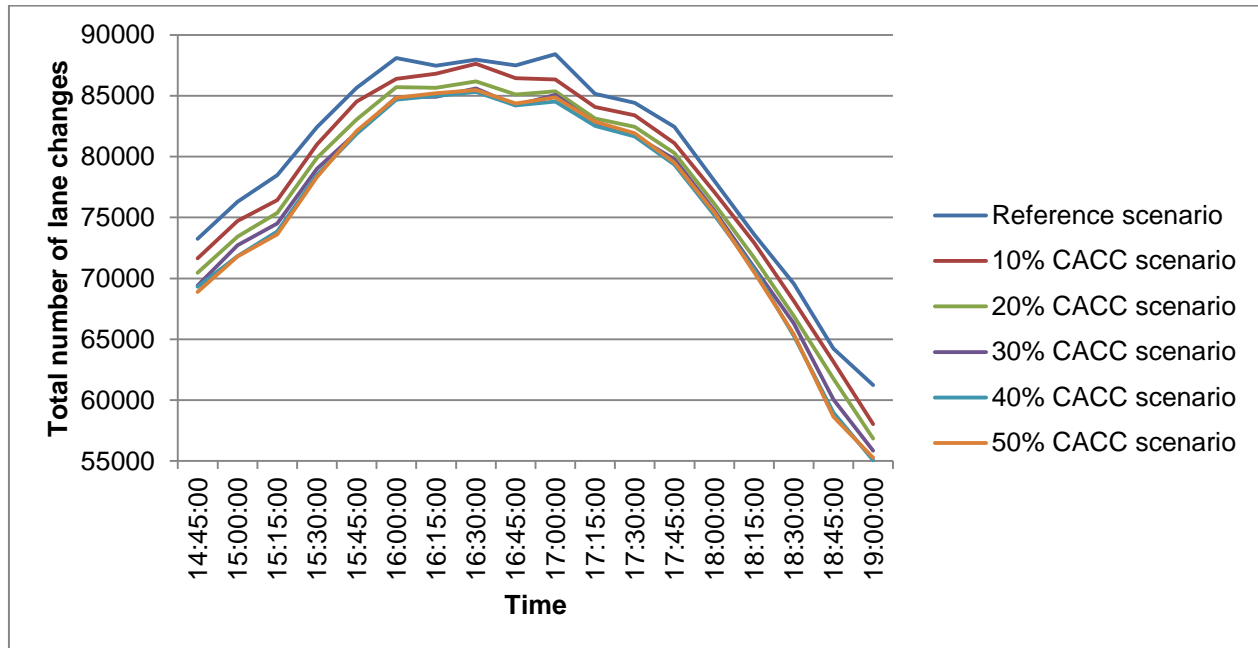


Figure 89 - Overview of the total number of lane changes in the CACC scenarios

The total number of lane changes reduces for increasing CACC percentages, similar to all ACC scenarios. However, the differences between 30%, 40% and 50% CACC are negligible, indicating that CACC users might change lanes more frequently than ACC users. This could be explained by the significant decrease in reaction time of CACC, which means that CACC users are able to change lanes more frequently in simulation, since smaller gaps are accepted and more evaluations of suitable gaps can be made. Therefore, changes in reaction time seem to have a significant effect on the number of lane changes.

6.2 Space-time diagrams of bottleneck locations

This subsection provides the space-time diagrams for the detector set locations as indicated in section 5.2.2. These detector sets are placed at locations where bottlenecks are found or expected. The space-time diagrams can be used to assess the length, severity and duration of congestion at these locations. Additionally, these space-time diagrams are computed for all equipment scenarios, providing a good overview of the impacts on specific bottleneck locations and bottleneck type. All space-time diagrams are discussed per detector set and subdivided per type of ACC or CACC.

6.2.1 Detector set 1

This detector set contains a weaving section at junction Ridderkerk. This weaving section could become a bottleneck, because weaving section has a limited length of approximately 150 meters, which means that many vehicles might have to change lanes over a limited road length.

6.2.1.1 ACC

The space-time diagrams of increasing percentages of ACC for this detector set are given in Figure 90. It becomes clear that speeds at the weaving section slightly reduce for increasing market penetration rates

of ACC, although the reductions in speed are not severe. These results can be explained by the fixed headway settings of ACC vehicles, which are also applied in the lane-changing algorithm. These headway settings limit the acceptable gaps for ACC vehicles, while the acceptable gaps for normal car users are not bounded by fixed headway settings. Also, ACC vehicles are driving at larger headways, which might reduce the potential capacity of roadways. Additionally, if vehicles merge directly in front of an ACC vehicle at gaps smaller than the desired headway set by the user, the ACC vehicle will try to adapt the headway towards the desired headway by lowering speed. This braking action might result in disturbances on the weaving section. The discussed features are expected to be the main reasons for deterioration in terms of traffic flow for the ACC scenarios at this location.

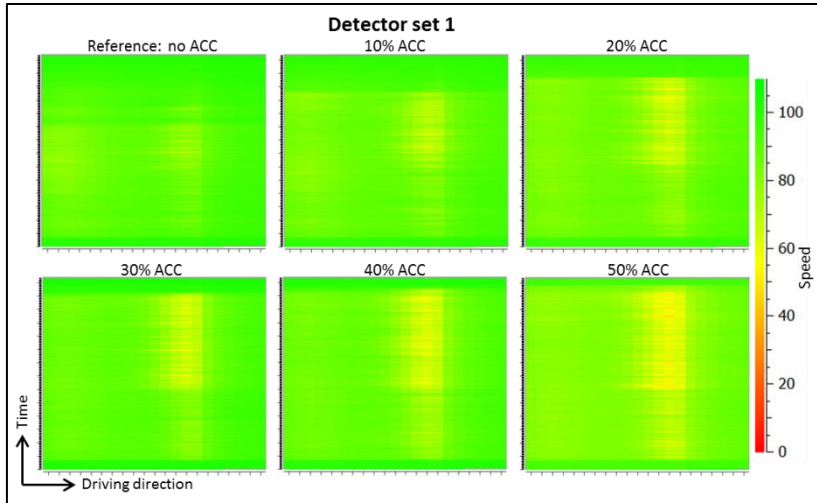


Figure 90 - Space-time diagrams for ACC scenarios at detector set 1

6.2.1.2 Newer ACC

Figure 91 shows the space-time diagrams of increasing market penetration rates of newer ACC vehicles at detector set 1.

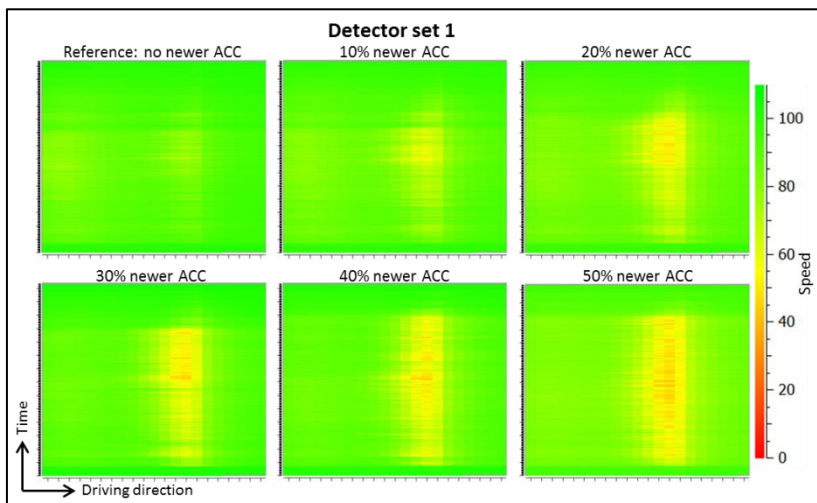


Figure 91 - Space-time diagrams for newer ACC scenarios at detector set 1

Similar to the ACC scenarios, the speeds at the weaving section reduce for increasing percentages of newer ACC. The main reason for this decrease is the desired headway defined, which limits the gaps allowed to merge and potentially increases braking movements of newer ACC vehicles to react upon

merging vehicles directly in front of the own vehicle. Both these consequences result in disturbances at the weaving section and contribute to the deterioration of traffic flow. However, the disturbance found for newer ACC are higher than those found for increasing percentages of ACC. The only difference between the vehicle types is a decrease in reaction time for the newer ACC systems, which implies that a reduction in reaction time has led to the deterioration. Due to this reduction in reaction time, the ACC vehicles are able to respond faster to vehicles merging in front of the own vehicle, which might increase the amount of braking actions leading to disturbances in speed. As a consequence, this braking response is probably amplified by the human drivers with larger reaction times. Additionally, the reductions in reaction time might also result in more (unexpected) braking maneuvers of ACC vehicles.

6.2.1.3 Improved ACC

The space time diagrams for increasing market penetration rates of improved ACC vehicles can be found in *Figure 92*. Again, deteriorations in speeds are found for increasing percentages of ACC. In comparison with the newer ACC space-time diagrams (*Figure 91*), the differences are that the improved ACC scenarios show some more disturbances, albeit that the differences are negligible. In combination with the space-time diagrams for percentages of ACC (*Figure 90*), it can be concluded that reaction time is the most important factor for the decrease in average speeds. Since the impact of the reduced headways for improved ACC systems was negligible, this congestion front is mainly caused by the lane-changing maneuvers, rather than due to capacity restrictions.

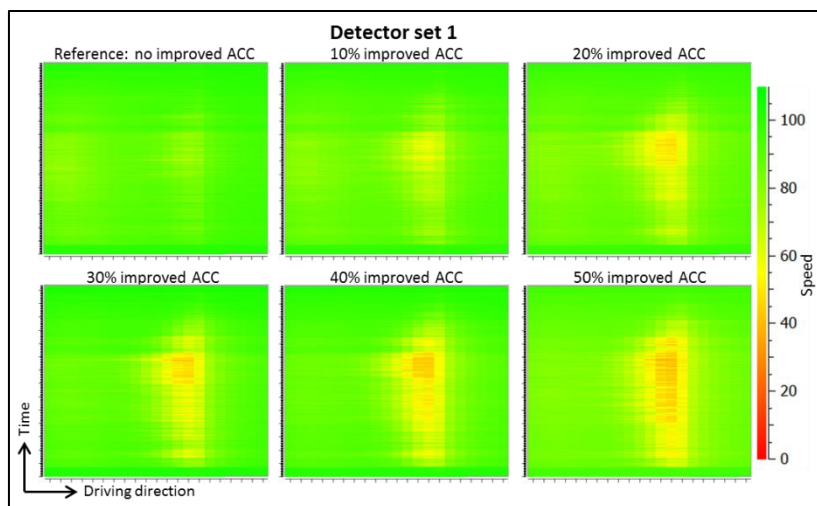


Figure 92 - Space-time diagrams for improved ACC scenarios at detector set 1

6.2.1.4 CACC

Figure 93 shows the space-time diagrams for the CACC scenarios. This congestion pattern is slightly worse in comparison with ACC (*Figure 90*). But, in comparison with the newer ACC and improved ACC (*Figure 91* and *Figure 92*), this congestion pattern has been improved. This suggests that still more congestion is occurring due to fixed headway settings at the weaving section, which probably have a significant effect on the gap acceptance model that determines whether or not possible gaps are large enough to merge into. Since the CACC scenarios show slightly more positive results, it can be concluded that these effects are reduced if both the fixed headway settings and reaction times decrease. At this bottleneck, the situation deteriorates due to the introduction of ACC, as well as CACC. This effect is mainly a result of introducing a fixed headway setting for the ACC and CACC vehicles, which has a direct effect on the determination of acceptable gaps to merge into. Since the manual drivers do not have a fixed headway setting in simulation, this user group does accept some gaps that are smaller than the fixed headway settings defined for ACC and CACC.

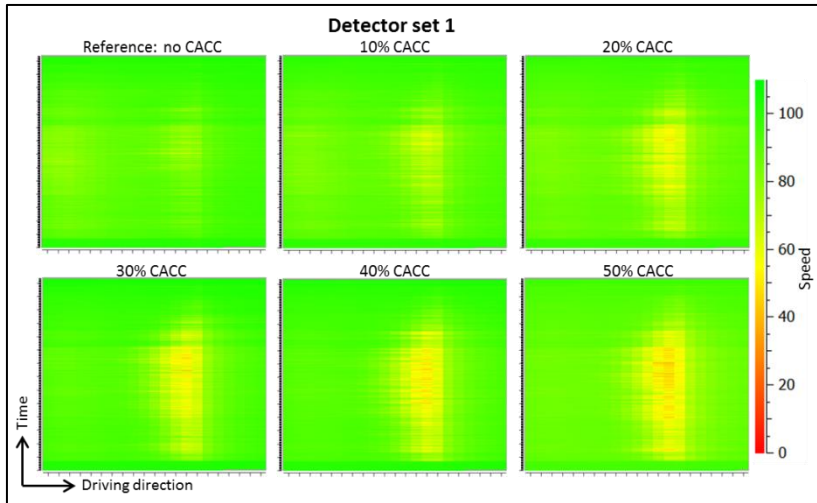


Figure 93 - Space-time diagrams for CACC scenarios at detector set 1

6.2.2 Detector set 2

This bottleneck consists of an on-ramp construction, where traffic from the main road and parallel road from the west merge at junction Ridderkerk, to continue in southeastern direction. The length of the section from where the two streams join to the end of the on-ramp lane is approximately 250 meters. This could potentially be a bottleneck, since the traffic demand at this section is relatively high and the merging traffic from the on-ramp could create some congestion.

6.2.2.1 ACC

Figure 94 provides the space-time diagrams of increasing percentages of ACC at detector set 2. It becomes clear that between 0% and 30% ACC penetration rates, the traffic situation becomes worse. From 30% to 50% ACC penetration, changes in speeds are hardly found, indicating that no further deterioration is found at these penetration rates. Since the ACC vehicles use fixed headway settings, ACC vehicles apply larger gaps in comparison with human car drivers, which might result in reductions in capacity. At 30% ACC penetration, the capacity of this bottleneck is probably reached for a short period of time and serious congestion starts occurring, although the duration of congestion is very limited. The fixed headway settings of ACC vehicles are important factors of this congestion. These headway settings are also applied for the lateral driving behavior. The spillback onto the main road upstream is limited.

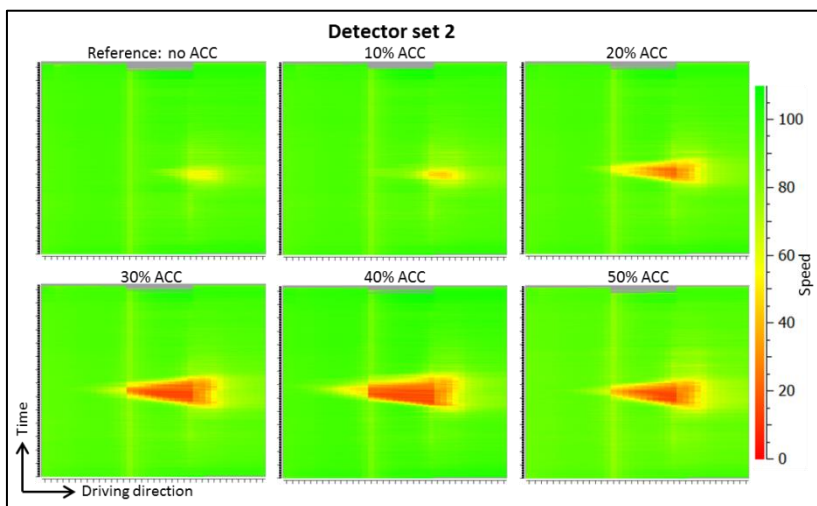


Figure 94 - Space-time diagrams for ACC scenarios at detector set 2

6.2.2.2 Newer ACC

The space-time diagrams of increasing market penetration rates of newer ACC at detector set 2 are shown in *Figure 95*. In these space-time diagrams, only small differences between different newer ACC scenarios can be found. In general, the traffic situation slightly deteriorates for increasing percentages of newer ACC, albeit very limited. Compared with *Figure 94*, the traffic situation has improved significantly. The only difference between these ACC types is the reduction in reaction time. Lower reaction times already solve the most important congestion problems. Decreased reaction times lead to faster responses of ACC vehicles, aiding in solving congestion. Additionally, lower reaction times could result in reductions in headway, if the speed is determined by the V_b component of the car-following model, which restricts the speed of a vehicle based on the presence of a lead vehicle and differences in normal decelerations.

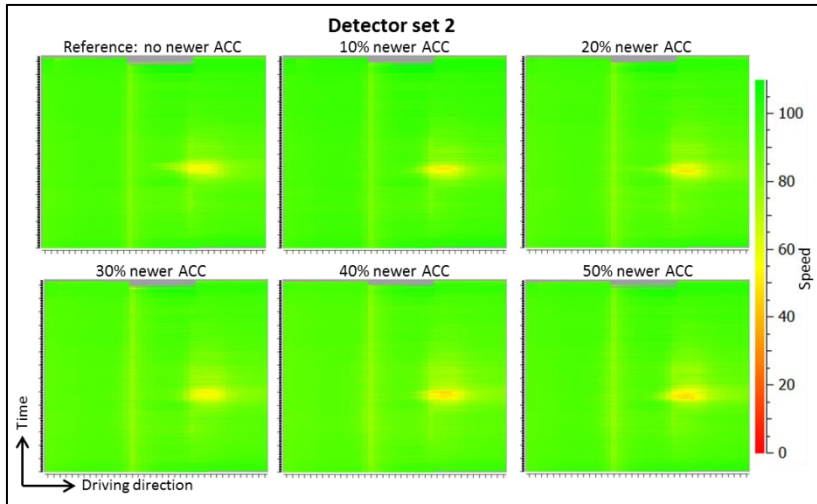


Figure 95 - Space-time diagrams for newer ACC scenarios at detector set 2

6.2.2.3 Improved ACC

Figure 96 provides the space-time diagrams of increasing percentages of improved ACC. In *Figure 96*, no to negligible differences can be found as a result of increasing penetration rates of improved ACC. In comparison with ACC and newer ACC (*Figure 94* and *Figure 95*), the traffic situation has been improved. At this bottleneck location, introducing the improved version of ACC will have no or small effects in terms of traffic flow, which is in line with the conclusions of van Arem et al. (2006) and VanderWerf et al. (2002).

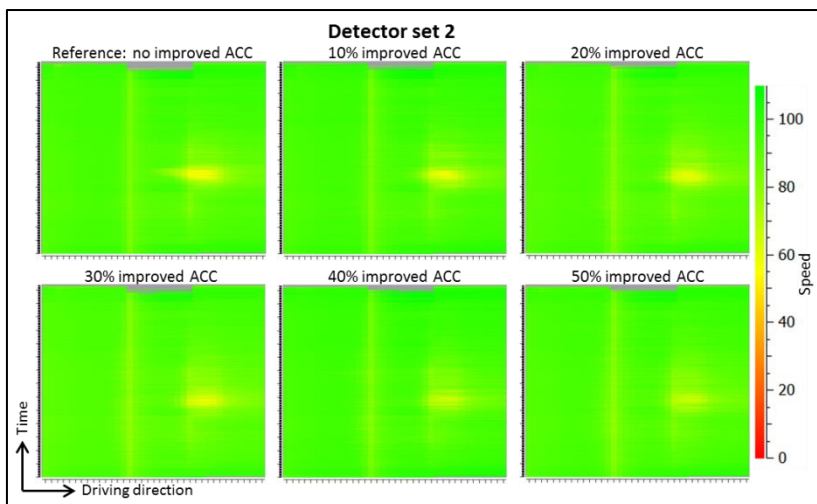


Figure 96 - Space-time diagrams for improved ACC scenarios at detector set 2

6.2.2.4 CACC

Figure 97 shows the space-time diagrams of scenarios with increasing market penetration rates of CACC. All ACC scenarios did not result in clear gains in average speed, while improvements are found for CACC. As van Arem et al. (2006) indicated, effects of ACC are only small, while the introduction of CACC shows signs of improvements. The results were expected to be similar, because that study was focused on a highway configuration with a lane drop, which is relatively similar to this on-ramp situation.

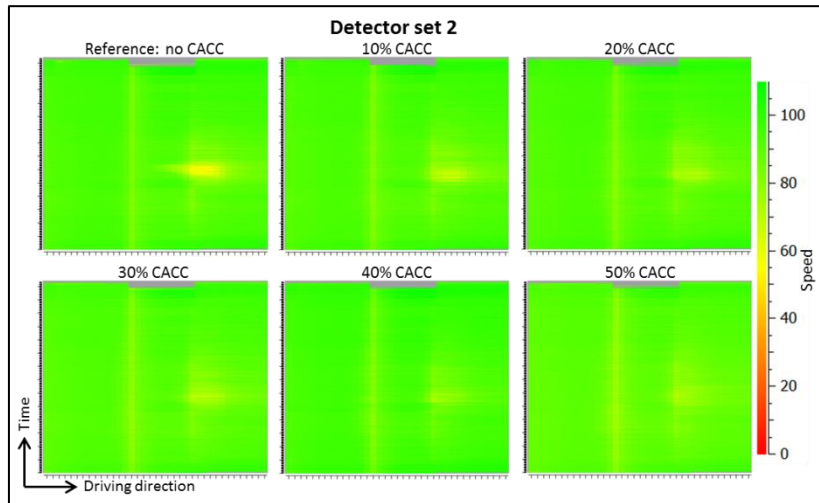


Figure 97 - Space-time diagrams for CACC scenarios at detector set 2

6.2.3 Detector set 3

The main bottleneck in this detector set is a weaving section of three lanes, where the traffic demand and amount of lane changes are relatively high, which could result in serious congestion. During the calibration procedure, this was one of the important congestion fronts with serious congestion on it. The length of this weaving section is approximately 500 meters, but it is expected (and modelled) that most drivers tend to change lanes early, because road signs are placed quite far upstream of the weaving section. The lane-changing behavior of vehicles could be considered as one of the most important causes of the congestion. The end of congestion could not be fully shown in the space-time diagrams, because the tail of congestion exceeds the network boundaries of the model. Therefore, it is important to note that the length of congestion might be longer and spills back further to the north of junction Ridderkerk, which is not visualized in any of the provided figures.

6.2.3.1 ACC

Figure 98 provides the space-time diagrams of increasing market penetration rates of ACC. Figure 98 shows that congestion is already found in the reference scenario. For increasing percentages of ACC, the start of congestion is found earlier, while the end of congestion is found at approximately equal points in time. This indicates that the duration of congestion increases for increasing percentages of ACC. The most important factors of this increase in congestion are the headways applied by the ACC vehicles, which result in larger distances between vehicles and probably leads to reductions in potential capacities. Here, the introduction of ACC vehicles results in deteriorations in the traffic situation, as found by several other studies (Marsden et al., 2001; Milanés & Shladover, 2014).

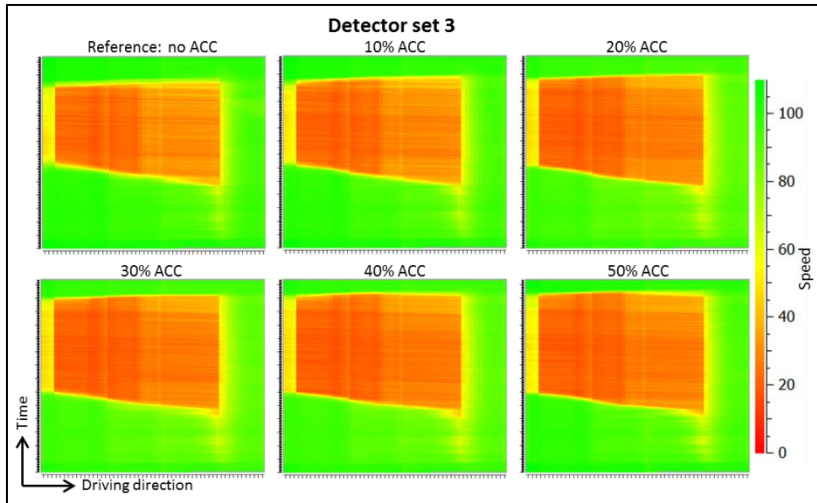


Figure 98 - Space-time diagrams for ACC scenarios at detector set 3

6.2.3.2 Newer ACC

Space-time diagrams for the newer ACC scenarios are shown in *Figure 99*. Contrary to the scenarios for ACC (*Figure 98*), the average speeds slightly increase for increasing penetration rates of newer ACC. This indicates that the traffic situation slightly improves as an effect of introducing ACC. An explanation for this effect is that the newer ACC vehicles still apply relatively large gaps, which provides space for merging vehicles and have lower reaction times, which enables the possibility to respond to speed changes at a quicker rate and more smoothly. Nevertheless, the decrease in congestion is still limited, indicating that the effects are relatively small, as indicated by VanderWerf et al. (2002).

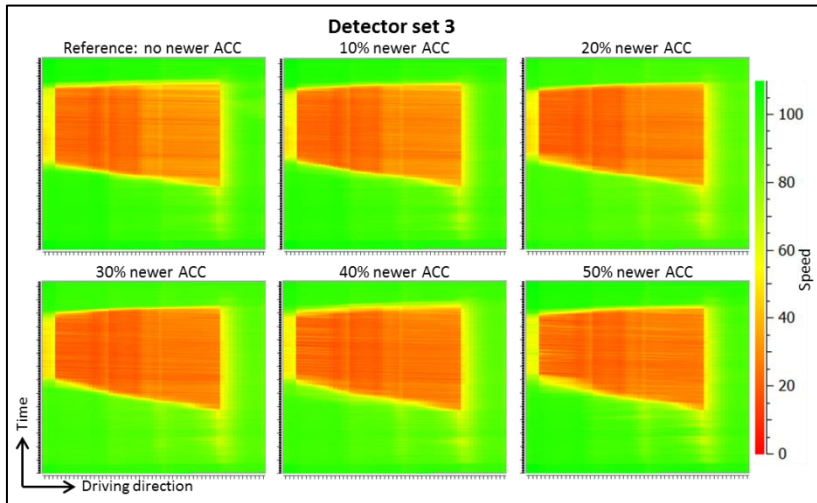


Figure 99 - Space-time diagrams for newer ACC scenarios at detector set 3

6.2.3.3 Improved ACC

Figure 100 shows space-time diagrams for increasing market penetration rates of improved ACC at detector set 3. Similar to the effects of newer ACC (*Figure 99*), the introduction of improved ACC are also positive. However, the results are more positive for the improved ACC scenarios. The results from 0% to 30% improved ACC penetration rates show similar patterns, while the largest improvements are found for the 40% and 50% improved ACC scenarios. This indicates that both reaction time and headway settings have an influence on the traffic flow at this bottleneck location. Decreases in desired headways and reaction times have a positive result, because the improved ACC vehicles react fast to their leading

vehicles and apply time headways that are slightly larger than the headways human drivers apply, but this comes with the advantages that braking actions are stabilized and disturbances due to braking actions are slightly smoothed by the improved ACC systems. The most important factors for the positive effects of improved ACC are the relatively short reaction times and the time headways applied, which on the one hand creates some space for merging vehicles and on the other hand decreases disturbances caused by braking actions and lane changes, as a result of the shorter reaction times of these systems. However, the gains found are still relatively small, which indicates that the congestion is not solved yet.

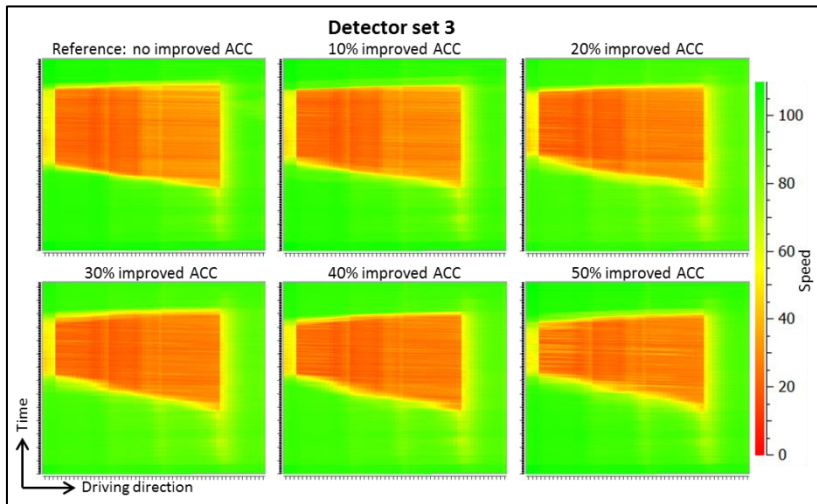


Figure 100 - Space-time diagrams for improved ACC scenarios at detector set 3

6.2.3.4 CACC

Space-time diagrams for scenarios with increasing CACC percentages are provided in *Figure 101*. Similar to the effects of newer ACC and improved ACC, the effects of CACC are positive. However, it should be noted that the effects of CACC are more clear and significant than the effects found for the other ACC systems. Low market penetration rates of CACC (up to 20% or 30%) only show small improvements, while large improvements are found for market penetration rates of 40% and 50%. A similar conclusion was drawn by van Arem et al. (2006), although the percentages for which the changes were found slightly differ, which could be explained by different assumptions with respect to the communication capabilities of the vehicles included in simulation.

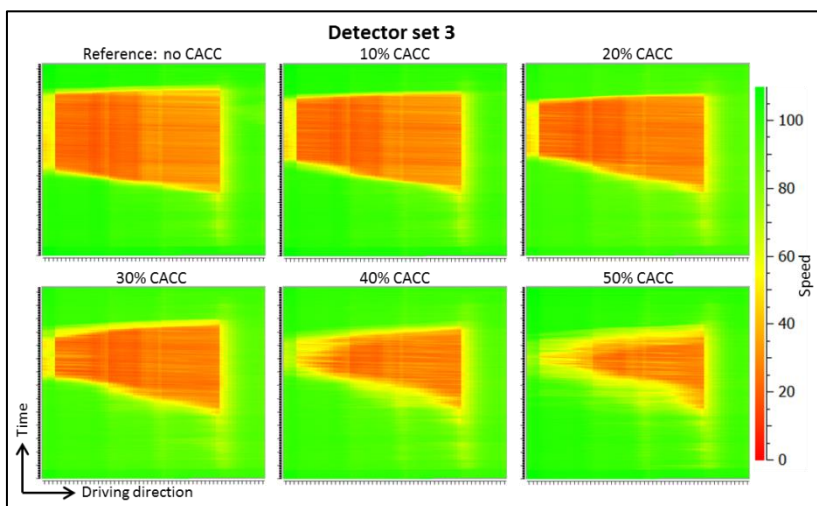


Figure 101 - Space-time diagrams for CACC scenarios at detector set 3

6.2.4 Detector set 4

The main bottleneck within this detector set is an on-ramp at junction Vaanplein, where the on-ramp lane drops off after approximately 200 meters. This road section has a downhill slope, meaning that congestion was modelled by applying extreme braking intensities, because it is expected that human drivers will apply larger braking rates than normal as a consequence of this downhill slope, as discussed in the calibration procedure. Additionally, the spillback towards the eastern part of the network is taken into account. This was one of the important congestion fronts in the calibration procedure. It is important to keep in mind that the congestion is mainly caused by a combination of lane-changing behavior, severe braking actions as a result of the downhill slope and the on-ramp construction at this road section.

6.2.4.1 ACC

Figure 102 shows the space-time diagrams for increasing penetration rates of ACC at detector set 4. A significant amount of congestion is found in the reference scenario. For increasing percentages of ACC, the amount of congestion decreases. The reason for this decrease in congestion are the lower desired and maximum decelerations of the ACC vehicles, which means that the extreme braking rates applied at the downhill slope are also less extreme in comparison with the braking rates of human drivers. This effect is also expected, since the ACC systems are bounded with certain braking rates, while human drivers might overreact and apply larger braking rates on downhill slopes. The introduction of ACC results in a decrease of the disturbances and shockwave effect at this location. This result is also found in a study on jam-avoiding adaptive cruise control (Kesting, Treiber, Schönhof, Kranke, et al., 2007).

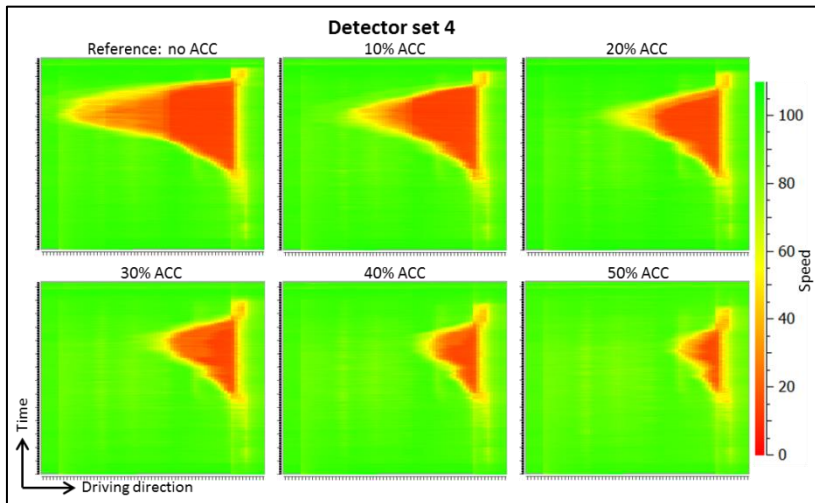


Figure 102 - Space-time diagrams for ACC scenarios at detector set 4

6.2.4.2 Newer ACC

The space-time diagrams for scenarios with increasing market penetration rates of newer ACC are provided in Figure 103. In comparison with the space-time diagrams for ACC (Figure 102), an improvement in traffic situation has been found. At 10% newer ACC penetration rate, the traffic situation is already comparable to the 30% ACC scenario. At 30% newer ACC, the congestion is only active over a short length, while the congestion is nearly solved in the 50% newer ACC scenario. This improvement in comparison with the ACC scenarios is caused by the reduced reaction time for newer ACC, which results in shorter and more adequate responses to lane changes and especially (extreme) braking actions, which dampens the shockwave and spillback effects caused by extreme braking actions even further.

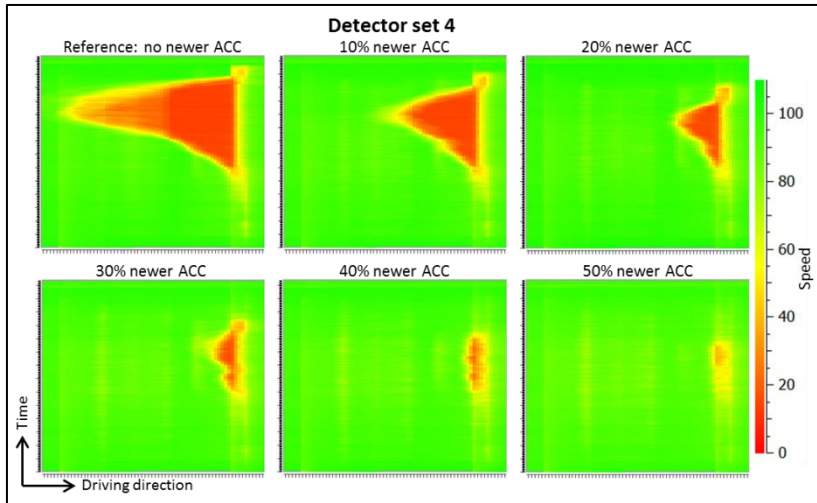


Figure 103 - Space-time diagrams for newer ACC scenarios at detector set 4

6.2.4.3 Improved ACC

Space-time diagrams for scenarios with increasing percentages of improved ACC at detector set 4 are shown in *Figure 104*. In comparison with the space-time diagrams for newer ACC (*Figure 103*), a small improvement in terms of speed and congestion lengths is found. As an example, the space-time diagram of the 20% improved ACC scenario resembles the space-time diagram of the 30% newer ACC scenario. This small improvement is caused by the reduced fixed headway settings, which ensures that the potential achievable throughput is increased and that smaller gaps/headways are accepted by the ACC systems, which makes it easier to merge and change lanes. The improved ACC systems are able to resolve the congestion faster. In the 40% and 50% improved ACC scenarios, no severe congestion is found, but only short temporary disturbances and reductions in speed are found, indicating that congestion might be solved as a result of stimulating the use of ACC technology.

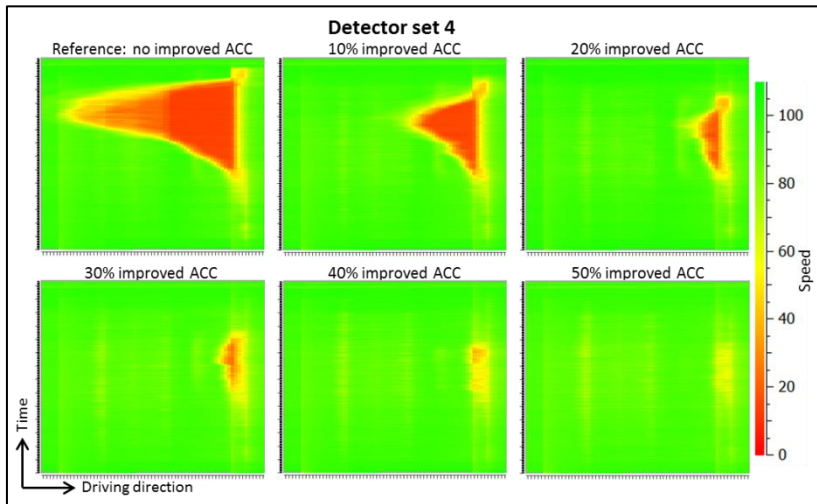


Figure 104 - Space-time diagrams for improved ACC scenarios at detector set 4

6.2.4.4 CACC

Space-time diagrams for scenarios with increased market shares of CACC at detector set 4 are shown in *Figure 105*. In comparison with the ACC scenarios, the congestion is solved at lower market penetration rates of CACC than is the case for the ACC versions, which indicates that the effects of CACC on traffic flow are more positive than those of ACC. However, the differences between the improved ACC scenarios

and CACC scenarios are relatively limited. For CACC, it is found that congestion is nearly solved at a 30% market penetration rate. Only some small disturbances are found at penetration rates of 30% and higher. However, it is important to note that it is assumed that all vehicles can send speed information to CACC vehicles, which means that this result might be optimistic. Shockwaves are dampened by the CACC systems, which indicates that CACC is a suitable candidate to improve traffic flow stability, which is in line with the conclusions of Milanés & Shladover (2014).

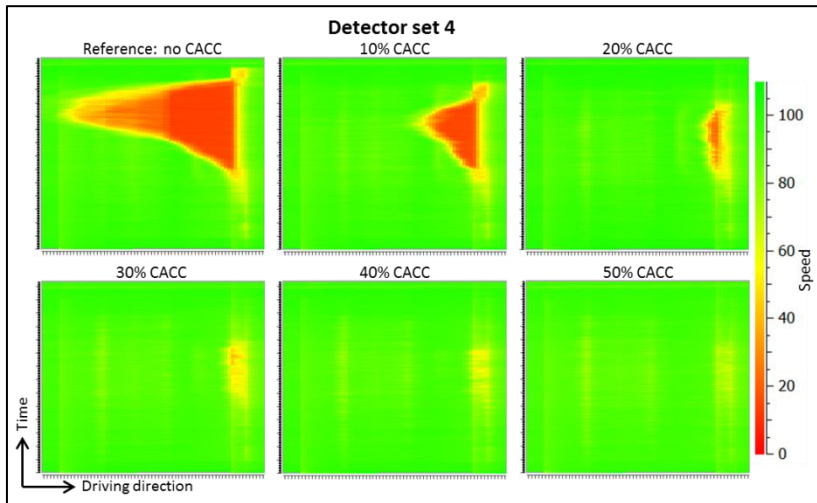


Figure 105 - Space-time diagrams for CACC scenarios at detector set 4

6.2.5 Detector set 5

The main bottleneck within this detector set is similar to detector set 4. But in this case, the spillback towards the city center of Rotterdam to the north of junction Vaanplein is considered. The congestion front considered in this detector set was one of the important congestion fronts to include in the calibration. The congestion is predominantly caused by lane-changing maneuvers and extreme braking actions as results of downhill road sections and an on-ramp. The length of the on-ramp where the congestion sets in is approximately 200 meters. When running the scenarios, it was found that the tail of congestion was not fully included in the figures of the reference scenario, which indicates that there might be more spillback than the current space-time diagrams suggest, although the amount of vehicles waiting to enter the network is low. In reality, some spillback could be expected into the city and lower level roads and at the nearest intersections with traffic lights. However, these areas fall outside of the scope of this research. The last road section included in this detector set is a lower level road of three lanes with a speed limit of 50 km/h. Although it is important to keep these notes on the lower level traffic network in mind, the effects of (C)ACC systems on traffic flow on the considered highways will hardly be influenced by it.

6.2.5.1 ACC

Figure 106 provides the space-time diagrams for scenarios with increasing percentages of ACC for detector set 5. It can be found that the differences between the reference scenarios and the 20% ACC scenario are relatively small. For scenarios with 30% ACC and more, some improvements are found. However, the congestion is not relieved in any of the simulated scenarios, although the congestion is significantly decreased in the 50% ACC scenario. This indicates that the introduction of ACC only has a small, but positive effect on this bottleneck (VanderWerf et al., 2002). The explanation for the decrease in congestion is that the braking rates applied by ACC systems are smaller, which has a stabilizing effect. Additionally, vehicles equipped with ACC apply a larger following distance, which increases the possibilities to merge for the on-ramp traffic. These reasons together ensure that the shockwaves caused by braking actions occur less frequently and are less severe.

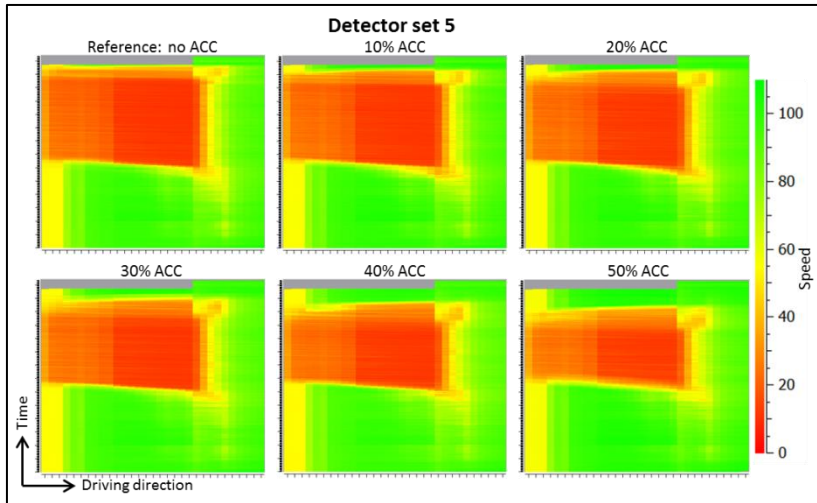


Figure 106 - Space-time diagrams for ACC scenarios at detector set 5

6.2.5.2 Newer ACC

In *Figure 107*, the space-time diagrams for the scenarios with increasing market penetration rates of newer ACC at detector set 5 can be found. The newer ACC systems clearly have a positive effect on the prevention of congestion at this bottleneck. The difference with the ACC vehicle type is that the reaction time of newer ACC vehicles is reduced to 0.4 seconds. Up until 20% newer ACC, the congestion is still quite severe, while the congestion decreases faster between 30% and 50% newer ACC scenarios, contradicting the findings that ACC can only have small effects on traffic flow (van Arem et al., 2006; VanderWerf et al., 2002). The studies that indicates that ACC has no or only a small effect only takes into account single lane capacities (VanderWerf et al., 2002) or a reduction in the number of lanes (van Arem et al., 2006), but do not take into account severe braking actions or on-ramp traffic. The congestion is nearly solved in the 40% and 50% newer ACC scenarios. From *Figure 106* and *Figure 107* can be concluded that increases or decreases in reaction times of ACC systems have a significant effect on traffic flow performance and congestion on these types of bottlenecks.

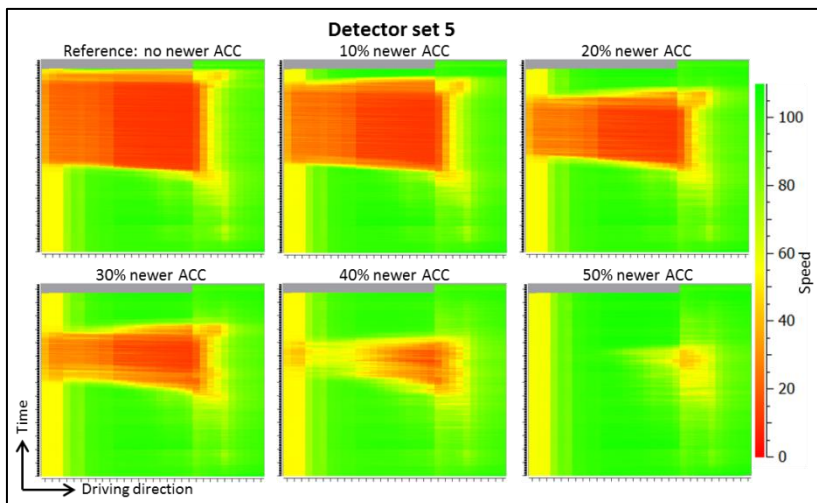


Figure 107 - Space-time diagrams for newer ACC scenarios at detector set 5

6.2.5.3 Improved ACC

Space-time diagrams for the improved ACC scenarios at detector set 5 are shown in *Figure 108*. It can be concluded that improved ACC systems are able to decrease the amount of congestion found at this

detector set. In comparison with the newer ACC systems (Figure 107), the traffic flow performance has been improved. However, the differences are smaller than the differences between ACC and newer ACC, which indicates that reducing reaction time is more effective to decrease the congestion than reductions in headways. Clearly, the improved version of ACC is able to solve the congestion at this location for 50% penetration rates. This indicates that ACC can already be an effective means to increase traffic flow stability, contradicting the results of Milanés & Shladover (2014), where the string stability is tested for changing leading vehicles speeds between 25 and 30 meters per second. However, in this situation, not only car-following behavior plays a role, but also extreme braking actions and lane-changing behavior.

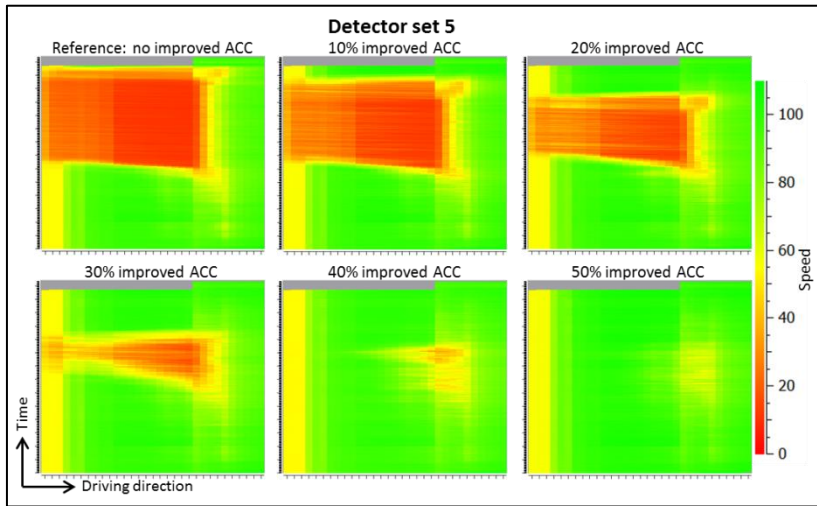


Figure 108 - Space-time diagrams for improved ACC scenarios at detector set 5

6.2.5.4 CACC

Space-time diagrams for scenarios with increased percentages of CACC are shown in Figure 109. For the 10% CACC scenario, the space-time diagram is very similar to the space-time diagram for improved ACC (Figure 108). However, the congestion is solved faster in the CACC scenarios. The congestion is more or less solved from CACC penetration rates of 30% or higher. This indicates that CACC is an effective means to improve traffic flow stability (Milanés & Shladover, 2014) at this bottleneck. Even at relatively low equipment percentages, increases were found if all other vehicles are able to send speed information to CACC vehicles.

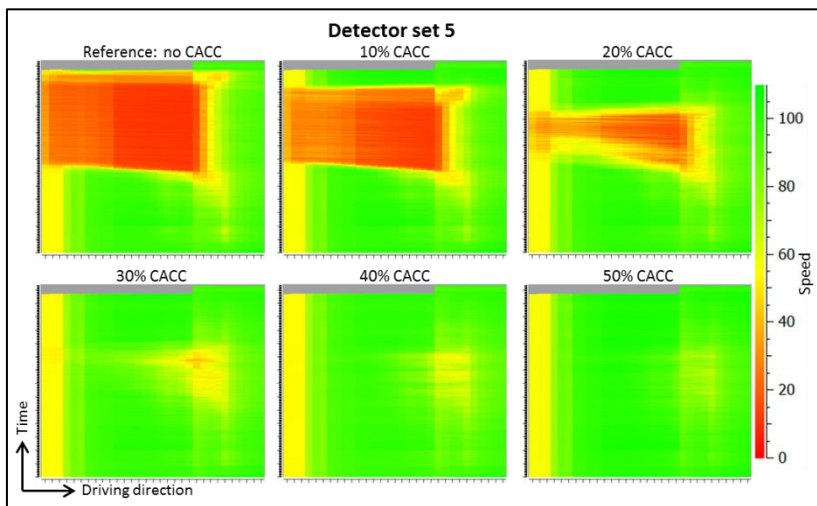


Figure 109 - Space-time diagrams for CACC scenarios at detector set 5

6.2.6 Detector set 6

The main bottleneck within this detector set is a reduction of lanes from 4 to 3 lanes. This means that the capacity is reduced, which might result in congestion.

6.2.6.1 ACC

Figure 110 shows the space-time diagrams for scenarios with increasing percentages of ACC for detector set 6. Between 0% and 20% ACC no significant differences are found. For 30% ACC market penetration rates and higher, the congestion slightly increases. This increase in congestion is caused by the fact that ACC systems apply fixed following distances that are larger than the following distances human drivers apply. This means that the potential achievable throughput decreases when the ACC percentage increases. The effects found for percentages higher than 20% ACC shows similarities with the results on capacity of AACC vehicles with time gaps of 1.55 seconds found in a study on single lane capacity (VanderWerf et al., 2002). Although small disturbances are found for ACC penetration rates higher than 20%, serious congestion does not yet occur, which means that the capacity limit is not reached yet.

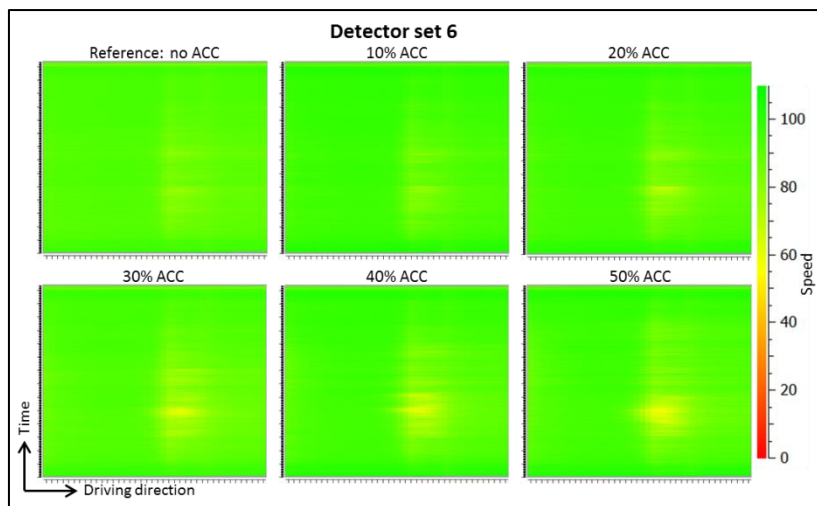


Figure 110 - Space-time diagrams for ACC scenarios at detector set 6

6.2.6.2 Newer ACC

Figure 111 shows space-time diagrams for increasing penetration rates of newer ACC at detector set 6.

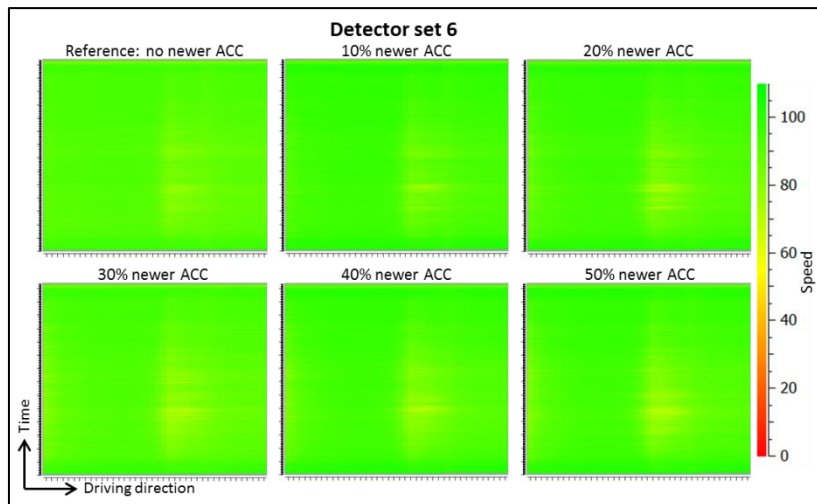


Figure 111 - Space-time diagrams for newer ACC scenarios at detector set 6

For this type of ACC, no significant effects found for increasing market penetration rates. A very small, but negligible decrease in average speeds could be found. The conclusion that ACC has a negligible effect on traffic flow is also supported by several other studies (van Arem et al., 2006; VanderWerf et al., 2002).

6.2.6.3 Improved ACC

Space-time diagrams for scenarios with increasing percentages of improved ACC are given in *Figure 112*. For the improved ACC scenarios, no clear differences are found. Again, this type of ACC does not have a significant effect on the traffic situation at this location. The conclusion that ACC has a negligible effect on traffic flow is supported by several other studies (van Arem et al., 2006; VanderWerf et al., 2002).

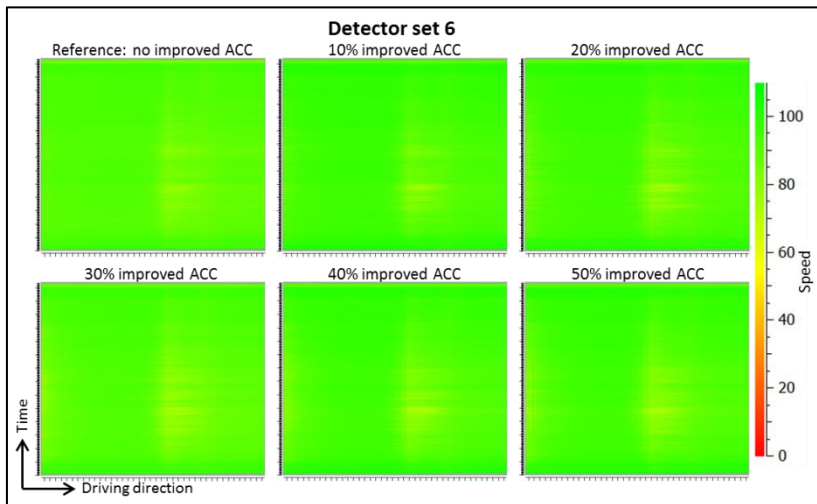


Figure 112 - Space-time diagrams for improved ACC scenarios at detector set 6

6.2.6.4 CACC

Space-time diagrams for CACC scenarios at detector set 6 are given in *Figure 113*.

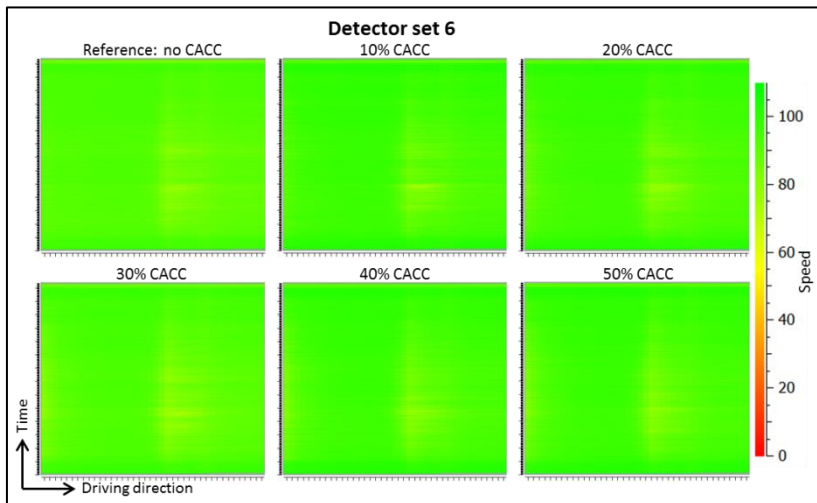


Figure 113 - Space-time diagrams for CACC scenarios at detector set 6

No extra disturbances are found as a result of increasing penetration rates of CACC. However, the only conclusion that can be drawn is that CACC does not deteriorate the traffic situation at this bottleneck. It is likely that the CACC vehicles will improve the traffic flow at this bottleneck, but this could not be stated with certainty, because no disturbances can be found in the reference scenario for at this location.

6.2.7 Detector set 7

The main bottleneck within this detector set is a weaving section of approximately 650 meters, which connects the main stream with the parallel stream. Congestion is expected somewhere on the weaving section (main stream) and spilling back towards the parallel stream again, as a result of a relatively high traffic demand traveling towards the downstream parallel stream, while the connector between main and parallel stream (both upstream and downstream) consists of a single lane.

6.2.7.1 ACC

Figure 114 provides the space-time diagrams for scenarios with increasing percentages of ACC at detector set 7. From 30% ACC and higher, congestion sets in as a result of the increased headways of ACC systems in comparison with human drivers. This is in line with the single lane capacity results found by VanderWerf et al. (2002), where increases are found for 20% ACC penetration rates, while higher penetration rates result in decreases of capacity. In Figure 114, the capacity limit is reached when the ACC percentage increases to 50%, because a significant increase in congestion is found for this scenario.

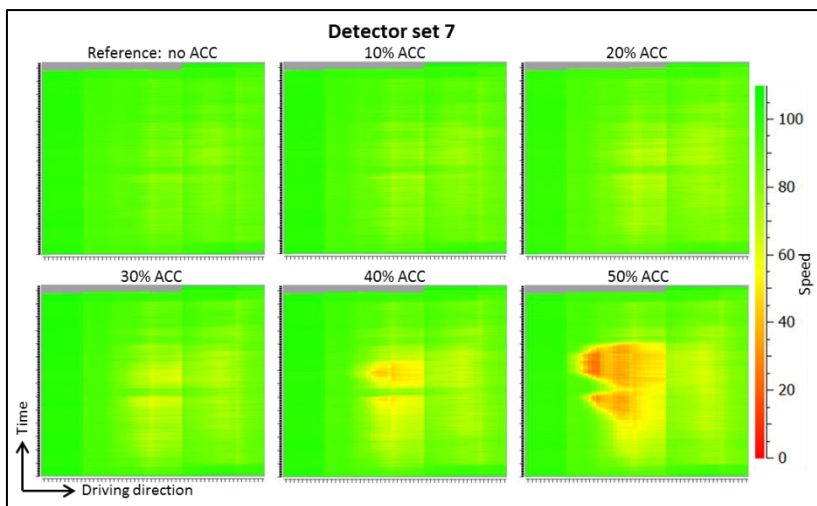


Figure 114 - Space-time diagrams for ACC scenarios at detector set 7

6.2.7.2 Newer ACC

Space-time diagrams for increasing market penetration rates of newer ACC are visualized in Figure 115.

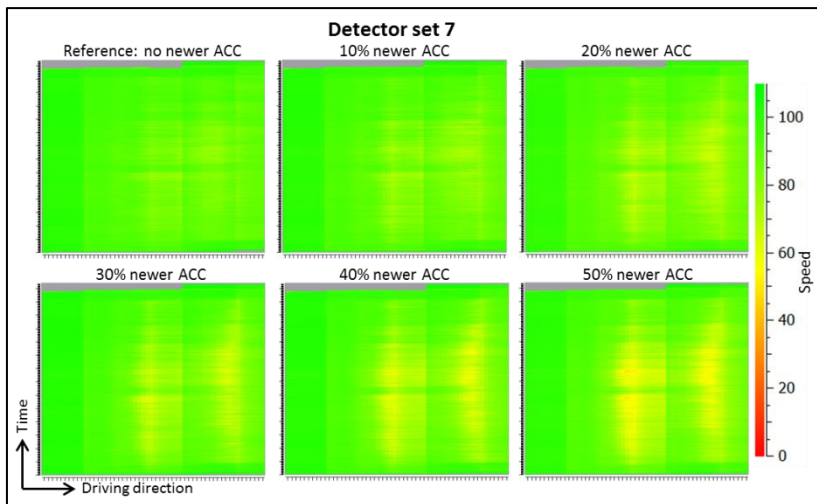


Figure 115 - Space-time diagrams for newer ACC scenarios at detector set 7

In comparison with the space-time diagrams for ACC (*Figure 114*), an improvement is witnessed for higher penetration rates. Although average speeds are generally reducing for increasing market penetration rates of newer ACC, the capacity limit is not reached in the 50% newer ACC scenario.

6.2.7.3 Improved ACC

Space-time diagrams for the improved ACC scenarios at detector set 7 are provided in *Figure 116*. When these space-time diagrams are compared with those of the newer ACC scenarios (*Figure 115*), no clear differences can be found, which indicates that the headway settings have a smaller impact on traffic flow on these types of bottlenecks than the reaction time settings. However, reductions in reaction time also influence the car-following behavior in Aimsun and thus indirectly have an impact on the headway applied. The effects of improved ACC on the traffic situation at this bottleneck are negative and small.

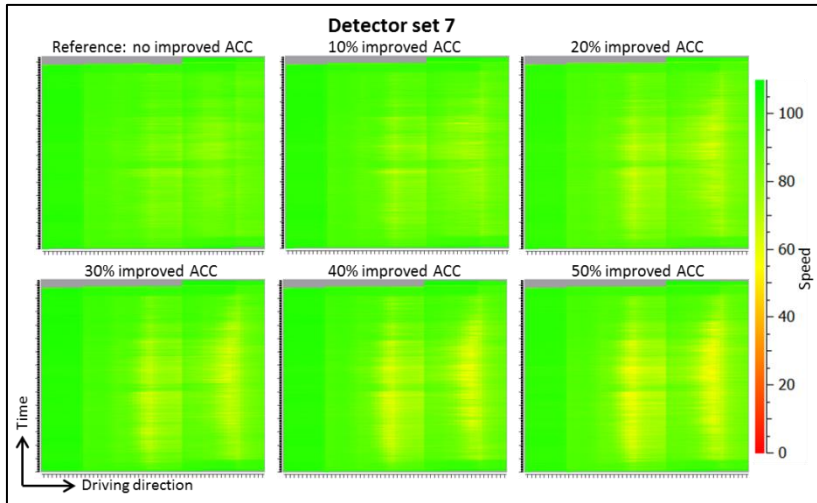


Figure 116 - Space-time diagrams for improved ACC scenarios at detector set 7

6.2.7.4 CACC

Space-time diagrams for the CACC scenarios at detector set 7 are provided in *Figure 117*.

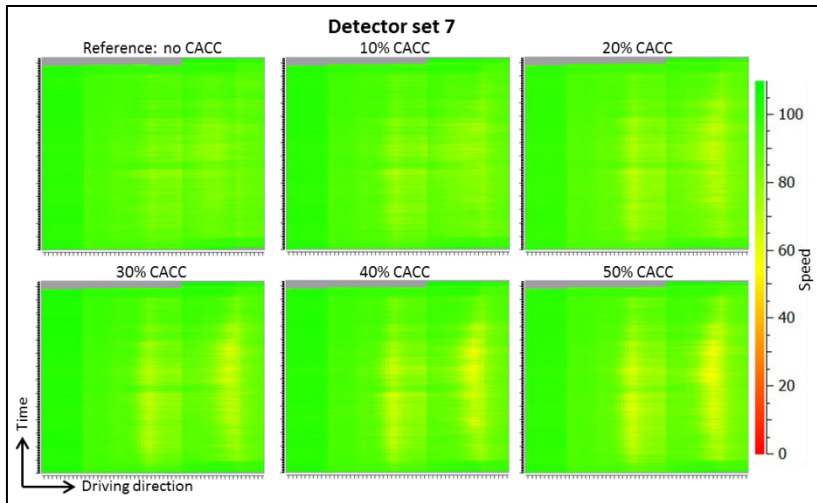


Figure 117 - Space-time diagrams for CACC scenarios at detector set 7

Similar to the ACC scenarios, deteriorations in the traffic situation are found for increasing market shares of CACC. The setting of the fixed headway seems to be the reason for the deterioration. This headway

setting plays an important role in the lane-changing behavior, which means that both ACC and CACC vehicles do not accept some gaps human drivers might accept and following vehicles with ACC or CACC systems will adapt their speeds, based on vehicles merging closely in front of the own vehicle.

6.2.8 Detector set 8

The main bottleneck within this detector set is a weaving section of approximately 850 meters, connecting the main road with the parallel road both upstream and downstream. Congestion is expected somewhere on the weaving section (main stream) and spilling back towards the parallel stream again, as a result of a relatively high traffic demand traveling towards the downstream parallel road, while the connection between main and parallel roads consists of a single lane both upstream and downstream. Congestion could occur if the capacity limit of the connection between the main road and downstream parallel road is reached or as a result of lane-changing behavior.

6.2.8.1 ACC

Figure 118 provides the space-time diagrams for scenarios with increasing percentages of ACC for detector set 8.

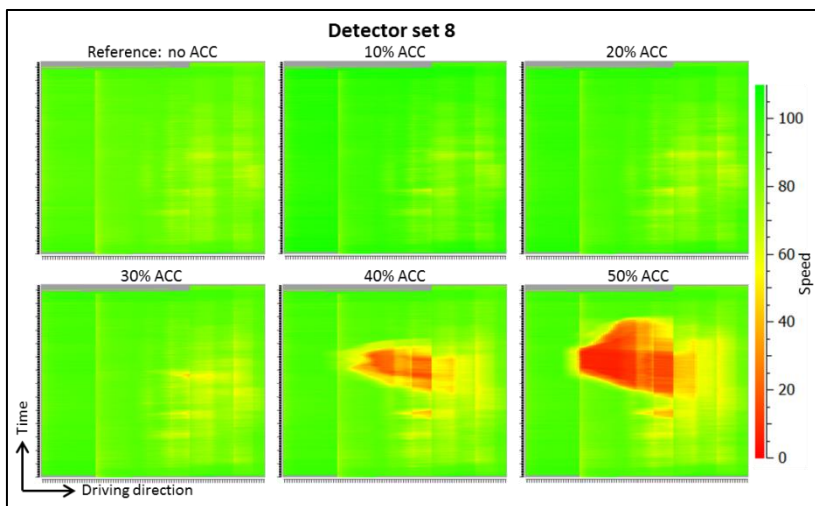


Figure 118 - Space-time diagrams for ACC scenarios at detector set 8

Between 0% and 20%, the differences between the space-time diagrams are negligible. For 30% penetration rates of ACC, small deteriorations are found. At 40% penetration rates, congestion occurs. The combination of the capacity limit of the connecting link and the lane-changing behavior of vehicles are the main reasons for the occurrence of congestion. For the 40% and 50% market penetration rate, the increase in congestion is significant.

6.2.8.2 Newer ACC

Space-time diagrams for increasing market penetration rates of newer ACC for detector set 8 are visualized in Figure 119. In comparison with the space-time diagrams for ACC (Figure 118), a significant improvement is witnessed for higher penetration rates. This improvement is caused by the reductions in reaction time for newer ACC. This suggests that the lane-changing behavior drastically improves when the ACC vehicles react faster. Additionally, the capacity limit of the connecting link is not reached, because newer ACC users are also able to drive at somewhat shorter headways in Aimsun, since the restriction of the V_b component are lowered as a result of the reduced reaction time. For increasing rates of newer ACC, only small speed reductions and disturbances are found for this detector set, but the capacity limit is not reached. This indicates that this type of ACC only has a small (but negative) effect (van Arem et al., 2006).

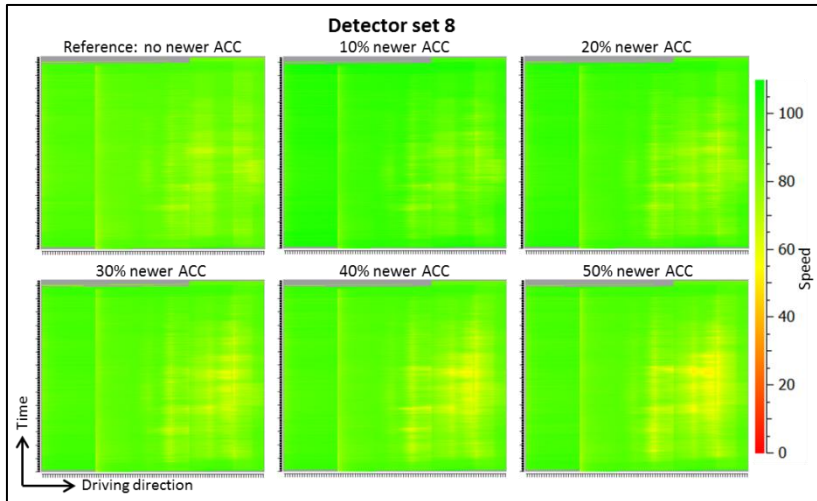


Figure 119 - Space-time diagrams for newer ACC scenarios at detector set 8

6.2.8.3 Improved ACC

Space-time diagrams for the improved ACC scenarios at detector set 8 are provided in Figure 120.

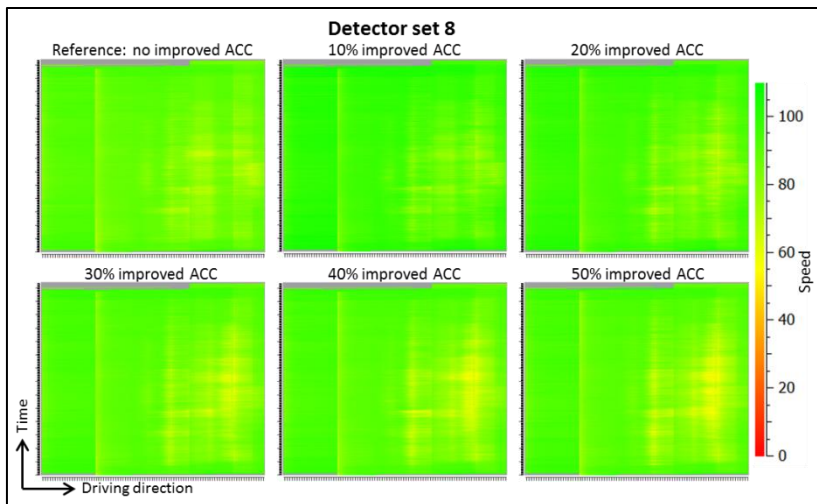


Figure 120 - Space-time diagrams for improved ACC scenarios at detector set 8

When these space-time diagrams are compared with those of the newer ACC scenarios (Figure 119), no clear differences can be found, which indicates that the headway settings have a smaller impact than the reaction time settings. The headway settings only seem to have a negligible impact. The effects of improved ACC on the traffic situation at this bottleneck are small, but negative, since speed disturbances increase for increasing market penetration rates of improved ACC.

6.2.8.4 CACC

Space-time diagrams for detector set 8 with scenarios of differing market penetration rates of CACC are given in Figure 121. Similar to the ACC scenarios, deteriorations in the traffic situation are found in the CACC scenarios. The setting of the fixed headway seems to be the most important reason for the deteriorations. Headway settings play an important role in the lane-changing behavior, meaning that both ACC and CACC vehicles do not accept some gaps human drivers will accept. Also, following vehicles with (C)ACC systems will adapt speed based on vehicles merging closely in front of the own vehicle.

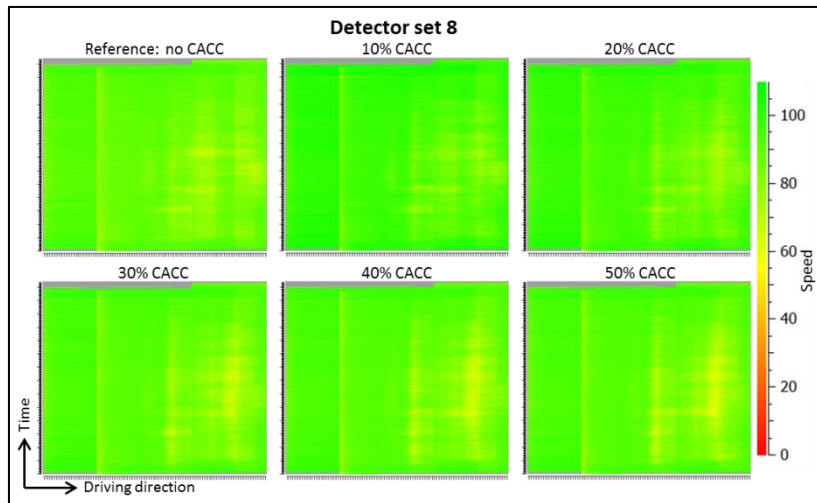


Figure 121 - Space-time diagrams for CACC scenarios at detector set 8

6.2.9 Detector set 9

The main bottleneck here is a short on-ramp of approximately 150 meters towards a 3-lane highway. The combination of the maximum capacity and merging behavior of on-ramp traffic might lead to congestion.

6.2.9.1 ACC

Figure 122 provides the space-time diagrams for scenarios with increasing percentages of ACC.

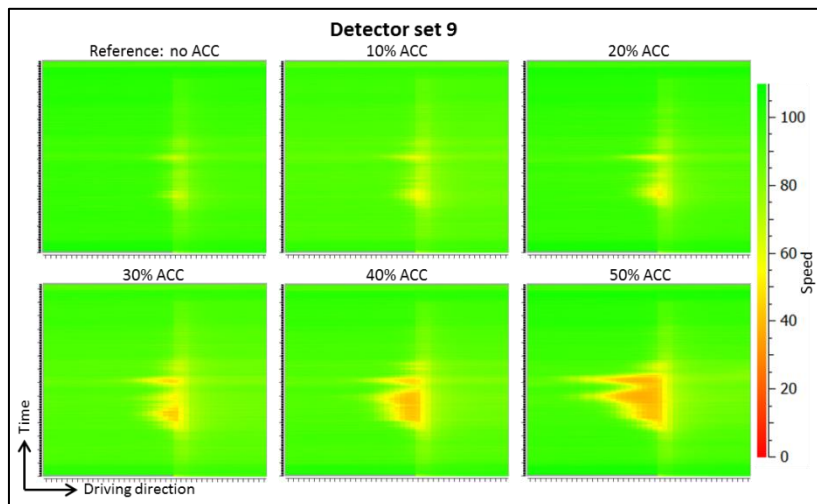


Figure 122 - Space-time diagrams for ACC scenarios at detector set 9

Between 0% and 20% ACC market penetration, the differences between the space-time diagrams are negligible. For higher penetration rates of ACC, the congestion gradually increases as a result of the larger headways of ACC vehicles, which means that the potential capacity reduces, the amount of acceptable gaps reduces and extra braking actions might be used to adapt to the defined headway.

6.2.9.2 Newer ACC

Space-time diagrams for increasing market penetration rates of newer ACC are shown in Figure 123. In comparison with the space-time diagrams for ACC (Figure 122), a significant improvement is found at higher penetration rates, which is caused by the reductions in reaction time. Small deteriorations in terms of traffic speeds are found for increasing percentages of newer ACC.

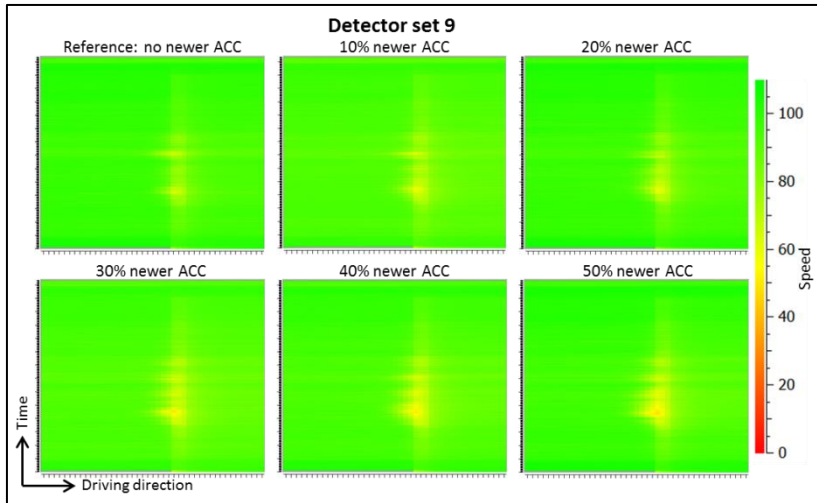


Figure 123 - Space-time diagrams for newer ACC scenarios at detector set 9

6.2.9.3 Improved ACC

Space-time diagrams for scenarios with increasing percentages of improved ACC are given in Figure 124.

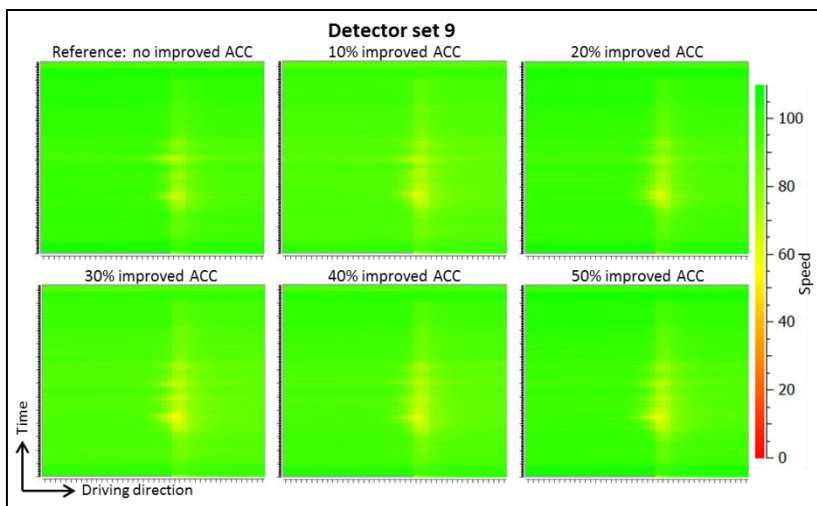


Figure 124 - Space-time diagrams for improved ACC scenarios at detector set 9

When these space-time diagrams are compared with those of the newer ACC scenarios (Figure 123), only small differences can be found, which indicates that the headway settings have a smaller impact than the reaction time settings. Regarding the space-time diagrams of the improved ACC penetration rates, no clear differences are found between the reference scenario and 50% improved ACC scenario. This indicates that this type of ACC has no effects on traffic flow performance, as was also found in several other studies (van Arem et al., 2006; VanderWerf et al., 2002).

6.2.9.4 CACC

Space-time diagrams for scenarios with differing market penetration rates of CACC for detector set 9 are given in Figure 125. Contrary to the ACC scenarios, very small improvements in traffic flow are found for increasing percentages of CACC at this bottleneck, indicating that the introduction of CACC systems in vehicles results in a reduction of congestion or disturbances at this bottleneck. However, the improvement found at this bottleneck is only small, because the reference scenario only showed some small disturbances. Because of this finding, one could not clearly state that introducing CACC has a clear

positive effect. On the other hand, it could be stated that increasing the market penetration rate does not have a negative effect on traffic flow performance at this bottleneck location. This effect might be reached by the combination of slightly larger headways applied in comparison with human drivers, which might provide more spaces to change lanes. Also, the reaction times of these vehicles have been reduced, enabling faster and smoother reactions to speed changes or closely merging vehicles.

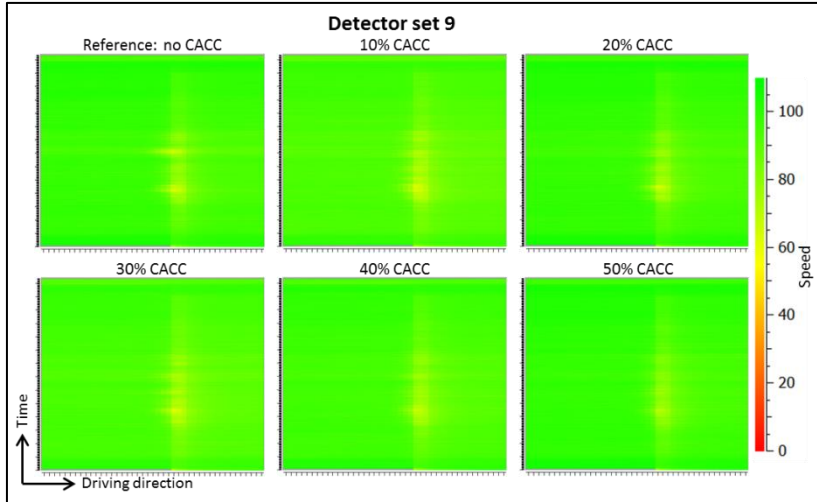


Figure 125 - Space-time diagrams for CACC scenarios at detector set 9

6.2.10 Detector set 10

This detector set consists of two weaving sections, where congestion is expected on the most upstream weaving section, which has a relatively limited length of approximately 250 meters. A capacity problem might occur on this weaving section as a consequence of high traffic demands and lane-changing behavior of drivers.

6.2.10.1 ACC

Figure 126 provides the space-time diagrams of the ACC scenarios at detector set 10.

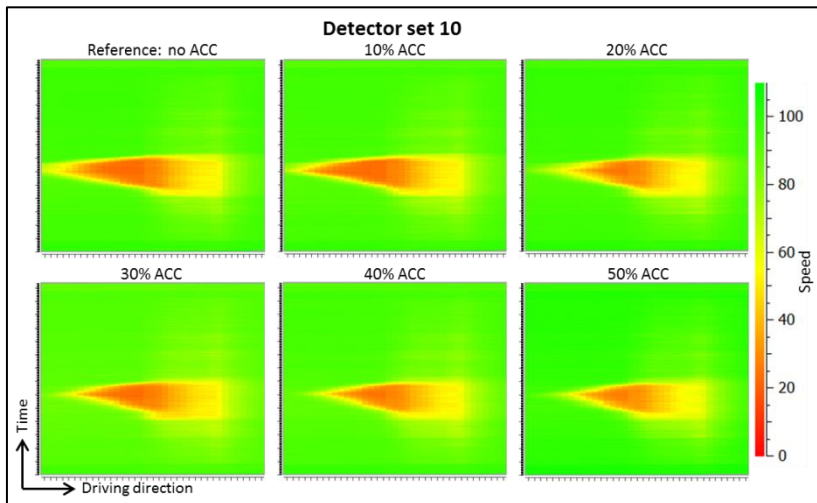


Figure 126 - Space-time diagrams for ACC scenarios at detector set 10

Very small improvements in terms of traffic flow and congestion lengths can be found for increasing percentages of ACC. This contradicts the expectation that potential capacity reduces when the penetration

rate of ACC increases. The improvement in traffic flow at this road stretch could be explained by two factors of ACC vehicles. First, lower accelerations and decelerations of ACC vehicles in comparison with human drivers might decrease the shockwave effects. Second, the larger headway settings of ACC vehicles provide more acceptable gaps on-ramp traffic. This might be important, since weaving requires many lane changes. Congestion occurs as results of lane-changing behavior and a high traffic demand.

6.2.10.2 Newer ACC

Space-time diagrams for increasing market penetration rates of newer ACC at detector set 10 are shown in *Figure 127*. Compared with the space-time diagrams for ACC (*Figure 126*), a significant improvement is found for newer ACC systems. Between the reference and 10% newer ACC scenarios, congestion reduced significantly. For newer ACC market shares of 30% and higher, no serious jam fronts are formed. These results correspond to the results of Davis (2004), who suggested that concentrations of 10% ACC were not sufficient to prevent traffic jams, while traffic jams can be suppressed by concentrations of 20%.

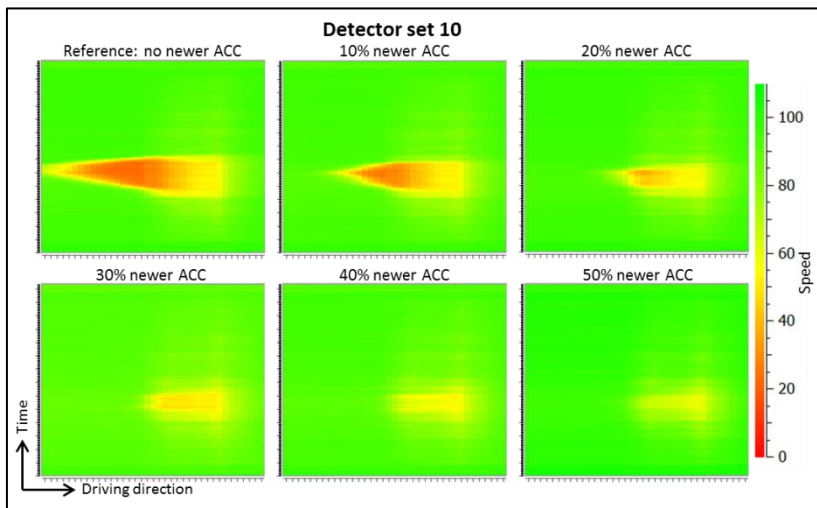


Figure 127 - Space-time diagrams for newer ACC scenarios at detector set 10

6.2.10.3 Improved ACC

Space-time diagrams for scenarios with increasing percentages of improved ACC are given in *Figure 128*.

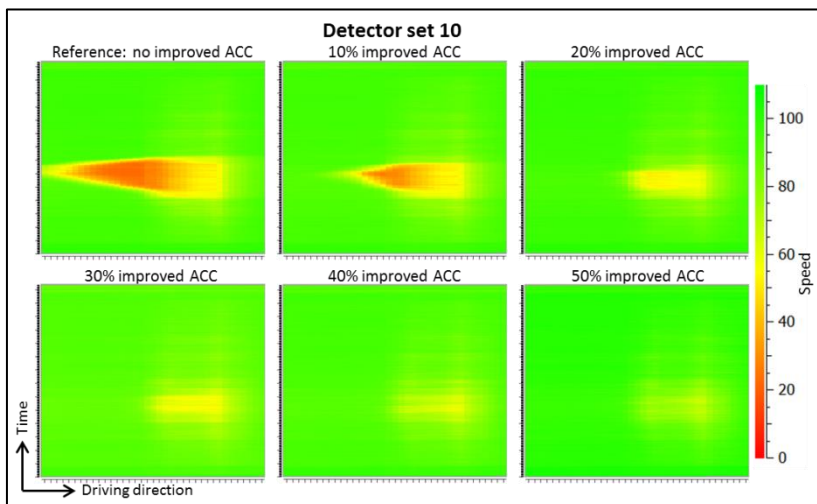


Figure 128 - Space-time diagrams for improved ACC scenarios at detector set 10

When these space-time diagrams are compared with the newer ACC scenarios (*Figure 127*), some gains as a result of the reduction in headway settings are found. The 30% newer ACC and 20% improved ACC scenario are similar. Reductions in headway settings lead to an increase in the amount of acceptable gaps for improved ACC vehicles to merge into, which means that making a lane change will become easier for this group of vehicles, while keeping the advantages of the smaller reaction times. Overall, increasing the market shares of improved ACC improves traffic flow at this bottleneck. Concentrations of 20% improved ACC and higher seem to suppress traffic jams, as was also indicated by Davis (2004).

6.2.10.4 CACC

Space-time diagrams for the CACC scenarios at detector set 10 are provided in *Figure 129*. Similar to the ACC scenarios, improvements in traffic flow are obtained for increasing rates of CACC. The improvements for CACC systems are larger than those for the different ACC systems simulated, as a result of the reduced reaction time and headway settings. The biggest improvements are found at low penetration rates, which is in contradiction with the results found by van Arem et al. (2006). However, this difference can be explained by the assumption that all other vehicles are able to send speed information to the CACC vehicles. For market penetration rates of 20% CACC or higher, there is no sign of congestion.

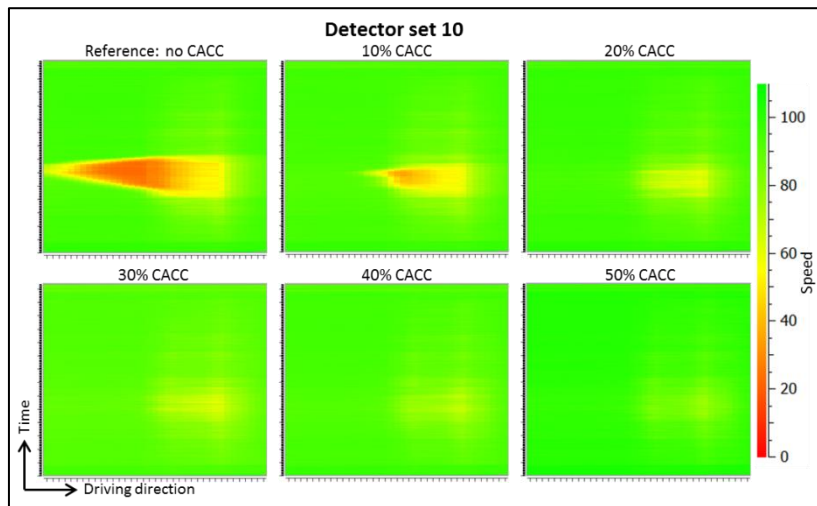


Figure 129 - Space-time diagrams for CACC scenarios at detector set 10

6.2.11 Overview of effects of ACC and CACC per bottleneck type

The detector sets and space time diagrams discussed contain different bottleneck types. This subsection gives a wrap-up of the effects found per bottleneck type. The following bottleneck types are discussed:

- **Extreme braking:** This bottleneck type consists of an on-ramp, which is a potential bottleneck on itself, and a downhill slope, where extreme braking might be applied to adjust following distances. The combination of lane-changing behavior and extreme braking could be seen as the most important reasons for congestion. Detector sets 4 and 5 are examples of this bottleneck type;
- **Lane drop:** A characteristic for this bottleneck is a decrease in the number of lanes, which could become a capacity problem and cause of congestion. This type is found in detector set 6;
- **On-ramp:** This type of bottleneck consists of on-ramps where congestion might occur as a result of short on-ramp lengths or high traffic demands. Detector sets 2 and 9 are considered in this bottleneck type. Please note that detector sets 4 and 5 could also be in this category, but these detector sets are not included in this category, because these are already in another category;
- **Weaving section:** This bottleneck type consists of weaving sections, where merging behavior plays an important role. Additionally, congestion is often found at weaving sections due to this merging behavior. This category includes detector sets 1, 3, 7, 8 and 10.

6.2.11.1 Effects of ACC and CACC on bottlenecks with extreme braking

In this subsection, a brief overview of the effects of ACC and CACC on bottlenecks with extreme braking is given. *Table 14* shows the effects for the corresponding detector sets and vehicle types. In order to give an indication of the effects of all the ACC types, a small comment on the space-time diagram of the 50% scenario is also included.

Table 14 - Overview of effects of (C)ACC on bottlenecks with extreme braking

	Detector set 4	Detector set 5
ACC	Positive effect, congestion in 50% scenario	Positive effect, serious congestion in 50% scenario
Newer ACC	Positive effect, disturbances in 50% scenario	Positive effect, small disturbances in 50% scenario
Improved ACC	Positive effect, small disturbances in 50% scenario	Positive effect, negligible disturbances in 50% scenario
CACC	Positive effect, no to negligible disturbances in 50% scenario	Positive effect, no to negligible disturbances in 50% scenario

Overall, all the ACC and CACC vehicle types have positive effects on bottlenecks where congestion is partly caused by extreme braking rates. This effect can be explained by the fact the ACC and CACC systems apply lower braking rates and have smaller reaction times. Additionally, more sophisticated versions of ACC show more positive effects. Concluding, ACC and CACC systems can solve congestion that occurs as a consequence of severe braking or excessive braking actions by manual drivers. However, it should be noted that the simulation ensures safe behavior, while this might not be true in reality.

6.2.11.2 Effects of ACC and CACC on lane drop bottlenecks

Here, a brief overview is given of the effects of ACC and CACC on lane drops. *Table 15* shows the effects for detector set 6 and the simulated vehicle types. In order to give an indication of the effects of all the ACC types, a small comment on the space-time diagram of the 50% scenario is included.

Table 15 - Overview of effects of (C)ACC on bottlenecks with a lane drop

	Detector set 6
ACC	Negative effect, some disturbances in 50% scenario
Newer ACC	Negligible negative effect, very small disturbances in 50% scenario
Improved ACC	No clear effect, no to negligible disturbances in 50% scenario
CACC	No clear effect, no to negligible disturbances in 50% scenario

In this study, it is concluded that ACC systems have no or a negative effect on lane drop situations, which could act as a capacity bottleneck. The newer ACC types showed very small negative effects, but do not show serious congestion in the 50% scenario. When improved ACC and CACC market shares increase, no effects were found, which indicates that it does not have a negative effect in terms of capacity. This result is also in line with the expectations, because larger headways result in lower potential capacities. Since this conclusion is based on a single detector set, these conclusions should be interpreted with care.

6.2.11.3 Effects of ACC and CACC on on-ramp bottlenecks

An overview is given of the effects of ACC and CACC on on-ramp bottlenecks, where congestion could occur as a result of merging behavior, high traffic demands or limited on-ramp lengths. *Table 16* shows the effects for the two corresponding detector sets and the simulated (C)ACC vehicle types. Small notes on the space-time diagram of the 50% scenarios are included, to indicate the effects of (C)ACC.

Both detector sets show negative effects for ACC and newer ACC. This is probably caused by the relatively large following distances of these systems, which might result in braking actions shortly after merging maneuvers, causing disturbances or congestion. Increasing penetration rates of improved ACC do not seem to have a significant influence on these bottlenecks, while CACC systems show positive

effects. When headways and reaction times of (C)ACC systems are reduced, the traffic situation near on-ramps is found to improve and disturbances are limited.

Table 16 - Overview of effects of (C)ACC on on-ramp bottlenecks

	Detector set 2	Detector set 9
ACC	Negative effect, some congestion in 50% scenario	Negative effect, serious congestion in 50% scenario
Newer ACC	Small negative effect, some disturbances in 50% scenario	Negative effect, increased disturbances in 50% scenario
Improved ACC	No clear effect, 50% scenario is similar to reference scenario	No clear effect, 50% scenario is similar to reference scenario
CACC	Positive effect, 50% scenario shows no significant disturbances	Positive effect, 50% scenario shows negligible disturbances

6.2.11.4 Effects of ACC and CACC on weaving sections

This subsection provides an overview of the effects of ACC and CACC vehicles on weaving sections. Table 17 explains the overall effects for the corresponding detector sets and vehicle types. In order to give an indication of the effects of all the ACC types, a small comment on the space-time diagram of the 50% scenario is included.

Table 17 - Overview of effects of (C)ACC on weaving sections

	Detector set 1	Detector set 3	Detector set 7	Detector set 8	Detector set 10
ACC	Negative effect, very small disturbances in 50% scenario	Negative effect, increase of congestion duration in 50% scenario	Negative effect, serious congestion in 50% scenario	Negative effect, serious congestion in 50% scenario	Small positive effect, serious congestion in 50% scenario
Newer ACC	Negative effect, small disturbances in 50% scenario	Positive effect, small decrease of congestion duration in 50% scenario	Negative effect, disturbances in 50% scenario	Negative effect, disturbances in 50% scenario	Positive effect, small disturbances in 50% scenario
Improved ACC	Negative effect, disturbances in 50% scenario	Positive effect, decrease of congestion duration in 50% scenario	Negative effect, small disturbances in 50% scenario	Negative effect, disturbances in 50% scenario	Positive effect, very small disturbances in 50% scenario
CACC	Negative effect, small disturbances in 50% scenario	Positive effect, decrease of congestion duration and length in 50% scenario	Negative effect, small disturbances in 50% scenario	Negative effect, small disturbances in 50% scenario	Positive effect, no disturbances in 50% scenario

It could be concluded that ACC systems generally have a negative effect on a weaving section, which can be explained by the larger following distances of ACC vehicles, resulting in decreases in potential capacity. For all other ACC types, both positive and negative effects are found on weaving sections. Negative effects could be obtained as a result of braking actions to adapt to the desired time headway and the decrease in potentially achievable capacities. However, positive effects could also be obtained, as a result of the larger following distances, which allows other vehicles to merge and the lower reaction times and maximum acceleration and deceleration rates, which might stabilize traffic.

In Table 17, it seems that results might differ per type of weaving section. Detector set 1 is a relatively short weaving section, where negative effects are found as a result of increasing market penetration rates of (C)ACC. The main reason for this might be the gap settings of (C)ACC vehicles, which could limit the amount of acceptable gaps. Congestion at detector set 7 and 8 occurs as a result of lane-changing

behavior and a limited capacity on the single lane connectors between the main and parallel road. Therefore, both lane-changing behavior and capacity limits play an important role at these bottlenecks. It is found that introducing (C)ACC has a negative effect on those weaving sections with limited capacities on connecting links. At detector sets 3 and 10, the capacity of the connector or the length of the weaving section is not limited enough to form additional bottlenecks. Therefore, the congestion at these detector sets is solely caused by lane-changing behavior. Therefore, it could be concluded that at weaving sections of very limited length or weaving sections with connections with limited capacity, the effects of introducing (C)ACC are generally negative. However, for normal weaving sections that do not suffer from connections with limited capacity or limited weaving section length, the effects of increasing the market penetration rates of (C)ACC are generally positive.

6.3 Results at section level

The speeds, flows, densities and number of lane changes at section level will be discussed in this subsection. The output of six selected road sections was analyzed and filtered for interesting results and conclusions, which will be discussed in this chapter. Unimportant and insignificant effects at lane level are filtered out. First, the average number of lane changes per vehicle type is elaborated upon. Subsequently, the speed, flow and density distribution over the lanes for section 108866 are discussed.

6.3.1 Lane changes per vehicle type

As Gorter (2015) indicated, the average number of lane changes of ACC is found to be lower in comparison with the average number of lane changes manual drivers apply. To check this, the average number of lane changes per vehicle type was considered for all the different scenarios and vehicle types.

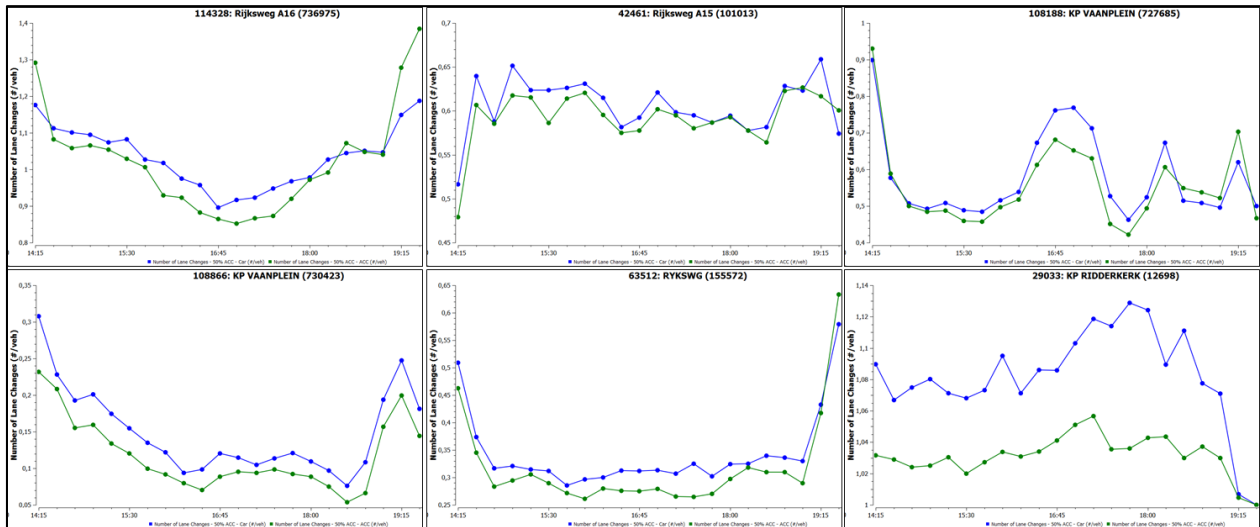


Figure 130 - Average number of lane changes of ACC (green) and car (blue) on six selected road sections

Figure 130 gives an overview of the average number of lane changes in the 50% ACC scenarios on all six selected sections for the car and ACC user class. It was chosen to select the 50% ACC scenarios, since the amount of vehicles of the different vehicle types are approximately similar in this scenario, which ensures a more reliable and fair comparison. Blue lines display the average number of lane changes for cars, while green lines indicate the average number of lane changes of ACC vehicles on the considered road section. For all selected road sections, the average numbers of lane changes are smaller for ACC vehicles. This confirms that ACC vehicles change lanes less frequently than manual drivers.

However, for newer ACC, improved ACC and CACC a different pattern with respect to the average number of lane changes on the selected sections was found. For all these types of ACC and CACC, the

average numbers of lane changes of (C)ACC users groups were generally found to be higher than those of the manual car drivers. As an example, the average number of lane changes in the 50% improved ACC scenarios of car (blue) and improved ACC (green) vehicle types are visualized in *Figure 131*. For the first four sections it is found that the average number of lane changes is higher for improved ACC. For the 5th section (i.e. weaving section), the average number of lane changes of both vehicle classes are relatively similar, while for the 6th road section, the average number of lane changes of manual car drivers is higher. Similar patterns are found for newer ACC and CACC. The differences between vehicle classes are smaller for newer ACC, but bigger for CACC. An explanation of these effects lies in the reduction of reaction time, which ensures that lane changes are increasingly possible, because minimum gaps to merge become smaller if reaction times decrease. This results in increases in the number of lane changes. As a result, the increases in the average number of lane changes are larger for systems with lower reaction times. This clearly is an effect of the simulation parameters used. If the ‘staying in overtaking lane’ tick box was selected, this effect would probably be less severe. However, this is not the full solution to this problem, since the vehicles staying in slow lanes could not be simulated by using this approach. For future research on this topic, it might be useful to add a factor that represents the willingness or threshold to perform lane-changing maneuvers.

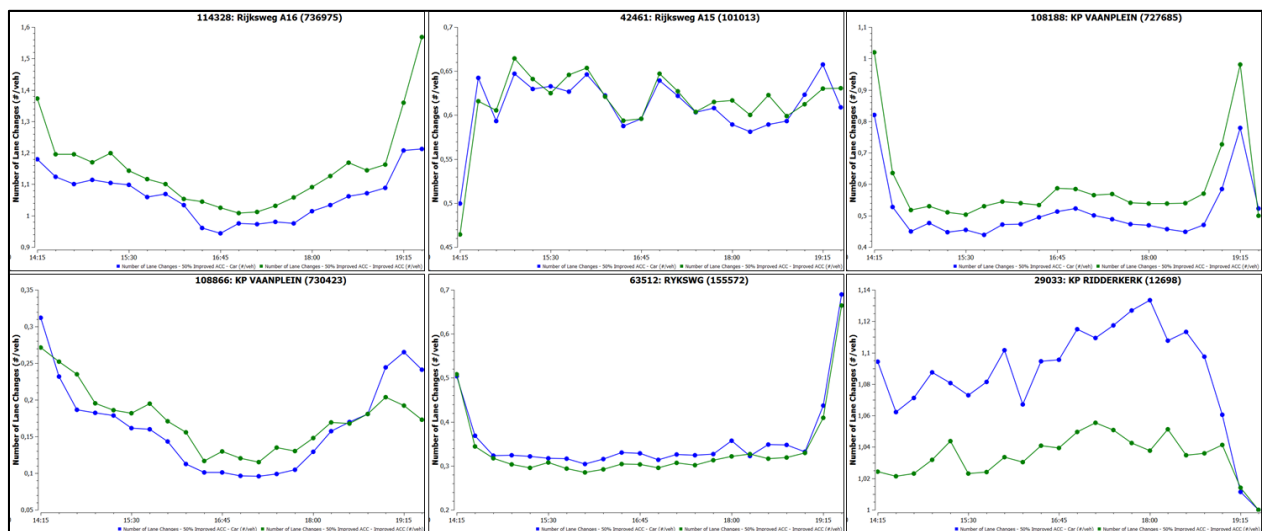


Figure 131 - Average number of lane changes of improved ACC (green) and car (blue) on six selected road sections

6.3.2 Speed differences between lanes

The speed differences between lanes were computed for all scenarios and selected sections in order to assess whether ACC and CACC have a homogenizing effect in terms of speed differences between lanes. In general, it was found that it is highly dependent on the road section layout and traffic situation on the road. Both small increases and decreases in speed differences between lanes were found as a result of increasing penetration rates of ACC or CACC. Next to the introduction of a new vehicle type, the local traffic situation might also be a reason for differences found.

However, for section 108866, which represents a road section at capacity conditions for a relatively long time period, some effects in terms of speed distributions between lanes were found, which indicates that ACC and CACC systems have a significant effect on speed distributions between lanes at road sections at capacity conditions. *Table 18* shows the average speed differences between the two lanes for all equipment scenarios. The average speed differences between the lanes are calculated as follows: First, the absolute speed difference between the two lanes is calculated per statistical time period, after which an average was computed by averaging over all the statistical time periods within simulation. This is a relatively easy method, although some information might be filtered out as a result of averaging.

Table 18 - Average speed differences between lanes on section 108866 at capacity

Average speed difference between lanes [km/h]	ACC	Newer ACC	Improved ACC	CACC
Reference scenario	2.45	2.45	2.45	2.45
10% penetration rate	2.56	2.31	2.07	1.93
20% penetration rate	2.45	2.41	2.12	1.83
30% penetration rate	2.64	2.50	1.85	1.38
40% penetration rate	2.77	2.10	1.51	1.45
50% penetration rate	2.67	1.62	1.27	1.30

In Table 18, higher penetration rates result in smaller average speed differences between lanes. This effect cannot be found for the ACC vehicle type. However, for the improved ACC and CACC a gradual decrease in speed differences between lanes could be found. With respect to the newer ACC vehicle type, this effect seems to be visible from 30% and onwards. Figure 132 illustrates the homogenizing effects on speed differences between lanes. This effect was found at this specific road section, but no clear effects were found for other road sections. Therefore, it is concluded that this effect is only found in traffic situations at or near capacity conditions. Concluding, both ACC and CACC systems have homogenizing effects on the speed differences between lanes at road sections at high traffic volumes near capacity.

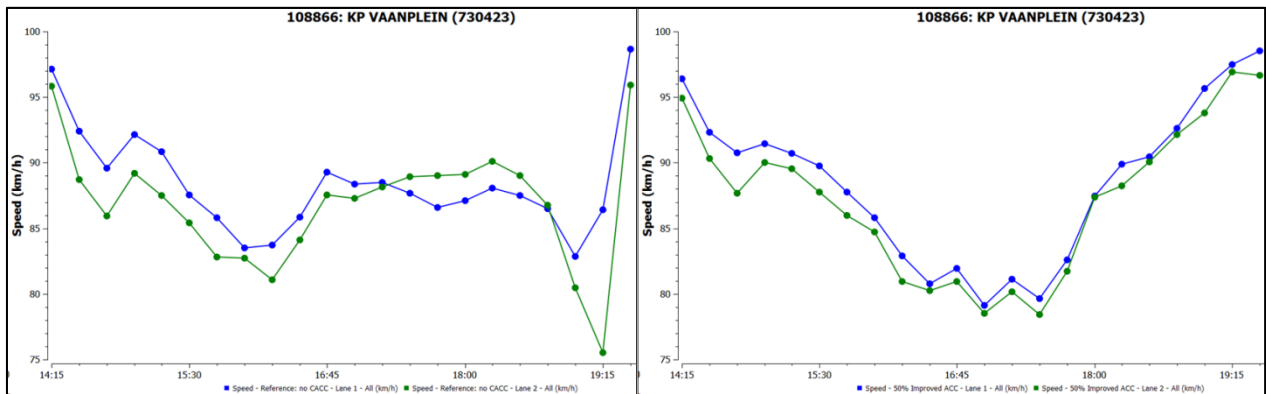


Figure 132 - Speed differences between lanes for reference and 50% improved ACC scenario on section 108866

Additionally, it was found that in free flow conditions average speeds decreased as a consequence of introducing ACC or CACC, which can be explained by the lower speed acceptance parameter of these vehicle types in comparison with the car class. Obviously, when congestion decreases as a result of increasing market penetration rates of ACC or CACC, the average speeds increased.

6.3.3 Density differences between lanes

The density differences between lanes were computed for all scenarios and selected sections in order to assess whether ACC and CACC have a homogenizing effect in terms of density differences between lanes. In general, it was found that it is highly dependent on the road section layout and traffic situation on the road. Both small increases and decreases in density differences between lanes were found as a result of increasing penetration rates of ACC or CACC. Next to the introduction of a new vehicle type, the local traffic situation might also be a reason for differences found.

For the two-lane road section at capacity (section 108866), a clear pattern was found. For the other selected road sections, no clear patterns due to increasing market penetration rates of (C)ACC were found. Both increases and decreases were found for the other road sections. Table 19 shows the average flow differences between the two lanes of section 108866 for all equipment scenarios. Average density differences between the lanes are calculated as follows: First, the absolute density difference between the two lanes is calculated per statistical time period, after which an average was computed by averaging over all the statistical time periods. The average lane densities are rounded to 2 digits. The results in Table 19

indicate that the density differences between lanes are reduced when penetration rates of (C)ACC increase. Generally, sophisticated versions of ACC gain larger improvements than older versions of ACC.

Table 19 - Average density differences between lanes on section 108866 at capacity

Average density difference between lanes [veh/km]	ACC	Newer ACC	Improved ACC	CACC
Reference scenario	4.27	4.27	4.27	4.27
10% penetration rate	4.08	3.96	3.61	3.66
20% penetration rate	3.82	3.45	3.15	2.91
30% penetration rate	3.59	2.95	2.56	2.40
40% penetration rate	3.38	2.34	2.27	2.20
50% penetration rate	3.13	2.07	1.99	2.08

The results in Table 19 indicate that ACC and CACC systems have a homogenizing effect in terms of differences in lane densities on road sections at capacity conditions. Also, Figure 133 shows a similar pattern, where it can be found that the disturbances in densities are reduced and that the differences in densities between lanes are reduced. This indicates an increase in traffic conditions with high traffic volumes as a result of increasing market penetration rates of ACC and CACC. For CACC, these effects are also expected in literature (van Arem et al., 2006).

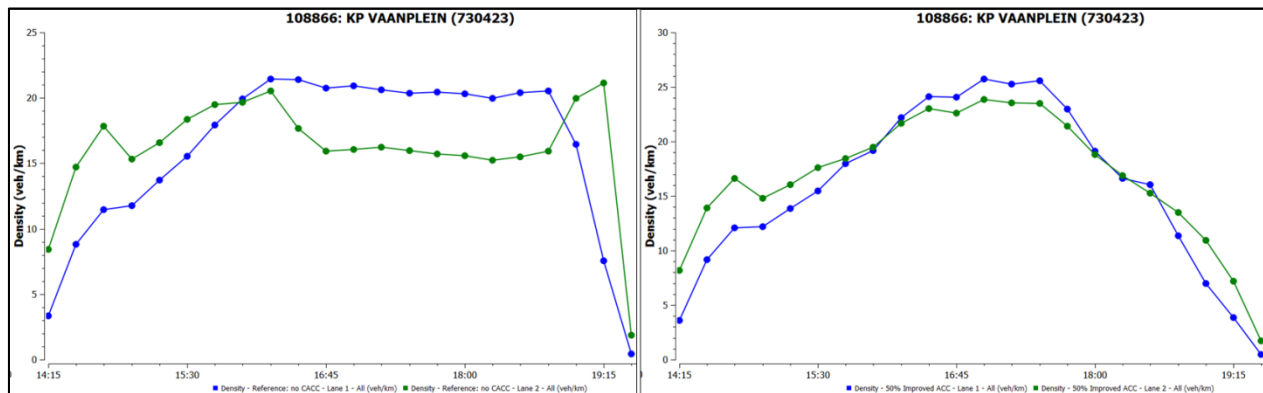


Figure 133 - Density differences between lanes for reference and 50% improved ACC scenario on section 108866

For other road sections, both small increases and decreases in differences between lane densities can be found. However, clear patterns are lacking. Therefore, the conclusion that increasing penetration rates lead to a homogenization in terms of density differences between lanes is only valid for road sections near and at capacity conditions.

6.3.4 Flow differences between lanes

The flow differences between lanes were computed for all scenarios and selected sections in order to assess whether ACC and CACC have a homogenizing effect in terms of flow differences between lanes. In general, it was found that it is highly dependent of the road section layout and traffic situation on the road. Both small increases and decreases in flow differences between lanes were found as a result of increasing penetration rates of ACC or CACC. Next to the introduction of a new vehicle type, the local traffic situation might also be a reason for differences found.

For many road sections, no clear patterns due to increasing market penetration rates of ACC or CACC were found. However, for the two-lane road section at capacity (section 108866), a clear pattern was found. Table 20 shows the average flow differences between the two lanes for all equipment scenarios. Average flow differences between the lanes are calculated as follows: First, absolute flow difference between the two lanes is calculated per statistical time period, after which an average was computed by averaging over all the statistical time periods. These averages are rounded to integer values. These

results indicate that the lane differences in flows are reduced when penetration rates of (C)ACC increase. Additionally, more sophisticated versions of ACC gain larger improvements than earlier versions of ACC.

Table 20 - Average flow differences between lanes on section 108866 at capacity

Average flow difference between lanes [veh/h]	ACC	Newer ACC	Improved ACC	CACC
Reference scenario	241	241	241	241
10% penetration rate	241	248	235	240
20% penetration rate	222	231	225	210
30% penetration rate	219	210	194	178
40% penetration rate	215	184	174	168
50% penetration rate	202	163	169	176

Figure 134 shows the flow differences between lanes for the reference scenario and the 50% improved ACC scenario. It can be concluded that the differences in flow between lanes are reduced for higher ACC penetration rates at a road section at capacity. It can be found that the traffic flow is also smoothed at higher penetration rates. Concluding, both ACC and CACC systems have homogenizing effects on the flow differences between lanes at road sections at high traffic volumes near capacity.

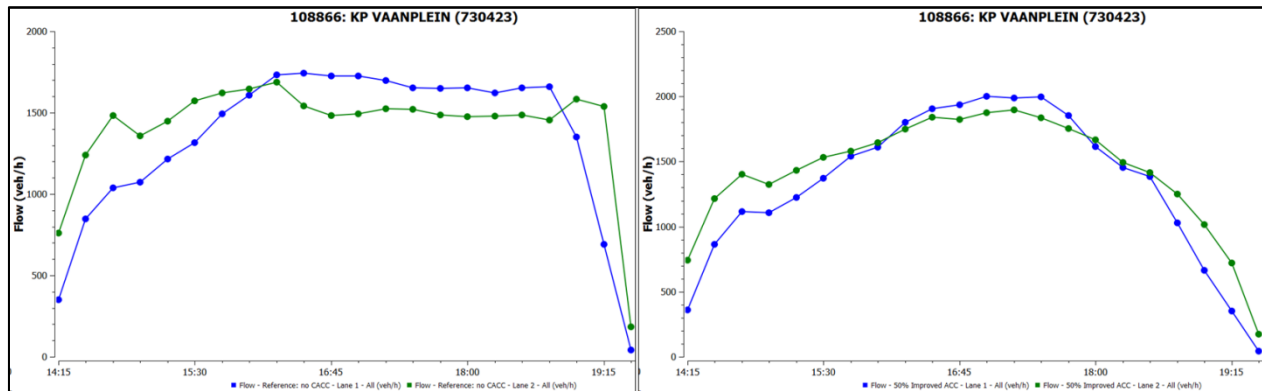


Figure 134 - Flow differences between lanes for reference and 50% improved ACC scenario on section 108866

For other road sections, no clear effects could be found. Therefore, it is concluded that this effect is only found in traffic situations at or near capacity conditions. This indicates that the main improvements in terms of homogenizing effects might be achieved in capacity conditions with high traffic volume, which is a conclusion that was also drawn in a study on the effects of CACC (van Arem et al., 2006).

7 Mesoscopic simulation

This chapter describes the process of translating the microscopic simulation results of ACC and CACC scenarios into a mesoscopic simulation, in order to find out whether it is possible to simulate similar effects as a result of increasing (C)ACC penetration rates. First, the mesoscopic parameter settings to represent the same effects of (C)ACC will be discussed. Subsequently, average results at network level will be provided for all microscopic scenarios to check whether the same patterns can be found or some effects are missing. Then, a short reflective and concluding review will be given to discuss whether the mesoscopic simulation model was able to represent microscopic simulation results, to indicate included or missing effects and to discuss the relation between microscopic and simulation input parameters.

7.1 Mesoscopic input parameters

In the mesoscopic model, there only are some parameters to change in order to describe driving behavior. Additionally, all section characteristics were already set and discussed in the calibration procedure, meaning that those mesoscopic section characteristics (jam density and reaction time factors) should not be changed at this stage of the research. The only parameters that could be changed are the mesoscopic parameters for the ACC and CACC user classes. Also, the vehicle characteristics that were already used in microscopic simulation, such as vehicle width, vehicle length, speed acceptance and maximum desired speeds, should not be changed as well. This leaves the mesoscopic reaction time and reaction time for front vehicle at traffic light and the probabilities over these reaction times as the only allowable parameters to change to represent ACC and CACC driving behavior by using mesoscopic simulations.

In order to find the corresponding input parameters for mesoscopic simulation, the average results at network level of the microscopic reference scenario and 50% market penetration scenarios of the various (C)ACC vehicle types will be used. The reference scenario is used to find initial differences in average simulation results at network level between microscopic and mesoscopic simulation. The reference scenario is constructed based on the general rule where the mesoscopic reaction time is the microscopic reaction time multiplied by 1.5, which results in a mesoscopic reaction time of 1.2 seconds for cars. As discussed in chapter 3, one of the important congestion fronts was not fully included in the mesoscopic reference scenario, while it is included in the microscopic reference scenario, which might provide differences between microscopic and mesoscopic results. The 50% equipage scenarios are used to find the best mesoscopic reaction times per (C)ACC type, based on the fit with microscopic simulation results. The 50% equipage scenarios were chosen, because the effects of (C)ACC systems should be clearer than for the other penetration rates. In subsection 7.2, the mesoscopic average results for all penetration rate scenarios will be computed and discussed. In order to have a fair comparison, the same random seeds from microscopic simulation are used (*Table 13*) for the mesoscopic simulations as well.

It is important to note that the space-time diagrams and indicators at section level are not used to reflect upon the mesoscopic simulation results. The space-time diagrams are not included, because the data computed for detectors on the same section will be exactly the same, which will only provide aggregated space-time diagrams that do not show the same level of detail as microscopic space-time diagrams. Data on the selected road sections was not included, because these would not provide additional insight in the relation between microscopic and mesoscopic modelling.

The mesoscopic input parameters used to represent (C)ACC driving behavior will be discussed per type in this subsection. The goodness of fit will be determined based on the coefficient of determination [R^2] as used previously in this report. The speed, density and delay time data will be the most important indicators to evaluate the fit. In this case, one would like to achieve a very high coefficient of determination, which indicates that the mesoscopic simulation results are similar to the microscopic simulation results. Next to the coefficient of determination, the speed, density and delay time patterns over time are also checked.

7.1.1 Mesoscopic reaction times for ACC scenarios

From subsection 6.1.1, it could be concluded that increasing penetration rates of ACC have a negative influence on delay time, speed and densities averaged over the whole network. This would indicate that the mesoscopic reaction time for ACC should be higher than the mesoscopic reaction times of the car user class (1.2 seconds). The increase in mesoscopic reaction time is needed to compensate the effects of the increased (fixed) headway and the smaller acceleration and deceleration rates.

Test simulations were performed to find out which mesoscopic parameters show corresponding results. The logic behind these tests was as follows: if the average speeds were too high, the reaction time of ACC vehicles was increased. If average speeds were too low, the reaction time of ACC vehicles was decreased. It was found that an ACC reaction time of 1.5 seconds provided the best fit with the microscopic scenario with 50% ACC. Additionally, the reaction time at traffic light was set to 2.1 seconds (0.1 seconds higher in comparison with the car user class) to compensate for the decrease in acceleration and deceleration. *Figure 135* shows the comparisons of the speed, density and total number of lane changes for the microscopic and mesoscopic reference and 50% ACC scenarios. The microscopic simulation results are indicated with solid lines, while the mesoscopic simulation results are indicated with dashed lines. In the delay time plot, it could be found that the mesoscopic scenario is slightly more optimistic than the microscopic reference scenario. Additionally, it could be found that the total number of lane changes is significantly lower in the mesoscopic scenarios. However, this could be explained by the differences in simulation approaches and the simplifications to allow for mesoscopic modelling. The 50% ACC simulation results are relatively similar for mesoscopic and microscopic simulations. In *Table 21*, the coefficients of determination are provided for the speed, density and delay time indicators.

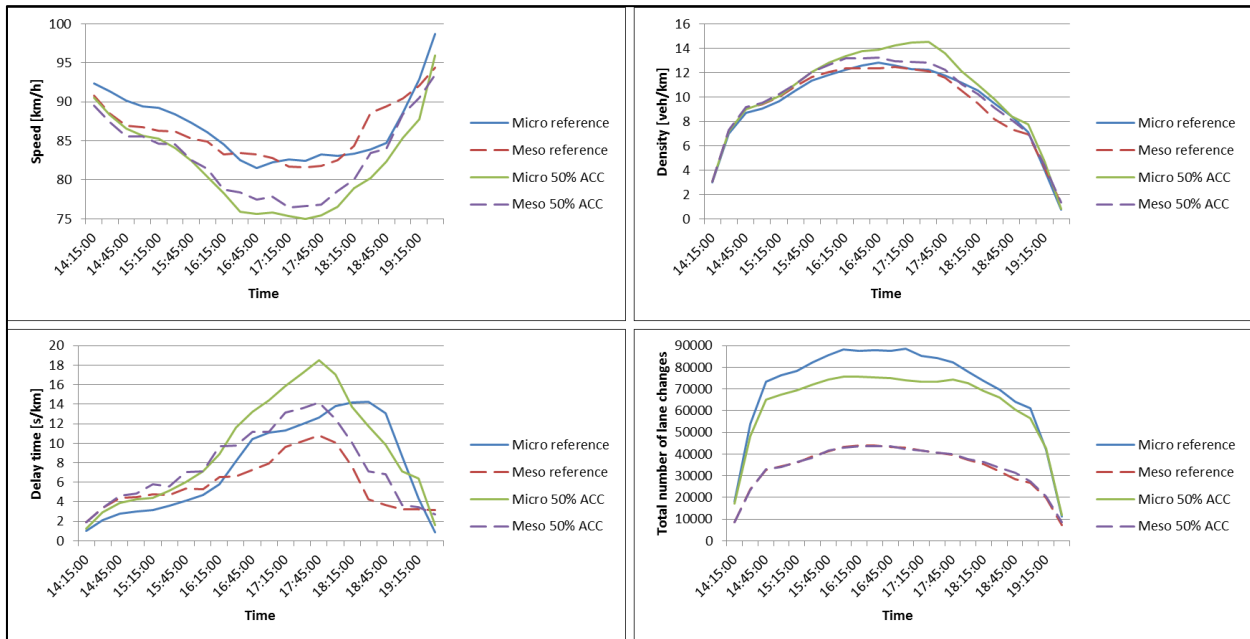


Figure 135 - Comparisons of speed, density, delay time and total number of lane changes for the microscopic and mesoscopic reference and 50% ACC scenarios

Table 21 - Corresponding coefficients of determination for comparison between microscopic and mesoscopic simulation results of ACC scenarios

Coefficient of determination [R ²]	Speed	Density	Delay time
Reference	0.727	0.976	0.446
50% ACC	0.947	0.981	0.894

From *Table 21*, it could be concluded that the mesoscopic simulation results of the 50% ACC scenario shows high coefficients of determination for delay time, speed and density. This indicates that the effects of ACC could be represented relatively well by selecting a mesoscopic reaction time of 1.5 seconds for the ACC user class. Additionally, the low R^2 -value for delay time in the reference scenarios could be explained by the fact that one congestion front is only included in the mesoscopic reference scenario to a limited extent, because an important cause of this congestion is the lane-changing behavior of drivers, which is more simplified in a mesoscopic simulation. Also, after approximately 18:00, there are large differences, which could be considered as outliers that significantly reduce the value of R^2 . If the R^2 is computed for the period between 14:00 up and to including 18:00, the corresponding coefficient of determination increases up to 0.927. Although the coefficient of determination for speed in the reference scenario is relatively low, the patterns are relatively similar, which indicates that the mesoscopic simulator is to some extent able to represent similar patterns and values as found in microscopic simulation. However, it is important to note that information could be filtered out as a consequence of the simplifications and the lack of some microscopic parameters.

7.1.2 Mesoscopic reaction times for newer ACC scenarios

From subsection 6.1.2, it could be concluded that increasing market penetration rates of newer ACC have some contradicting effects in terms of speed, density and delay time. In general, speeds are decreased as a consequence of increasing newer ACC market penetration, which seems to indicate an increase in congestion. However, the average delay time was also decreased, which indicates a relief of congestion as a consequence of increasing penetration rates of newer ACC. In order to represent the microscopic results of newer ACC, an increase in reaction time with respect to the rule of thumb is required to compensate the effects of headway settings and smaller acceleration and deceleration rates. In comparison with the mesoscopic reaction time for ACC, a decrease in mesoscopic reaction time is required, since the microscopic reaction time was reduced as well.

For the determination of mesoscopic reaction times for newer ACC, it was chosen to pick a slightly lower mesoscopic reaction time in comparison with the car vehicle class, because the delay time should be decreased. The differences found in speeds and densities are considered to be due to the lower maximum desired speeds as a result of lower speed acceptance parameters for newer ACC systems. After multiple tests, it was found that a mesoscopic reaction time of 1.05 seconds did resemble and fit the average microscopic results of the 50% newer ACC scenario the best, in terms of speed, density and delay time patterns over time and corresponding coefficients of determination. This mesoscopic reaction time could be considered as a compromise, because decreases in mesoscopic reaction time result in higher average speeds and decreases in delay time, while both speed and delay times were reduced in the microscopic simulation results. This notion already indicates that the mesoscopic simulator is not fully able to show the exact same effects as found in microscopic simulation. The mesoscopic reaction time at traffic light was set to 2.1 seconds to compensate for the effect of decreased accelerations of (newer) ACC systems.

Figure 136 shows the comparisons of the average speed, density, delay time and total number of lane changes for the microscopic and mesoscopic reference and 50% newer ACC scenarios. The microscopic simulation results are indicated with solid lines, while the mesoscopic simulation results are indicated with dashed lines. The delay time plot shows that the delay has been decreased in the 50% newer ACC scenario, although the decrease in delay time is bigger in the microscopic scenario. In terms of speed and density, no significant changes in mesoscopic results are visible in the graphs. Additionally, the total number of lane changes is significantly lower in the mesoscopic scenarios, which could be explained by differences in simulation approaches and simplifications made to allow for mesoscopic modelling. In *Table 22*, the coefficients of determination between microscopic and mesoscopic reference and 50% newer ACC scenarios are provided for the speed, density and delay time indicators.

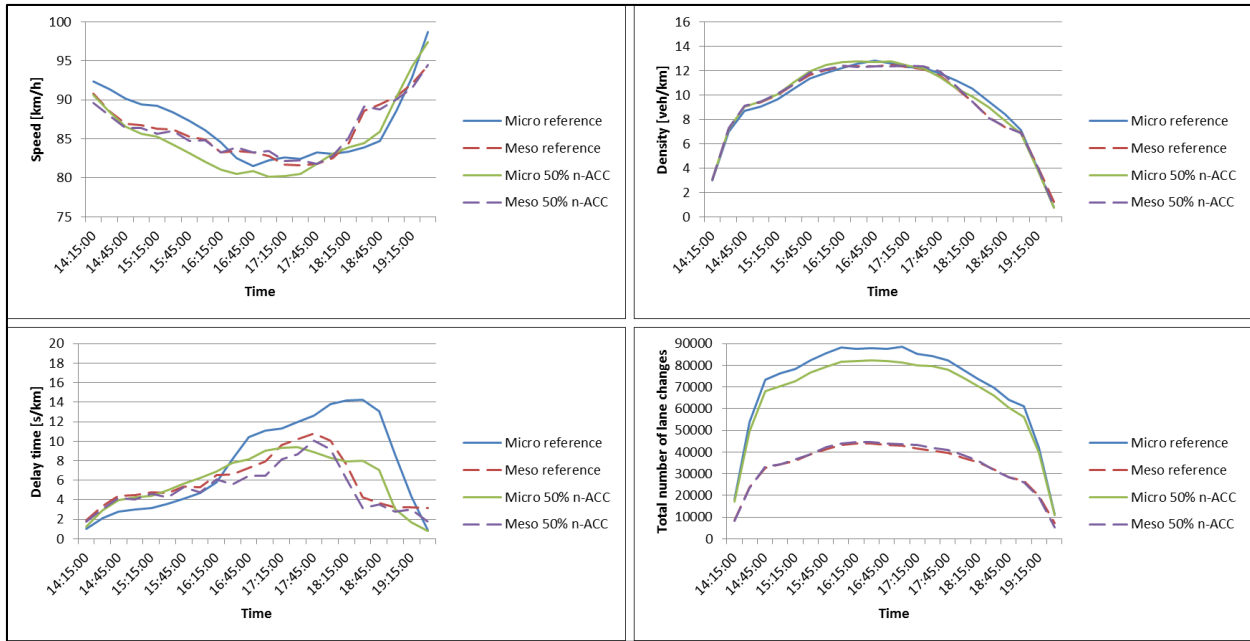


Figure 136 - Comparisons of speed, density, delay time and total number of lane changes for the microscopic and mesoscopic reference and 50% newer ACC scenarios

Table 22 - Corresponding coefficients of determination for comparison between microscopic and mesoscopic simulation results of newer ACC scenarios

Coefficient of determination [R ²]	Speed	Density	Delay time
Reference	0.727	0.976	0.446
50% newer ACC	0.877	0.992	0.681

In Table 22, the 50% newer ACC scenario shows high coefficients of determination for speed and density. However, the mesoscopic patterns of delay time and speed over time show some significant differences with the microscopic simulation results. This indicates that the mesoscopic simulation is not able to fully represent the microscopic simulation results. It also seems that differences between subsequent market penetration scenarios are much smaller in mesoscopic simulation, which is a logic effect of simplifications to allow for mesoscopic modelling. Additionally, when efforts are made to increase the fit in terms of speed, the fit in terms of delay time is reduced, which is an important reason for making a compromise.

7.1.3 Mesoscopic reaction times for improved ACC scenarios

From the microscopic simulation results, discussed in subsection 6.1.3, it was found that improved ACC systems generally have a positive effect on average speed, density and delay time. In general, average density and delay time were found to decrease for increasing improved ACC penetration, which indicates decreases in congestion. Since the improved ACC systems can apply smaller following distances than newer ACC, the mesoscopic reaction time for improved ACC should be set lower than 1.05 seconds.

For the determination of mesoscopic reaction times of improved ACC, it was chosen to pick a reaction time lower than 1.0 seconds, because the mesoscopic reaction time should be lower in comparison with the newer ACC vehicle class. After multiple test simulations with mesoscopic reaction time factors of 0.6, 0.7, 0.8, 0.9 and 1.0 seconds, it was found that a mesoscopic reaction time of 0.9 represented the data from microscopic simulations the best. The decrease of 0.15 seconds with respect to the newer ACC system is explained by the decreased minimum headway settings, resulting in smaller following distances.

Figure 137 shows the comparisons of the speed, density, delay time and total number of lane changes of the microscopic and mesoscopic reference and 50% improved ACC scenarios. The microscopic results

are indicated with solid lines, while the mesoscopic simulation results are indicated with dashed lines. Corresponding coefficients of determination between microscopic and mesoscopic results for speed, density and delay time indicators are provided in *Table 23*. The delay time plot shows that the delay has been decreased in the 50% improved ACC scenarios, although the decreases in delay time are more severe for the microscopic scenario. With respect to the mesoscopic results of speed and density, only small deviations between the reference and 50% improved ACC scenarios can be found, while clearer differences in speed can be found for microscopic scenarios. As discussed, the number of lane changes found in mesoscopic simulations is significantly lower. Concluding, the mesoscopic simulator is able to represent the microscopic patterns in terms of increases and decreases in speed, density and delay time, although the severity of these changes is not represented as well as in microscopic simulation.

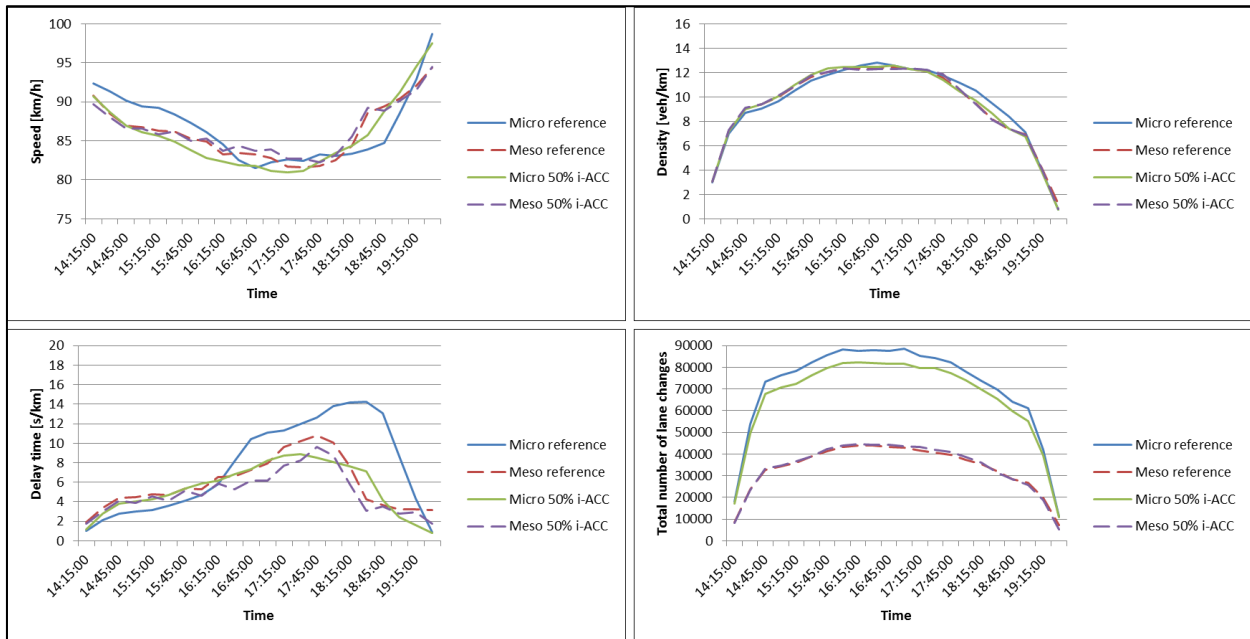


Figure 137 - Comparisons of speed, density, delay time and total number of lane changes for the microscopic and mesoscopic reference and 50% improved ACC scenarios

Table 23 - Corresponding coefficients of determination for comparison between microscopic and mesoscopic simulation results of improved ACC scenarios

Coefficient of determination [R ²]	Speed	Density	Delay time
Reference	0.727	0.976	0.446
50% improved ACC	0.917	0.996	0.767

In *Table 23*, high coefficients of determination for speed, density and delay time are found between microscopic and mesoscopic 50% improved ACC scenarios, indicating a good fit. However, mesoscopic patterns of delay time and speed show some differences with the corresponding microscopic simulation results. This indicates that mesoscopic simulation gives a good approximation of microscopic simulation results, but cannot be used to fully represent similar results as microscopic simulation.

7.1.4 Mesoscopic reaction times for CACC scenarios

From the microscopic simulation results on the average effects of CACC, discussed in subsection 6.1.4, it was found that CACC systems have positive effects on average speed, density and delay time. Generally, average density and delay time were found to decrease for increasing penetration rates of CACC, which clearly indicates decreases in congestion and improvements in traffic flow. Since CACC systems can apply shorter following distances than ACC systems as a result of the communication abilities of CACC, mesoscopic reaction time for CACC should be set lower than the reaction times of previous ACC systems.

To select a proper mesoscopic reaction time for the CACC vehicle class, the general rule of thumb is used as a reference. The microscopic reaction time was set to 0.2 seconds. The rule of thumb describes that the mesoscopic reaction times should approximately be the microscopic reaction time, multiplied with 1.5, which results in a mesoscopic reaction time of 0.3 seconds. Mesoscopic reaction times between 0.2 and 0.4 were tested, with steps of 0.025 seconds. It was found that a mesoscopic reaction time of 0.25 seconds provided the best fit with the microscopic simulation results. This is in contrast with all the reaction times used for the ACC systems, where all mesoscopic reaction times used were higher than the microscopic reaction time multiplied with 1.5, while all systems show smaller acceleration and deceleration rates. For the ACC types discussed, the mesoscopic reaction times were increased to compensate for these smaller decelerations and the constant gap policy applied. However, microscopic simulation results also indicated that CACC systems might have a stabilizing effect on traffic flow, which could be compensated by lowering mesoscopic reaction times.

Figure 138 shows the comparisons of the speed, density, delay time and total number of lane changes for the microscopic and mesoscopic reference and 50% CACC scenarios. The microscopic simulation results are indicated with solid lines, while mesoscopic simulation results are indicated with dashed lines. The corresponding coefficients of determination between microscopic and mesoscopic results are provided for the speed, density and delay time indicators in Table 24. The delay time plot indicates that the delay time is decreased in the 50% CACC scenarios, although the decreases in delay time are more severe for the microscopic scenario. Small deviations between the mesoscopic speed results of the reference and 50% CACC scenario are found, while microscopic simulation results show larger differences between these scenarios. As discussed, the number of lane changes found in mesoscopic simulations is significantly lower, as a result of differences in simulation approaches and the simplifications to allow for mesoscopic modelling. From Figure 138, it could be concluded that the mesoscopic simulation provides patterns in terms of average speed, density and delay time that are relatively similar to the microscopic simulation results, although the extent and severity of the differences between scenarios is significantly lower, which is mainly caused by the simplifications to allow for mesoscopic modelling and the reduced amount of parameters available to describe driving behavior in mesoscopic simulation.

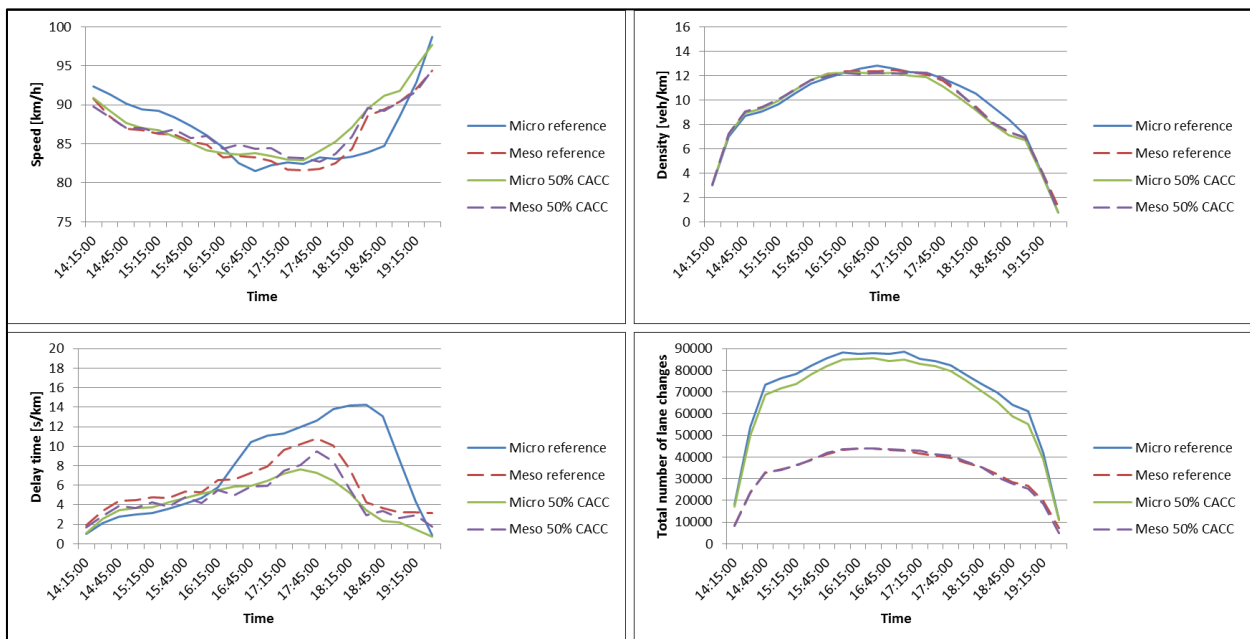


Figure 138 - Comparisons of speed, density, delay time and total number of lane changes for the microscopic and mesoscopic reference and 50% CACC scenarios

Table 24 - Corresponding coefficients of determination for comparison between microscopic and mesoscopic simulation results of CACC scenarios

Coefficient of determination [R ²]	Speed	Density	Delay time
Reference	0.727	0.976	0.446
50% improved ACC	0.930	0.997	0.859

From Table 24 could be concluded that the simulation results of the 50% CACC scenario shows high coefficients of determination for speed, density and delay time. This indicates that the effects of CACC could be represented quite well by selecting a mesoscopic reaction time for CACC of 0.25 seconds. However, it should be noted that despite of the high values for R², there also are some significant differences between mesoscopic and microscopic simulation results, which is clearly visualized in the speed and delay time plots in Figure 138.

7.2 Mesoscopic averages at experiment level

This subsection will discuss the mesoscopic simulation results of average speed, density and delay time for all the scenarios and (C)ACC types over the whole network. By evaluating and comparing these results with the corresponding microscopic simulation results, described in section 6.1, an insight could be gained in whether it is possible to represent the effects of (C)ACC by using mesoscopic simulations. The statistics on the total number of lane changes were not included in this analysis, because significant differences were found as a result of differences in simulation approaches and the simplifications to allow for mesoscopic modelling. Therefore, adding an analysis on the total number of lane changes would not provide additional insights on this part of the research.

7.2.1 Mesoscopic average simulation results for ACC scenarios

This subsection describes the average results in terms of speed, density and delay time found from mesoscopic simulations. These results are compared with the microscopic simulation results from section 6.1.1 to check whether mesoscopic simulations provide results similarly to microscopic simulation results.

7.2.1.1 Speed

The average speeds resulting from mesoscopic simulation of ACC scenarios with increasing penetration rates are provided in Figure 139. These average speeds refer to the average journey speed of individual vehicles, averaged over all vehicles leaving the network within a statistical time period.

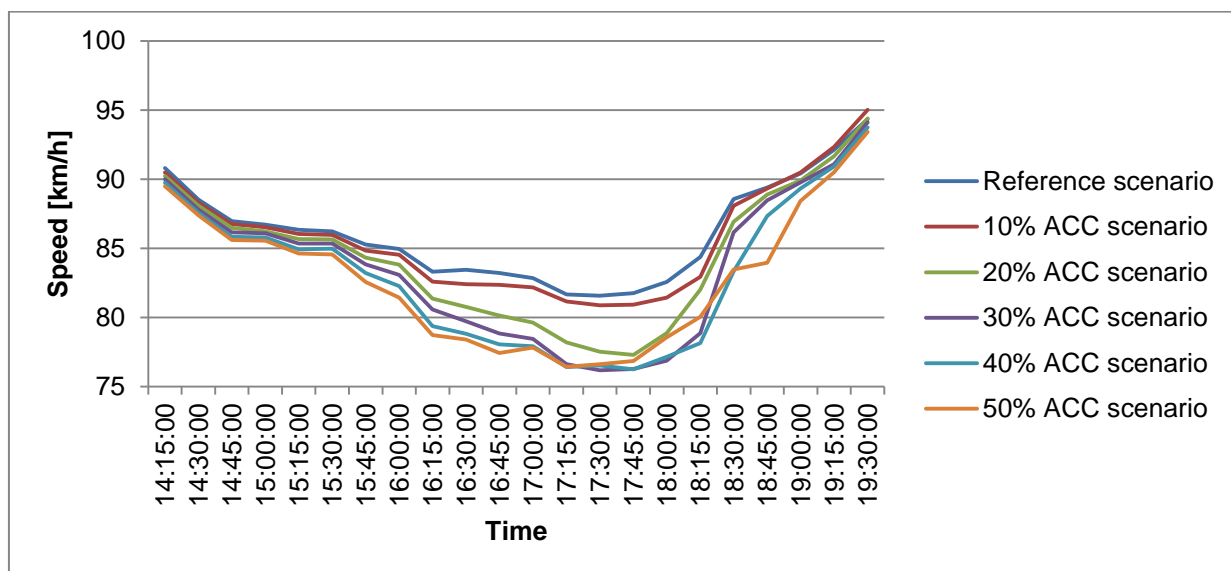


Figure 139 - Overview of average speeds over time resulting from mesoscopic simulation of ACC scenarios

In the early time period, these mesoscopic speed patterns are similar to the speeds obtained by microscopic simulation (*Figure 74*). However, in the microscopic simulation results, the speed differences were higher for high penetration rates, while this is not true in the mesoscopic simulation results. Additionally, between 17:30 and 18:30, the average speeds of the 30% and 40% ACC scenarios are lower than the average speeds of the 50% ACC scenario, while this pattern is not observed in the microscopic simulation results. Nevertheless, the shape of the mesoscopic speed plots is very similar to the microscopic speed plots, which indicates that the mesoscopic simulator performs relatively well on representing the effects of ACC in terms of average speed, albeit that the deviations between consecutive penetration rate scenarios are significantly smaller in mesoscopic simulation.

7.2.1.2 Density

The average densities over the network resulting from mesoscopic simulations are provided in *Figure 140*. These average densities refer to the average densities all over the network, which means that it only provides some information, since dense road sections could be compensated by empty road sections. However, it will indicate the amount of vehicles on the network and might give an indication of the amount of congestion. The warm-up and cooldown period to fill the network are not shown in this graph.

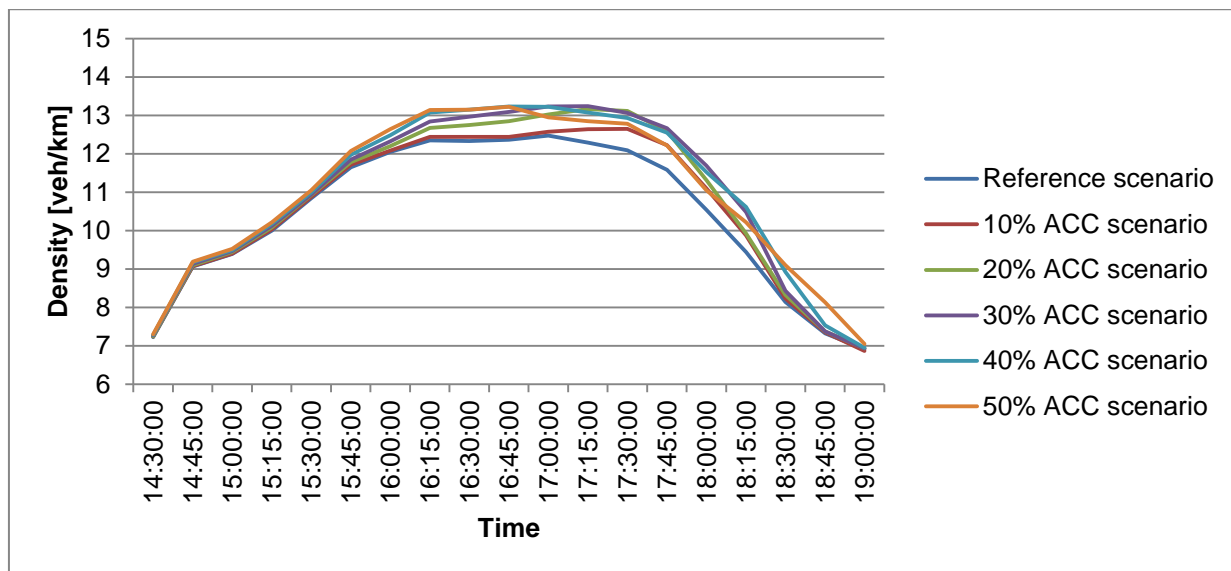


Figure 140 - Overview of average densities over time resulting from mesoscopic simulation of ACC scenarios

In the mesoscopic density plots for ACC (*Figure 140*), the density for increasing percentages of ACC is higher at early time steps. However, at later time periods, the densities were found to be highest for penetration rates between 20% and 40%, which is definitely not in line with the microscopic simulation results on the effects of ACC on average density (*Figure 75*). In the microscopic simulation results, higher penetration rates of ACC result in significant increases in average density. This pattern is not found in the mesoscopic simulation results. Additionally, in the microscopic simulation results, the increases in density became more significant for ACC percentages above 40%. The density patterns from mesoscopic simulation are not considered to be satisfactory representing the microscopic simulation results, because there are some vital differences in the patterns and expected consequences of ACC.

7.2.1.3 Delay time

The delay times for increasing penetration rates of ACC are shown in *Figure 141*. These averages refer to delay time on a full journey and are calculated at the moment that the vehicle leaves the network. This graph should be compared with the microscopic delay time results of different ACC scenarios (*Figure 76*).

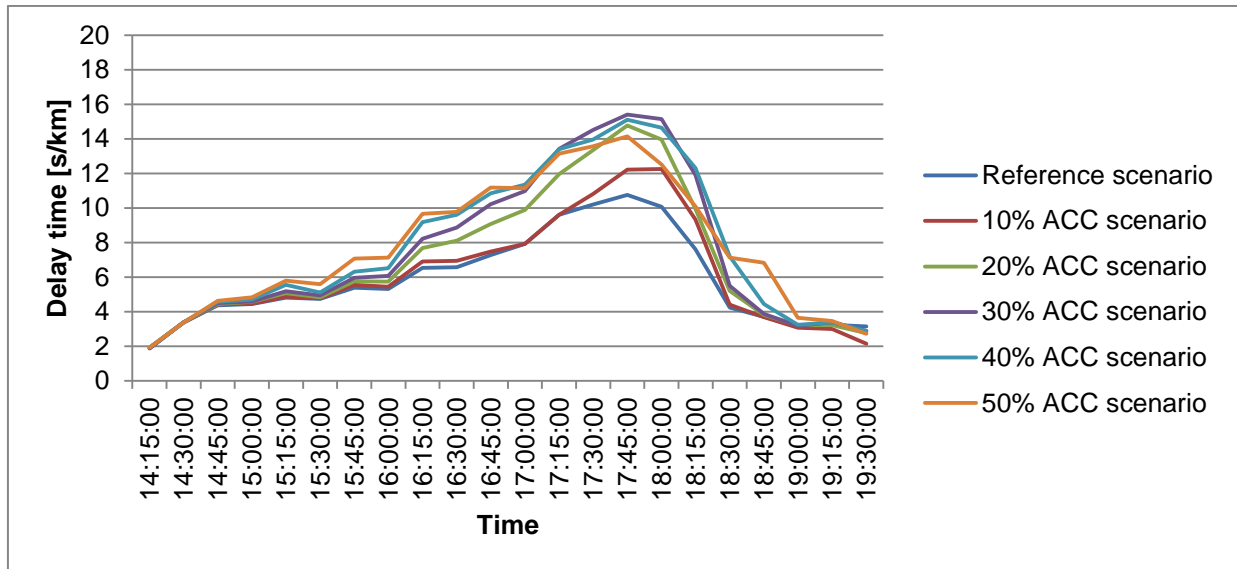


Figure 141 - Overview of average delay time resulting from mesoscopic simulation of ACC scenarios

At early time periods, the delay increases when ACC penetration rates increase. However, after 17:15, the delay time is highest for the 20%, 30% and 40% ACC scenario, which is not found in microscopic simulation. The largest differences between scenarios in *Figure 141* are found for lower penetration rates, while they should be found for higher penetration rates as concluded from *Figure 76*. Also, delay times found in microscopic simulation are generally higher than those found from mesoscopic simulation of ACC scenarios. Although a relatively similar pattern is found, mesoscopic simulation results do not show the same effects as microscopic simulation due to the simplifications to allow for mesoscopic simulation.

7.2.2 Mesoscopic average simulation results for newer ACC scenarios

Mesoscopic simulation results of newer ACC scenarios are provided and reflected in this subsection.

7.2.2.1 Speed

The average journey speeds from mesoscopic simulation for are provided in *Figure 142*.

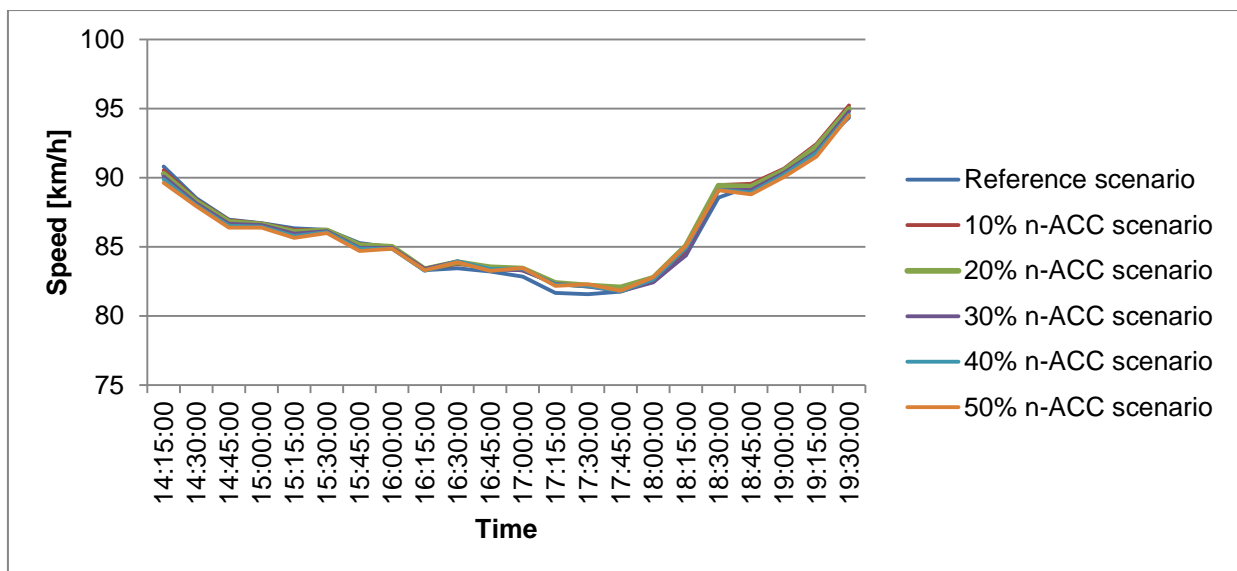


Figure 142 - Overview of speed over time resulting from mesoscopic simulation of newer ACC scenarios

In the average speeds resulting from mesoscopic simulation, the differences between the average speeds for different market penetration rates are negligible. However, in the microscopic simulation results (*Figure 78*), the speed differences are visible and much clearer. In general, microscopic simulations report decreasing speed for increasing penetration rates of newer ACC. The general shapes of the speed plots are similar to those from microscopic simulation, although no clear differences can be found between speeds for the different penetration rate scenarios. This indicates that the mesoscopic simulator is not able to represent the same effects as the microscopic simulator in terms of average traffic speed.

7.2.2.2 Density

The average densities resulting from mesoscopic simulation are provided in *Figure 143*. These average densities refer to the average densities all over the network, which means that it only provides some information, since dense road sections could be compensated by empty road sections. However, it will indicate the amount of vehicles on the network and gives an indication of the amount of congestion. The warm-up and cooldown period to fill the network are not shown in this graph.

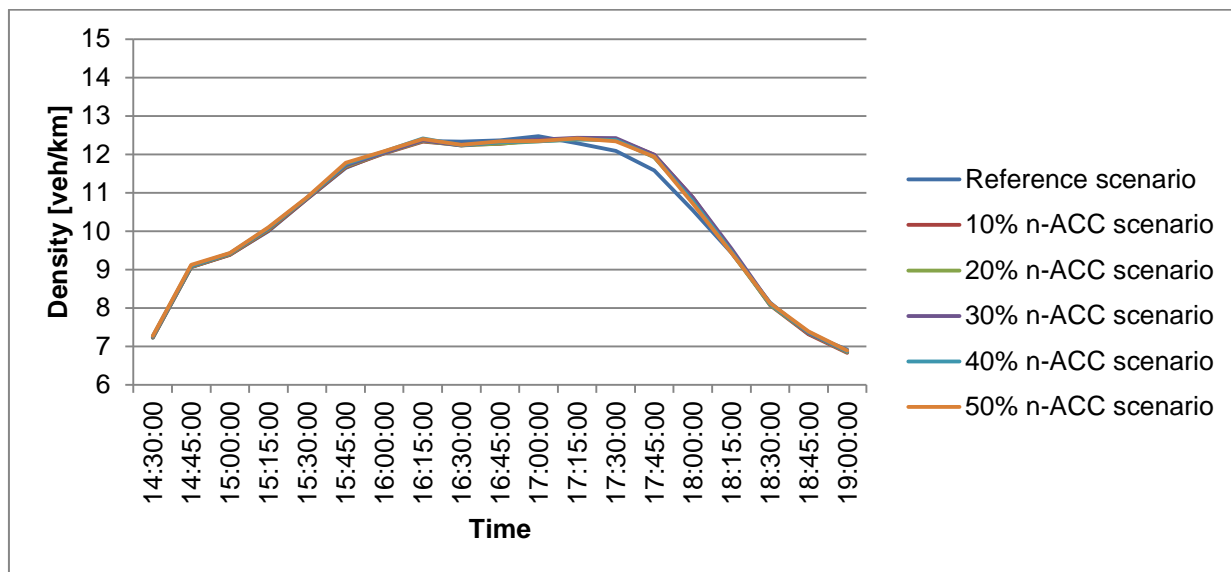


Figure 143 - Overview of density over time resulting from mesoscopic simulation of newer ACC scenarios

In the mesoscopic density plots for newer ACC, the densities for all scenarios with newer ACC are very similar. The only small difference is that the reference scenario has slightly lower densities between 17:00 and 18:00, which indicates that introducing newer ACC might lead to an increase in congestion. Additionally, in the microscopic simulation results, the density is higher at early time steps for higher newer ACC penetration rates, while it is lower at late time steps. This effect is not found in the mesoscopic simulation results. Again, mesoscopic simulation results show relatively similar values, but does not show the severity of differences between scenarios found in microscopic simulation. Therefore, mesoscopic simulation does not seem to be capable of producing the same effects on traffic flow, caused by increasing market penetration rates of newer ACC, as found from microscopic simulation results.

7.2.2.3 Delay time

The delay times for increasing penetration rates of newer ACC are shown in *Figure 144*. These averages refer to delay time on a full journey and are calculated at the moment that a vehicle leaves the network. All the delay times of individual vehicles are averaged over a statistical time period to provide average delay times per time period. This graph should be compared with the microscopic average delay time results of different ACC scenarios, displayed in *Figure 80*.

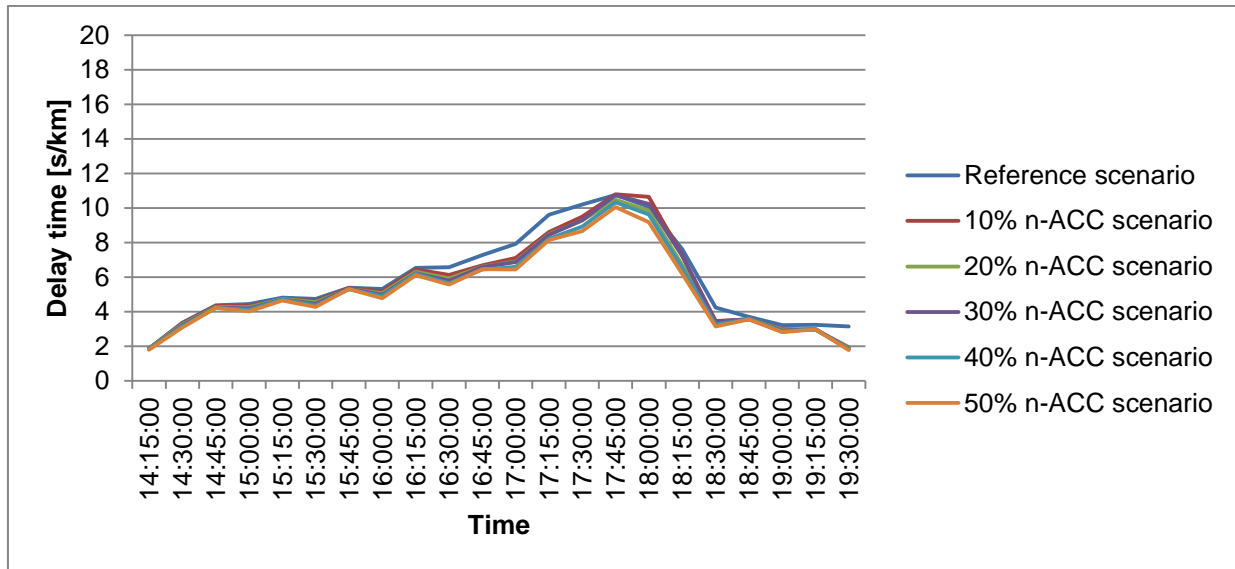


Figure 144 - Overview of average delay time resulting from mesoscopic simulation of newer ACC scenarios

In Figure 144, increases in newer ACC rates lead to reductions in delay time. This reduction is found for the whole simulation period, which contradicts the microscopic results, where delay time increases for high penetration rates of newer ACC in early time periods. On average, a decrease in delay time is found for increasing newer ACC equipage in microscopic simulation. The mesoscopic simulation is partly able to represent microscopic results of delay time. This indicates that mesoscopic simulations could be used as first indication of the effects on delay time, although these are less clear than in microscopic simulation.

7.2.3 Mesoscopic average simulation results for improved ACC scenarios

This subsection describes the average speed, density and delay time resulting from mesoscopic simulations. These results will be compared with microscopic simulation results, defined in section 6.1.3.

7.2.3.1 Speed

Average speeds for improved ACC scenarios derived from mesoscopic simulation are given in Figure 145.

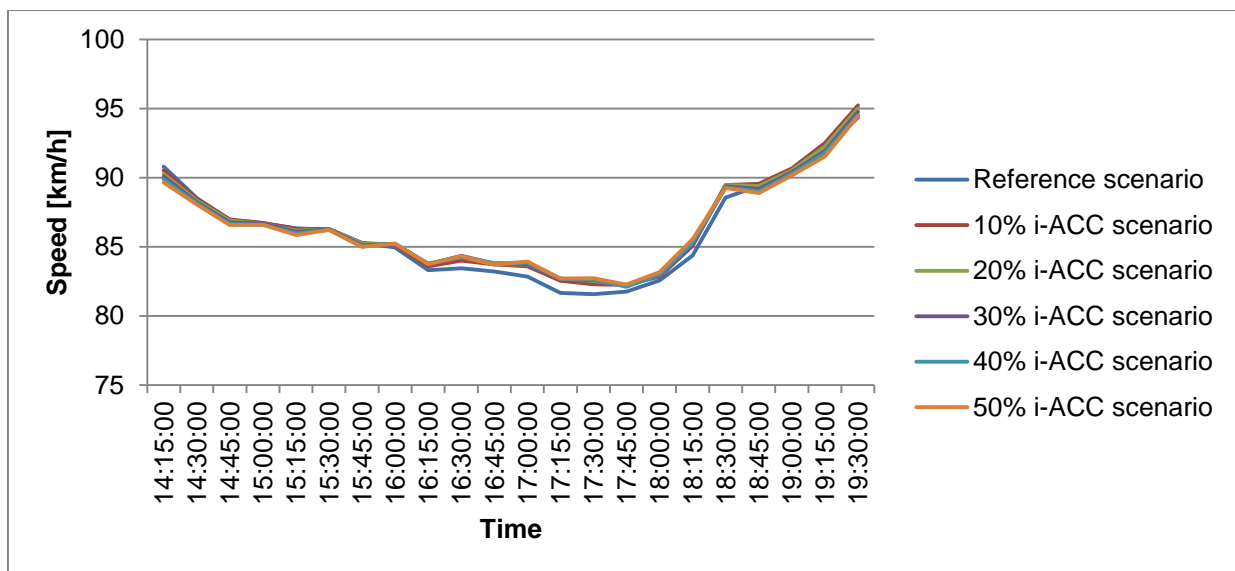


Figure 145 - Overview of speed over time resulting from mesoscopic simulation of improved ACC scenarios

In *Figure 145*, differences between average speeds for different market penetration rates are negligible. If a close look is taken at the figure, one could see that the average speed is highest for the 50% improved ACC scenario. Only the reference scenario shows significantly lower speeds. However, speed differences are much more visible and clear in the microscopic simulation results. Generally, microscopic simulation results show decreasing speeds for increasing penetration rates of newer ACC. The overall shapes of the speed plots are similar to those obtained by microscopic simulation, although no clear differences can be found between speeds for the different penetration rates. This indicates that the mesoscopic simulator is partly able to represent the same effects as the microscopic simulator in terms of average traffic speed.

7.2.3.2 Density

The average densities of the improved ACC scenarios resulting from mesoscopic simulation are provided in *Figure 146*. These average densities refer to the average densities all over the network, so it only provides some information, since dense sections could be compensated by empty sections. However, it indicates the amount of vehicles on the network and the amount of congestion. The warm-up and cooldown period are excluded from the graph. This graph should be compared with the microscopic average densities for improved ACC scenarios, displayed in *Figure 83*.

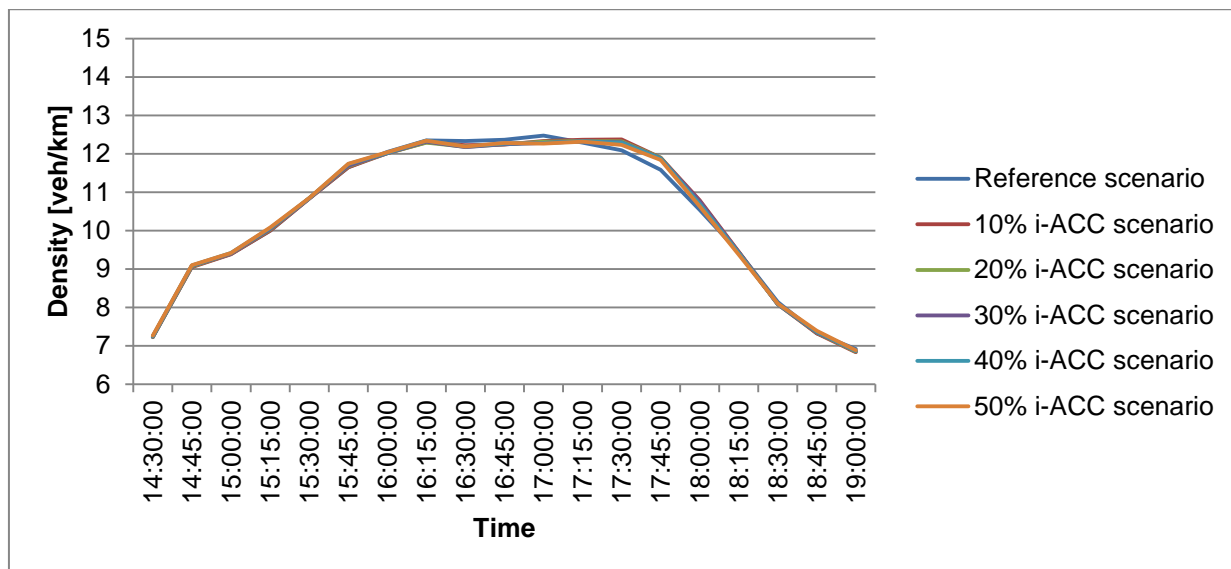


Figure 146 - Overview of density over time resulting from mesoscopic simulation of improved ACC scenarios

In the mesoscopic density plots for improved ACC (*Figure 146*), the densities for all scenarios with newer ACC are similar. The reference scenario reports higher values in the peak period between 16:00 and 17:30, but this is compensated afterwards. In the microscopic simulation results (*Figure 83*), density is higher for higher improved ACC percentages at early time steps, while it is lower at late time periods. This effect is not visible in the mesoscopic simulation results. Again, the mesoscopic simulation results shows relatively similar values, but does not show the differences between the scenarios found in microscopic simulation. Therefore, the mesoscopic simulation does not seem to be fully capable of representing the same effects of improved ACC on traffic flow as found in microscopic simulations.

7.2.3.3 Delay time

The delay times for increasing penetration rates of improved ACC are given in *Figure 147*. The averages refer to delay time on a full journey and are calculated at the moment that the vehicle leaves the network. This graph should be compared with the microscopic delay time results of improved ACC, displayed in *Figure 84*.

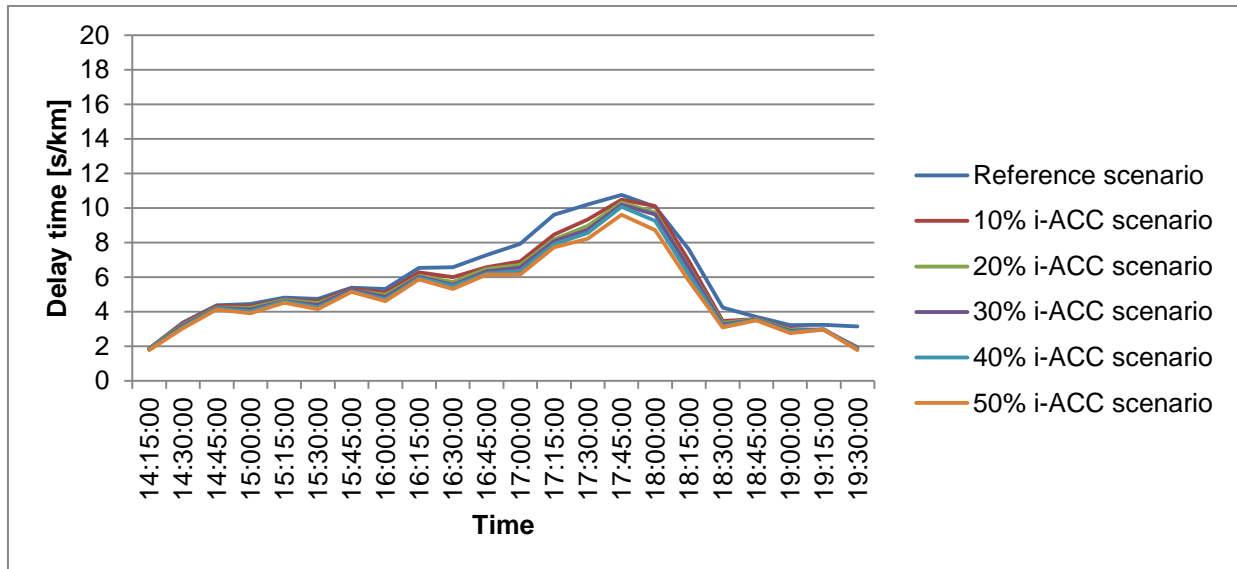


Figure 147 - Overview of average delay time resulting from mesoscopic simulation of improved ACC scenarios

Mesoscopic simulation results on delay time suggest that increases in the market penetration rate of improved ACC systems leads to reductions in delay time, similar to microscopic simulation results (Figure 84). However, the patterns are only slightly different at early time periods. The severity of differences in delay time is shown much clearer in microscopic simulation results, although the general patterns are very similar. Therefore, mesoscopic simulation is able to represent microscopic results on delay time, but delay time patterns of improved ACC scenarios show some small differences between microscopic and mesoscopic simulation. This indicates that mesoscopic simulations could be used to indicate the results.

7.2.4 Mesoscopic average simulation results for CACC scenarios

Here, mesoscopic simulation results of CACC scenarios are reflected and compared with section 6.1.4.

7.2.4.1 Speed

Average speeds for CACC scenarios derived from mesoscopic simulation are given in Figure 148.

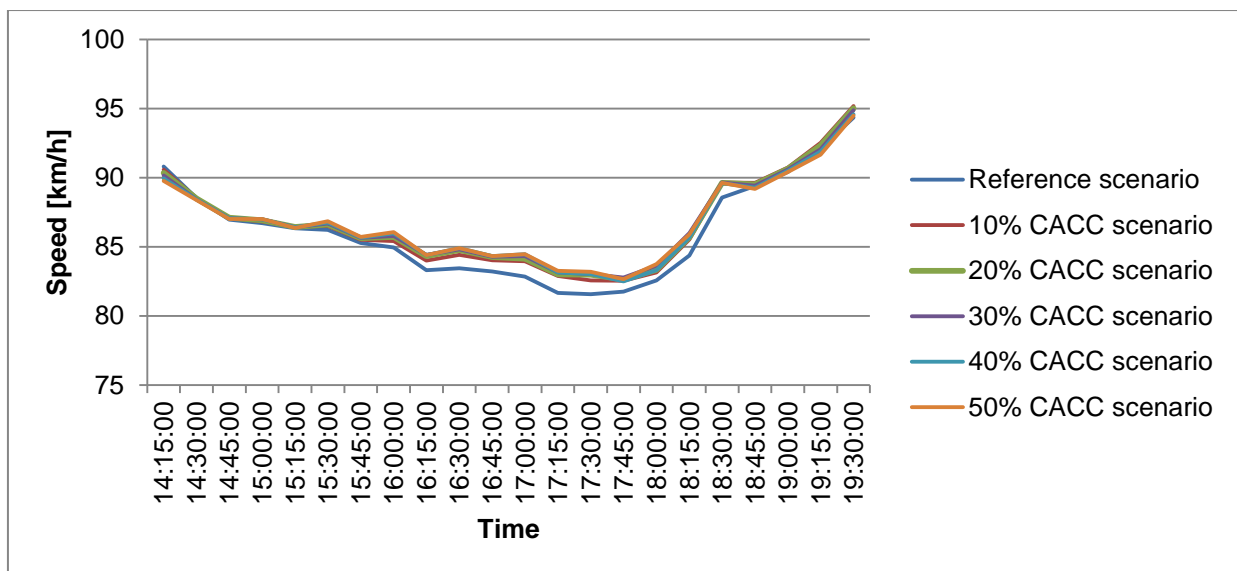


Figure 148 - Overview of speed over time resulting from mesoscopic simulation of CACC scenarios

With respect to average speeds resulting from mesoscopic simulation of CACC scenarios, the differences between penetration rates of 10% to 50% CACC are very small. In comparison with the reference scenario, there is a significant difference between 16:00 and 18:30. However, some clear speed differences in average speed for different penetration rates of CACC can be found in the microscopic simulation results (*Figure 86*). This indicates that the severity of differences between scenarios cannot be shown as clearly in mesoscopic simulation, which also means that it costs more effort to compute the effects of CACC on traffic flow when using mesoscopic simulations. In *Figure 148*, the highest average speeds are found for the 50% CACC scenario, similar to the microscopic simulation results. The overall shapes of the speed plots are similar to those obtained from microscopic simulation, although no clear differences can be found between speeds for different penetration rates, which indicates that mesoscopic simulations provide relatively similar results and patterns in terms of average speed, but is unable to clearly show differences between scenarios with differing penetration rates, because the differences between the different penetration scenarios are smaller and less clear in mesoscopic simulation.

7.2.4.2 Density

Figure 149 provides average densities over the network resulting from mesoscopic simulations of CACC scenarios. The average densities refer to the average densities all over the network, which means that it only provides some information. However, it gives an indication of the amount of vehicles on the network and the amount of congestion. The warm-up and cooldown period are excluded from the graph. These results could be compared with the microscopic simulation results displayed in *Figure 87*.

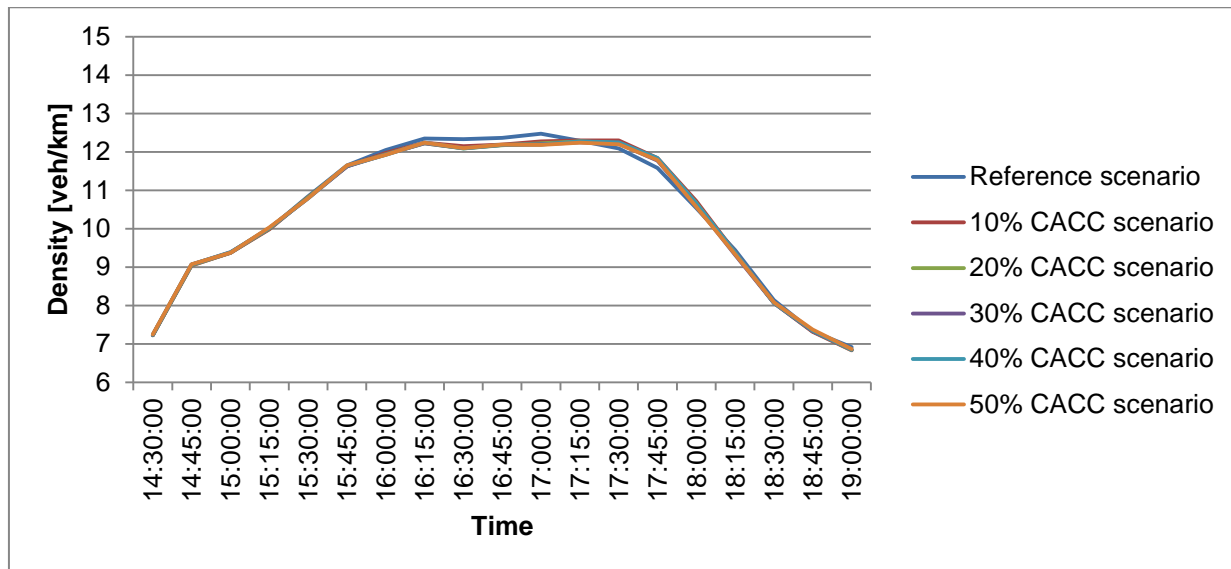


Figure 149 - Overview of density over time resulting from mesoscopic simulation of CACC scenarios

The mesoscopic simulation results of CACC scenarios on average density are very similar for all scenarios with CACC vehicles included. The differences between CACC market penetration rates of 10% to 50% are negligible. The only significant difference is found with respect to the reference scenario. The reference scenario reports higher values in the peak period between 16:00 and 17:30, but this is compensated afterwards. Additionally, in microscopic simulation results (*Figure 87*), average density is higher for higher CACC penetration rates at early time steps, while it is lower at late time periods. This effect is not found in the mesoscopic simulation results. Again, the mesoscopic simulation results show relatively similar values and patterns, but do not show the differences between the scenarios as well as microscopic simulation results. Therefore, the mesoscopic simulation does not seem to be capable of fully representing similar effects on traffic flow as found by performing microscopic simulations.

7.2.4.3 Delay time

Mesoscopic simulation results of average delay times of CACC scenarios are shown in *Figure 150*. These average delay times are over a full journey, with respect to ideal travel times at maximum desired speed. The mesoscopic simulation results are compared with microscopic simulation results (*Figure 88*).

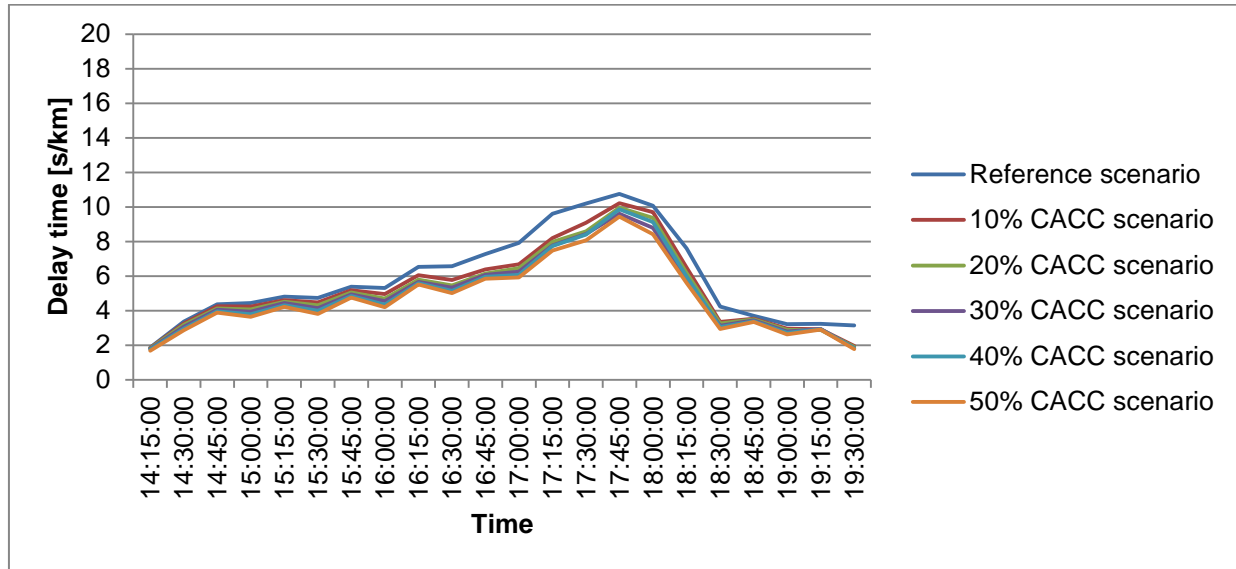


Figure 150 - Overview of average delay time resulting from mesoscopic simulation of CACC scenarios

In mesoscopic simulation results on delay time, increases in CACC market penetration rates lead to reductions in delay time over the whole simulation period. In microscopic simulations, a similar pattern is found. In mesoscopic simulation results, there are significant differences between the reference, 10% and 20% CACC scenario, which are also found in microscopic simulation. In both simulation types, differences between subsequent CACC scenarios are lower when penetration rates increase. The reference scenario shows different values for mesoscopic and microscopic simulation, although the build-up of delay is similar. Therefore, this might explain the smaller differences found in mesoscopic simulation. Mesoscopic simulations might be used to show the effects of rising CACC penetration rates on delay time, although results should be analyzed with care, because there might be significant differences in comparison with microscopic simulations, due to simplifications in mesoscopic behavioral models. It is important to note that mesoscopic simulation results suggest that the severity of delay in the reference and low penetration scenarios was not shown properly. Also, differences in delay time between subsequent CACC scenarios are much clearer in microscopic simulation results. Therefore, it is advised to only use mesoscopic simulations as an indication of these effects. Microscopic simulations are advised for detailed analyses.

7.3 Review of mesoscopic simulation results

This subsection provides a brief review on the mesoscopic simulation results and whether the mesoscopic simulator is able to provide similar results as microscopic simulations. Additionally, the relations between mesoscopic and microscopic simulations with respect to the simulated scenarios are discussed.

The rule of thumb for converting microscopic reaction times into mesoscopic reaction times was used for mesoscopic simulation of the reference scenario. The microscopic reaction time of cars (0.8 seconds) was multiplied with 1.5 to obtain a mesoscopic reaction time of 1.2 seconds, which was then used as input for the mesoscopic simulations of the reference scenario. For all types of ACC and CACC, the average microscopic simulation results were used to find mesoscopic reaction times that provided a good fit with microscopic simulation results on average speed, density and delay time found in section 6.1.

In general, the patterns and propagation of speed, density and delay time over the simulated time periods found by mesoscopic simulation are relatively similar to the patterns found in microscopic simulation. This indicates that both microscopic and mesoscopic simulations should provide relatively similar results. However, it is important to note that there also are some significant differences found in the results.

One of the important congestion fronts was not fully included in mesoscopic simulations of the reference scenario in this study, because it was impossible to create serious congestion at this location within the defined boundaries of reaction time factors. This resulted in significant differences between microscopic and mesoscopic simulation results in terms of congestion and delay time for the reference scenarios. Also, delay time and speed increases are found at an earlier point in time in mesoscopic simulation results, because the mesoscopic simulator applies instantaneous speeds. Also, disturbances such as braking maneuvers to adjust headways are not taken into account in mesoscopic simulation, while these disturbances could cause congestion and extend the duration of congestion. Another reason might be that in the microscopic simulation, all vehicle parameters were drawn from a truncated normal distribution with spreads, while the mesoscopic simulations were performed with the same fixed mesoscopic reaction times for all vehicles within the same vehicle class, which makes the traffic mix more uniform than it was in microscopic simulation. As results of these characteristics, the effects of congestion were found to be less severe in mesoscopic simulations.

Subsequently, the total amount of lane changes found in mesoscopic simulation was significantly lower than in microscopic simulation. The mesoscopic simulator only takes some types of lane changes into account. On the one hand, the necessary lane changes to reach the final destination, lane changes to divide the vehicles over the lanes and lane changes to obtain gains in terms of travel time are used in mesoscopic simulation. However, the microscopic simulation also evaluates lane changes to help other vehicles to merge and (multiple) lane changes for overtaking maneuvers, while these lane changes are probably not taken into account in mesoscopic simulation. This indicates that mesoscopic simulations of situations where lane-changing behavior plays an important role should be interpreted with care. However, it is expected that differences in the total number of lane changes could be significantly reduced by selecting the 'penalize slow lanes' and 'penalize shared lanes' options, which were not selected in performing this research. Additionally, lane changes resulting from mesoscopic modelling should increase when section lengths reduce, because the mesoscopic simulator only takes into account the moment and location (i.e. lane) at which the respective vehicles enter and leave the respective road sections. If section lengths reduce, the number of lane changes should increase, because more lane changes would be performed to decrease travel time, which indirectly also represents overtaking behavior. The current network lay-out and mesoscopic simulation parameters are unsuitable to evaluate effects of (C)ACC on lane-changing using mesoscopic simulation, indicating that further research is required.

With respect to the mesoscopic simulation results of scenarios with differing penetration rates of (C)ACC, some conclusions could also be drawn. It was found that the effect of increasing penetration rates of (C)ACC on speed, density and delay time could be represented with mesoscopic simulation, albeit with much smaller differences between the equipage scenarios. The differences in speed, density and delay time as results of differing penetration rates of (C)ACC was often found very small or negligible in mesoscopic simulation, while microscopic simulations reported significant differences. This effect is caused by differences in reference scenarios, reduced variance between vehicles of the same vehicle class in mesoscopic simulations and the simplifications to allow for mesoscopic simulation. Also, it is in the line of expectations that mesoscopic simulations provide a more averaged view of the effects, as a result of the simplifications to allow for mesoscopic simulation. Therefore, it could be concluded that mesoscopic simulations could be used as indications on the effects of (C)ACC on average speed, density and delay time, but differences between different penetration rates found by mesoscopic simulation are not as clear as in microscopic simulation, which means that microscopic simulation is advised for detailed analyses.

Table 25 gives an overview of the mesoscopic reaction times used, as well as the corresponding microscopic reaction times and mesoscopic reaction times according to the rule of thumb ($R_{meso} = 1.5 * R_{micro}$). For the car user class, the rule of thumb was used to obtain a mesoscopic reaction time of 1.2 seconds. It is important to note that the car user class does not use a set headway (i.e. converted time gap setting), while all (C)ACC systems use a set headway. Test simulations showed that two cars with exactly the same parameter settings follow each other at headways of approximately 1.0 seconds in unrestricted situations. For ACC vehicles it was found that the rule of thumb did not provide the best fit with microscopic simulation results. The best fit was found when the multiplication factor used was increased to 1.875. This increase was presumably needed to compensate for the relatively large headway settings and lower acceleration and deceleration rates of the ACC user class. For the newer ACC user class, a factor of 2.625 was used to compensate for these effects. A factor of 2.25 was used to compensate the same effects for the improved ACC user class. Obviously, different factors are used and the rule of thumb does not apply for the mesoscopic reaction times when using fixed headways. The highest multiplication factor used to determine the mesoscopic reaction time was found for the newer ACC user class, which has a relatively short reaction time, but relatively high mean time headway. These components seem to be of importance for determining the factor to calculate mesoscopic reaction times. While microscopic reaction times for newer ACC and improved ACC are the same, the multiplication factor used for improved ACC is lower, because the restrictions on the headway in microscopic simulation are less severe for this user class, which means that the compensation of this effect could also be reduced. However, for the ACC user class was found that a multiplication factor of 1.25 provided the best fit with microscopic simulation results. In this case, the factor is lower than the rule of thumb, which might be explained by the set mean time headway that is lower than the unrestricted time headway car drivers were generally found to apply and the decreased acceleration and deceleration rates, which might make braking actions more smooth and stabilize disturbances in microscopic simulations, if the microscopic reaction time is small enough. However, clear relations between microscopic parameter settings and mesoscopic reaction times when using fixed headway settings were not found in this study. Further research is required to gain more insight into this relationship.

Table 25 - Overview of microscopic and mesoscopic reaction time and compensations

	Microscopic reaction time used in simulation [s]	Microscopic mean time headway [s]	Mesoscopic reaction time according to the rule of thumb ($R_{micro} * 1.5$) [s]	Mesoscopic reaction time used in simulation [s]	Factor used
Car	0.8	- (≈ 1.0)	1.2	1.2	1.5
ACC	0.8	1.6	1.2	1.5	1.875
Newer ACC	0.4	1.6	0.6	1.05	2.625
Improved ACC	0.4	1.2	0.6	0.9	2.25
CACC	0.2	0.8	0.3	0.25	1.25

Overall, mesoscopic simulations could be used to represent similar results as found with microscopic simulation. However, it is very important to be aware of differences in simulation results that can be found as a reason of the simplifications to allow for mesoscopic modelling. Also, the effects of differing penetration rates of ACC and CACC on traffic flow are less clear in mesoscopic modelling. Additionally, the multiplication factors needed to convert microscopic parameter settings of (C)ACC user classes into mesoscopic reaction times differ for the user classes defined in this research. It seems that microscopic reaction times and mean time headway settings have the most significant influence on the multiplication factor needed to convert microscopic reaction times into mesoscopic reaction times. Also, differences in acceleration and deceleration parameters are expected to have an effect on this multiplication factor. However, clear relations between changes in microscopic parameter settings and mesoscopic reaction times were not found. Therefore, mesoscopic simulation results should be interpreted with care and further research is required on the relations between microscopic and mesoscopic parameter settings.

8 Conclusions and recommendations

This chapter contains the main conclusion and recommendations of this research. The conclusions are given for the content of this research, where the research goal is to gain insight in the effects of ACC and CACC on traffic performance in realistic traffic situations on the highway. Subsequently, recommendations with respect to (C)ACC systems, modelling in Aimsun and future research are provided.

8.1 Conclusions

With respect to ACC systems, both positive and negative effects on traffic flow are found in literature and this research. In this research, current ACC systems were found to have a negative effect on traffic flow, especially due to the combination of the relatively high reaction time (0.8 seconds) and large following distances (mean time headway of 1.6 seconds) modelled. The newer ACC systems defined in simulation represent newer ACC systems that apply the same following distances as current ACC systems, but have the capability to detect vehicles on adjacent lanes and have significantly lower reaction times (0.4 seconds). These newer ACC systems both show positive and negative effects on traffic flow. On average, the effects of newer ACC systems are more positive than negative. Improved ACC systems, where both reaction time (0.4 seconds) and following distances (mean time headway of 1.2 seconds) are reduced with respect to current ACC systems, predominantly show positive effects on traffic flow. For CACC systems that have further decreased reaction times (of 0.2 seconds) and following distances (mean time headway of 0.8 seconds) between vehicles, positive effects on traffic flow was found. Please note that the driving behavior of all user classes was described by the empirical car-following model of Gipps (Gipps, 1981, 1986b). To model (C)ACC driving behavior, the available parameters were manipulated in such a way that it represents (C)ACC driving behavior.

For the (current) ACC systems included in simulation, average speeds over the network decrease for increasing market penetration rates of ACC. The average densities and delay time over the network increase for increases in ACC equipage. The deteriorations in average speed, density and delay time are more severe for the 40% and 50% ACC scenario, which means that the problems at local bottlenecks become more severe at high penetration rates. This effect appears to be caused by reaching capacity limits at these sections and bottlenecks. The total number of lane changes on the network reduces for increasing penetration rates of ACC, which indicates that ACC drivers tend to stay in their lane more often. In general, the introduction of ACC results in deteriorations in traffic flow.

In general, the introduction of newer ACC lowers average speed at early time periods. However, at some point in time, a small improvement in average speed can be gained with respect to the reference scenario without any ACC vehicles. This increase can already be gained at 10% market penetration rates of newer ACC. Further increases do not lead to significant changes in average speed. Additionally, at the early evening peak densities increase for increasing percentages of newer ACC, as a result of lower speed acceptance parameter settings for these vehicles, resulting in slightly larger travel times. After 17:30 hours approximately, the congestion is resolving and average densities decrease for increasing percentages of newer ACC, which indicates that the congestion is solved at an earlier moment in time. Average delay time decreases as a result of the introduction of newer ACC. A 10% market penetration rate significantly reduces delay time in comparison with the reference scenario, as a result of relieving congestion at the bottlenecks with severe braking, while limited further gains can be found up to 30%. Between 30% and 50% newer ACC, substantial improvements are found again, because congestion is solved at multiple local bottlenecks. Additionally, the number of lane changes reduces for increasing rates of newer ACC.

For the improved version of ACC, the results are very similar to the results for newer ACC. The small differences are that some effects are found at earlier moments in time or for lower penetration rates of ACC, indicating some small further improvements in traffic flow in comparison with newer ACC scenarios.

The CACC systems show the biggest improvements of all systems. However, this is under the assumption that all vehicles send speed information to CACC systems. From the start of congestion (approximately 16:15) until the end of simulation, average speeds increase and densities decrease for increasing CACC penetration rates. Average delay time is significantly reduced for all increasing percentages of CACC as a result of decreases in congestion at local bottlenecks, although improvements become smaller for higher penetration rates, which indicates that at a certain penetration rates, no extra gains could be achieved.

In the simulation results of all simulated (C)ACC scenarios, the average delay time at early time periods was always higher than for the reference scenario, while average speeds were always lower. This effect is a direct result of the speed acceptance parameter used to describe (C)ACC driving behavior. The speed acceptance parameter describes the degree of acceptance of speed limits. The maximum desired speed of a vehicle at any point inside the network is either the maximum desired speed of that vehicle or the speed acceptance multiplied with the maximum speed on the specific road section the vehicle is driving. The speed acceptance parameters of (C)ACC users was set lower than the speed acceptance parameter of manual car drivers, which means that at early time periods of simulation, when the driving behavior is not yet restricted by local traffic effects, vehicles equipped with (C)ACC will drive slower. This leads to increases in delay time for manual car drivers, because their speeds might be restricted by the speed of a leading (C)ACC equipped vehicle. Therefore, decreases in speed and increases in delay time at early time periods are basically put in the simulation results by selecting these parameter settings.

When the effects of ACC and CACC systems are analyzed for bottlenecks with extreme braking, lane drops, on-ramps and weaving sections, the following results were found:

- With respect to bottlenecks where extreme braking rates are applied, an increase in market penetration of (C)ACC vehicles results in positive effects, because these systems apply smaller deceleration rates, which leads to a stabilization of traffic. This effect is partly caused by selecting lower deceleration rates for (C)ACC systems. More sophisticated versions of ACC resulted in more positive effects, as results of further reduced reaction times and following distances;
- With respect to lane drops, ACC systems show a negative effect, because the potential capacity is reduced as a consequence of larger following distances (fixed time headways). Additionally, the newer ACC scenarios also showed very small increases in disturbances, but no serious congestion was found, which indicates that the capacity limit was not close to being reached. For increasing rates of improved ACC and CACC, no clear effects were found, which indicates that these systems do not have a negative effect at lane drops;
- At on-ramps, ACC and newer ACC showed negative effects as a result of relatively high desired time headways, resulting in braking actions that might be amplified further upstream if vehicles merge at headways shorter than the desired time headway. For improved ACC, no differences with the reference situation were found, which indicates that the mean time headway should at least be as small as 1.2 seconds to prevent increases in congestion near on-ramps, as a result of increasing market penetration rates of (C)ACC. For increasing penetration rates of CACC, a positive effect was found. This might be explained by the decreases in reaction time and time headway, which limits the consequences of braking actions as results of merging vehicles;
- At weaving sections, the effects of ACC are generally negative as a result of larger following distances of ACC vehicles, which results in decreases in potential capacity. For all other (C)ACC types, both positive and negative effects are found on weaving sections. It seems that this effect is mainly due to the lay-out and characteristics of the respective weaving sections considered. At weaving sections of limited length or weaving sections with connections with limited capacity, the effects of introducing (C)ACC are generally negative. However, for normal weaving sections that do not suffer from connections with limited capacity or very limited weaving section length, the effects of increasing the market penetration rates of (C)ACC are generally positive.

For road sections at capacity, it was found that increasing market penetration rates of (C)ACC have a homogenizing effect on speed, density and flow differences between lanes. This effect was only found for road sections at capacity. Additionally, the average amount of lane changes per vehicle type was tested on six characteristic road sections, where it was found that ACC vehicles indeed apply less lane changes than human car drivers. However, for newer ACC, improved ACC and CACC, the average amount of lane changes was generally higher than human car drivers, which should not be the case according to Gorter (2015). However, this effect could be explained by the reductions in reaction time, which ensures that the minimum acceptable gaps in the gap acceptance model reduce. Therefore, a reduction in reaction time directly leads to an increase in the average amount of lane changes found in simulation.

Although microscopic simulations provided credible and reasonable results to assess the effects of ACC and CACC on traffic flow, the microscopic simulator is not fully able to simulate all specifications and features of ACC and CACC. Firstly, the simulator does not always apply the defined minimum desired time headway, because it is sometimes overruled by the V_b component of the car-following model, which will not happen in reality. This is one of the consequences of applying a safe distance car-following model. Additionally, it is currently impossible to model activation and deactivation of these (C)ACC systems. Especially on section level, it might be interesting to temporarily change driving behavior and parameters as a result of deactivating (C)ACC systems. Also, it should be able to influence lane-changing behavior in an additional way, to model the (C)ACC users that tend to change lanes less frequently. Additionally, the reaction time applies for both longitudinal and lateral driving behavior, while current ACC systems react fast to vehicles in longitudinal direction, but slower or do not react at all to vehicles in lateral direction. Another effect that cannot be captured in microscopic simulations in Aimsun yet, is that the CACC vehicles can only use a single type of driving behavior, while these systems would function as an ACC if the leading vehicle has no communication abilities and as CACC if the leading vehicle is able to communicate. Since the assumption that all vehicles have the capability to communicate with CACC vehicles was made in this research, microscopic simulation results of CACC scenarios are more positive than in studies where communication abilities between vehicles are taken into account as a (variable) vehicle characteristic.

In the exploration on whether it is possible to obtain similar results as found in microscopic simulation by using mesoscopic simulation, it was found that the general rule of thumb to translate microscopic reaction times into mesoscopic reaction times ($R_{meso} = 1.5 * R_{micro}$) did not provide satisfactory results when fixed headway settings were used in microscopic simulation. Actually, the multiplication factors that provided the best fit between microscopic and mesoscopic simulation results were different for every (C)ACC user class defined in this research. The microscopic reaction time and mean time headway parameter seem to have the most significant influence on the multiplication factor needed to translate microscopic reaction times into mesoscopic reaction times. Generally, it seems that the more restricting the (microscopic) time headway parameters are with respect to the microscopic reaction time settings, the higher the multiplication factor should be. Also, changes in acceleration and deceleration parameter settings seem to have an effect on the multiplication factor. However, clear relations between changes in microscopic parameter settings and mesoscopic reaction times when using fixed headways were not found. Therefore, mesoscopic simulation results should be interpreted with care and further research is required on the relations between microscopic and mesoscopic parameter settings.

In general, mesoscopic simulations could be used to obtain relatively similar results as found in microscopic simulation. However, it is very important to be aware of the differences in simulation results that can be found as a result of the simplifications to allow mesoscopic modelling. Generally, traffic flow patterns of microscopic and mesoscopic simulations seem to be relatively similar. However, microscopic simulations are more accurate in describing the severity of traffic flow effects caused by increasing

penetration rates of (C)ACC. Furthermore, the effects of changes in market penetration rates of ACC or CACC vehicle types on traffic flow characteristics are smaller and less clear when using mesoscopic simulations. Subsequently, the total amount of lane changes found in mesoscopic simulation was significantly lower than in microscopic simulation as a result of the network lay-out and simplifications to allow mesoscopic simulation. However, it is expected that differences in the total number of lane changes could be significantly reduced by selecting the 'penalize slow lanes' and 'penalize shared lanes' options, which were not selected in performing this research. Also, the total number of lane changes resulting from mesoscopic modelling increase when section lengths reduce, because the mesoscopic simulator only takes into account the moment and location (i.e. lane) at which a vehicle enters and leaves the road sections. Additionally, adding some spread over mesoscopic reaction times might also increase the number of lane changes found in mesoscopic simulation. The current network lay-out and mesoscopic simulation parameter settings are unsuitable to evaluate effects of (C)ACC on lane-changing using mesoscopic simulation. Therefore, it could be concluded that mesoscopic simulations could be used as indications on the effects of (C)ACC on average speed, density and delay time, but differences between different penetration rates found in mesoscopic simulation are not as clear as in microscopic simulation. Accordingly, for detailed analyses of traffic flow effects of different market penetration rates of ACC and CACC it is advised to use microscopic simulations.

8.2 Recommendations

Based on this research, several recommendations can be made. These recommendations are described in this subsection. First, recommendations for further research and how to improve this research will be provided. Subsequently, some recommendations on ACC and CACC systems will be given. Afterwards, recommendations on traffic flow on highways will be provided. Finally, recommendations on how to improve traffic modelling (of intelligent vehicles) in Aimsun will be provided.

8.2.1 Recommendations for improvement and further research

This research only gave an overview of expected effects of ACC and CACC on a part of the A15 highway, with three large junctions and multiple bottlenecks. The input parameters for describing (C)ACC driving behavior were mainly conducted from different sources of literature. However, car manufacturers are reluctant to share information on the specifications of (C)ACC systems, which means that the input parameters with respect to for example, braking abilities and system reaction times could be different in practice. More research and communication between research and car manufacturers is required to increase the realism and level of detail of research studies. Also, new developments in these systems could lead to different effects on traffic flow. Therefore, it is important to gain more insight on the system capabilities and when these systems provide positive and negative effects. This knowledge could, for example, be gained by performing field tests. Also, it might be interesting to find out whether these systems also have an effect on waiting queues at traffic lights or in the inner city.

Not only the systems itself, but also the influences of the systems on the users of the systems should be researched to find out whether drivers stay alert and are still aware of the traffic situations. Many different studies are devoted to this topic, but results differ from positive to negative behavioral adaptations.

An important assumption in this research was that (C)ACC systems were always activated and that all other vehicles were able to communicate with CACC vehicles. Thus, on- and off switching of these systems was not included, while many drivers tend to overrule the systems in complex traffic situations (Viti et al., 2008), which could have a significant effect on driving behavior and traffic flow (Pauwelussen & Feenstra, 2010). It is important to study the effects of this on- and off switching behavior and whether it brings advantages or disadvantages, both locally and network-wide. Although this topic is frequently studied (among others: (Klunder et al., 2009)), more insight should be gained. Additionally, it would have

been of added value to this study if the ACC or CACC systems could have been deactivated at specific locations where these systems have a negative effect on traffic flow, to find out whether the local traffic situations would improve if these systems cannot be used at certain bottlenecks or bottleneck types. Next to this, the communication abilities of the vehicles could be added as a parameter to give a more realistic overview on the effects of CACC systems on traffic flow.

This study examined the effects of ACC and CACC systems on a part of the A15 highway. However, it would be interesting to also study the same effects on other highways or on highways in other countries to find out whether results are similar. It could be that the results are very specific for the selected road section or traffic demand. Additionally, computing and analyzing data of the effects of ACC and CACC on more typical bottlenecks, such as weaving sections and on-ramps will provide more insight on the traffic flow effects on these bottlenecks and increases the database. If more data is gathered, conclusions could be drawn with higher certainty. Likewise, this is expected to prove the significance of the effects.

With respect to the modelling part of this research, improved car-following models should be considered to find out if different assumptions in car-following behavior show similar results. In this study, the Gipps car-following model (Gipps, 1981, 1986b) that was designed to describe human driving behavior was manipulated in such a way that it described (C)ACC driving behavior to a satisfactory extent. However, implementing car-following models designed to describe (C)ACC driving behavior might provide different results. Also, the mesoscopic models were not fully able to represent microscopic simulation results. Therefore, further research is required to find out how to convert changes in microscopic parameter settings into mesoscopic reaction times. Currently, there is no clarity on the exact relation between microscopic parameter settings and mesoscopic reaction times when using fixed headways.

8.2.2 Recommendations with respect to ACC and CACC systems

The current ACC systems need to be improved in order to have a positive effect on traffic flow. There are two important improvements to be made on reaction time and time headway settings. Currently, time gap (i.e. net headway) settings of ACC vehicles are still significantly larger than the time gaps manual drivers usually adopt. This has a negative effect on the potential achievable capacity of roadways. These effects will be minimized if smaller time gap settings can be used. With respect to reaction times, improvements should be made to reduce reaction times when vehicles from adjacent lanes merge in front of a vehicle with ACC activated, which reduces the frequency and severity of braking actions of ACC vehicles that adapt their headways to merging vehicles. The ability to detect vehicles on adjacent lanes is an important improvement. However, it should be noted that some of the newer ACC systems commercially available are already able to detect vehicles on adjacent lanes. Additionally, it is important that the ACC and CACC systems are able to work at full speed range.

In order to significantly reduce the negative effects of ACC on traffic flow, the reaction time and time headways of these systems should minimally be at certain threshold values before the effects on traffic flow could be considered positive. In this research was concluded that the maximum reaction time of these systems should be 0.4 seconds or lower. The maximum time headway should be decreased to 1.6 seconds, while the mean time headway should be approximately 1.2 seconds.

In this research, the assumption was made that all vehicles were able to send speed information to CACC equipped vehicles, which is currently not possible yet. Therefore, it is advised that when the market penetration rates of CACC systems increase, all manually driven and ACC vehicles should be equipped with vehicle-awareness devices that can transmit speed and location information to CACC systems. This could be achieved by installing a DSRC radio that frequently broadcasts a message with speed and location data, which provides the advantage that vehicles equipped with CACC are always able to efficiently make use of the CACC system (Shladover et al., 2012).

8.2.3 Recommendations with respect to traffic flow

In this subsection, general recommendations with respect to average network-wide traffic flow effects of vehicles equipped with (C)ACC are provided. Furthermore, recommendations on traffic flow effects of (C)ACC systems at specific bottleneck types and traffic situations will be provided

When looking at the average traffic flow effects found in this research, some recommendations with respect to maintaining or improving traffic flow effects on highways could be given. Firstly, the market penetration rates of ACC systems that are not able to detect vehicles on adjacent lanes, have relatively high reaction times and maintain time headways near 1.6 seconds should not be increased actively, because these systems were found to have negative effects on traffic flow and will increase average delay times.

When ACC vehicles are able to detect vehicles on adjacent lanes and reaction times are approximately 0.4 seconds and the mean time headway is near 1.6 seconds, the effects of ACC on traffic flow are predominantly positive. However, some negative results were also found, depending on the bottleneck types, traffic demand and time of day. Therefore, it might be useful to start promoting ACC systems if the ACC systems have reached these or better system specifications. However, decreasing the mean time headway would provide more positive results. When market penetration rates of these types of ACC increase, positive effects on average delay time were found in this study.

If following distances of these ACC systems decrease towards mean time headways of approximately 1.2 seconds, the traffic flow effects of increasing penetration rates of ACC systems predominantly show positive effects in terms of average speeds and delay times. Therefore, it can be advised to heavily promote the purchase and use of ACC systems, if these systems have achieved the described system specifications, because positive effects on traffic flow can be achieved by increasing market penetration rates of these ACC systems.

A positive effect on traffic flow is expected as results of the introduction of CACC vehicles. Therefore, the development of these systems is very important and should be supported. Also, if vehicles equipped with CACC systems are commercially available, it is important to stimulate the purchase of vehicles equipped with CACC systems. However, the improvements on traffic flow will be more significant if all vehicles are able to communicate with CACC vehicles, which could be achieved by installing vehicle awareness devices, such as a DSRC radio in non-CACC vehicles (Shladover et al., 2012). If all vehicles are able to communicate with CACC vehicles, a significant positive effect on traffic flow can be achieved, even at low penetration rates of CACC and in mixed traffic.

When specific traffic situations or bottleneck types are considered, the following recommendations could be made, based on the results found in this research:

- At road sections where extreme or severe braking actions are a cause of congestion, it is advisable to keep ACC and CACC systems activated, because these vehicles will apply less severe braking actions and will have a stabilizing effect on traffic flow. Additionally, these systems ensure that congestion caused by these severe braking actions will be decreased or resolved;
- At road sections with a lane drop, it is advisable to switch off ACC systems, because these systems generally decrease the potential capacity of this road section as results of the relatively large fixed time headway settings. Therefore, it is advised to place a road sign with a message to deactivate ACC systems at road sections upstream of a lane reduction. For CACC systems, no significant effects were found, which indicates that it does not make a difference whether these systems are activated or deactivated at these bottleneck types. However, since it is assumed that all vehicles have the ability to communicate with CACC vehicles, which is not the case in reality, it is also advised to deactivate these systems to minimize negative effects;

- It is advisable to deactivate (simple) ACC systems near on-ramps, because braking actions to adapt to the relatively large time headway settings will have negative effects on traffic flow near on-ramps with high traffic demands. If ACC system specifications show reaction times of 0.4 seconds maximum and maximum mean time headways of 1.2 seconds, ACC systems could stay activated, because no negative effects are found. Further improved versions of ACC could even have positive effects in this case. Increasing market penetration rates of vehicles equipped with CACC systems were found to have a positive effect on traffic flow near on-ramps, which indicates that it is advisable to keep these systems activated near on-ramps;
- Simple ACC systems should be deactivated at weaving sections, because these systems generally have a negative effect on traffic flow at weaving sections, as a result of relative large following distances applied by ACC systems. At weaving sections with limited lengths or connections with limited capacity, the effects of (C)ACC are generally negative, which means that it is advised to deactivate these systems at these types of weaving sections. However, for weaving sections that are not restricted by limited lengths of the weaving section or limited capacities of connections, the effects of increasing penetration rates of sophisticated (C)ACC systems are generally positive. Therefore, it is advised to activate more sophisticated types of (C)ACC at weaving sections where there are no significant restrictions of the length of the weaving section or capacity of connections. At this type of weaving sections, disturbances are mainly caused by lane-changing behavior;
- It is profitable to activate ACC or CACC on road sections at capacity or in congestion, because this will have a homogenizing effect on speed, flow and density differences between lanes. This suggests that traffic is stabilized. Additionally, this also appears to increase traffic safety, since speed differences between lanes are reduced when market penetration rates of (C)ACC increase.

8.2.4 Recommended improvements for traffic modelling in Aimsun

Since modelling and simulating intelligent vehicles in Aimsun was an important element of this research, some recommendations on both microscopic and mesoscopic traffic modelling in Aimsun could be made. Additionally, some recommendations on simulation output are presented.

Based on this research, the following recommendations with respect to microscopic traffic modelling (of intelligent vehicles) are presented:

- To model (current) ACC systems more accurately, the microscopic reaction time should be split into two separate reaction times for longitudinal car-following behavior and lateral lane-changing behavior. From personal experiences in driving with activated ACC systems, it was found that the ACC system reacts fast to a leading vehicle driving in the same lane. However, if a vehicle from an adjacent lane merges directly in front of the vehicle equipped with ACC, it takes a relatively long time before the merging vehicle is detected by the ACC system. Currently, the simulation model uses a single reaction time to describe both these types of reaction times. When reaction times are split, this enables the option to more accurately model vehicles with ACC systems that are unable to detect vehicles on adjacent lanes, by selecting low reaction times for the longitudinal car-following behavior and relatively high reaction times for the lateral lane-changing behavior;
- To model (C)ACC more accurately, a lane-changing willingness (or laziness) parameter should be added as vehicle parameter. This would ensure that the (un)desire to change lanes or overtake other vehicles could be represented with a value or factor, which includes the possibility to differentiate between user classes that often change lanes to overtake other vehicles and drivers that tend to stay in the same lane. Also, this enables the possibility to more accurately model (C)ACC users with short reaction times and a tendency to stay in the same lane;
- To model (C)ACC more accurately, include the possibility of activating and deactivating intelligent systems. Therefore, it should be possible to temporarily change the driving behavior of a vehicle

- class. Changes in the driving behavior might be triggered by local traffic characteristics or at certain road sections or road types inside the network;
- To allow for more realistic modelling of (C)ACC driving behavior, include the possibility of applying a constant time gap policy for intelligent vehicles, which is not restricted by the V_b component of the current car-following model;
 - In order to improve the accuracy of modelling (C)ACC even more, improved car-following models or platforms should be considered to enable the possibility to look more vehicles ahead and model interaction between vehicles. Especially when modelling CACC driving behavior, it is important to include interaction between vehicles.

Furthermore, the following recommendations for mesoscopic modelling of intelligent vehicles are made:

- Conduct further research to gain more insight in the relations between microscopic parameter settings and mesoscopic reaction times, especially when using fixed headway settings, before directly using mesoscopic simulations to evaluate the effects of intelligent vehicles on traffic flow;
- Model lane changes more accurately by reducing the lengths of road sections and selecting the 'penalize slow lanes' and 'penalize shared lanes' options.

Based on this research, the following recommendations on simulation output and indicators to describe the effects of increasing market penetration rates of (C)ACC are presented:

- Include an indicator that provides the average number of lane changes per vehicle type over the whole network in order to gain insight in the lane-changing behavior of specific vehicle types. This indicator should be added for microscopic and mesoscopic simulation;
- Adding an indicator on traffic safety to the microscopic simulation output might add value, even though the car-following model is a safe distance or collision avoidance model. Therefore, it might be a good suggestion to add surrogate safety measures, such as Time-to-Collision (TTC), Post Encroachment Time (PET), Time Exposed Time-to-collision (TET), Time Integrated Time-to-collision (TIT), Crash Index (CI) or Modified Time-to-Collision (MTTC) as discussed by Archer & Kosonen (2000), Gettman & Head (2003), Minderhoud & Bovy (2001) and Ozbay, Yang, Bartin, & Mudigonda (2008). To indicate traffic safety in mesoscopic simulation results, an equivalent indicator should be added.

8.3 Reflection

The importance of reflection in science is high. In a three-year case study, Baird, Fensham, Gunstone, & White (1991) concluded that reflection does not only improve the quality of an individuals practice, but also improves knowledge, awareness and control of themselves. Therefore, a reflection on this research is provided in this subsection.

Before starting with my master thesis, I had to determine the topic in which I liked to do research. From the courses I followed, I found out that the fields of intelligent vehicles, traffic flow, traffic simulation and traffic management interested and inspired me the most. Therefore, I started looking for a thesis assignment involving one or a combination of these topics. Shortly after, I found an assignment on using traffic simulations to gain more insight in the effects of (C)ACC on traffic flow. In my opinion, this was a very inspiring and interesting research topic and assignment, even despite of my relatively limited experience with traffic simulation.

The English business magnate Richard Branson once said: "If somebody offers you an amazing opportunity but you are not sure you can do it, say yes – then learn how to do it later!" This quote was quite applicable, although I was sure I could do it, I knew I would have to work hard for it. Therefore, at the start of this research, I directly got my hands dirty and started experimenting and playing with the traffic simulation program, Aimsun, to learn how to use it. Additionally, I had to study literature and gain more

insight in the topic to formulate the research problem, goals and questions. After all, this process went well and motivated me even more.

After determining the research outline, the calibration of the model and network was the following step. The calibration process took much more time than I expected, because it was quite hard to make the simulation output fit real traffic data and to get both the microscopic and mesoscopic reference scenarios representative. I experienced the calibration of the microscopic model as a complicated process, because many changes were required as a result of differences between mesoscopic and microscopic modelling approaches. However, after some serious effort, the models and network were calibrated to a satisfactory extent, which was joyful, because it is the foundation of the research and is very important for determining the influences of ACC and CACC on traffic flow.

Subsequently, the driving behavior of the ACC and CACC vehicles had to be modelled, which involved testing with the simulation model and comparing the results with literature, which was quite an interesting thing to do. It also sharpened my modelling, problem-solving and analyzing skills, because it is important to understand why specific parameter settings have to be changed and what effect it has on simulation output. When the driving behavior of these vehicles was defined, it was time to design and run scenarios with differing market penetration rates of these vehicles.

During and after running the scenarios, it was time to analyze the results and find out what influences these vehicles had on the simulation results and traffic flow. This was one of the most interesting parts of this research, because I found several effects, but also got even more curious about the effects of these vehicles. I hope and think that the results presented in this research provide some valuable information and insights on the effects of ACC and CACC on traffic flow. Because of the promising results, I got inspired to increase the number of bottlenecks to assess the effects on traffic flows. At late stages of the research, all simulations were run again, in order to improve the quality of the research. Although, it was quite annoying to gather results and analyze the data all over again, I think it definitely increases the quality of this study and I am satisfied that this decision was made. In my opinion, some interesting results were gathered, which have not been indicated in literature yet. I am especially proud of the different effects found for some specific bottleneck types on a realistic traffic network.

Also, a quick-scan on the extent to which mesoscopic simulation could be used to show similar traffic flow effects for (C)ACC scenarios was performed. Before starting with this part of the research, I was doubtful whether it was possible to represent microscopic simulation results using mesoscopic simulations. To some extent, it was possible to represent these results, but some clear differences were also found. Unfortunately, clear relations between microscopic and mesoscopic simulation parameters were not found yet. However, the results found in this part research provided insight into the relation between microscopic and mesoscopic modelling and gave direction to further research topics.

The last part of this research was writing the report. Luckily, I already started writing the report during the research period. Nevertheless, it was quite intense to finish writing the report and fine-tune it further. Although, this was a time-consuming part of the research, I tried and, in my opinion, managed to write the report in a clear and understandable way and to give a wide and clear overview of the effects of ACC and CACC on traffic flow found in this research.

Overall, I am confident and satisfied with the results of this research and I hope this research will contribute to the knowledge about the effects of (Cooperative) Adaptive Cruise Control and the field of research on traffic simulation and intelligent vehicles. In my opinion, one of the main contributions is that the effects of (C)ACC are explored on a realistic network with multiple bottlenecks, where bottlenecks could be of different bottleneck types.

Bibliography

- Ahn, S., & Cassidy, M. J. (2007). *Freeway traffic oscillations and vehicle lane-change maneuvers*. Paper presented at the Transportation and Traffic Theory 2007. Papers Selected for Presentation at ISTTT17.
- Alkim, T. P., Bootsma, G., & Looman, P. (2007). *The assisted driver: systems that support driving*. Delft: Rijkswaterstaat.
- Alkim, T. P., Schuurman, H., & Tampere, C. M. J. (2000). *Effects of External Cruise Control and Cooperative Following on Highways: an Analysis with the MIXIC Traffic Simulation Model*. Paper presented at the IEEE Intelligent Vehicles Symposium, Proceedings.
- Archer, J., & Kosonen, I. (2000). *The potential of micro-simulation modelling in relation to traffic safety assessment*. Paper presented at the ESS conference proceedings, Hamburg.
- Baird, J. R., Fensham, P. J., Gunstone, R. F., & White, R. T. (1991). The importance of reflection in improving science teaching and learning. *Journal of research in Science Teaching*, 28(2), 163-182.
- Barth, M., Boriboonsomsin, K., & Wu, G. (2014). Vehicle Automation and Its Potential Impacts on Energy and Emissions *Road Vehicle Automation* (pp. 103-112): Springer.
- Bianchi Piccinini, G. F., Rodrigues, C. M., Leitão, M., & Simões, A. (2015). Reaction to a critical situation during driving with adaptive cruise control for users and non-users of the system. *Safety science*, 72, 116-126.
- Bose, A., & Ioannou, P. (2003). Mixed manual/semi-automated traffic: a macroscopic analysis. *Transportation Research Part C: Emerging Technologies*, 11(6), 439-462.
- Brackstone, M., & McDonald, M. (1999). Car-following: a historical review. *Transportation Research Part F: Traffic Psychology and Behaviour*, 2(4), 181-196.
- Browand, F., McArthur, J., & Radovich, C. (2004). Fuel saving achieved in the field test of two tandem trucks. *California Partners for Advanced Transit and Highways (PATH)*.
- Bu, F., Tan, H.-S., & Huang, J. (2010). *Design and field testing of a cooperative adaptive cruise control system*. Paper presented at the American Control Conference (ACC).
- Davis, L. C. (2004). Effect of adaptive cruise control systems on traffic flow. *Physical Review E - Statistical, Nonlinear, and Soft Matter Physics*, 69(6 2), 066110-066111-066110-066118.
- Deng, Q., & Ma, X. (2015). *A Simulation Platform for Autonomous Heavy-duty Vehicle Platooning in Mixed Traffic*. Paper presented at the Transportation Research Board 94th Annual Meeting.
- Gettman, D., & Head, L. (2003). Surrogate safety measures from traffic simulation models. *Transportation Research Record: Journal of the Transportation Research Board*(1840), 104-115.
- Gipps, P. G. (1981). A behavioural car-following model for computer simulation. *Transportation Research Part B: Methodological*, 15(2), 105-111.
- Gipps, P. G. (1986a). A model for the structure of lane-changing decisions. *Transportation Research Part B: Methodological*, 20(5), 403-414.
- Gipps, P. G. (1986b). Multsim: a model for simulating vehicular traffic on multi-lane arterial roads. *Mathematics and Computers in Simulation*, 28(4), 291-295.
- Google. (2016). Typical traffic. Retrieved May 2, 2016, from <https://www.google.nl/maps/@51.8621491,4.4795055,13z/data=!5m1!1e1>
- Gorter, C. M. (2015). *Adaptive Cruise Control in Practice: A Field Study and Questionnaire into its influence on Driver, Traffic Flows and Safety*. (Master of Science Transport and Planning), Delft University of Technology, Delft.
- Hoedemaeker, M., & Brookhuis, K. A. (1998). Behavioural adaptation to driving with an adaptive cruise control (ACC). *Transportation Research Part F: Traffic Psychology and Behaviour*, 1(2), 95-106.
- Hourdakis, J., Michalopoulos, P. G., & Kottommannil, J. (2003) Practical Procedure for Calibrating Microscopic Traffic Simulation Models. *Transportation Research Record* (pp. 130-139).
- Jha, M., Gopalan, G., Garms, A., Mahanti, B., Toledo, T., & Ben-Akiva, M. (2004). Development and Calibration of a Large-Scale Microscopic Traffic Simulation Model. *Transportation Research Record: Journal of the Transportation Research Board*, 1876, 121-131.
- Kerner, B. S., & Klenov, S. L. (2003). Microscopic theory of spatial-temporal congested traffic patterns at highway bottlenecks. *Physical Review E*, 68(3), 036130.

- Kesting, A., Treiber, M., & Helbing, D. (2010). Enhanced intelligent driver model to access the impact of driving strategies on traffic capacity. *Philosophical Transactions of the Royal Society of London A: Mathematical, Physical and Engineering Sciences*, 368(1928), 4585-4605.
- Kesting, A., Treiber, M., Schönhof, M., & Helbing, D. (2007). Extending adaptive cruise control to adaptive driving strategies. *Transportation Research Record: Journal of the Transportation Research Board*, 16-24.
- Kesting, A., Treiber, M., Schönhof, M., & Helbing, D. (2008). Adaptive cruise control design for active congestion avoidance. *Transportation Research Part C: Emerging Technologies*, 16(6), 668-683.
- Kesting, A., Treiber, M., Schönhof, M., Kranke, F., & Helbing, D. (2007). Jam-avoiding adaptive cruise control (ACC) and its impact on traffic dynamics *Traffic and Granular Flow'05* (pp. 633-643): Springer.
- Kikuchi, S., Uno, N., & Tanaka, M. (2003). Impacts of shorter perception-reaction time of adapted cruise controlled vehicles on traffic flow and safety. *Journal of transportation engineering*, 129(2), 146-154.
- Klunder, G., Li, M., & Minderhoud, M. (2009). Traffic flow impacts of adaptive cruise control deactivation and (re) activation with cooperative driver behavior. *Transportation Research Record: Journal of the Transportation Research Board*(2129), 145-151.
- Labuhn, P. I., & Chundrik, W. J. (1995). Adaptive cruise control: Google Patents.
- Liang, K.-Y., Mårtensson, J., & Johansson, K. H. (2013). *When is it fuel efficient for a heavy duty vehicle to catch up with a platoon?* Paper presented at the 7th IFAC Symposium on Advances in Automotive Control, Tokyo, Japan, September 4-7, 2013.
- Madi, M. Y. (2016). Investigating and Calibrating the Dynamics of Vehicles in Traffic Micro-simulations Models. *Transportation Research Procedia*, 14, 1782-1791.
- Marsden, G., McDonald, M., & Brackstone, M. (2001). Towards an understanding of adaptive cruise control. *Transportation Research Part C: Emerging Technologies*, 9(1), 33-51.
- Mehlenbacher, B., Wogalter, M. S., & Laughery, K. R. (2002). *On the reading of product owner's manuals: Perceptions and product complexity*. Paper presented at the Proceedings of the Human Factors and Ergonomics Society Annual Meeting.
- Milanés, V., & Shladover, S. E. (2014). Modeling cooperative and autonomous adaptive cruise control dynamic responses using experimental data. *Transportation Research Part C: Emerging Technologies*, 48, 285-300.
- Milanés, V., & Shladover, S. E. (2015). Handling Cut-In Vehicles in Strings of Cooperative ACC Vehicles. *Journal of Intelligent Transportation Systems*, 1-14.
- Minderhoud, M. M., & Bovy, P. H. (2001). Extended time-to-collision measures for road traffic safety assessment. *Accident Analysis & Prevention*, 33(1), 89-97.
- Moriasi, D. N., Arnold, J. G., Van Liew, M. W., Bingner, R. L., Harmel, R. D., & Veith, T. L. (2007). Model evaluation guidelines for systematic quantification of accuracy in watershed simulations. *Transactions of the ASABE*, 50(3), 885-900.
- Mullakkal-Babu, F. A., Wang, M., Van Arem, B., & Happee, R. (2016). Full Range Adaptive Cruise Control for String Stability [Preprint, for review only]. *2016 IEEE Intelligent Vehicles Symposium*.
- Munoz, J. C., & Daganzo, C. F. (2002). The bottleneck mechanism of a freeway diverge. *Transportation Research Part A: Policy and Practice*, 36(6), 483-505.
- National Data Warehouse for traffic information. (2014). Average traffic flows for 2014.
- National Data Warehouse for traffic information. (2016). Loop detector data 2016.
- Nau, R. F. (2016). Statistical forecasting: notes on regression and time series analysis. Retrieved June 30, 2016, <http://people.duke.edu/~rnau/rsquared.htm>
- Ozbay, K., Yang, H., Bartin, B., & Mudigonda, S. (2008). Derivation and validation of new simulation-based surrogate safety measure. *Transportation Research Record: Journal of the Transportation Research Board*(2083), 105-113.
- Papacharalampous, A. E., Wang, M., Knoop, V. L., Ros, B. G., Takahashi, T., Sakata, I., . . . Hoogendoorn, S. P. (2015). *Mitigating Congestion at Sags with Adaptive Cruise Control Systems*. Paper presented at the Intelligent Transportation Systems (ITSC), 2015 IEEE 18th International Conference on.
- Pauwelussen, J., & Feenstra, P. J. (2010). Driver behavior analysis during ACC activation and deactivation in a real traffic environment. *Intelligent Transportation Systems, IEEE Transactions on*, 11(2), 329-338.

- Rudin-Brown, C. M., & Parker, H. A. (2004). Behavioural adaptation to adaptive cruise control (ACC): implications for preventive strategies. *Transportation Research Part F: Traffic Psychology and Behaviour*, 7(2), 59-76.
- SAE International. (2014). SAE International Technical Standard Provides Terminology for Motor Vehicle Automated Driving Systems [Press release]. Retrieved February 24, 2016, from http://www.sae.org/servlets/pressRoom?OBJECT_TYPE=PressReleases&PAGE=showRelease&RELEASE_ID=2715
- Schakel, W. J., & van Arem, B. (2014). Improving traffic flow efficiency by in-car advice on lane, speed, and headway. *Intelligent Transportation Systems, IEEE Transactions on*, 15(4), 1597-1606.
- Schakel, W. J., van Arem, B., & Netten, B. D. (2010). *Effects of cooperative adaptive cruise control on traffic flow stability*. Paper presented at the Intelligent Transportation Systems (ITSC), 2010 13th International IEEE Conference on.
- Shladover, S., Su, D., & Lu, X.-Y. (2012). Impacts of Cooperative Adaptive Cruise Control on Freeway Traffic Flow. *Transportation Research Record: Journal of the Transportation Research Board*, 2324, 63-70.
- Strand, N., Nilsson, J., Karlsson, I. C. M., & Nilsson, L. (2011). Exploring end-user experiences: Self-perceived notions on use of adaptive cruise control systems. *IET Intelligent Transport Systems*, 5(2), 134-140.
- Transport Simulation Systems. (2014). Aimsun 8.1 Dynamic Simulators Users' Manual.
- Transport Simulation Systems. (2015). Aimsun. Retrieved February 15, 2016, from <https://www.aimsun.com/wp/aimsun/>
- van Arem, B., van Driel, C. J., & Visser, R. (2006). The Impact of Cooperative Adaptive Cruise Control on Traffic-Flow Characteristics. *Intelligent Transportation Systems, IEEE Transactions on*, 7(4), 429-436.
- van Driel, C. J. G., & van Arem, B. (2010). The impact of a congestion assistant on traffic flow efficiency and safety in congested traffic caused by a lane drop. *Journal of Intelligent Transportation Systems: Technology, Planning, and Operations*, 14(4), 197-208.
- van Twuijver, M., & Pol, M. (2004). *Car Owners' Experiences with In-car Speed Controlling Systems in the Netherlands*. Paper presented at the Proceedings of the European Transport Conference (ETC) 2004, Held 4-6 October 2004, Strasbourg, France.
- VanderWerf, J., Shladover, S. E., Miller, M., & Kourjanskaia, N. (2002). Effects of adaptive cruise control systems on highway traffic flow capacity. *Transportation Research Record: Journal of the Transportation Research Board*, 1800, 78-84.
- Viti, F., Hoogendoorn, S. P., Alkim, T. P., & Bootsma, G. (2008). *Driving behavior interaction with ACC: results from a Field Operational Test in the Netherlands*. Paper presented at the Intelligent Vehicles Symposium, 2008 IEEE.
- Vits, A., Hodac, I., Mossé, O., & Jaaskelainen, J. (2002). Final Report of the eSafety Working Group on Road Safety. *Information Society Technologies and European Commission*.
- Wang, M., Daamen, W., Hoogendoorn, S. P., & van Arem, B. (2015). Cooperative Car-Following Control: Distributed Algorithm and Impact on Moving Jam Features.

Appendix A - Validation check

This Appendix will handle all the different detector locations used for the validation check. The speed and flow plots over time will be given for the loop detector data, mesoscopic simulation results and microscopic simulation results. In some cases, calibration counts will also be provided.

The validation locations are shown and numbered in *Figure 151*. The loop detector was collected by the National Data Warehouse for traffic information (2016), NDW. The application Dataack, developed by Royal HaskoningDHV and PathMobility, was used to read the loop detector data. This application stores all the detector data and can be used to visualize patterns in the detector data. In this case, speed and density plots over some detectors were used to store the speeds and flows from 14:15 to 19:30 for every time step of 15 minutes. These values will be compared with the microscopic and mesoscopic simulation results. For flow comparisons, the first and last time periods (i.e. warmup and cooldown period) are excluded. The flow and speed plots will be shown per location and an explanation on the results is added. In the explanation, the goodness of fit will be discussed and elaborated upon.

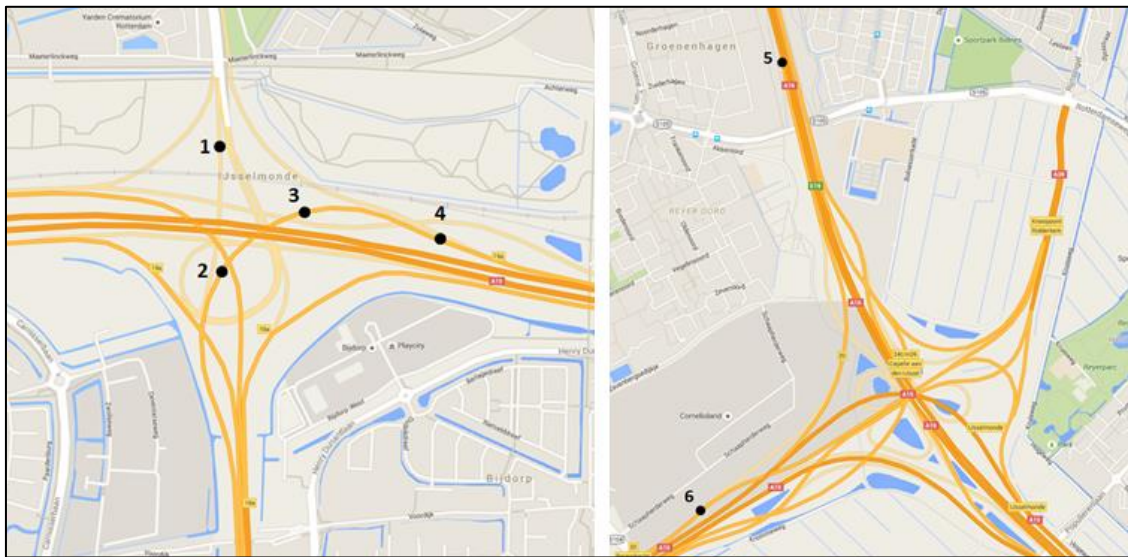


Figure 151 - Loop detector locations

The critical locations where the simulation results and NDW data are compared are locations where congestion occurs or where the traffic is put on the network. These locations are chosen to be at the junctions Vaanplein and Ridderkerk, because the most important congestion fronts were found at these locations. Loop detector data of 2016 will be used to validate the calibration. Data of 2016 is used, which is in line with the congestion patterns displayed by Google (2016) and this data is expected to show the effect of the extended A4, which was completed at the end of 2015. First, an average of the available loop detector data from the 1st of January 2016 until the 31st of March 2016 is used. This average is computed for weekdays, while Saturdays, Sundays and public holidays are filtered. Secondly, the loop detector data of a representative day with a significant amount of congestion will be used. The reason for this is that the average congestion patterns are often smaller than representative congestion patterns, because some days could be free of congestion. February 29, 2016 was found to show a representative amount of congestion and was chosen as the representative day. Additionally, the calibration has been performed in such a way that some serious congestion has been found, which means that in some cases the simulation results are expected to fit the representative day better than an average weekday.

To indicate the model fit with the traffic data, the R^2 statistic is used. The coefficient of determination [R^2] is a statistic that gives information about the goodness of fit of a model. An R^2 of 1 indicates that the model

fits the data perfectly, while a R^2 of 0 indicates that the model does not fit the data at all. Values of R^2 range from 0 to 1 and represent the proportion of the variance in the measured data that can be explained by the model. Higher values indicate less error variance. In general, R^2 values above 50% are considered to be acceptable (Moriassi et al., 2007), although this is very dependent on the type of study that is conducted. Although, this statistic is oversensitive to high extreme values (outliers) and insensitive to additive and proportional differences between model prediction and measured data (Moriassi et al., 2007). Generally speaking, a R^2 of 0.75 or higher is considered to be satisfactory for this study, because this indicates that the standard deviation of the errors is exactly one-half of the standard deviation of the dependent variable, which means that at least 50% of the standard deviation is explained by the model (Nau, 2016). However, lower values of this statistic might also be considered to be acceptable if the deviations can be explained.

Whenever possible, the microscopic and mesoscopic speed and flow simulation results are compared with the average weekday, representative day and calibration values. The coefficient of determination is depicted for any of these combinations and tested.

Detector location 1

This detector is located at the north side of junction Vaanplein. *Figure 152* shows the flows from simulation and traffic data per 15 minute periods.

Table 26 gives the corresponding coefficients of determination.

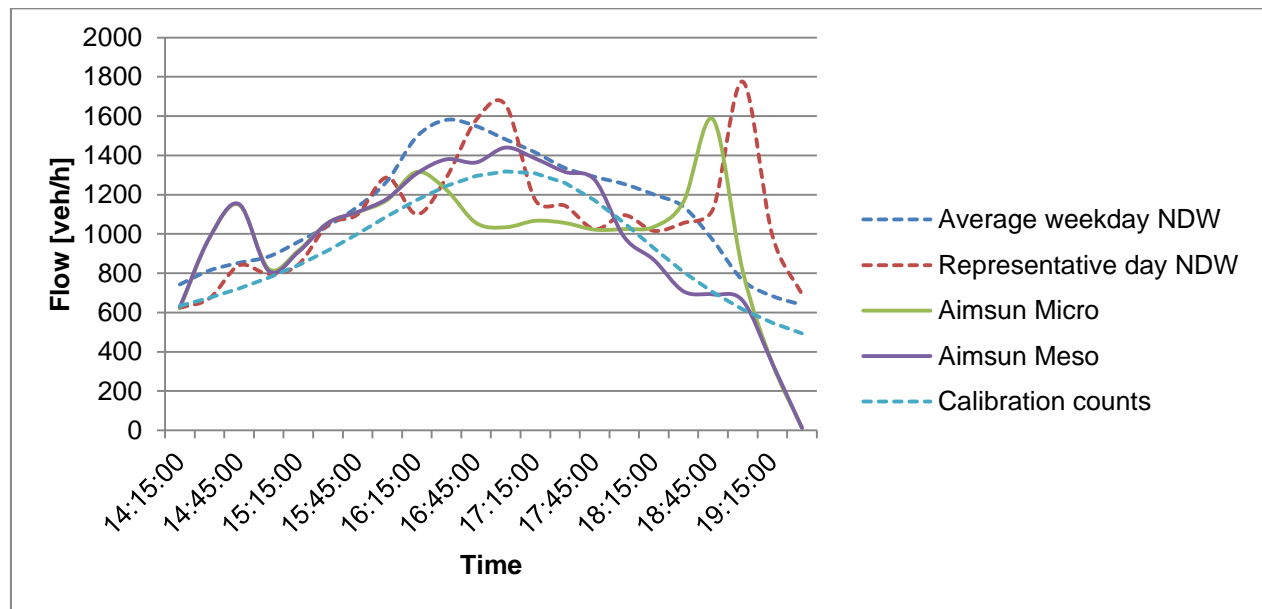


Figure 152 - Flows per 15 minutes for detector location 1

Table 26 - Coefficients of determination [R^2] for the flows at detector location 1

	Micro	Meso
Average weekday	0.219	0.671
Representative day	0.005	0.069
Calibration counts	0.121	0.795

For the mesoscopic simulation results for detector location 1, the simulation results are within the acceptable margin with respect to the calibration counts. Additionally, the mesoscopic simulation flows resemble the pattern of the average weekday, except for some outliers. The microscopic simulation flows show very low R^2 -value and require some attention. However, if the flow over time at detector location 1 is

compared with the flow pattern at the representative weekday (*Figure 152*), it is found that the pattern is very similar. Both the microscopic simulation flows and representative day flows show two serious peaks. However, the peaks in the microscopic simulation results are somewhat shifted in time and are found at earlier time periods. The microscopic flows peak at approximately 16:15 and 18:45, while the peaks for the representative day are found at approximately 17:00 and 19:00. Since these peaks are found for different time periods, these differences contribute to decreasing values of R^2 , since extreme outliers are found in these occasions. In terms of validation, the combination of the microscopic flows and representative day flows is accepted, because the patterns are very similar, but slightly shifted in time.

Figure 153 shows the speeds from simulation and traffic data per 15 minute periods, while *Table 27* provides the corresponding coefficients of determination.

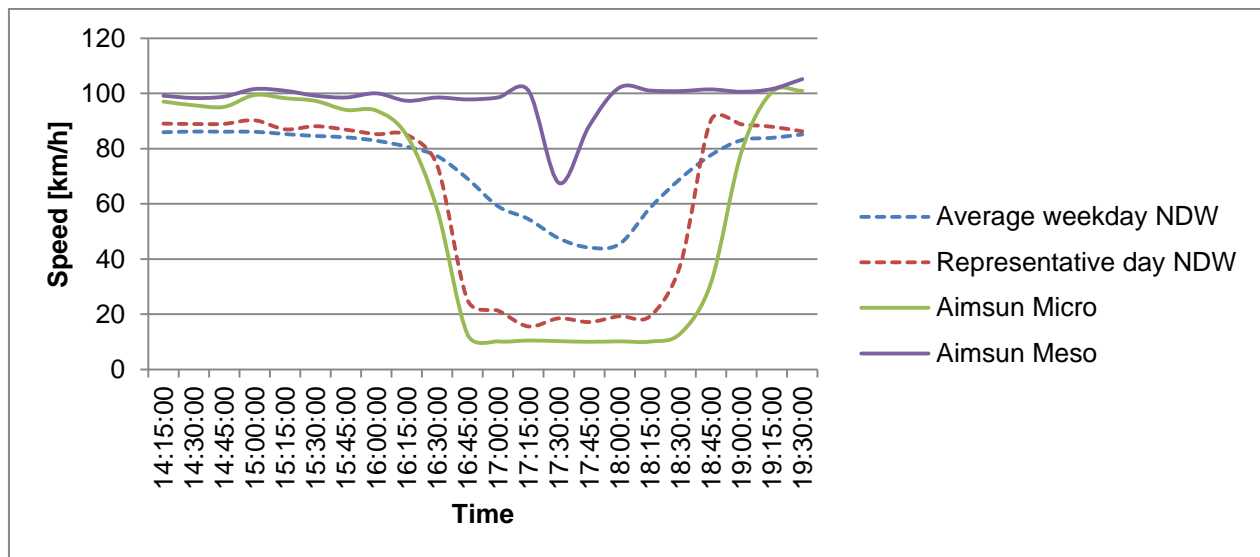


Figure 153 - Speeds per 15 minutes for detector location 1

Table 27 - Coefficients of determination [R^2] for the speeds at detector location 1

	Micro	Meso
Average weekday	0.809	0.238
Representative day	0.853	0.151

From *Figure 153*, it can be concluded that the microscopic simulation pattern follows the speed pattern of the representative day very well. Also, the average day shows a similar pattern. The coefficients of determination for the microscopic speeds are both above the acceptable limits. In the mesoscopic speed patterns, some congestion is found over a significantly smaller period of time. However, this could be explained by the fact that almost no congestion and speed reduction was found in the simulation. One of the most important reasons for this congestion are the lane changes and braking rates downstream, which cannot be modelled as efficiently in the mesoscopic simulation, due to simplifications in the behavioral models.

However, the mesoscopic speed results are relatively far off, because this location does not suffer serious congestion in the mesoscopic simulation, while the average and representative weekday show more congestion (*Figure 153*). It is expected that this congestion front is caused by lane-changing behavior of drivers and some braking actions downstream, which cannot be modelled as efficiently in the mesoscopic simulation, due to simplifications. Therefore, the severity of congestion at this location could not be included sufficiently in the mesoscopic simulation. However, since the reason for this problem is known, this flaw is still accepted in terms of validation, because the mesoscopic simulation does show some

congestion in a comparable pattern, albeit that the severity and duration of congestion is significantly lower.

Detector location 2

This detector is located at junction Vaanplein. *Figure 154* shows the flows from simulation and traffic data per 15 minute periods. *Table 28* gives the coefficients of determination between simulation results and traffic data.

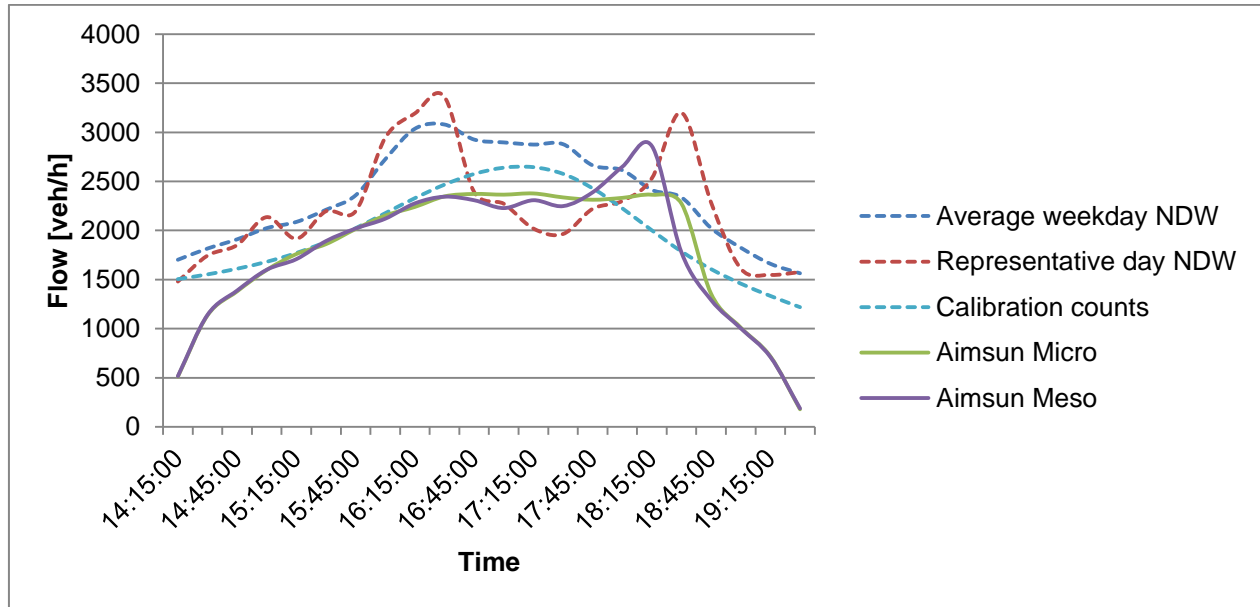


Figure 154 - Flows per 15 minutes for detector location 2

Table 28 - Coefficients of determination [R^2] for the flows at detector location 2

	Micro	Meso
Average weekday	0.807	0.697
Representative day	0.407	0.299
Calibration counts	0.777	0.685

From *Figure 154* can be concluded that both the microscopic flow pattern follows the average weekday and calibration counts relatively well. The corresponding coefficients of determination are also above the limit of 0.75 for these combinations (*Table 28*). However, the mesoscopic simulation flow pattern does show a peak, similar to the representative day. However, when looking at the flow patterns from mesoscopic simulation, it is found that the calibration counts are similar until 16:30, after which a similar flow pattern as the representative weekday is found. Although, the peak is slightly shifted in time, which results in decreasing values of R^2 . Additionally, this road section requires some time to be filled and flushed, which takes more than one time period for these locations and also contributes to decreasing values of R^2 due to outliers. Nevertheless, the mesoscopic simulation results show a comparable flow pattern if the calibration counts and representative weekday are considered at different time periods. The deviations can be explained, meaning that these flow patterns could be accepted in terms of validation.

Figure 155 shows the average speeds resulting from mesoscopic and microscopic simulation and the traffic data per 15 minute periods. *Table 29* provides the corresponding coefficients of determination of combinations of simulations and traffic data.

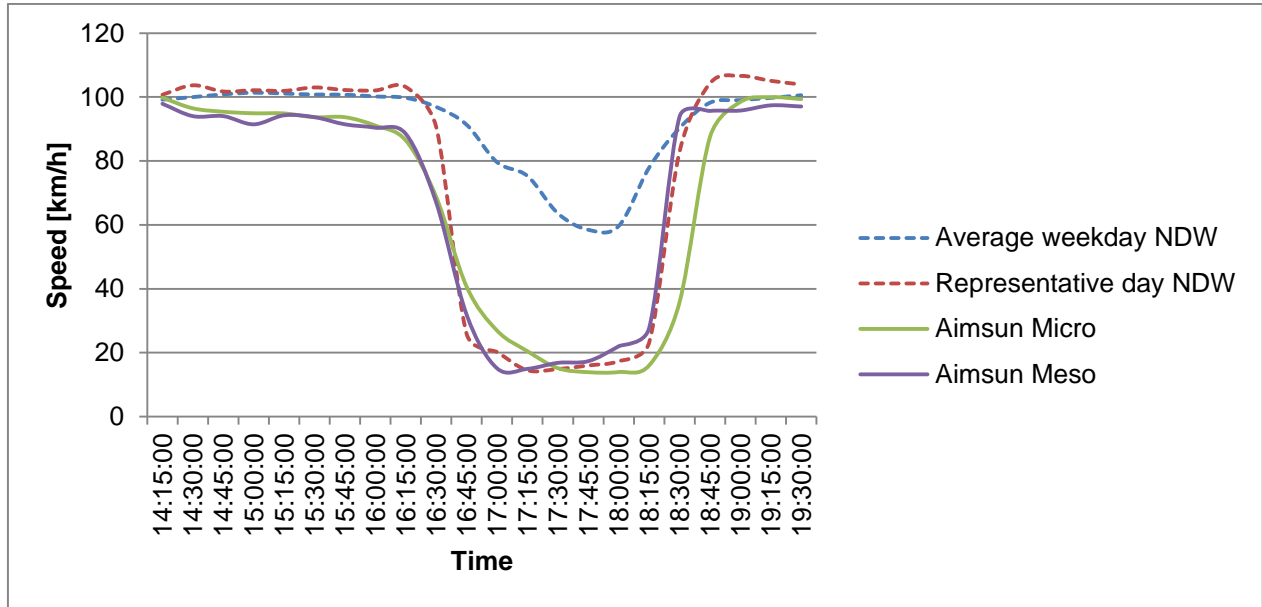


Figure 155 - Speeds per 15 minutes for detector location 2

Table 29 - Coefficients of determination $[R^2]$ for the speeds at detector location 2

	Micro	Meso
Average weekday	0.840	0.798
Representative day	0.911	0.970

In Figure 155, the microscopic and mesoscopic simulation speeds are very similar to the speed pattern of the representative day. However, the average weekday also shows a similar behavior, with smaller speed decreases. Table 29 shows that all the coefficients of determination are acceptable in all cases.

Detector location 3

This detector is also located at junction Vaanplein. Figure 156 shows the flows from simulation and traffic data per 15 minute periods. Table 30 provides the corresponding coefficients of determination.

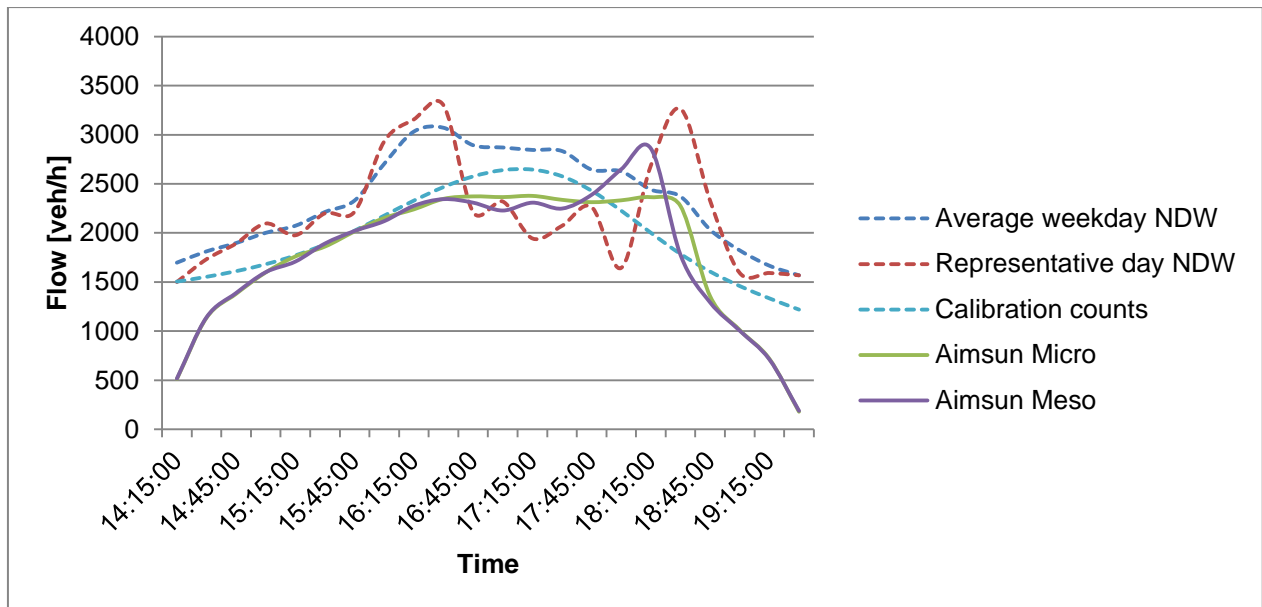


Figure 156 - Flows per 15 minutes for detector location 3

Table 30 - Coefficients of determination [R^2] for the flows at detector location 3

	Micro	Meso
Average weekday	0.817	0.709
Representative day	0.313	0.200
Calibration counts	0.777	0.685

The flows resulting from microscopic simulation follow the flow patterns of the average weekday and calibration counts relatively well, as can be seen in *Figure 156*. This is also shown in *Table 30*, where it is indicated that the coefficients of determination are above 0.75. The mesoscopic simulation flows could not be validated directly. Like detector location 2, it is found that the calibration counts are similar to the mesoscopic flow results until 16:30, after which a similar flow pattern as the representative weekday is found. Although, the peak is slightly shifted in time, which results in decreasing values of R^2 . Additionally, these links need quite some time to be filled and flushed, which takes more than one time period for these locations and also contributes to decreasing values of R^2 due to outliers at the start and end of simulation. Nevertheless, the mesoscopic simulation results show a comparable flow pattern if the calibration counts and representative weekday are considered at different time periods. The deviations can be explained, meaning that these flow patterns could be accepted in terms of validation.

Figure 157 provides the speeds from simulation and traffic data per 15 minute periods. *Table 31* gives the corresponding coefficients of determination for combinations of simulation results and traffic data used for calibration and validation.

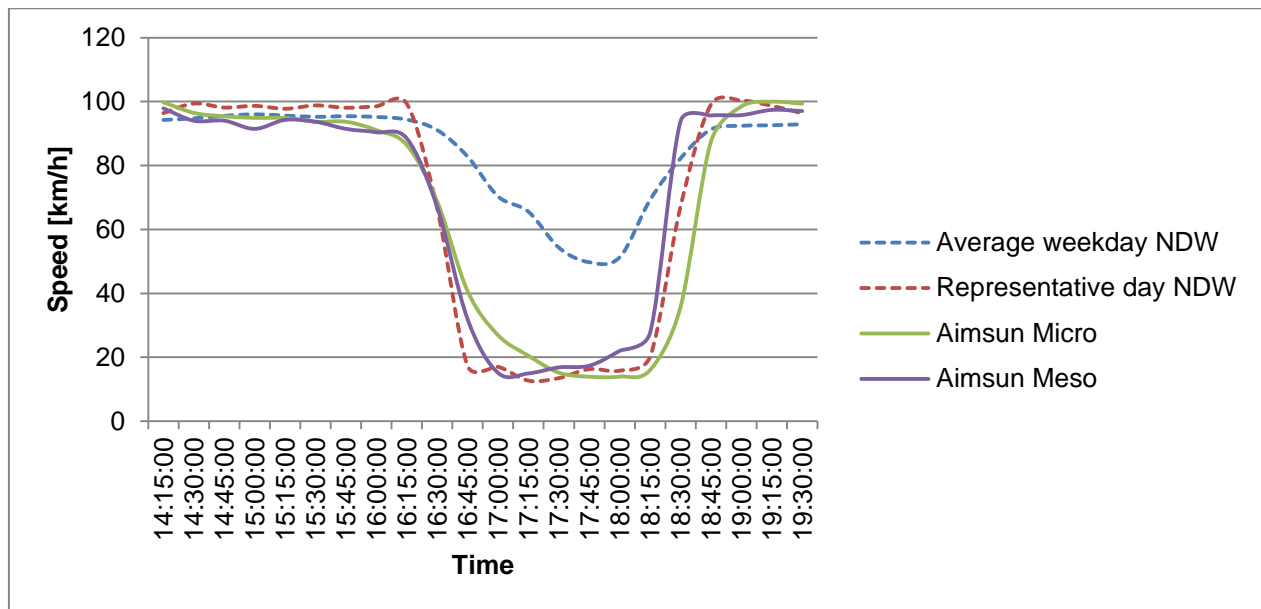


Figure 157 - Speeds per 15 minutes for detector location 3

Table 31 - Coefficients of determination [R^2] for the speeds at detector location 3

	Micro	Meso
Average weekday	0.863	0.817
Representative day	0.933	0.956

From *Figure 157* can be concluded that the speed patterns resulting from microscopic and mesoscopic simulation are very similar to the representative day at this detector location. Additionally, the average weekday also shows a similar pattern. *Table 31* also indicates that the goodness of fit is within the acceptable margins and is validated. The coefficients of determination are very high for the combinations of simulations results with traffic data from the representative day

Detector location 4

This detector is also located at junction Vaanplein. *Figure 158* shows the flows from simulation and traffic data per 15 minute periods. *Table 32* provides the corresponding coefficients of determination for combinations of simulation results with traffic data.

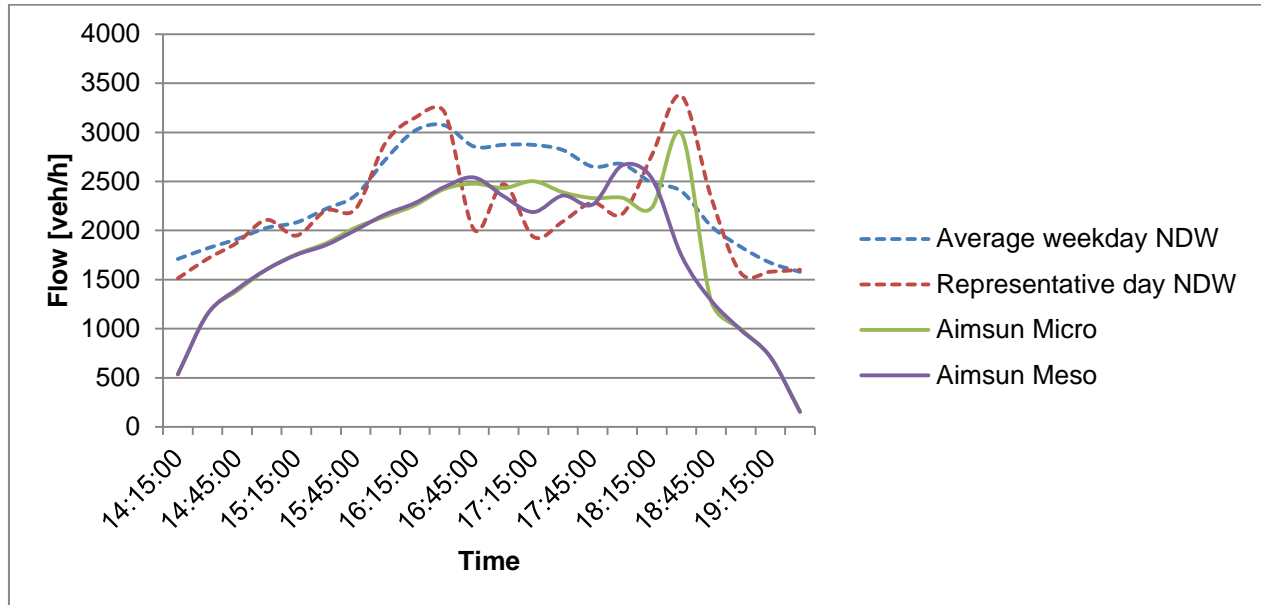


Figure 158 - Flows per 15 minutes for detector location 4

Table 32 - Coefficients of determination [R^2] for the flows at detector location 4

	Micro	Meso
Average weekday	0.733	0.815
Representative day	0.449	0.266

Flows from mesoscopic simulation follow the patterns found at the average weekday relatively well. *Table 32* shows that the coefficient of determination is within the acceptable limits for the average weekday, which could probably be explained by the fact that the difference between mesoscopic simulation results and the average weekday stays approximately constant. Additionally, the difference between mesoscopic simulation flows and the average weekday flow is approximately in the same range along the entire simulation period, which results in a coefficient of determination above 0.75 meaning that the mesoscopic simulation results is considered to be validated. Since the average of the representative day is closer to the averages resulting from simulation, the influences of outliers between the simulation results and the days from data are considerably larger.

The microscopic simulation flows do not have a R^2 -value above 0.75, which means that further explanation is required. The microscopic simulation flow results at detector location 4 resemble the flow patterns of the average weekday until 18:00, but are constantly found to be approximately 500 vehicles per hour lower. From 18:00 and onwards, the same peak as the representative weekday is found, albeit slightly less severe. When comparing with the representative weekday, a very similar pattern is found between 16:30 and 19:30. Therefore, the microscopic flow results for this detector location are also validated, since it seems to be a combination of patterns from the average and representative weekday selected for validation.

Figure 159 shows the speeds from microscopic, mesoscopic simulation and traffic data per 15 minute time intervals. *Table 33* gives the corresponding coefficients of determination.

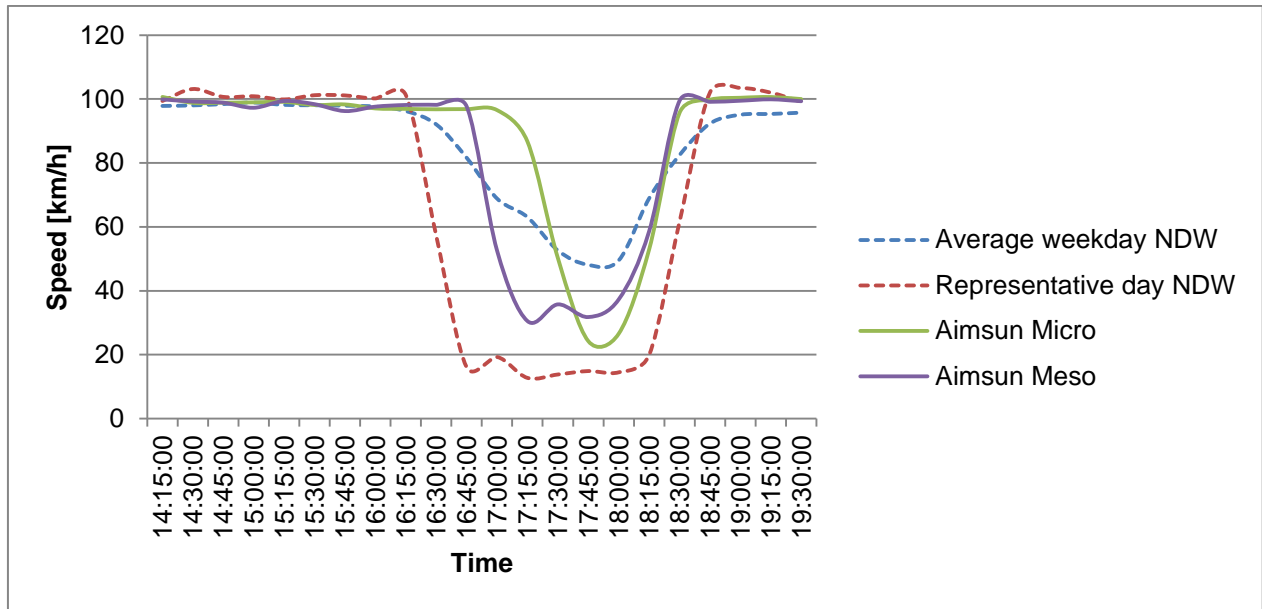


Figure 159 - Speeds per 15 minutes for detector location 4

Table 33 - Coefficients of determination [R²] for the speeds at detector location 4

	Micro	Meso
Average weekday	0.766	0.902
Representative day	0.493	0.714

Again, the speed patterns from simulation are similar to speed patterns from traffic data. In fact, the simulation results are generally in the middle of the average weekday and representative weekday. Both microscopic and mesoscopic simulation show an acceptable fit with respect to the average weekday.

Detector location 5

This detector is located at junction Ridderkerk and is at the approximate tail of the congestion. Figure 160 shows the flows from simulation and traffic data. Table 34 provides the coefficients of determination.

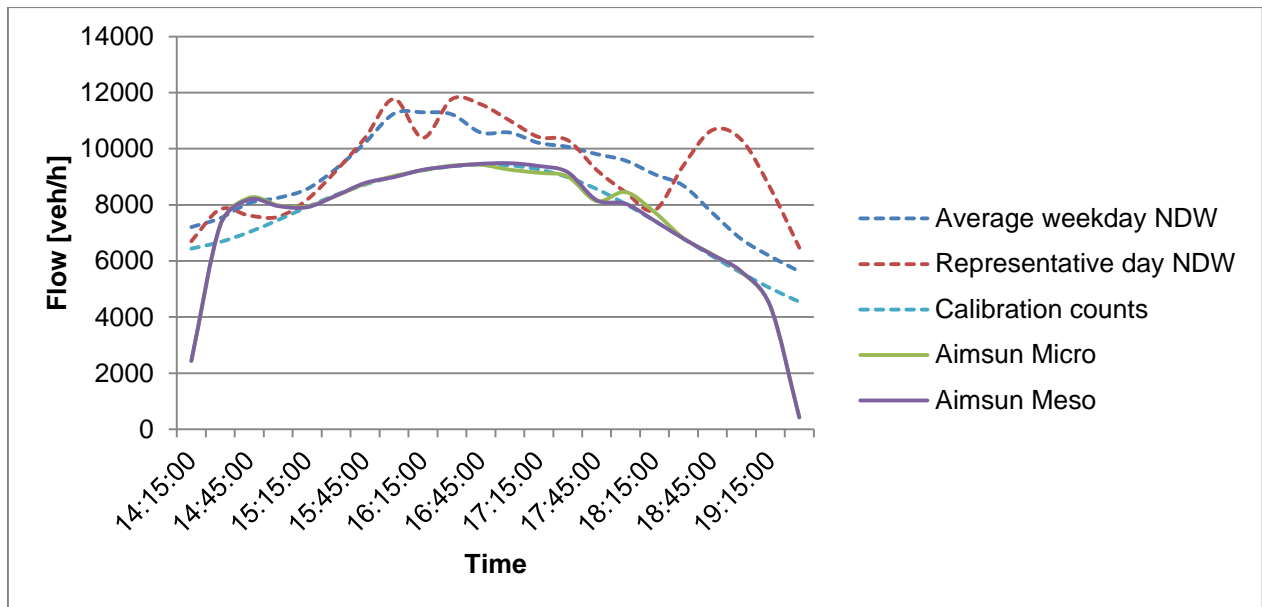


Figure 160 - Flows per 15 minutes for detector location 5

Table 34 - Coefficients of determination [R^2] for the flows at detector location 5

	Micro	Meso
Average weekday	0.824	0.818
Representative day	0.143	0.175
Calibration counts	0.920	0.934

From Figure 160 could be found that both microscopic and mesoscopic flow patterns follow the average weekday and calibration counts very well. All coefficients of determination with respect to the average weekday and calibration counts are above 0.75, meaning that the simulation results are validated.

Figure 161 shows the speeds from simulation and traffic data per 15 minute periods. Table 35 gives the corresponding coefficients of determination.

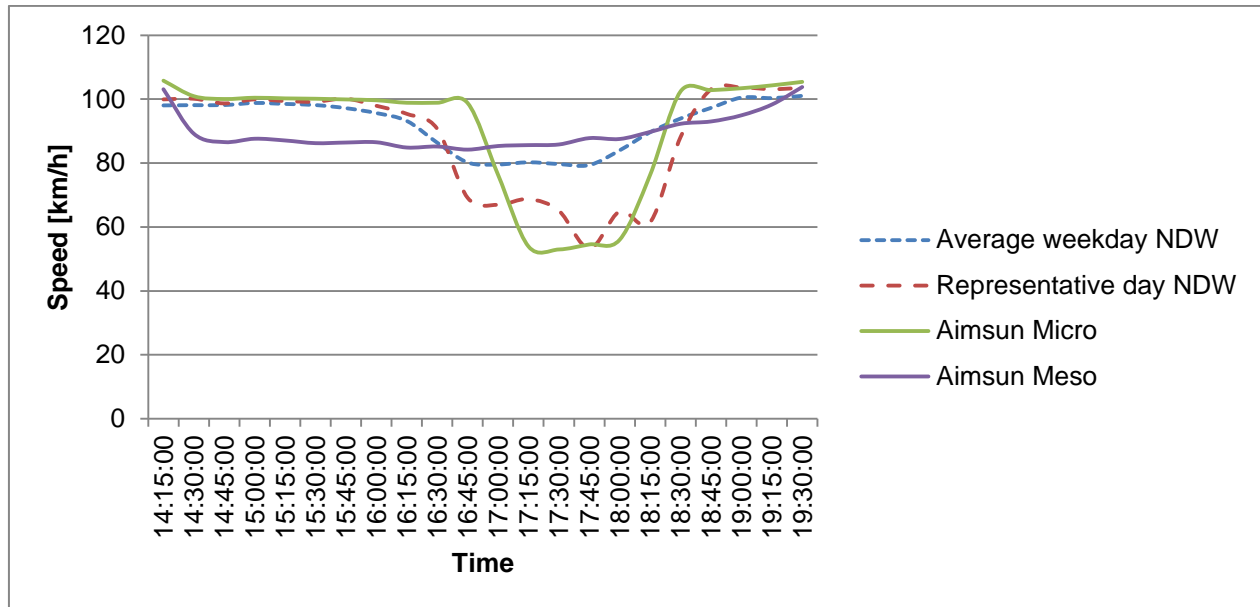


Figure 161 - Speeds per 15 minutes for detector location 5

Table 35 - Coefficients of determination [R^2] for the speeds at detector location 5

	Micro	Meso
Average weekday	0.660	0.286
Representative day	0.764	0.177

With respect to the speed patterns at detector location 5, the microscopic simulation results are relatively similar to the representative day, with a coefficient of determination of above 0.75. While the mesoscopic speed results resemble the speeds at the average weekday, the coefficient of determination is relatively low for this combination, because the averages are very close to each other, which means that deviations account stronger than in cases where averages are further away from each other. The speed difference between the mesoscopic speeds from simulation and the speeds at an average weekday are very close to each other, since the maximum speed difference is only 12 km/h. This maximum speed difference is low, which means that these results are also accepted in terms of validation. Additionally, note that the congestion has spilled back to this location in microscopic simulation, but not in mesoscopic simulation.

Detector location 6

This detector is also located at junction Ridderkerk. This location could be considered as the approximate head or start of the congestion front. Figure 162 shows the flows from simulation and traffic data per 15 minute time periods. Table 36 gives the corresponding coefficients of determination for combinations of simulation results and traffic data.

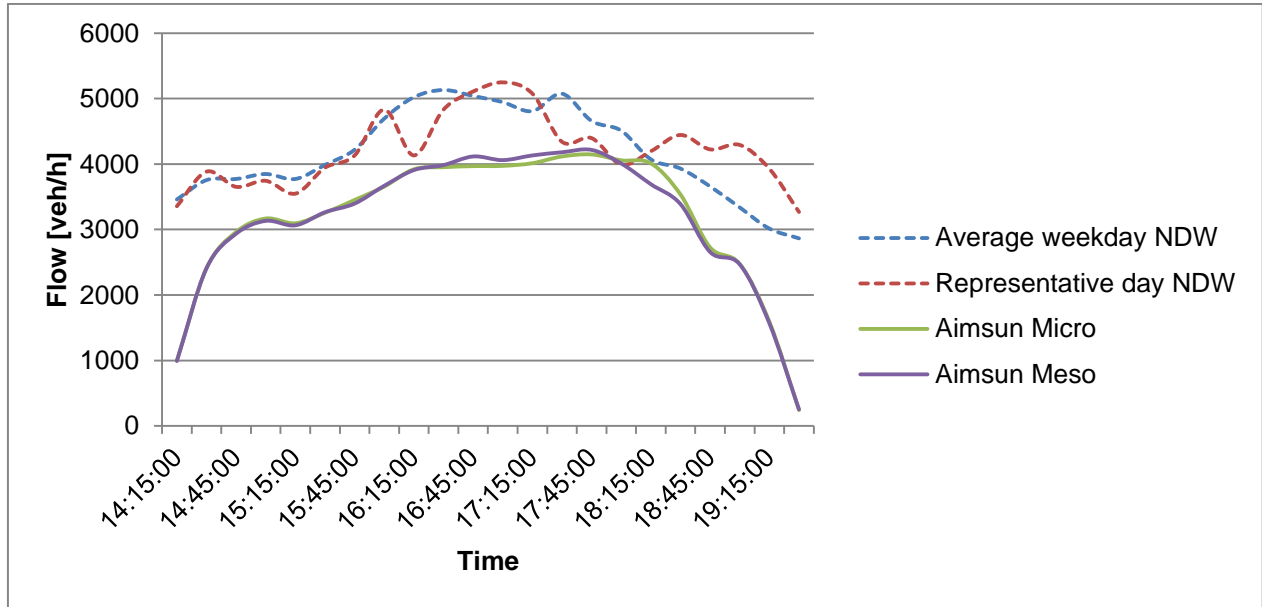


Figure 162 - Flows per 15 minutes for detector location 6

Table 36 - Coefficients of determination [R²] for the flows at detector location 6

	Micro	Meso
Average weekday	0.784	0.852
Representative day	0.278	0.332

Figure 162 shows that flows from simulation are structurally lower than flows from traffic data. There might be two reasons for this. First, there has been a sharp increase in traffic between 2014 (year of calibration counts) and 2016. Secondly, the detector data might also contain data of the off-ramp, which is very close to the considered detector and main road. Nevertheless, the flow patterns are similar. The representative days show some more fluctuations in comparison with the simulation results and average weekday. Table 36 indicates that the mesoscopic and microscopic flow results have an acceptable goodness of fit with respect to the average weekday. These flows are validated, because the R²-values are above 0.75.

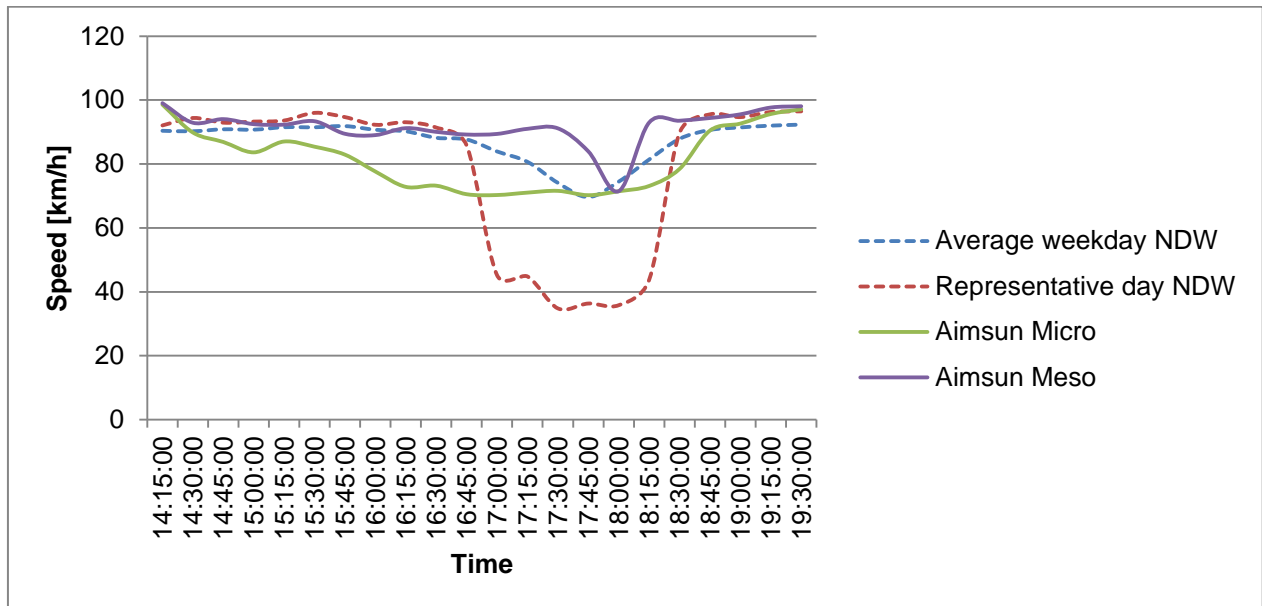


Figure 163 - Speeds per 15 minutes for detector location 6

Table 37 - Coefficients of determination [R^2] for the speeds at detector location 6

	Micro	Meso
Average weekday	0.464	0.430
Representative day	0.476	0.349

Figure 163 shows the speeds from simulation and traffic data per 15 minute periods. Table 37 gives the corresponding coefficients of determination. At detector location 6, the coefficients of determination are too low. This location can be considered as the approximate head or source of congestion. The representative day shows serious congestion, while the average weekday does only show mild congestion. The microscopic simulation reports speeds that are somewhat reduced from the start of simulation, while the mesoscopic simulation results show some congestion, but only for a limited time period (Figure 163). The expected reason for the relatively poor fit is that the detector is located at a single place, while the simulation results are obtained as an average speed over a road section, which influence the results. Most of the congestion in the simulation is shown just upstream of this road section, which means that congestion is not fully shown in the simulation results. If the microscopic and mesoscopic speed results are compared with the speeds found for the average weekday, the simulation results seem to have a relatively similar pattern as the average weekday. However, the mesoscopic simulation shows a decrease in speed over a shorter period in time, while the microscopic simulation shows a decrease in speed for a longer period of time. Additionally, the speed differences are all below 20 km/h. The discussed reasons together justify that these speed patterns are also accepted in terms of validation.